Institut für Neurobiologie
der Universität Ulm

Behavioral aspects of neuronal control in the foregut of the two crab species *Cancer pagurus* and *Cancer borealis*

Dissertation
zur
Erlangung des Doktorgrades Dr. rer. nat.
der Fakultät für Naturwissenschaften
der Universität Ulm

Vorgelegt von
Florian M. Diehl
aus Kempten

Ulm 2012

Dekan: Prof. Dr. Joachim Ankerold

Erstgutachter: PD Dr. Wolfgang Stein

Zweitgutachter: Prof. Dr. Harald Wolf

Abgabe der Doktorarbeit: 13.11.2012

Tag der Promotion: 18.12.2012

"I don’t know anything, but I do know that everything

is interesting if you go into it deeply enough."

Richard Feynman (1918 - 1988)

Table of Contents

CHAPTER 1 Abstract 1
CHAPTER 2 Introduction 3
2.1 Invertebrate model systems in neuroscience 3
2.2 Cancer, the edible crab: a model system for neurobiology 4
2.2.1 The stomatogastric ganglion 6
2.2.2 Projection neurons modulate motor pattern generators in the STG 8
2.2.3 Endoreceptors activate projection neurons 9
2.2.4 Exteroceptors activate projection neurons 13
2.2.5 Other pathways that activate the gastric mill 14
2.2.6 Differentiability of gastric mill rhythms by analysis of neuronal output 14
2.2.7 Anatomical properties of the stomach and the gastric mill 16
2.2.7.1 The medial tooth protractor system 19
2.2.7.2 The lateral tooth protractor system 20
2.2.7.3 The medial and lateral tooth retractor system 21
2.3 Purpose and goals of this work 21
CHAPTER 3 Materials and Methods 25
3.1 Solutions used 25
3.2 Preparations 25
3.2.1 *In vivo* preparation 25
3.2.1.1 Positioning of electrodes on dorsal side 26
3.2.1.2 Positioning of electrodes on ventral side 27
3.2.2 *In situ* muscle preparation 30
3.3 Electrophysiology 32
3.3.1 Extracellular recording and stimulation 33
3.3.2 Construction of extracellular electrodes 34
3.4 Sensory Stimulation *in vivo* 35
3.4.1 VCN-type gastric mill rhythm initiation 35
3.4.2 POC-type gastric mill rhythm initiation 36
3.5 Video Endoscopy 36
3.6 Data Analysis 37
3.7 3-D Modeling and drawings of dried stomach preparations 37
CHAPTER 4 Results 39
4.1 Selective activation of a commissural projection neuron is possible *in vivo* 39
4.1.1 Similarities of spontaneous MCN1 activities *in vivo* and *in vitro* 41
4.1.2 MCN1 does not affect the esophageal motor neuron 42
4.1.3 Lesioning of MCN1 axon affects pyloric CPG *in vivo* 45
4.1.4 MCN1 activation *in vivo has similar effects* on the gastric mill CPG compared to *in vitro* 46
4.1.5 Summary 47
4.2 Activation of distinct pathways initiating gastric mill rhythms *in vivo* 47
4.2.1 Mechanical activation of the VCN-pathway *in vivo* 48
4.2.1.1 Characterization of lateral tooth movement during VCN stimulation 50
4.2.1.2 Hepatopancreatic duct activity affects the initiation of the VCN-elicited gastric mill rhythm 51
4.2.2 Electrophysiological activation of the POC-pathway *in vivo* 53
4.2.2.1 Characterization of lateral tooth movement during POC stimulation 56
4.2.2.2 Hepatopancreatic duct activity affects the initiation of the POC-elicited gastric mill rhythm 61
4.2.2.3 Variability of tooth movement changes during POC-elicited gastric mill rhythms 62
4.2.2.4 Protraction movement of teeth during VCN-elicited gastric mill rhythms does not change over time 66
4.2.3 Summary and characterization of VCN- and POC elicited rhyhms *in vivo* 68
4.3 Application of *in vitro* spike patterns in the *in vivo* preparation 69
4.3.1 Quantitative analysis of differences between two types of *in vitro* patterns 70
4.3.2 *Distinct characteristics in lateral* tooth movements during stimulation with *in vitro patterns* 75
4.4 The gm6 muscle faithfully reproduces stimulations with in vitro patterns 82
4.4.1 *Distinct characteristics of in situ* muscle contractions during stimulation with *in vitro* data 83
4.5 Characterization of tooth movements during three distinct gastric mill rhythms in vivo 88
4.5.1 Duty cycles of motor neurons in standardized gastric mill patterns 89
4.5.2 Burst characteristics and gastric mill periods in standardized gastric mill patterns 92
4.5.3 Intraburst firing frequencies in standardized gastric mill patterns 92
4.5.4 Analysis of gastric mill teeth movement elicited by standardized stimulation 93
4.5.4.1 Standardized gastric mill rhythms elicit distinct movement output in the lateral teeth 96
4.5.4.2 Standardized gastric mill rhythms elicit distinct movement output of the medial tooth 101
4.5.5 Summary of chapter 4.5 104

4.6 Lateral- and medial tooth movement depends on motor neuron spike-frequency 105
4.6.1 Summary of chapter 4.6 107
4.7 Emergent effects during rhythmic muscle contractions influence tooth movement 108
4.7.1 Lateral and medial tooth protractions are decoupled 108
4.7.2 Retractions of the medial- and lateral tooth are coupled 109
4.7.2.1 The medial tooth retractor subsystem 109
4.7.2.2 The lateral tooth retractor subsystem 111
4.7.2.3 Muscles gm2 & gm3 do not participate in retraction 113
4.7.3 3D-modeling visualizes functional coupling of gastric mill teeth 114
4.7.4 Summary of chapter 4.7 119
CHAPTER 5 Discussion 121
5.1 Contribution of a single projection neuron on motor output *in vivo* 122
5.2 Different gastric mill activation pathways elicit distinct behaviors *in vivo* 124
5.2.1 Investigation of a mechanosensory gastric mill activation pathway 124
5.2.2 Implications of noise and functional relevance of variability of behavior in the gastric mill 129
5.2.3 Different methods to investigate the neuronal network, musculature and anatomy of the stomatogastric system in the crab 132
5.2.4 Varying contribution of a protractor muscle on movement during several modes of VCN-type stimulations 134
5.2.5 Investigation of a non-sensory gastric mill activation pathway 136
5.2.6 Consistent contribution of a protractor muscle on movement during several modes of POC-type stimulations 139
5.2.7 Behavioral relevance of three different types of gastric mill rhythms 140
5.2.8 An active hepatopancreatic duct enables the induction of gastric mill rhythms in vivo 142
5.3 Coupling and decoupling of tooth movement systems in the gastric mill is mediated by an intrinsic muscle 144
5.4 Outlook 148
CHAPTER 6 Bibliography 150

List of Abbreviations

Ganglia

Abbreviation	Description
CG	cerebral ganglion
CoG	commissural ganglion
STG	stomatogastric ganglion
TG	thoracic ganglion

Nerves

Abbreviation	Description
coc	circum esophageal commissure
dgn	dorsal gastric nerve
dvn	dorsal ventricular nerve
ion	inferior esophageal nerve
ivn	inferior ventricular nerve
lgn	lateral gastric nerve
lvn	lateral ventricular nerve
mvn	medial ventricular nerve
pdn	pyloric dilator nerve
poc	post esophageal commissure
son	superior esophageal nerve
stn	stomatogastric nerve

Neurons

Abbreviation	Description
AB	anterior burster
AGR	anterior gastric receptor
CPN2	commissural projection neuron 2
DG	dorsal gastric motor neuron
GPR1	gastropyloric receptor 1
GPR2	gastropyloric receptor 2
IC	inferior cardiac motor neuron

IV	inferior ventricular neuron
LG	lateral gastric motor neuron
LP	lateral pyloric motor neuron
LPG	lateral posterior gastric motor neuron
MCN1	modulatory commissural neuron 1
MCN5	modulatory commissural neuron 5
MCN7	modulatory commissural neuron 7
OMN	esophageal motor neuron
PD	pyloric dilator motor neuron
PSR	posterior stomach receptor
PY	pyloric constrictor motor neuron
VCN	ventral cardiac neuron

Muscles

Abbreviation	Description
gm1	gastric mill muscle 1
gm2	gastric mill muscle 2
gm3	gastric mill muscle 3
gm4	gastric mill muscle 4
gm5	gastric mill muscle 5
gm6	gastric mill muscle 6
gm8	gastric mill muscle 8
gm9	gastric mill muscle 9

Other

Abbreviation	Description
CNS	central nervous system
CPG	central pattern generator
°C	degrees celsius
GMR	gastric mill rhythm
Hz	Hertz
kHz	Kilohertz
min	minute
mMol	millimol
MT	Medial Tooth Unit
ms	millisecond

PR	pyloric rhythm
s	second
S	Siemens
Stim	stimulation
STNS	stomatogastric nervous system
V	Volt

Chemical formulas

Abbreviation	**Description**
$CaCl_2 \bullet 2H_2O$	calciumchloride dihydrate
$NaCl$	sodium chloride
$MgCl_2 \bullet 6H_2O$	magnesium chloride hexahydrate
KCl	potassium chloride

1. Abstract

Neuronal networks compute cues from the environment using specialized sensors and they actuate the musculature, eliciting directed behavioral output. Investigating rhythmic movement patterns in invertebrates has been a successful method in neuroscience to understand the principles of neuronal control. A successful model system for the past decades has been the stomatogastric nervous system (STNS) of decapod crustaceans. Rhythmic behavior in the foregut, which contains the gastric mill and the pyloric filter apparatus, is controlled by a network of neurons constituting central pattern generators. The initiation, modulation and termination of activity in these central pattern generators is performed by paracrine inputs from projection neurons and endocrine inputs from hormones in the blood stream. How this modulation is controlled and whether the large flexibility caused by these influences is relevant for behavioral output and ultimately the survival of the organism, is still subject to debate.

The experiments in this work were conducted on *in vivo* preparations of two brachyuran species (*Cancer pagurus & Cancer borealis*). They demonstrate that modulatory and sensory pathways, which were previously established in *in vitro* studies, were sufficient to elicit rhythmic activity of motor neurons *in vivo* as well. The movement of the gastric mill teeth during these motor patterns revealed that the different pathways elicited readily discernible movement patterns on the behavioral level. While several aspects of the motor patterns could be traced from the neuronal activity to muscle force production and finally tooth movement, several movement properties were not predicted by the neuronal activity alone. The concerted interaction of motor neurons, muscles and ossicle dynamics *in vivo* thus has to be appreciated to study these emergent properties. While the stomatogastric nervous system has been a model for investigating motor pattern generation for several decades, linking the combination of the comprehensive knowledge about the neuronal network with behavioral and ethological experiments, could reveal new insights into what methods organisms evolved to respond adequately to changing environmental cues.

2. Introduction

2.1 Invertebrate model systems in neuroscience

Evolutionary processes of natural life have produced a mind-boggling variety of species on this planet. The cells of multicellular individuals are arranged in different tissues enabling the organism to sustain itself and produce offspring. One key factor to accomplish this is the ability to perceive the world. Sensory organs have evolved to control, and provide feedback while, moving through the environment by walking, swimming or flying. One method in neurobiology has been to investigate the central nervous system to find out about how information is extracted from the world and the state of the own body, computed and then used to elicit behaviors. It has been found, however, that the nervous system, as well as the organs innervated by it, show highly complex interactions which are very difficult to entangle scientifically. Academic experience tells us that the best way to deal with a complex system is to break it up into smaller bits and investigate those in isolation. Organisms and environments are very complex, which made the partitioned investigation of organisms, organs and cells neccessary. Some model systems in neuroscience have been very successful and provided a very good understanding about the neuronal architecture, underlying behavioral output.

For the investigation of the effects of neuronal activity onto behavior, the study of locomotion and movement in general has been very rewarding scientifically. Some of the first modern scientific experiments have been conducted on the locomotor system of invertebrates and vertebrates, mainly because movement is easily observable and quantifiable (Humboldt 1797). Investigations on invertebrate organisms revealed that the control of rhythmic movements such as walking, swimming or flying, is performed by central pattern generators in the nervous system. Those are networks of motor neurons, which are usually interconnected such that these neurons endogenously generate rhythmic activity (Grillner & Wallen 2002; Calabrese 1995; Pearson 2006). The action potentials then elicit rhythmic contraction and relaxation in the muscles. Feedback from sensory neurons innervating the muscles provides information about the current state of the musculature and position of limbs. The interaction of many central pattern generators and feedback pathways in the nervous system are necessary for the animal to successfully evade dangers, find food and mates (Holmes et al. 2006).

For a more detailed investigation of the architecture of the central pattern generators as well as the sensory pathways, invertebrates also serve as a valuable model organisms (Marder et al. 2005; Sattelle & Buckingham 2006). The knowledge aggregated from studies on invertebrate nervous systems encompasses the sub cellular

level (Hille 1986), the network level (Nusbaum & Beenhakker 2002) and the behavioral level (Calabrese 2003). This has enabled scientists to gain a detailed understanding, not only about the typical neurobiological architecture of this clade, but also about our own (Flash & Hochner 2005; Dickinson 2006).

One invertebrate model system of which the neuronal basis of motor control is understood exceptionally well, is the stomatogastric nervous system of decapod crustaceans (Govind et al. 1975; Pearson 1908). Neurons in this nervous system form central pattern generators (CPGs) (Marder & Bucher 2001), which innervate a complex digestive system consisting of the esophagus, the foregut and the mid- and hindgut (Icely & Nott 1992; Yonge 1924). Through the esophagus the food is ingested, and transported into the foregut. There, the food is chewed by a complex apparatus of teeth - the gastric mill (Heinzel 1988). However, oppose to other invertebrate model systems in which behavioral assays have been established as successful means of experimentation (Stephens et al. 2008; Katz 1996), the behavioral output of the stomatogastric system of crustaceans, i.e. chewing, has not been investigated very much. Since the classic works of Heinzel et al. (1988), there was no other study investigating the interaction of the neurons, muscles and bones in the stomatogastric system in a holistic manner. The work presented here thus connects a well-characterized neuronal model system for pattern generation with behavioral studies by establishing an *in vivo* experimental assay for the stomatogastric system of the brachyuran crab species *Cancer pagurus* and *Cancer borealis*.

The following chapters will give current information about the stomatogastric system beginning with a gross description of the crustaceans used in my studies and then focussing on the structure of the stomatogastric nervous system. Special focus will be given to the central pattern generators and the extero- and proprioceptors controlling movement. Then the musculature driven by these CPGs, and lastly the anatomical structure in which these muscles move are described in detail. Finally, motivation and description for the research shown in this work is given as well.

2.2 *Cancer*, the edible crab: a model system for neurobiology

Decapod crustaceans are one of the most successful order of animals on this planet. Members of the Decapoda can be found as high as *2,000 m* above sea level and as low as *6,000 m* in the abyssal region of the ocean (Ng et al. 2008). Within the Decapoda, the infraorder of the Brachyura is the most diverse. All brachyuran crabs have in common that the abdomen is reduced under the thorax and the head region is fused

to the carapace. This is called "carcinisation", an evolutionary trend in this clade, which forms a highly resistive and compact shell (Ng et al. 2008). The ten pereiopods form eight walking legs (four pairs) and two chelates (one pair of chelipeds) for cutting and holding of prey.

Information about the food size and texture are gathered by specialized appendages. Around the esophagus, three maxillipeds with flagella and two maxilla are located. They cannot only perceive tactile and olfactory information about the food they also push it towards the mandibles (Reddy 1935). The mandibles chop the food into small enough pieces, which are able to proceed through the esophagus. The esophagus contains olfactory sensors, which can perceive noxae and toxins. The ingestion of the hormone ecdysone, for example, can have toxic effects on animals, which grow via molting (Robertson & Laverack 1979; Tomaschko et al. 1995). Therefore, highly sensitive olfactory sensors perceive this hormone which leads to immediate egestion of the food without further harm for the animal. If the food is considered not harmful, it passes through the esophagus via peristaltic movements of the musculature. The food is thus moved into the cardiac sac, the largest portion of the foregut (Spirito 1975). The cardiac sac is comprised of a rigid tissue, which holds the food, but can also be drastically inflated during molting (Ayali 2009). During digestion, the musculature of the cardiac sac performs peristaltic movements, which mixes the digestive enzymes with the food to help pre-digestion (Barker & Gibson 1977; Heinzel et al. 1993; Huxley 1880). The food is then chewed in a specialized structure in the foregut, the gastric mill, by two symmetrically organized lateral teeth and one medial tooth. Coordinated rhythmic pro- and retractions of these teeth can cut or grind larger food particles (Patwardhan 1935b; Heinzel 1988). The ground food is passed into the pylorus by the cardio-pyloric valve while several setae perform further filtering of coarse food particles in the pylorus (Icely & Nott 1992). A complex arrangement of intrinsic ossicles and muscles form the pyloric duct in which nutrients are filtered and transported to the midgut (Govind et al. 1975; Yonge 1924). The pancreatic function of the hepatopancreas is performed via the anterior midgut caeca, which form the hepatopancreatic duct and insert posterior of the pylorus (Schultz 1976; McGaw 2006). The aforementioned digestive enzymes, produced by the hepatopancreas, are passed through the aforementioned duct into the pylorus and the lumen of the cardiac sac (Icely & Nott 1992). The midgut caeci also mark the transition from the foregut to the midgut (McGaw & Reiber 2000). Here, in the midgut, the enzymatic digestion takes place. Arborisations of the midgut caeca form blind-ending tubuli through which nutrients are passed into the hepatopancreas (Icely & Nott 1992; Johnson 1980). The end of the midgut is marked by the posterior midgut caeca. Indigestible particles and waste are transported to the hindgut, which ends in the anus (Smith 1978).

Research on the neuronal control of rhythmic movements during digestion has been focused on the investigation of the foregut. Both, the gastric mill and the pyloric filter apparatus, are moved by rhythmic contractions of a complex array of intrinsic and extrinsic muscles (Maynard & Dando 1974; Patwardhan 1935b). These muscles are innervated by *~26* motor neurons (depending on the species), which are located in the stomatogastric ganglion (STG) (Larimer & Kennedy 1966; Maynard & Selverston 1975; Hermann 1977). This ganglion is located dorsally, between the cardiac sac and the carapace, within the ophthalmic artery (Maynard & Selverston 1975). The synaptic connections between the motor neurons in the STG and their interconnection with other ganglia shall be described in more detail in the following.

2.2.1 The stomatogastric ganglion

The neurons in the stomatogastric ganglion form two central pattern generators (Bal et al. 1988; Hooper 2000). One of the central pattern generators controls the pylorus, which controls the dilation of the pyloric valve, filtering and the peristalsis, and moves the food further into the midgut. The pyloric central pattern generator's pacemaker ensemble consists of the anterior burster (AB) neuron and two pyloric dilator (PD) neurons (Nusbaum & Beenhakker 2002). Due to the mostly inhibitory synapses onto the other neurons of the pyloric CPG (see fig. 1), all pyloric follower neurons are rhythmically active and form robust burst patterns. The rhythmic pattern of activity elicited by the neurons in the pyloric CPG is highly robust. This has been shown in the *in vivo* preparation as well as, completely isolated from other inputs, in the *in vitro* preparation. These neurons perform rhythmic bursting at a cycle periods between *0.5 - 2 s* (Bal et al. 1988).

The second central pattern generator in the STG controls the gastric mill teeth and runs at a cycle period that is about *10x* slower than that of the pyloric rhythm (*6 - 25 s*, and see Selverston et al. 2009). In contrast to the pyloric CPG, the gastric mill CPG does not possess pacemaker neurons in the crab. The gastric mill CPG is thus not continuously active. Rather, rhythmic bursting activity in the gastric mill neurons is elicited and maintained by inputs from other ganglia and sensory neurons (Combes et al. 1999; Selverston et al. 2009; Powers 1973). Modulatory projection neurons in the paired commissural ganglia (CoGs) activate the gastric mill CPG by releasing neuromodulatory and classical transmitter onto the STG motor neurons (Stein 2009; Nusbaum 2012).

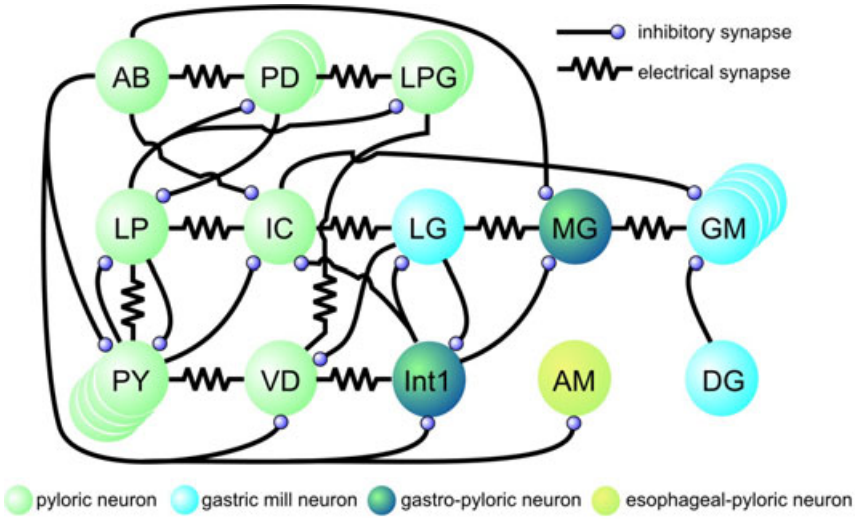

Figure 1: Synaptic connections of neurons in the STG. Schematic shows all neurons in the ganglion colored according to their affiliation to the pyloric-, gastric- and esophageal CPGs. Neurons (circles) colored in green show neurons belonging to the pyloric CPG. Neurons associated with the gastric mill CPG are shown in cyan. The pyloric constrictor motor neuron (PY), the pyloric dilator motor neuron (PD), the lateral posterior gastric motor neuron (LPG) and the gastric mill motor neurons (GM) exist as several copies in the STG. Adapted from Stein (2009).

Once activated, the gastric mill motor neurons fire in an alternating fashion due to reciprocal inhibitory synapses between the lateral gastric neuron (LG) and the interneuron 1 (Int 1) (Johnson & Hooper 1992; Nusbaum & Beenhakker 2002). The LG neuron innervates the protractor muscles of the lateral teeth (gm5, gm6, gm8). Four other neurons in the gastric mill CPG, the gastric mill (GM) neurons, innervate the protractor muscle of the medial tooth (gm1). Simultaneous activity of the GM neurons and LG thus characterize the protraction phase of a gastric mill rhythm. The dorsal gastric (DG) neuron and Int 1 are active in alternation to the protractor neurons. The DG neuron innervates the retractor muscle (gm4) and characterizes the retraction phase of the gastric mill rhythm.

The gastric mill CPG is thus activated by several pathways, which are relayed via the projection neurons. These pathways can also modulate the activity patterns of the gastric mill motor neurons thus eliciting different neuronal outputs (Hedrich et al. 2009). In the following, these pathways and their effects on the CPGs in the stomatogastric ganglion are described in more detail.

2.2.2 Projection neurons modulate motor pattern generators in the STG

The commissural ganglia contain more than *500* neurons. A few of these, which are known to affect the CPGs in the STG, have already been investigated in more detail (Nusbaum et al. 2001; Stein 2009). Extensive studies of the connections between the projection neurons and the neurons in the STG revealed complex feedforward and feedback pathways (Coleman et al. 1992; Kirby & Nusbaum 2007), which are described in more detail in the following.

The modulatory commissural neuron 1 (MCN1) was the first projection neuron to be identified (Coleman et al. 1992). Its axon projects via the inferior esophageal nerve (*ion*), the stomatogastric nerve (*stn*), to the network of motor neurons in the STG. MCN1 excites all gastric mill motor neurons (including the interneuron Int1) and pyloric neurons (see fig. 2, far left and Stein et al. 2007). It forms additional electric synapses to LG and the inferior cardiac (IC) neuron. Thus, MCN1 modulates both CPGs. MCN1 also receives feedback from the STG neurons. When LG is activated, it presynaptically inhibits MCN1, thus terminating MCN1 input onto both CPGs. During retraction, with LG mediated inhibition missing, MCN1 activates both CPGs (Coleman & Nusbaum 1994; Stein 2009).

Similar to MCN1, the modulatory commissural neuron 5 (MCN5) projects, similar to MCN1, via the *ion* and *stn,* to the STG (Norris et al. 1996). There, it forms excitatory synapses with the gastric mill neuron DG, and inhibits LP (lateral pyloric neuron), PY (pyloric constrictor neurons), VD (ventral dilator neuron) and IC (see fig. 2, left). In addition to the

The modulatory commissural neuron 7 (MCN 7) projects via the subesophageal nerve *son* and the *stn* to the STG (Blitz & Nusbaum 1999). It possesses chemical excitatory synapses onto the gastric mill neurons LG and DG, as well as the pyloric neurons IC and VD (see fig. 2, right).

The last of the identified projection neurons is the commissural projection neuron 2 (CPN2) which projects via the *son* and the *stn* to the STG. It excites the gastric mill neurons GM and LG, and inhibits DG as well as IC (see fig. 2, far right). However, all known proprioceptors and exteroceptors that affect the CPGs in the stomatogastric ganglion have strong effects onto the projection neurons in the CoGs and thus onto the output of the CPGs.

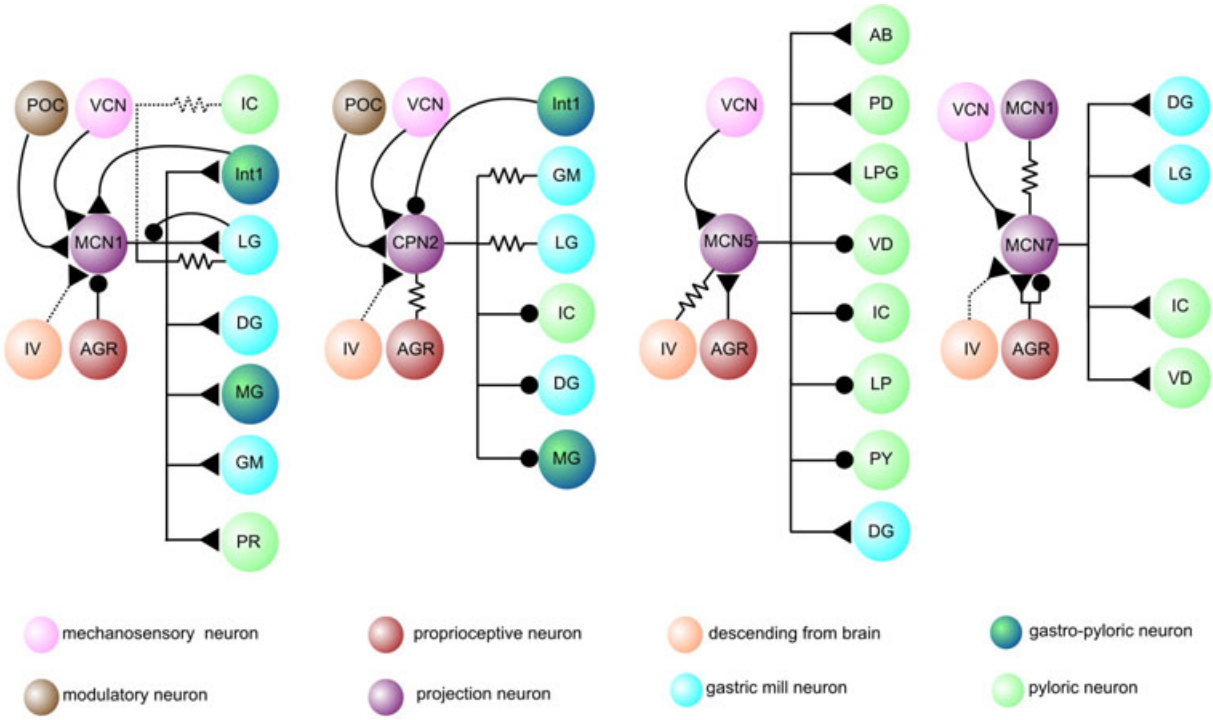

Figure 2: Synaptic interconnection between projection neurons and STG neurons. **Far left**: MCN1 receives input from several receptors. It modulates the pyloric rhythm and initiates a gastric mill rhythm. **Left:** CPN2 only affects gastric mill and gastro-pyloric cells. It receives feedback inhibition from Int1. **Right:** MCN5 receives input from IV and AGR (inhibitory) and synapses with pyloric neurons, and one gastric mill neuron (DG). **Far right:** MCN7 synapses with MCN1 and excites pyloric as well as gastric mill neurons. Adapted from Stein (2009).

2.2.3 Endoreceptors activate projection neurons

Several proprioceptors are arranged around the stomach wall and the musculature to monitor the state of the system and provide feedback. In the following, these receptors are described and the known innervations and feedback mechanisms illuminated.

The soma of the anterior gastric receptor (AGR) is situated slightly rostral to the STG. One of its axons projects via the dorsal gastric nerve *dgn* and ramifies laterally to the protractor muscle of the medial tooth, the paired gm1 muscle(Larimer & Kennedy 1966). AGR projects a second axon caudally via the *stn* and the *son* to the CoGs and excites CPN2 and MCN7; MCN1 is being inhibited by AGR (Smarandache & Stein 2007). AGR possesses two types of activity: a tonic activity pattern, and a bursting activity pattern. Bursting occurs when the gm1 muscle stretch is increased, which can be achieved either by activation of the GM motor neurons or passive stretch on the muscle. Rhythmic AGR bursting entrains a gastric mill rhythm, which

means that the gastric mill cycle duration accommodates to the duration of the AGR bursts (Smarandache & Stein 2007). Tonic AGR activity, in contrast, modulates the response of the gastric mill pattern generator to different sensory input (Daur et al. 2009).

The bilaterally symmetric gastropyloric receptor 1 (GPR 1) innervates the lateral tooth protractor muscle gm8a (see fig. 3); the gastropyloric receptor 2 (GPR 2) innervates the gastric mill muscle gm9 associated with the gastric mill as well as the cardio-pyloric valve muscle 3a (cpv3a) which is associated with the pyloric valve (Katz et al. 1989). GPR 2 computes input from two different motor systems since the gm9 muscle is innervated by the medial gastric neuron MG and the cpv3a muscle is innervated by LP. Due to the arrangement of the muscles passive stretch, elicited by other muscles inserting at the same ossicles, can also cause an activation of these receptor cells (Katz et al. 1989). Both, GPR 1 & 2, are serotonergic cells, which project to the STG and also the CoGs. In the STG the GPR neurons activate the pyloric neurons LP (Katz 2001) and inhibit the PY neurons. This causes an increase in intraburst firing frequency of the pacemaker neurons AB and PD, as well as a decrease in pyloric period. GPR can initiate a gastric mill rhythm, however, only for the duration of the stimulation. GPR has also distinct effects on the gastric mill neuron DG, which innervates the retractor muscle gm4. Contraction of this muscle causes passive stretch in gm9 and can thus activate GPR 2. This activation causes activation of DG and the induction of plateau potentials (Katz 2001). GPR thus builds a positive feedback loop with the gastric mill CPG. As shown by Blitz et al. (2004) GPR 1 & 2 cannot, contrary to AGR, entrain a gastric mill rhythm. GPR 2 also forms excitatory synapses onto all known projection neurons in the CoGs (Blitz et al. 2004).

The ventral cardiac neurons (VCN), for example, can inhibit GPR 2 effects on the projection neurons, when active. The VCNs are located in the cardiac gutter and project axons by the ventral cardiac nerve *vcn* and the *dpon* (dorsoposterior esophageal nerve) to the CoGs *(Beenhakker et al. 2004)*. Several cell bodies traverse the stomach cuticle and function as pressure receptors. The VCN modulate the activity of both CPGs in the stomatogastric ganglion.

While the pyloric cycle period is decreased and the intraburst firing frequency of LP is diminished *(Beenhakker et al. 2004)*, a distinct gastric mill rhythm with strong overlapping bursting of LG and DG is elicited. Initiation and maintenance of this gastric mill rhythm depends on projection neurons' activity in the CoGs: all identified CoG projection neurons (MCN1, 5, 7, CPN2) receive input from the VCNs.

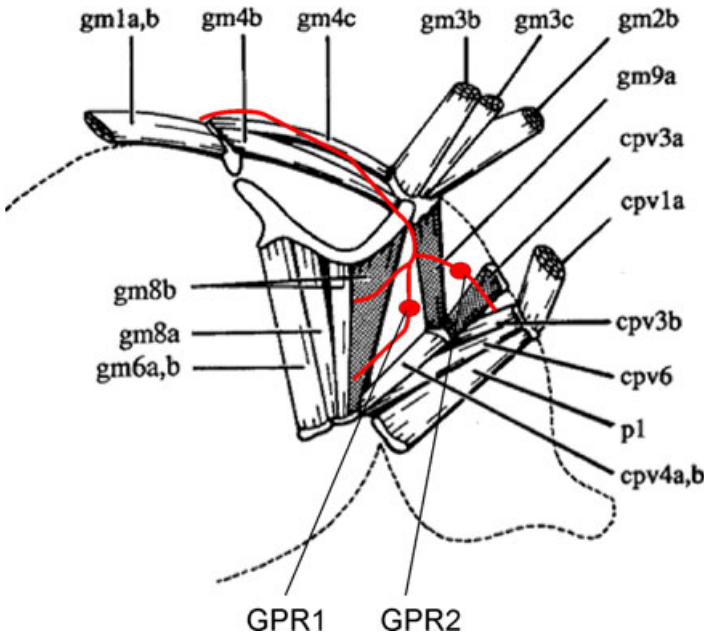

Figure 3: Schematic of innervation of the gastropyloric receptors. Schematic drawing shows lateral view of the gastropyloric region. The *lvn* and its ramifications is shown in red; the two stretch receptors are shown as red dots; the GPR1 & 2 innervated muscles are shaded in grey. Adapted from Katz et al. (1989).

MCN1 & CPN2 are inhibited during VCN activity, while the other two projection neurons receive excitatory synaptic inputs. Based on previous research on other invertebrates, the VCNs are assumed to exert a similar function as the stretch receptors in the foregut of flies and crickets (Rice 1970; Möhl 1972), namely the detection of the amount of food in the gut.

Lastly, the posterior stomach receptors (PSR) consist of ~*50* somata aggregated in a cell cluster in the posterior stomach nerve (*psn*) on top of the stomach wall (Dando & Laverack 1969). It could be shown in the lobster *Jasus lalandii* that the PSR neurons activate the esophageal central pattern generator (Nagy & Moulins 1981). The PSR neurons innervate projection neurons in the CoG as well, and elicit a distinct gastric mill rhythm. Interestingly, PSR can presynaptically inhibit the anterior gastric receptor AGR (Barriere et al. 2008; Blitz & Nusbaum 2011). Presynaptic inhibition of PSR onto AGR suppresses the activation of the projection neurons via AGR, thus eliciting a PSR-elicited version of the gastric mill rhythm.

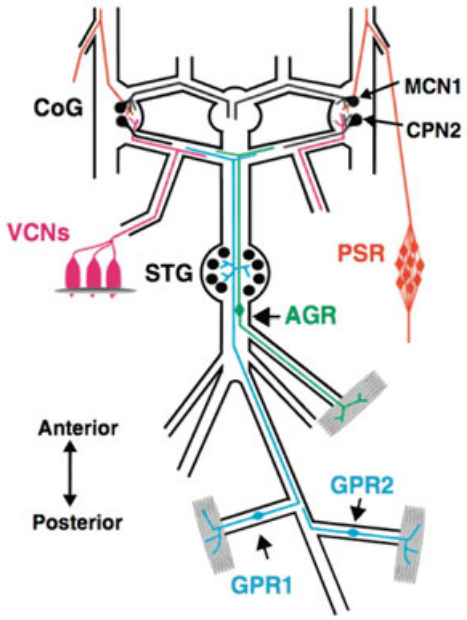

Figure 4: Known proprioceptors in the foregut of decapod Crustacea. Summarizing schematic highlighting the known proprioceptors in the stomatogastric nervous system. The ventral cardiac neurons (VCNs, pink) innervate the cardiac gutter and synapse with the CoGs. The anterior gastric receptor (AGR, green) sends feedback about the gm1 muscle to the CoGs. The gastropyloric receptors (GPR1 & 2, blue) innervate gm8 & gm9/cpv3 muscles and are the only receptors that synapse in both, STG and CoGs. The posterior stomach receptors (PSR, orange) innervate the posterolateral stomach wall and form synapses with the CoGs as well as inhibitory synapses with AGR. Adapted from Blitz & Nusbaum (2011).

The exact mode of function of the PSR neurons is not exactly known, it is assumed however, that strong movements of the zygocardiac ossicles can excite the PSR neurons thus eliciting feedback and changing the mode of chewing. To summarize all known endoreceptors in the stomatogastric nervous system figure 4 shows a schematic summarizing the four known types of receptors and their axonal projections.

2.2.4 Exteroceptors activate projection neurons

The only source of information about the food prior to ingestion originates from the antennae located at the rostral part of the carapace (see fig. 5). Marine animals in general are highly dependent on chemical stimuli (Carr & Derby 1986). Olfactory cues are used by crustaceans to regulate orientation (Lohmann et al. 2008), evasive behaviors (Weissburg et al. 2012), and associative learning (Abramson & Feinman 1990; Dimant & Maldonado 1992; Steullet et al. 2002).

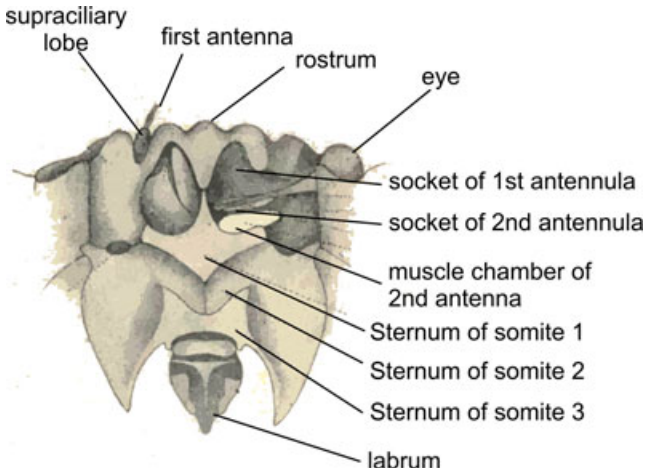

Figure 5: Ventral view of the pre-oral cephalic region. Drawing shows the sockets of the first antenna and the antennulae. The left antennae have been removed to show antennal sockets. Adapted from Pearson (1908).

It has also been shown previously that the antennae play crucial roles in feeding and the initiation of activity in the stomatogastric system of the animal (Hamilton & Ache 1983; Hedrich 2008). The olfactory information is parsed to the cerebral ganglion (CG) for computation and integration with other sensory cues (Schmidt et al. 1992). The inferior ventricular (IV) neurons in the cerebral ganglion project via the inferior ventricular nerve *(ivn)* and form excitatory synapses onto the projection neurons MCN1, MCN7 and CPN2, as well as electric synapses onto MCN5 (Beenhakker et al. 2004; Coleman & Nusbaum 1994; Wood et al. 2000). The projection neurons ultimately activate the motor pattern generators in the STG.

2.2.5 Other pathways that activate the gastric mill

Besides being influenced by sensory pathways, the gastric mill CPG can be activated by neuromodulatory pathways: neurons projecting through the post-esophageal commissure (POC) are known to synapse onto previously described projection neurons in the CoGs (Blitz et al. 2008) and to elicit a gastric mill rhythm. The location of the POC neurons' somata is not yet known; but it is assumed that they are located in the circumesophageal connective between the POC and the thoracic ganglion (see fig. 12 and fig. 14). The POC neurons themselves may relay sensory inputs from the thoracic ganglion towards the CoGs and the STG or they could be activated be other, internal factors of unknows origin.

2.2.6 Differentiability of gastric mill rhythms by analysis of neuronal output

The targeted activation of projection neurons in *in vitro* preparations of the crab elicited gastric mill rhythms in the central pattern generators in the STG. Analysis of the rhythmic output of the motor neurons revealed significant differences depending on the stimulus paradigm used to activate the projection neurons. The following chapter gives an overview of the various types of gastric mill rhythms elicited by three different activation pathways: the cerebral IV neurons, the mechanosensory VCNs and the neuromodulatory POC neurons.

The information gathered from olfactory sensors in the antennae activates the inferior ventricular (IV) neurons in the cerebral ganglion (Hedrich 2008). The IV neurons project via the ivn to STG and COGs where they synapse onto STG motor neurons and CoG. Activation of the IV neurons elicits a distinct gastric mill rhythm in the STG motor neurons (Hedrich & Stein 2008). The period of the elicited gastric mill rhythm was identical to the period of the stimulation of the IV neurons, i.e. IV neuron activity entrains the gastric mill rhythm. Compared to other types of gastric mill rhythms (see below), the duty cycles were significantly shorter for all gastric mill motor neurons, the LG, DG and the GMs.

The ventral cardiac neurons (VCN) elicited distinct burst patterns in the STG motor neurons (Beenhakker et al. 2004). LG showed longer duty cycles (***6.5 ±1.5 s***, from Beenhakker et al. (2004)), compared to other gastric mill rhythms. Both DG and LG showed higher intraburst firing frequencies (***11.5 Hz*** and ***13.6 Hz*** on average) compared to the other gastric mill rhythms.

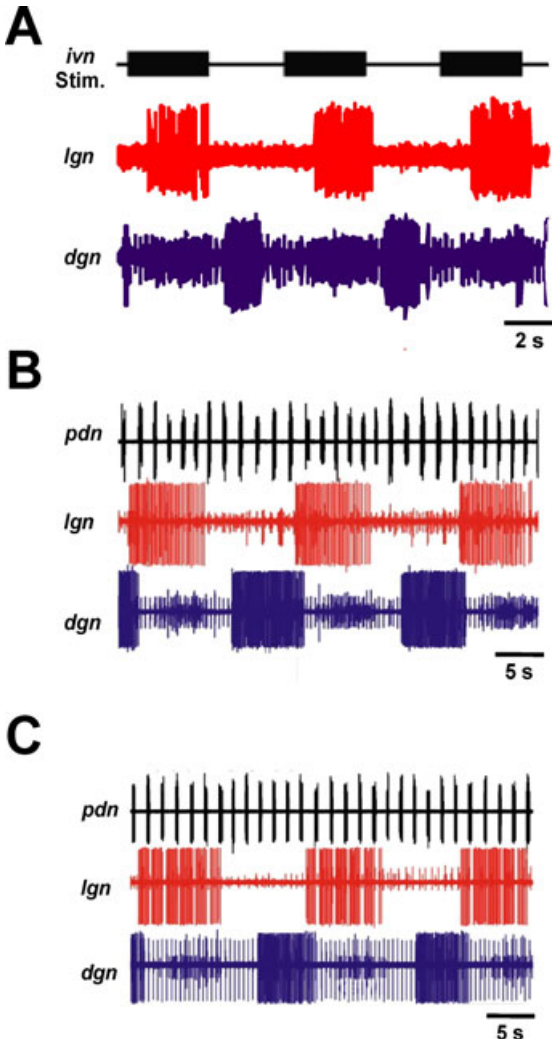

Figure 6: Bursting of motor neurons during three types of GMRs. **A** shows bursting of LG on the *lgn* (red trace) and DG on the *dgn* (blue trace) during stimulation of *ivn* (top trace). **B** shows bursting of LG and DG during stimulation of the VCNs. The pyloric pacemaker PD activity on the *pdn* (black trace) is shown as control. **C** shows bursting of LG and DG during stimulation of the POC neurons. Note that there are gaps in the LG bursts that are timed with the ocurrence of PD activity (top trace). PD is electrically coupled to the AB neuron (see fig. 1) and reflects its activity pattern. Adapted from M. P. Nusbaum & D. Blitz.

High motor neuron firing frequency means strong muscle activation and in case of LG and DG, the overlapping activation of two antagonistic muscles could lead to significant cocontrations. It has not been shown, however, whether this overlap has effects on the movement of the gastric mill teeth.

In the POC-elicited version of the gastric mill rhythm, the pyloric pacemaker neuron AB inhibits the commissural neuron MCN1 in each pyloric cycle (Blitz et al. 2008). This pyloric inhibition feeds forward to the gastric mill neuron LG, interrupting the LG burst with pyloric-timed gaps (burstlets, see fig. 6 C). It was assumed that this gapped burst pattern has an impact on the behavioral output, thus making the CPG activation via a different pathway behaviorally relevant. White et al. (2011) showed that the distinct burst pattern of LG during a POC-elicited gastric mill rhythm indeed has significant effects on the isolated protractor muscle (gm6). It has not yet been shown, however, whether this effect is retained on the behavioral level in vivo as well.

2.2.7 Anatomical properties of the stomach and the gastric mill

The aforementioned motor neurons in the STG innervate a complex network of muscles in the foregut. These muscles insert to calcified bones (ossicles) which hold the stomach wall and also form the chewing apparatus in the gastric mill as well as the filtering valve in the pylorus (Mocquard 1883). The arrangement of the ossicles and muscles has been described for brachyuran crabs (Brösing et al. 2002; Pearson 1908; Patwardhan 1935a), as well as for representatives of the Palinuridae and Nephropidae (Kennedy & Cronin 2006; Maynard & Dando 1974; Patwardhan 1935b). Despite this anatomical knowledge, the interaction of musculature and ossicles during mastication in the gastric mill has never been thuroughly analyzed. To avert confusion over the nomenclature of the foregut structures, the terminology from the latest summarizing publication (Kennedy & Cronin 2006) was used in this work.

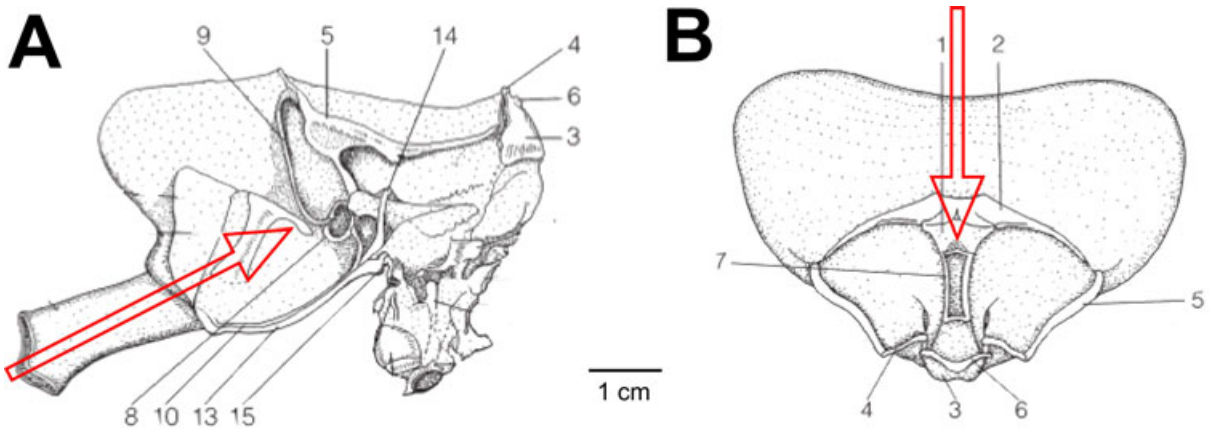

Figure 7: Generic schematic of the brachyuran stomach. **A** shows a lateral view of the stomach without musculature. Numbers refer to the nomenclature of ossicles (see table 1). **B** shows dorsal view of the stomach without musculature. Red arrows in **A** and **B** indicate the position of the endoscope and its view direction. Adapted from Kennedy & Cronin (2006).

Number	Name
1	mesocardiac ossicle
2	pterocardiac ossicle
3	pyloric ossicle
4	exopyloric ossicle
5	zygocardiac ossicle
6	propyloric ossicle
7	urocardiac ossicle
8	pectineal ossicle
9	prepectineal ossicle
10	postpectineal ossicle
13	inferior lateral cardiac ossicle
14	subdentate ossicle
15	lateral cardiopyloric ossicle

Table 1: List of ossicles in the foregut of brachyuran crustacea. Numbers correspond to those given in figures in this work. Nomenclature given here according to Kennedy & Cronin 2006.

In the following the structure and the innervating muscles of the gastric mill are described in more detail. For simplicity's sake, it is assumed that the anatomical situation for each lateral tooth is the same. Therefore paired, symmetric structures are referred to in singular. The anatomy of the ossicles and muscles is shown in figure 7. The nomenclature is given in table 1.

Since the experiments presented in this work will largely rely on data acquired via an endoscope inserted into the cardiac sac (see chapter 3.4.5 on page 36 and fig. 14), it is worthwhile to focus on the ossicles which are visible through the endoscope. A screenshot image from the digital camera connected to the endoscope is shown in figure 8. The prominent features are the two lateral (LT) and the single medial tooth (MT). The coloration of the cusps of the teeth is possibly due to plaque formation. The accessory teeth (AT) are claw-like structures, which are thought to hold the food, thus facilitating chewing and chopping of the food by the teeth (Heinzel et al. 1993).

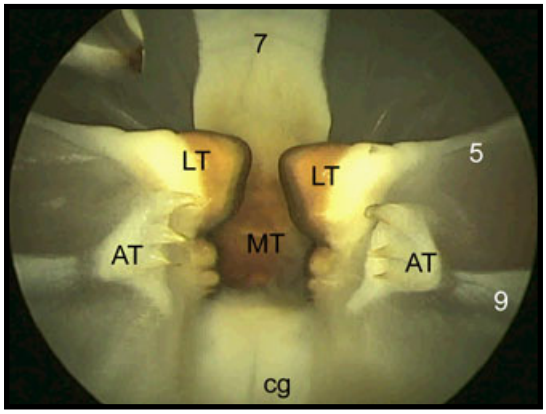

Figure 8: Gastric mill chamber viewed through the endoscope. The lateral teeth (LT), medial tooth (MT) and accessory teeth (AT) are visible. The cardiac gutter (cg) is below the gastric mill teeth. The ossicles visible are numbered according to the nomenclature in table 1 on page 17.

The cardiac gutter (cg) is located below the gastric mill teeth and is part of the closing mechanism of the pyloric valve. Several ossicles are visible in figure 8 as well. The most prominent one is the urocardiac ossicle (*7*), which ends ventrally in the calcified medial tooth. The anterior fibula of the zygocardiac ossicle (*5*), forming the lateral tooth, is also visible. The preperinecteal ossicle (*9*) is fused with the accessory teeth and with the dorsal fibula of the zygocardiac ossicle (out of view in fig. 8).

2.2.7.1 The medial tooth protractor system

To provide a synopsis of the complex arrangement of muscles the schematic of the gastric mill ossicles and most stomatogastric muscles shown in figure 9 provides a visual overview. The protractors of the medial tooth consist of the gm1 muscles. These are paired muscles, which are sub divided into the gm1a (lateral) and the gm1b (medial) fiber bundle. The gm1a bundles are rostrally attached to the carapace, and insert caudally into the pterocardiac ossicle. The gm1b bundles insert rostrally into the carapace and are caudally into the mesocardiac ossicle, which is attached to the urocardiac ossicle.

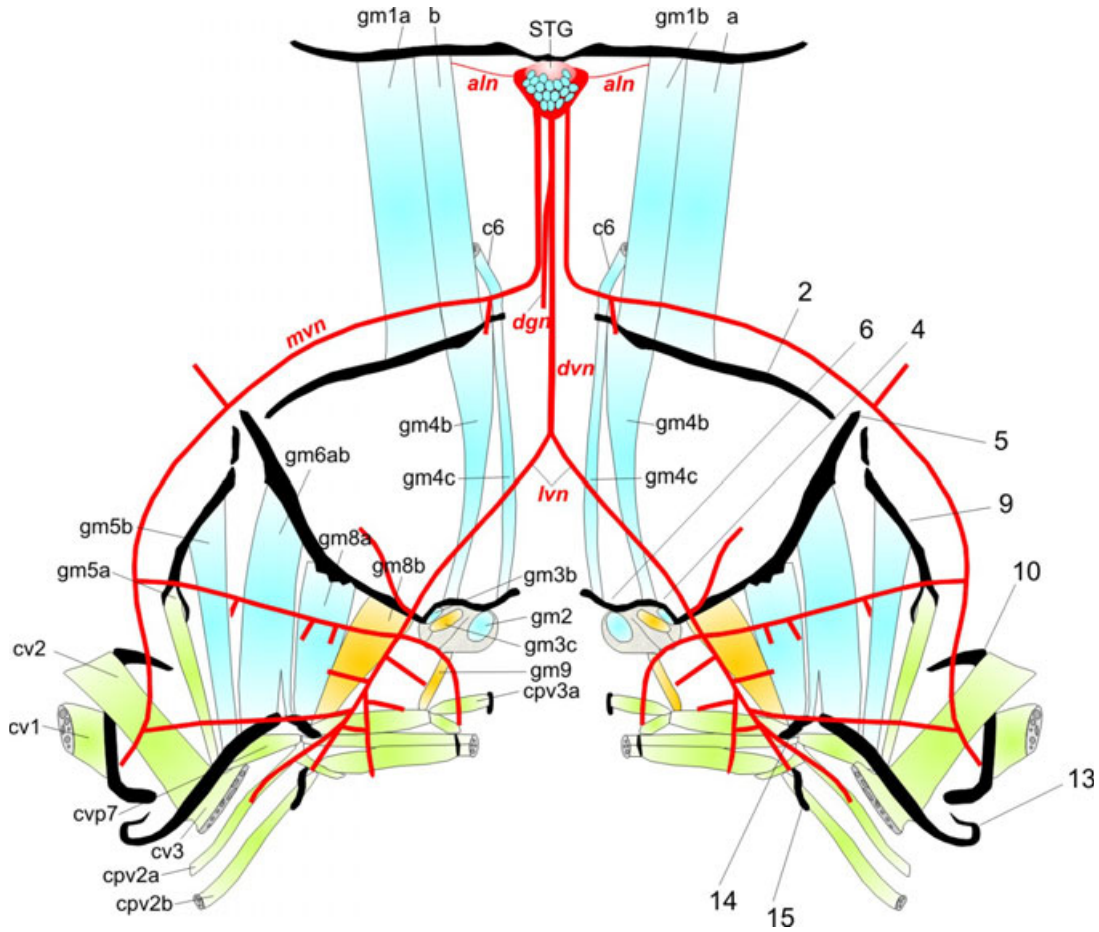

Figure 9: Schematic of the flattened stomach of brachyuran crustaceans. Muscles belonging to the gastric mill (cyan), muscles belonging to the pylorus (green) and muscles attributed to both (orange), are shown. Nerves are shown in red. Ossicles are shown in black. Numbers indicate ossicles according to table 1. Adapted from Weimann et al. 1991.

The gm2/3 muscles are the second extrinsic muscles, which are important for the protraction of the medial tooth. These muscles insert dorsally at the branchial lobe of the carapace, and ventrally at the propyloric ossicle. The latter is fused with the pyloric ossicle which itself protrudes towards the cardium and fuses with the urocardiac ossicle (medial tooth), forming a hinge-like structure.

Interaction of these muscles leads to protraction of the medial tooth. Contraction of the gm1 muscle leads to rostrodorsal movement of the medial tooth. The pyloric ossicle is pulled in rostral direction during contraction of the gm2/3 muscles. The hinge-like connection between the pyloric and the urocardiac ossicle elicits a dorso-rostral movement of the tooth during protraction.

2.2.7.2 The lateral tooth protractor system

The protractors of the lateral tooth are the gm5ab, gm6 and gm8ab muscles (Weimann et al. 1991; Heinzel 1988). The gm8ab and gm6 both insert dorsally into the zygocardiac ossicle. Ventrally, the gm8ab fully inserts into the subdentate ossicle, while gm6 only partially inserts into this ossicle. The rostral part of gm6 inserts into the inferior lateral cardiac ossicle. gm5ab inserts dorsally into the prepectineal ossicle, and ventrally into the inferior lateral cardiac ossicle.

For the protraction of the lateral tooth, a hinge-like structure formed by the fusion of the subdentate ossicle and the zygocardiac ossicle has a key function. During protraction, the gm8 and gm6 muscles pull these two ossicles towards each other (Heinzel 1988). This leads to a closing movement of the calcified tooth structures of the zygocardiac ossicle inside the stomach.

The gm5 muscle, which is also innervated by LG, moves the accessory tooth. The accessory tooth is a claw-like protrusion from the prepectineal ossicle (Pearson 1908; Cochran 1935). Three other gastric ossicles are fused to the pectineal ossicle: the prepectineal ossicle proceeds dorsally, the postpectineal ossicle proceeds in ventral direction, and the subdentate ossicle proceeds in caudal direction, from the pectineal ossicle. The gm5ab muscles insert dorsally at the prepectineal ossicle and ventrally at the inferior lateral cardiac ossicle. The muscles pull these two ossicles towards each other, thereby moving the accessory teeth inside the cardiac sac towards the midline.

2.2.7.3 The medial and lateral tooth retractor system

The retraction of the medial tooth is elicited by contraction of the gm4 muscle. This muscle is subdivided into the paired gm4b and the gm4c bundles (see fig. 9). Each bundle inserts rostrally into the mesocardiac ossicle. Caudally, however, the gm4c bundle inserts into the pyloric ossicle, while the gm4b bundles insert into the exopyloric ossicles. Contraction of the gm4 muscle moves the mesocardiac ossicle caudally, thus stretching the gm1 muscle. The contraction of the gm4 muscle simultaneously moves the pyloric and propyloric ossicles rostrally, thus stretching the gm2 and gm3 muscles. The pyloric and propyloric ossicles are fused to the urocardiac ossicle. The caudal movement of the mesocardiac ossicle and the rostral movement of the urocardiac ossicle, elicit a ventro-caudal movement of the medial tooth towards the pyloric valve (retraction).

Retraction of the lateral teeth has been described previously in the lobster (Heinzel 1988). In these nephropid crustaceans the gm2 and gm3 muscles are innervated by the LPG motor neuron. Contraction of these muscles moves the exopyloric ossicle caudally. The exopyloric ossicle is fused to the zygocardiac ossicle. Thus, contraction of the gm2 and gm3 muscles translates onto the zygocardiac ossicle, which elicits retraction of the lateral tooth. In the crab, the LPG neuron is not active during gastric mill rhythms. It is therefore not known, how retraction of the lateral teeth in cancrid crustaceans is realized.

2.3 Purpose and goals of this work

As shown in the previous chapters, the detailed knowledge about the flexibility rhythmic motor pattern output in the stomatogastric nervous system has been described briefly. The knowledge on the behavioral output of this system, however, is rather limited. It is therefore not clear, whether the plasticity in activity of stomatogastric neurons is of behavioral relevance. While the advances in our understanding of the dynamics of the nervous system shall by no means be trivialized it seems evident that some aspects of neuronal dynamics cannot be explained without studying their functional context. Neuromodulatory influences in vivo, as well as the properties of the effectors (the muscles) and the anatomical arrangement of muscles and ossicles may contribute substantially to the dynamics and the performance of complex behaviors. In the stomatogastric system, the functional consequences of these factors for the behavior are unknown. In other model systems, the behavioral output is very well investigated, but the knowledge about architecture of the nervous system is not as detailed as in the STNS (Dickinson 2006; Harris-Warrick 2011). The investigation of the be-

havioral output of the stomatogastric system, combined with analyses of previously published data on the STNS, would provide important insights into the processes of neuronal and muscular interaction during behavior. To study these interactions in the *in vivo* preparation of the crab, the following goals were posed.

1. **Developing techniques to record and stimulate neurons *in vivo.*** To establish the *in vivo* preparation, it is necessary to develop a minimally invasive experimental setup but allows stable recordings in the intact animal. This includes the construction and refinement of a holding device for the animal, as well as the manufacturing of extracellular electrodes, which can be used on the in vivo preparation.

2. **Stimulation of known pathways *in vivo* and comparison with *in vitro* data.** It is unknown whether the neuromodulatory system has the same effects on the activity of the nervous system *in vivo* as it has *in vitro.* To test this, a single neuromodulatory pathway that elicits a distinct gastric mill rhythm *in vitro* was selected. It has been shown previously that lesion of the MCN1 axon terminates all gastric mill activity in the isolated nervous system, indicating a unique function of this neuromodulatory pathway for the gastric mill system. It is not yet known, if this is also the case *in vivo*, or if the influences of sensory inputs or other modulatory pathways *in vivo* are capable of compensating for the missing input from MCN1. This will be tested in the *in vivo* preparation via lesion experiments on the inferior esophageal nerve (*ion*) and simultaneous recording of the motor nerves. The data gathered in these experiments will also be compared to *in vitro* experiments, previously conducted in the laboratory of W. Stein (Ulm University, Germany).

3. **Stimulation of proprioceptors in the *in vivo* preparation.** It is unclear whether sensory pathways that are able to elicits a particular version of the GMR *in vitro* can also elicits that version of the rhythm *in vivo*, In fact, it is unclear whether they can elcit a rhythm at all. The advantage of the *in vivo* preparation (compared to the isolated prep.) is that all internal sensors remain intact. This allows for experiments in which specific receptors are stimulated and their effects on the gastric mill rhythm can be monitored. The receptors which will be stimulated in these *in vivo* experiments are the VCN neurons. The cardiac gutter can be stimulated via an esophageally applied probe, the VCNs can be stimulated without additional surgery. The characteristics of the gastric

mill rhythm elicited by the VCNs has been described in detail in the isolated nervous system. If the VCNs elicit similar pattern *in vivo*, despite other neuromodulatory and sensory inputs, is unclear. It will therefore be tested, whether the activation of these neurons is possible and whether it has the same effects (initiation of a gastric mill rhythm) known from experiments conducted in *in vitro* and *in situ* preparations (Beenhakker & Nusbaum 2004). The differences in neuronal firing between *in vivo* and *in vitro* preparations will be tested as well. Parameters such as burst duration, interburst frequency and cycle duration will be recorded *in vivo* and compared to *in vitro* data.

4. **Stimulation of neuromodulatory pathways in the *in vivo* preparation***.* The gastric mill CPG can be activated in *in vitro* preparations by a neuromodulatory pathway, which was described by Blitz et al. (2008). Neurons projecting through the post-esophageal commissure (POC) activate the gastric mill and the pyloric CPG in a characteristic manner pattern in the *in vitro* preparation. Whether it is possible to activate this pathway *in vivo* will be tested. Experiments, in which the POC neurons are stimulated via extracellular electrodes, will be conducted. If an activation of the gastric mill via the POCs is possible *in vivo,* the output of the STG motor neurons will be recorded and compared to *in vitro* data. This analysis will show if these two types of gastric mill rhythms are qualitatively equal in the *in vivo* and in the *in vitro* preparations.

5. **Analysis of muscle response to motor nerve stimulation.** Whether neuronal activity patterns can be faithfully transfered to the behavioral levele depends on the dynamics of the effector muscles. Hence, before the movement of the teeth can be fully understood the contractile responses of the muscles need to be investigated more closely. The response of the gm6 muscle to standardized stimulation has been investigated before by White (2011). In my studies, I will use realistic stimulus patterns, extracted from motor neuronal activity patterns *in vitro*, because previous studies demonstrate that muscles can exhibit highly dynamic properties (Thuma & Hooper 2010; Hooper 2004) that might not be caught by standardized, non-varying stimuli. A stimulation with realistic stimulus patterns may thus reveal previously unknown dynamics of the muscular system. The muscle being investigated will be the gm6 muscle, analogous to the studies by White (2011).

6. **Analysis of tooth movements during stimulation with three different types of gastric mill rhythms.** It can be assumed that *in vivo* responses to stimulation of sensory and other pathways will be highly dynamic. Despite efforts of keeping experimental conditions comparable across all the experiments, many uncontrollable and unknown factors can cause variability in the output of the stomatogastric system. Also, very little is known about the interactions of the musculature with the ossicle structure during rhythmic movement of the gastric mill. Studies showing high complexity on the level of the ossicles (Hobbs & Hooper 2009) suggest that emergent effects may add to the flexibility of the system or allow for previously unknown ways of movement of the teeth in the gastric mill. To study the contribution of muscles and ossicles on the resulting movement output, the motor nerves in the in vivo preparation will be transected, thus removing all motor activity that drives the gastric mill muscles. This also terminates all effects from modulatory, sensory and CPG neurons and effectively removes all intrinsic flexibility of the nervous system. The motor nerves will then be stimulated simultaneously via three extracellular electrodes placed on the dorsal side of the animal. The stimuli will consist of stimulus patterns based on averaged data from in vitro recordings of various types of gastric mill rhythms conducted previously in the lab of W. Stein (Ulm University, Germany) and M. Nusbaum (University of Pennsylvania, USA). Since defined motor patterns are used, the resulting tooth movements can be recorded and analyzed to extract motor primitives from the data. During stimulation, lesion experiments will be conducted to test which muscles are key elements for certain motor primitives.

3. Materials and Methods

Experiments were conducted on the stomatogastric system of either *Cancer pagurus* or *borealis* specimen. Male *Cancer pagurus* used for experiments conducted at Ulm University (Germany) were bought from Feinfisch (Neu-Ulm, Germany). Male Cancer borealis used for experiments conducted at University of Pennsylvania (Philadelphia, USA) were bought from The Marine Biological Laboratory (Woods Hole, MA, USA). All animals were kept in salt-water tanks at constant temperature between ***8 – 11ºC*** and salinity level of ***1.025 g/cm³*** (artificial reef salt, AquaMed). Animals were kept on a ***12/12*** (day/night) cycle. Animals were kept in tanks either alone or in groups of max. ***12*** individuals. All experiments were conducted in accordance with the policy on humane care and use of laboratory animals (OLAW & NIH) and German regulations for keeping of animals and animal experiments (TierSchG).

3.1 Solutions used

All preparations were perfused with saline solution at a temperature of ***8 – 11ºC***. Temperature was kept constant using a peltier element (constructed after plans provided by Nadim, F., Rutgers University, New Jersey, USA). The saline solution was composed of $NaCl(440\ \frac{mMol}{l})$, $KCl(11\ \frac{mMol}{l})$, $CaCl^{2+} \bullet 2H_2O(13\ \frac{mMol}{l})$, $MgCl^{2+} \bullet 6H_2O(26\ \frac{mMol}{l})$.

The pH was adjusted between ***7.4 – 7.6*** using $Trisma(12\ \frac{mMol}{l})$ and $Maleic\ acid(5\ \frac{mMol}{l})$.

3.2 Preparations

3.2.1 *In vivo* preparation

For *in vivo* preparations animals were put on ice for ***20 – 40*** minutes to anesthetize the animal. The animal was then fixed in a custom-made holder with rubber bands to restrain legs and claws. The holder was put in a custom-made plexiglass box constructed after the prototypes of Prof. H.-G. Heinzel (Zoologisches Institut, Universität Bonn, Germany) which was then filled with ice to keep the animal cool during the experiments.

Prior to each *in vivo* experiment the contents of the stomach were controlled via the endoscope. Empty cardiac sac and no visible enzymatic fluids in the stomach suggested no feeding and were thus evaluated unlikely to exhibit gastric mill activity. If the stomach was full and/or the cardiac sac was filled with digestive enzymes this animal was chosen for an experiment. Prior to the experiment, however, the stomach had to be emptied via a suction tube to free the view onto the gastric mill structure. A *2-3 mm* silicone tube was connected to a large syringe. The loose end of the tube was inserted into the esophagus and the cardiac sac. Vacuum was applied via the syringe and the contents of the stomach were sucked out.

Before starting the surgery, the mouthparts of the animal were stilted to reveal the mandibles. These were clipped using bone rongeurs to allow access for the endoscope to the esophagus. Additionally *2 x 0.5 cm* stripes of cellulose were soaked in cold saline, rolled up and inserted into the pterygostoma to keep the gills from drying out.

If necessary, the claw tip ends were clipped with the rongeurs to guarantee access to the ventral side of the animal for the surgery (see below).

3.2.1.1 Positioning of electrodes on dorsal side

The dorsal carapace was opened to insert extracellular electrodes for recording and stimulation to the motor nerves. The carapace was opened using a precision drill (Proxxon GmbH, Föhren, Germany) and a rectangular window was cut into the carapace (see fig. 10). In rostrocaudal direction the window ranged from the frontal to the metagastric part of the carapace (for anatomy see: Kennedy & Cronin 2006); mediolaterally it ranged from the orbital to the branchial lobe. After removing the carapace the hypodermis was removed to reveal the dorsal side of the stomach. Care was taken to keep the ophthalmic artery, which proceeds rostrocaudally along the midline of the carapace, intact in order to maintain the integrity of the blood stream and therefore the health of the animal. After removing connective tissue from the motor nerves with fine scissors (Fine Science Tools GmbH, Heidelberg, Germany) a syringe connected to the saline flask was attached to a self-built clamp on a swivel joint. This clamp was attached to the plate of the crab holder using neodym magnets to perfuse the wound with cooled saline. Next, the extracellular hook electrodes were positioned. Each extracellular electrode (construction described in chapter 3.3.2 on page 34) was fixed to a swivel joint mount which was locked to a dovetail rail on the base plate of the crab-holder. A total of three electrodes could be attached to the plate of the holder. Each electrode was roughly positioned close to the nerve; fine positioning and loading of the nerve onto the hook electrodes was performed through a microscope (Stemi 2000, Zeiss, Oberkochen, Germany). The hook ends of the electrode wire

were slid under the nerve. Then the nerve segment was carefully lifted into the crook of the wire with a hand-held hook. Once the nerve was in place, the isolation tubing was pulled over the nerve using forceps (Fine Science Tools GmbH, Heidelberg, Germany), thus electrically sealing the nerve segment from the surroundings.

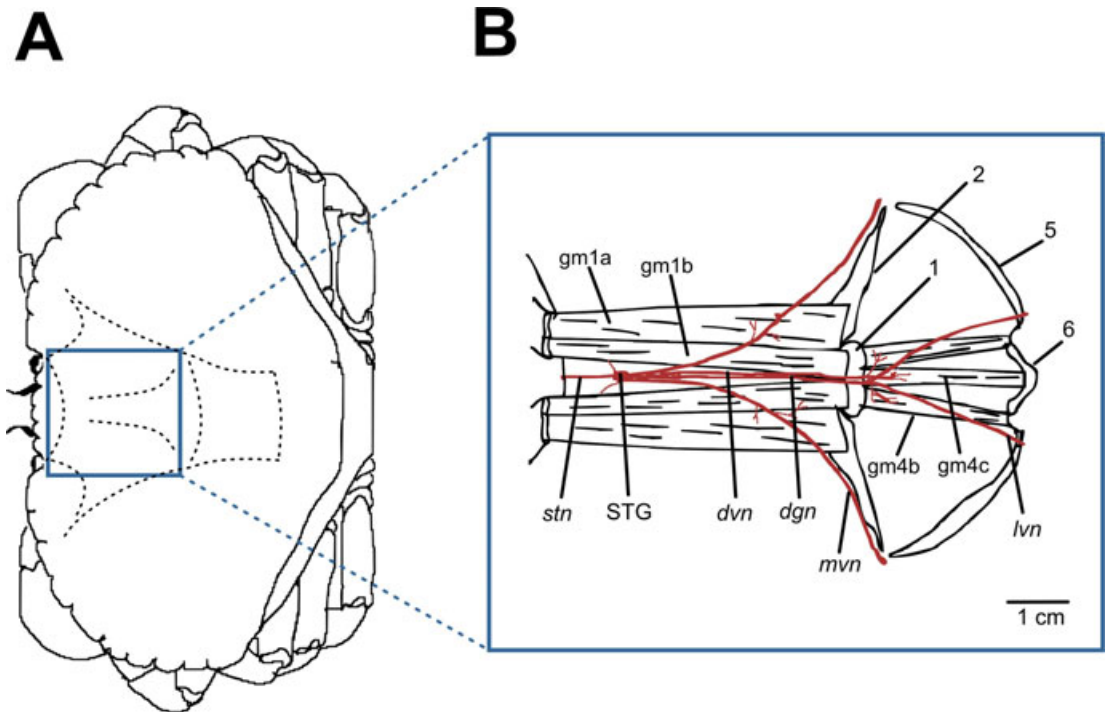

Figure 10: Dorsal view of in vivo preparation. **A** shows the dorsal carapace with edges of apodemes (dashed lines). Blue square marks the region of surgery. **B** shows the pro- and retractor muscles of the medial tooth and the dorsally visible ossicles. The nervous system is marked in red; *stn*: stomatogastric nerve, *dvn*: dorsoventral nerve, *dgn:* dorsal gastric nerve, *mvn:* medial ventricular nerve, *lvn*: lateral ventricular nerve. Numbering of ossicles according to table 1.

3.2.1.2 Positioning of electrodes on ventral side

To expose the circum-esophageal connective (COC) and the post-esophageal Commissure (POC) the carapace was opened in rostrocaudal direction from the 1st to the 4th thoracic sternite and in mediolateral direction to the coxae of the 1st pereopods (see red section marked "B" in figure 11). After removing hypodermis and midgut gland both connectives are visible behind the ventral thoracic artery and its branchings. During surgery, a syringe provided fresh chilled saline to prevent the wound from drying out. The electrode was positioned such that the artery remained unharmed when the COC was recorded or stimulated (see fig. 12). Until the connectives could be reached and electrodes applied, a large volume of midgut gland and

connective tissue had to be removed. To keep the nerves stable and perfused with saline, the syringe was kept in place while the animal was turned upright again and the experiment was conducted. The previously described surgery was conducted on a workbench under a microscope.

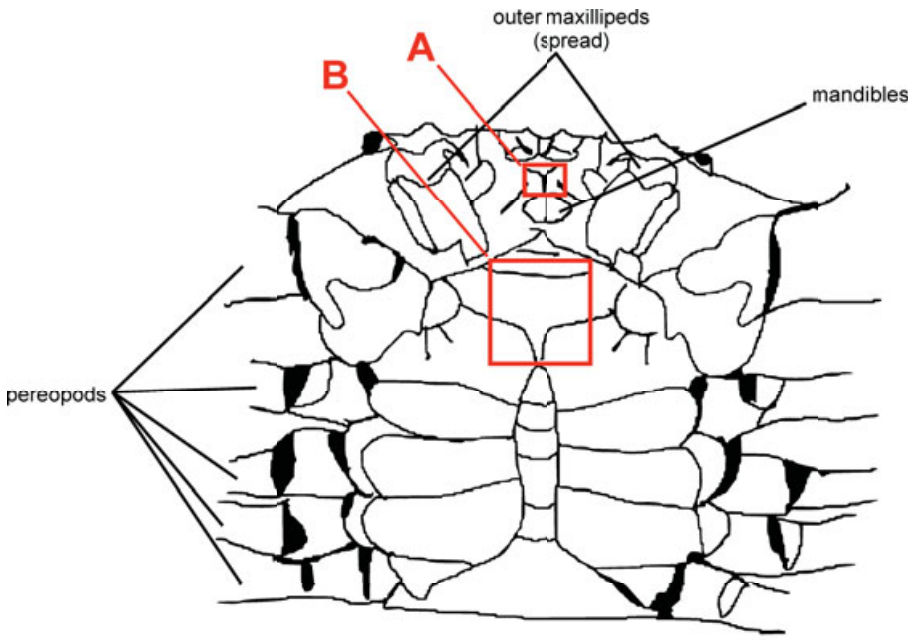

Figure 11: Ventral view of *in vivo* preparation. Ventral side of crab before surgery is shown. Areas where the carapace was opened are marked by red boxes (**A** and **B**); **A** was used for access to the *ion*; area **B** was used for access to the COC and POC.

In experiments where ventral and dorsal side were opened to place recording or stimulation electrodes, the sequence of surgeries was as follows:

1. The ventral electrode was placed.
2. The ventral wound was sealed with Vaseline; the syringe was kept in place to maintain saline perfusion to the uncovered nerves.
3. The holder with the animal was turned to make the dorsal side of the animal accessible.
4. The dorsal electrode(s) and the saline perfusion were put in place.
5. The animal holder was carried to the rig and placed inside to conduct the experiment.

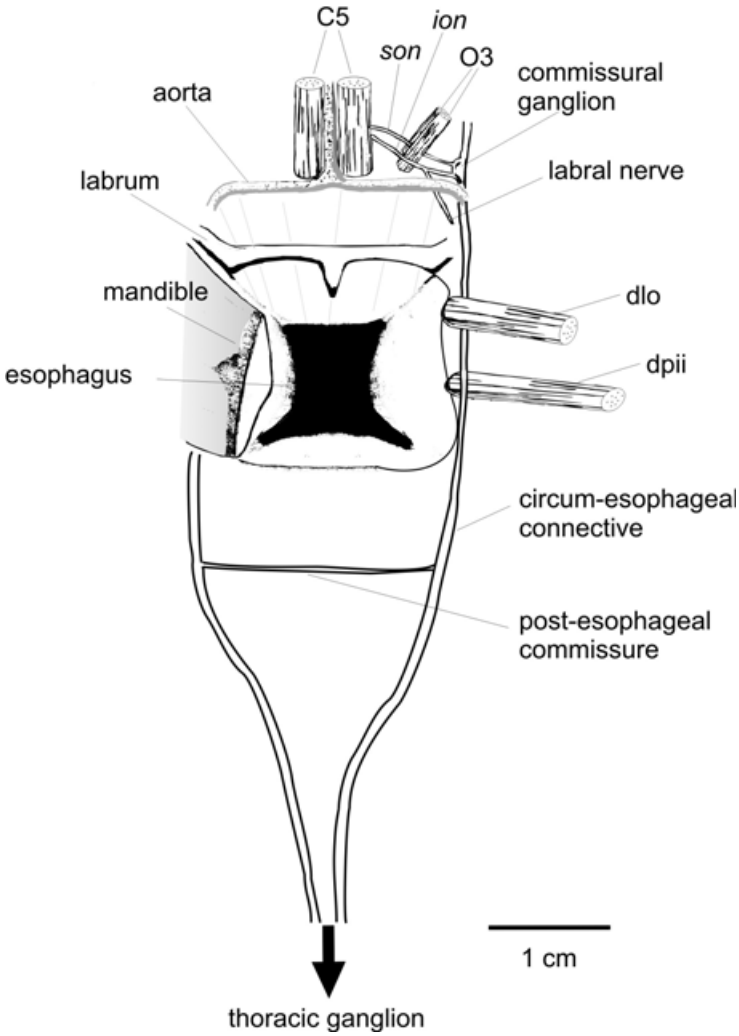

Figure 12: The location of the esophageal connective *in vivo*. Semi-schematic drawing with carapace and connective tissue removed on one side (right). The Commissural Ganglion containing the projection neurons is shown. Below the esophagus, the artery and connective tissue are not shown. C5 = cardiac muscle 5; O3 = esophageal muscle 3; *ion* = inferior esophageal nerve; *son* = superior esophageal nerve. dlo = dilator lateralis esophagii; dpii = dilator internus pylorici inferior; POC = post esophageal commissure.

In experiments in which the *ion* was stimulated, the section above the labrum was opened (as shown in the red section marked "A" in figure 11). Ligaments, connective tissue and the c5 muscles were removed as well. On each side, the *ion* passes by the O3 muscle (see fig. 12). The *ion* from one side was mounted on an extracellular hook electrode. Depending on the experimental design, the nerve segment leading to the commissural ganglion was cut to prevent the influence of other projection neurons and to investigate the response of the nervous system to the *ion* lesion. Stimuli (***1 ms*** pulses, ***20 Hz***) were applied via a Master 8 stimulator (A.M.P.I., Jerusalem, Israel).

Voltage was increased until a GMR was initiated, detectable via an initiation of LG bursting. A syringe connected to the cooled saline reservoir was applied to prevent the wound from drying out. Additional extracellular recording electrodes were applied after opening the dorsal carapace, either to the *dvn* or the *lvn*.

3.2.2 *In situ* muscle preparation

The animals were put on ice for ***20 - 40 minutes*** to be anesthetized before the stomach was removed. First, all peropods were removed with bone rongeur forceps. Then the 1st - 3rd maxillipeds, all maxillae and the mandibles were removed.

Next, the hepatic, branchial and mesobranchial sections of the dorsal carapace were opened from both sides (Bierman & Tobin 2009; Stein 2006). The hypodermis including extracellular musculature below the proto- meso- and metagastric carapace was carefully detached with a small spatula. A coronal cut was made through the frontal and metagastric carapace and the resulting carapace segment was removed. Next, the frontal and orbital parts of the carapace towards the labrum were removed. The mouth and labrum were held with a venous clamp while the muscles, ossicles and cartilage were cut. The stomach was then removed from the animal; the pylorus was removed from the stomach posterior of the ampullae. The stomach was intersected dorsosagittally from the esophagus to the lateral cardio-pyloric ossicles. Two intersections from the midline were made, beginning at the anterior tips of each inferior lateral cardiac ossicle, towards the zygocardiac ossicle, so that the gastric mill can be unfolded. The tips of the teeth were clipped before the stomach was spread dorsal side up into a glass bowl filled with blackened Sylgard. After filling the bowl with cooled saline, the stomach was pinned to the Sylgard. Since the dorsal side of the stomach is placed upwards, the nervous system can be revealed after carefully removing remaining hypodermis, cartilage and hepatopancreas.

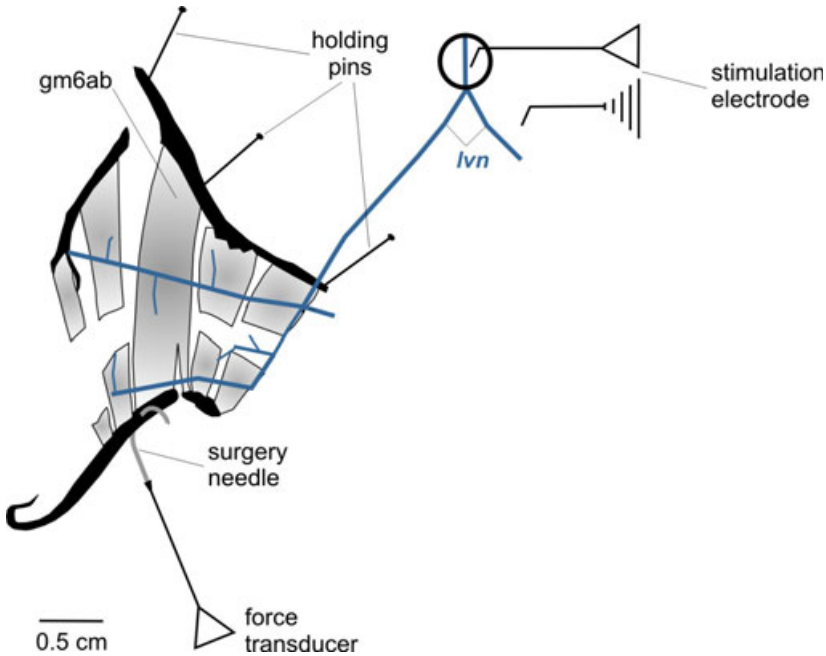

Figure 13: Schematic of setup for in situ experiments on gm6 muscle. Ossicles are shown in black, muscles in grey. All muscles but gm6 were lesioned prior to the experiment. The motor nerve *lvn* (blue) was stimulated via an extracellular wire electrode. The inferior lateral cardiac ossicle was pierced with a surgery needle to attach to the force transducer.

In order to stimulate the gm6 muscle the dorsal ventricular nerve (*dvn*) had to be stimulated using an extracellular wire electrode (see fig. 13). For this, stomach wall and nervous system were transsected sagittally between the pterocardiac and the zygocardiac ossicle. The *dvn* was cleared from cartilage to allow for best conduction of voltage during stimulation. Next, all ossicles and muscles had to be cut or removed which would perturb the gm6 force measurements. The stomach was moved from the bowl into a petri dish filled clear Sylgard and cooled saline. The stomach was pinned out using stainless steel minute pins. First, the unpaired ossicles along the midline were transsected to separate both sides of the stomach from each other; i.e. the mesocardiac-, urocardiac-, propyloric- and pyloric ossicles were cut. Next, the prepectineal ossicle was cut and the connection of the subdentate ossicle and the zygocardiac ossicle was severed to free the gm6 muscle. The ossicles which connect the gastric mill to the ampullae and the pyloric region (lateral cardio-pyloric ossicles, anterior supra-ampullary ossicles, anterior pleuropyloric ossicles), were also cut. Next, all the muscles connecting to the same ossicles as the gm6 muscle were severed, leaving only gm6 intact. A *0.2 mm* diameter hole was pierced through the subdentate ossicle to hold the force transducer (see fig. 13).

The loose end of the nerve was fixed to the sylgard with *0.5 mm* thick pins from stainless steel wire. A Vaseline well was constructed around a *0.5 cm* segment of the nerve which rose above the saline level. Next, a stainless steel wire (*0.075 mm*, Good Fellow, Cambridge, England) was fixed into the Sylgard inside the Vaseline well serving as stimulation electrode. A second wire was placed outside the well as reference electrode.

An atraumatic suture needle and prolene thread (M-3, Ethicon, Somerville, NJ, USA) was used to affix the subdentate ossicle to an isometric force transducer (*0 – 5g*, *10x* amplifier & digitizer, Harvard Apparatus, USA). Data from the muscle activity was digitized using a power 1401 Mk.2 unit (CED, Cambridge, UK).

3.3 Electrophysiology

Unless otherwise stated in this section, the equipment used during experiments conducted in Ulm (Ulm University, Germany) and Philadelphia (University of Pennsylvania, USA) was of the same product series.

Depending on the experimental design, the electrodes were applied dorsally and or ventrally. When the movement of the teeth was recorded, an endoscope was inserted past the mandibles and through the esophagus into the cardiac sac to enable a view of the gastric mill. Due to the design of the crab holder, a maximum of *3* electrodes could be applied during an experiment. Figure 14 shows the application of extracellular electrodes and endoscope in the intact animal.

To conduct experiments to stimulate and record the *ion*, the frontal side of the carapace above the esophagus was opened, ligaments and other tissues removed, and a hook electrode was applied.

During experiments in which the motor nerves were stimulated, the electrodes were applied dorsally through the window in the carapace. The motor nerves were decentralized, meaning that *mvn*, *dvn* and *dgn* were cut caudally of the STG. These decentralized nerves were loaded onto the hook electrodes and sealed. After electrodes were applied, the preparation was adjusted such that the endoscope could be applied past the mandibles, through the esophagus and into the cardiac sac.

For experiments in which the POC neurons were stimulated, the frontal carapace was opened below the esophagus. The digestive gland was removed until the aorta and the circum-esophageal commissure (COC) were visible. A segment of the left or right COC was applied to the hook electrode, and afterwards decentralized from the thoracic ganglion to inhibit feedback caused by the stimulation. In some experiments, a second electrode was applied dorsally to the *lvn* to record the effect on the motor neurons.

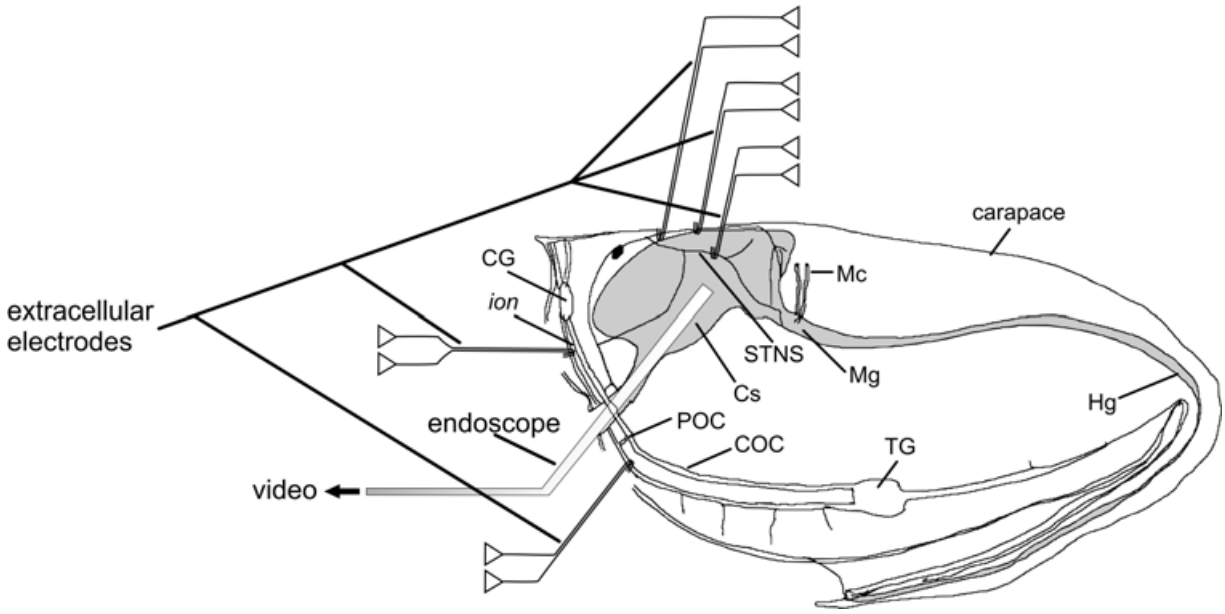

Figure 14: Sagittal schematic of *Cancer sp.* The stomach area is shown in grey. Mc: anterior midgut caeca, Mg: midgut, Cs: cardiac sac, Hg: hindgut, CG: cerebral ganglion, TG: thoracic ganglion, POC: post-esophageal commissure, COC: circum-esophageal commissure.

3.3.1 Extracellular recording and stimulation

The recording electrodes which were used during the *in vivo* experiments were connected to a differential AC amplifier (model 1700, A-M Systems, Carlsborg, USA) which amplified the voltage difference between the recording hook electrode to which the nerve is attached and the reference electrode which is placed in the body cavity of the animal. In experiments at the University of Pennsylvania, the signal was further amplified and filtered (model 410, Brownlee Precision, Palo Alto, USA). After amplification, the signal was sent to the A-D converter Power 1401 Mk. 2 (CED, Cambridge, UK). The digitized signal was then recorded and saved on a Windows 7 PC using the Spike2 software (Version 6.12 – 7.12, CED, Cambridge, UK).

Stimuli (*in vivo* and *in vitro*) were applied via a stimulator unit (University of Pennsylvania: S88, Grass Instruments, West Warwick, USA; Ulm University: SD9, Grass Instruments, West Warwick, USA and Master8, AMPI, Jerusalem, Israel) which was connected to a stimulus isolation unit (SIU5, Grass Instruments, West Warwick, USA). The extracellular stimulation electrodes were connected to the SIU. In experiments in which stimuli of constant duration and frequency were applied, the SD9 and Master8 were configured accordingly. In experiments in which recordings from *in vitro* experiments were replayed, the stimulator unit was connected to the computer via the

A-D converter, which was able to send a digital output signal to the stimulator unit. The duration of a single stimulus was set to 1ms in all experiments to guarantee comparability. The amplitude of the voltage had to be set manually depending on the quality of the seal around the electrode.

3.3.2 Construction of extracellular electrodes

The extracellular electrodes for stimulating and recording the nerves *in vivo* were to be manufactured individually. The tip of a *5 cm* piece of silver wire (*0.1 mm* or *0.075 mm*, insulation *0.01 mm* (PFTE), Good Fellow, Cambridge, England) was bent into a hook, into which the nerve was placed during experiments. A second piece of silver wire was bent in the same way. The insulation was removed from the part of the wire, which formed the hook. Both wires were placed next to each other on a flat surface *0.5 – 1 mm* apart; a syringe needle (*16* gauge) and parafilm was used to fix both wires to the syringe. Both wires were fixed to the needle such that the hooks were at a distance of *~1 cm* to the syringe tip. The parafilm was heated carefully with a gas lighter to seal perfectly. Silicone tubing (*1.5 cm*) of *1.8 mm* (I.D.) and *1.9 mm* (O.D.) was slid over parafilm and wires all the way to the plastic screw-end of the needle. A second piece of silicone tubing (*1 cm*) of *1.9 mm* (I.D.) and *2 mm* (O.D.) was slid over the first silicone tube. This second silicone tube was used to slide over and seal the wire hooks during an experiment; therefore the hooks had to be bent such that the second silicone tube could be slid over them with ease (see Figure).

Next the other ends of the silver wires were fixed to an insulated wire which was connected to the extracellular pre-amplifier. Then the needle was connected to a syringe (*10 ml*) which had been pre-filled with Vaseline. The cord was secured to the syringe with duct-tape.

This configuration was then clamped into a ball joint mount or any other suitable mounting.

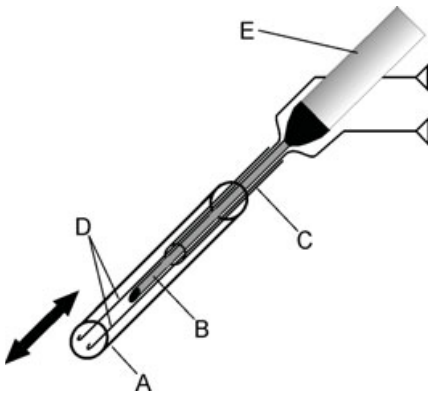

Figure 15: Schematic of the extracellular electrode used *in vivo*. **E** and **B** represent the syringe tube, filled with Vaseline, and the syringe tip. **D** are the silver wires unto which the nerve was placed. The hooks were fixed to the syringe tip by a piece of latex tubing **C**. A larger latex tube **A** is slid over **B**, **C** and **D**.

3.4 Sensory Stimulation *in vivo*

In order to activate the pathways of the gastric mill rhythms in a realistic fashion, several pathways were stimulated *in vivo*. The animals can perceive olfactory, visual and tactile stimuli via different sensors. Very little is known about the integration of these different sensory modalities. As shown by Fleischer (1981), the rhythmic activity of the gastric mill CPG shows dependency on illumination of the eyes. A suppression of chewing behavior was recorded after sudden illumination, and an initiation of such behavior during dark phases. The impact of light on the behavior was not tested directly in this work. However, care was taken that animals were on a night phase when they were taken out of the salt-water tank before an experiment.

The other modalities were used to actively initiate gastric mill rhythms *in vivo.* The procedures for this during an experiment are described in the following.

3.4.1 VCN-type gastric mill rhythm initiation

The somata of the VCNs are located in the cardio-pyloric valve between the cardio-pyloric ossicles. Their functionality in the stomatogastric nervous system was first described by Beenhakker et al. (2004). Albeit performed in *in vitro* preparations, this study showed a profound effect on the neurons of the gastric mill CPG.

To stimulate the gastric mill via this pathway *in vivo* the cardiac gutter was lightly touched with a small diameter probe (*<0.2 mm*) which was inserted into the cardiac sac via the esophagus. The cardiac gutter was stroked repetitively until a gastric mill rhythm (GMR) was initiated. If no GMR could be initiated, stimulation was terminated after *~ 30 s*.

3.4.2 POC-type gastric mill rhythm initiation

For stimulation of the POC neurons *in vivo* surgery as described in chapter 3.2.1.2 (see page 27) was performed. The amplitude of the stimulus voltage was raised until a visible reaction in behavior (tooth movement) was observed. Change in activity in these projection neurons has direct effects on the STG (White & Nusbaum 2011), resulting in retraction of the teeth and interruption of currently ongoing gastric mill rhythms.

3.5 Video Endoscopy

To monitor the movement output of the musculature and the motor neurons controlling the gastric mill an endoscope of *5.3 mm* diameter and *300 mm* length (*30º* view angle) was used (Panoview, Richard Wolf GmbH, Knittlingen, Germany). The endoscope contained a LED unit to illuminate the inside of the stomach. The endoscope was connected to a video camera (TECAM-3, Richard Wolf GmbH, Knittlingen, Germany). The camera recorded the video signal in PAL (*25 Hz* sampling rate, *640 × 480* pixels) and synchronized with the electrophysiological data via the plugin software "spike2video" provided with the Spike2 (Version 7.x) software package.

The video data had to be translated into two-dimensional data, which could then be analyzed. For this task, a software written for Matlab (Mathworks, Natick, USA) for auto tracking points in video files was used (Hedrick 2008). This software is able to track any change in contrast within a predefined window of *9 - 100* pixels. The change in contrast was determined via the extended Kalman filter (Pillow et al. 2010; Fahrmeir 1992). As tracking points the tips of the lateral teeth and the tip of the medial tooth were used (if possible, small markings or other segments of stark contrast changes were used to track tooth movement).

After a tracking point was added to each frame in the video, all *X*-coordinates and *Y*-coordinates and the number of the corresponding frame were saved to file. The data was imported into Spike2 as a waveform channel. Since the position of the endoscope, and therefore the angle of view, is different in each experiment, no absolute

method of measurement could be applied to quantify the movement of the teeth. Therefore, the tooth movement was quantified with a relative measuring unit dubbed "Medial Tooth unit" (***MT***). The widest width of the medial tooth was measured in each video and the number of pixels in ***X***-axis were measured and defines as ***1 MT***. The movement amplitudes (i.e. number of pixels in ***X***-axis) of the lateral teeth were then normalized to this value.

3.6 Data Analysis

The computer recorded the signal from the A-D converter at a sampling rate of ***10 kHz***. The action potentials recorded extracellularly, if quality sufficed, were analyzed and sorted using principal component analysis (Jurjut et al. 2009; Gabbay 2000). This waveform component analysis method is integrated into the Spike2 software bundle and was adjusted for signal to noise ratio and overall signal amplitude for each data file. When the pyloric rhythm was analyzed the onset of a burst in the Posterior Dilator Neuron (PD) was defined as the start of a pyloric cycle. Spikes, cycle periods and other parameters were acquired from the raw data via custom scripts using the Spike2 native scripting language. The output of these scripts was then exported to MS-Excel (MS-Office 2003, 2004, 2010, Microsoft Corp., Redmont, USA) and OriginPro (Version 7.0 - 8.6G, OriginLab, Northampton, USA).

Statistical Analyses were performed OriginPro, MS-Excel and SigmaStat (Version 3.1, Systat Software Inc., Chicago, USA). When results of statistical tests are shown, the significance levels (***p***-values) are shown above the data or described in the figure text. Figures were processed in CorelDraw (Version 10 -12, Corel Corp., Ottawa, Canada). Images and photographs were processed for this publication using WolframAlpha (Wolfram Research, Champaign, USA) and Adobe Photoshop Lightroom (Version 4, Adobe Corp., San Jose, USA). This publication was written in Mellel (Version 3, RedleX, Tel Aviv, Israel) and Scrivener (Version 2.1 - 2.3, Literature&Latte, Cornwall, UK). The bibliography was generated using MagicManuscripts within Papers (Version 0.9 - 2.2, Mekentosj, Amsterdam, Netherlands).

3.7 3-D Modeling and drawings of dried stomach preparations

A digital model of the stomach musculature and ossicles was constructed using Blender (Version 2.41 - 2.63a, Blender Foundation, Amsterdam, NL) based on photographs of a dried stomach of *Cancer borealis*.

The procedure for curing a crab stomach is as follows. The previously described (see chapter 3.2.2 on page 30) dissection applies until the stomach is completely freed from the rest of the animal. Instead of transferring it into a saline-filled dish for further preparation, the stomach was immersed in a *10% K-OH* solution. The solution was brought to a boil for *30 - 60* minutes so all ligaments, muscles, and other tissue are removed. Afterwards the stomach was put into *90%* ethanol for one hour at room temperature. This dried the stomach wall and the cardiac sac, making it more rigid.

This preparation was photographed using an Olympus E600 digital camera with a Soligor *f2.5* macro lens on Triopo tripod and an external flash unit (Metz 50 AF-1). The images were imported into Blender as planes to build the model from.

Drawings were created with a digital tablet (Intuos 3, Wacom, Saitama, Japan) in the graphics editor Gimp (Version 2.8, GNU license) and ported to CorelDraw (Version 12, Corel, Ottawa, Canada) for further processing.

4. Results

The previous decades of studies on the stomatogastric nervous system of crustaceans have shown that the two central pattern generators located in the stomatogastric ganglion elicit distinct activity patterns. Most studies were performed *in vitro*, which provide stable conditions and allows for a variety of experimental setups to scrutinize the neurons' activities. In the *in vitro* condition, however, the nervous system is devoid of input from sensory neurons and from cerebral control. Neuromodulators and neurohormones usually present in the hemolymph (DeKeyser et al. 2007) are also missing in the intact *(in vivo)* preparation, in contrast, all these parameters are preserved and functional. The question remains whether these factors (sensory inputs and neuromodulation) affect the activity of the CPGs in the stomatogastric nervous system to extents that cannot be reproduced in the isolated (*in vitro*) nervous system and whether the flexibility observed *in vitro* is also present *in vivo*. Therefore, I conducted experiments in the fully intact animal to show that the selective activation of the central pattern generators in the STG is possible *in vivo*. These experiments will also provide results that can be compared to previously acquired data *in vitro*, and allow for a statistical analysis of differences in motor neuron activities *in vitro* and *in vivo*. In the intact animal all muscles are intact as well. Hence, the correlations between motor neuron activity and muscle contraction as well as the actual behavior - the chewing movements of the teeth - can be analyzed. Consequently, the spike pattern of the motor neurons and the movement output itself can be used to infer the underlying mechanisms of the chewing patterns in the gastric mill.

The results are arranged as follows: firstly, I present the experiments focusing on the nervous system and its centers of control. Secondly, I provide data investigating the neuromuscular interface. Thirdly, I present movement data showing the interplay between the musculature and the bone structure.

4.1 Selective activation of a commissural projection neuron is possible *in vivo*

The stomatogastric ganglion contains neurons of two distinct central pattern generator networks. The output of the pyloric CPG is highly stable and autonomous. The gastric mill CPG, however, is episodic and only activated when certain projection neurons in the paired commissural ganglia are active. One of these projection neurons is the modulatory commissural neuron 1 (MCN1). Its modulatory effects on the gastric mill CPG have been shown previously (Coleman et al. 1995; Stein et al. 2007) in studies *in vitro*. In some studies it could also be shown that several projection neu-

rons can be activated simultaneously and modulate activity of the motor neurons in the STG (Beenhakker et al. 2007) when sensory pathways are stimulated (Stein, 2009). In particular, MCN1 is contributes to most sensory responses, but albeit this fact, activation of MCN1 alone is sufficient to elicit gastric mill rhythms *in vitro* (Coleman & Nusbaum 1994; Smarandache & Stein 2007; Stein et al. 2007). It is still unclear if this holds also true *in vivo*. Additional factors such as fluctuations of the concentration of neuromodulators in the hemolymph or simultaneous sensory input could alter or override the effects of single projection neurons onto the STG. Thus, I conducted experiments in which MCN1 was activated extracellularly in the otherwise unaltered *in vivo* preparation. This type of experiment should also be able to answer the question whether the stimulation of MCN1 *in vivo* elicits similar, different or no activities at all in STG neurons compared to the *in vitro* situation. The commissural neuron MCN1 was stimulated with an extracellular hook electrode on the *ion* (according to chapter 3.2.1.2, page 27). The resulting motor activity was monitored using extracellular electrodes on the *dvn* or *lvn* (see fig. 16).

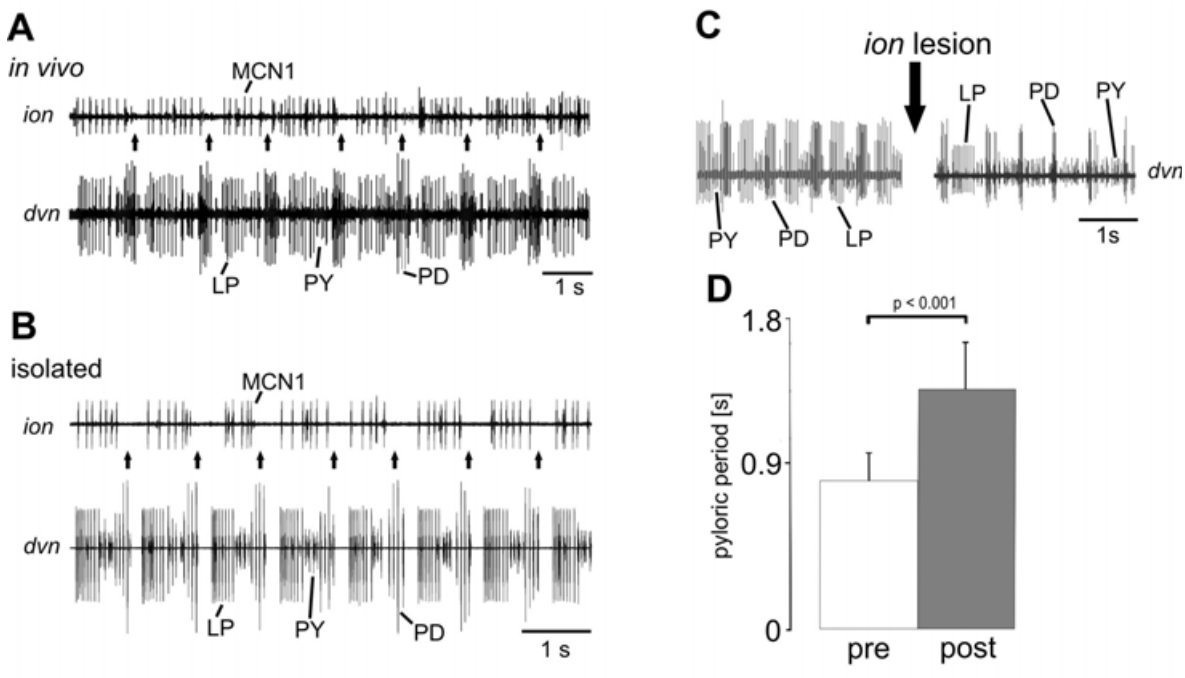

Figure 16: MCN1 affects the CPGs in the stomatogastric ganglion**A** *In vivo* recording of *ion* and *dvn.* Note pyloric-timed gaps (arrows) indicating POC-rhythm. **B** *In vitro* recording of *ion* and *dvn.* Note pyloric-timed gaps in MCN1 activity. Data recorded & edited by U.B.S. Hedrich (see Hedrich et al. 2011) **C** *In vivo* recording of *dvn* during lesion of *ion.* Segment shows activity *30 s* after lesion. **D** Statistical analysis of effect of *ion* lesion on pyloric period (N=*5*).

4.1.1 Similarities of spontaneous MCN1 activities *in vivo* and *in vitro*

Before experiments on the effects of the projection neuron MCN1 on the central pattern generators *in vivo* could be conducted, the experimental design was tested, whether it harmed or disturbed the animal in way significantly changing the activity of this projection neuron. Thus, control experiments were conducted in which the surgery was performed (see chapter 3.2.1.2 on page 27 and fig. 14) and the *ion* was recorded via an extracellular electrode (see fig. 15). In a total of *11* animals the *ion* was recorded *in vivo* and in each one MCN1 showed spontaneous activity. In *7* of these animals MCN1 showed a firing patterns as shown in figure 16 A, i.e. MCN1 showed distinct bursts that were separated by a gap. In these cases MCN1 was firing at *11.2 Hz* (± *5.2 Hz*) and each burst was *0.88 s* long (± *0.28 s*). *In vitro,* these interburst pauses are elicited by inhibitory feedback from the pyloric CPG. The anterior burster (AB) neuron possesses an inhibitory synapse onto MCN1, thus synchronizing the projection neuron with the pyloric CPG (Blitz et al. 2004; Stein 2009). To demonstrate

the pyloric timing *in vivo* as well, I compared the timing of the MCN1 burst with the pyloric cycle period, which was assessed by the burst initiation of the pyloric dilator (PD) neuron. PD is electrically coupled to the AB neuron and thus reflects AB activity. The MCN1 burst occupied ***78.6%*** (***±12.4***) of the pyloric cycle in the ***7*** *in vivo* preparations. MCN1 bursts were initiated ***0.3 s*** (***±0.03***) after the PD activity terminated. The low standard deviation demonstrates that the timing of MCN1 depended on that of the pyloric pacemaker. The *in vivo* experiments thus demonstrate that MCN1 shows similar firing patterns compared to previous *in vitro* experiments. They also show that the activity patterns of MCN1 are modified via the same pathways already described in previous publications based on *in vitro* experiments.

4.1.2 MCN1 does not affect the esophageal motor neuron

The MCN1 axons project via the inferior esophageal nerve (*ion*) to the STG. The *ion* does not contain solely the MCN1 axon. There are at least two additional neurons that project through the *ion*: the Esophageal Modulatory Neuron (OMN) and the Modulatory Commissural Neuron 5 (MCN5). It is thus unclear whether the effects after transection of the *ion* (see chapter 4.1.1 on page 41) occurred because of the interruption of MCN1 activity or any of the other neurons projecting via the *ion*. In all my experiments, MCN5 was active at very low firing rates, which do not significantly affect the STG motor patterns (Coleman et al. 1992). OMN, however, showed continuous bursting in all experiments. I thus tested whether OMN activity influences either the STG motor circuits or MCN1. Recordings of the *ion* in the *in vivo* preparation revealed action potential amplitudes of all three neurons to be consistent with previously published experiments conducted *in vitro (Stein et al. 2005)*. Exemplary, a segment from an *in vivo* recording is shown in figure 17 A (inset). Spike sizes were similar in all experiments (***N=11***), which allowed an easy identification of OMN spike activity. I first tested whether the cycle periods of MCN1 and the pyloric rhythm changed in correlation with OMN activity. Significant changes in MCN1 and/or the pyloric activity during OMN activation would provide evidence for previously unaccounted for modulatory effects of OMN *in vivo*. First, recordings with spontaneous OMN activity were analyzed. Figure 17 A shows that the MCN1 activity as well as the pyloric period vary during and in-between OMN bursts as well. To test whether there was a significant correlation between MCN1 activity and OMN activity I measured the firing frequency of MCN1 during active and silent periods of OMN activity. The different units recorded extracellularly on the *ion* were separated using principal component analysis (PCA) method. MCN1 was firing at ***19.39 Hz*** (***±9.6***) during OMN interbursts and with ***21.1 Hz*** (***±4.4***) during OMN bursts (***N=5***), i.e. there was no significant difference between

these two situations (***p=0.23***, Student's t-Test). The short fluctuations in MCN1 firing frequency (see figure 17 A, middle) were pyloric timed and thus likely resulted from the inhibitory synapse of AB onto MCN1 (Blitz & Nusbaum 2012). During OMN bursting, these pyloric bouts in MCN1 activity continued, supporting the hypothesis that OMN does not influence MCN1 activity.

It is possible, however, that OMN activates other projection neurons in the CoGs, bypassing MCN1 but nonetheless activating the motor neurons in the STG. Since extracellular electrodes applied on the motor nerves recorded the activities of the pyloric neurons, I analyzed whether pyloric activity changed during OMN activity. Data from ***5*** *in vivo* experiments show the pyloric cycle period and firing frequency during OMN bursting (see fig. 17 B).

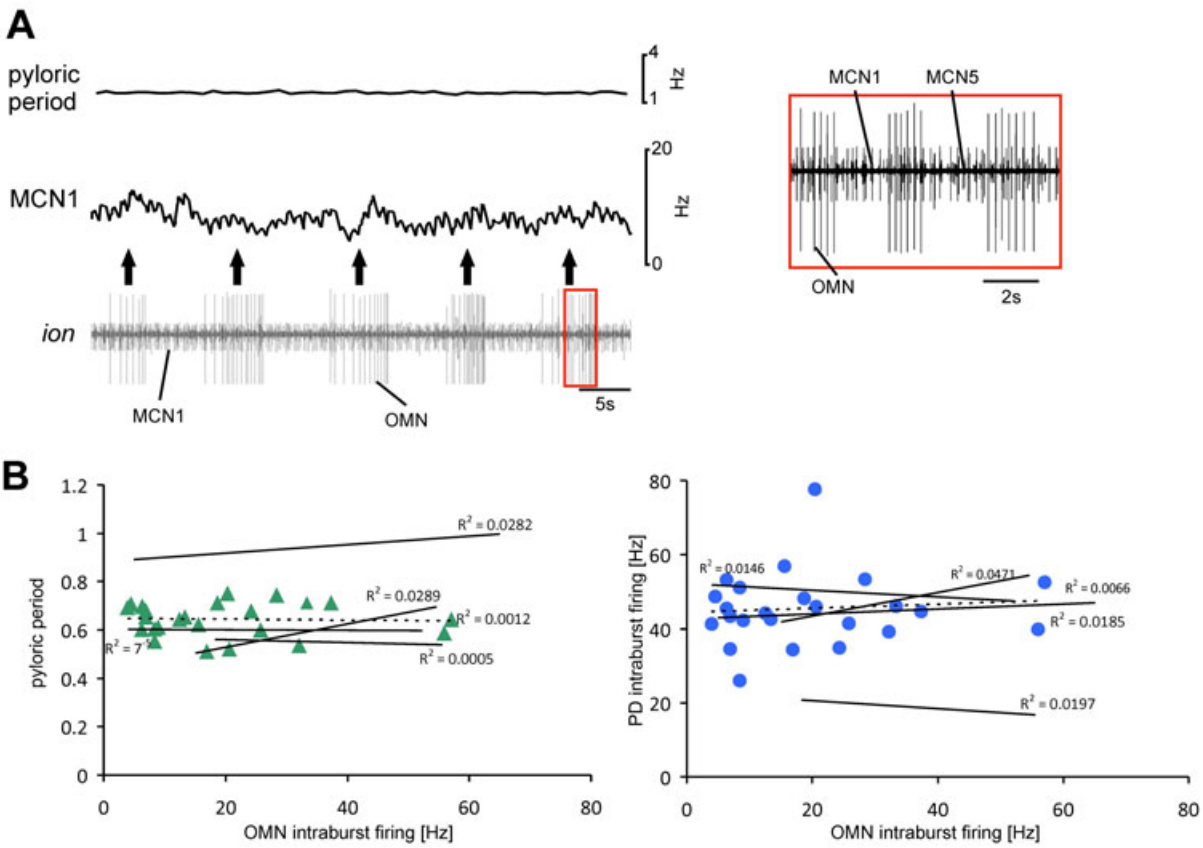

Figure 17: No significant effects of OMN bursting on the pyloric pacemaker kernel and MCN1. **A** *ion in vivo* recording showing spontaneous bursting activity of OMN and no significant changes in MCN1 spiking and in pyloric period. Right shows the marked segment in *ion* recording expanded. **B** shows OMN intraburst firing frequencies and pyloric periods during OMN bursts (left). Right graph shows linear fits and R^2 values of OMN intraburst firing frequencies and PD intraburst firing frequencies. Graphs show linear fits. As an example, the corresponding data to one fit (dashed line) is shown (colored data points).

If OMN had an effect on the activity of the pyloric pacemaker ensemble, linear fits computed for these data should show a slope, indicating a correlation between the two. However, as can be seen for the analysis of the pyloric period, none of the fits show a significant correlation with OMN activity (see fig. 17 B, left). Since the observation of the period disregards other changes such as the neuronal firing frequency, the pyloric dilator (PD) neuron was also analyzed (see fig. 17 B, right). This data shows PD intraburst firing frequency plotted against OMN intraburst firing frequency. The linear fits show no significant slope, suggesting that no correlation between OMN and PD activity is present *in vivo*.

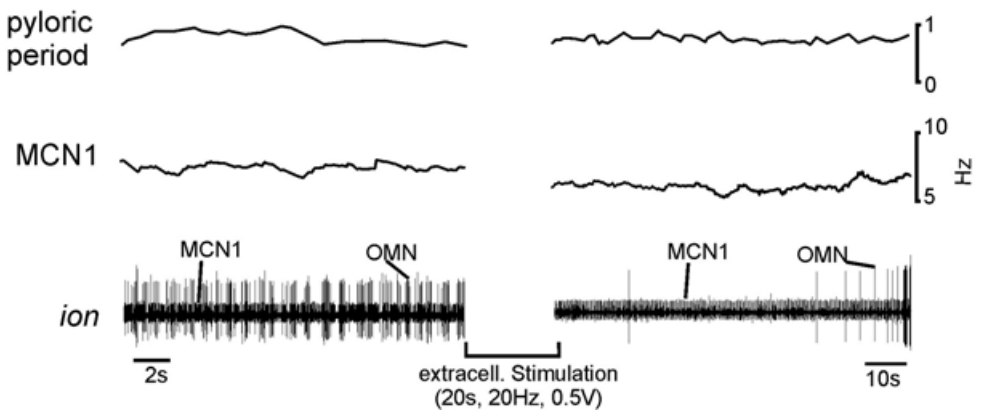

Figure 18: Extracellular stimulation of OMN. **Left:** *ion* recording *30 s* prior to stimulation. Firing frequencies of MCN1 and pyloric period are shown above. **Right:** *ion* recording *30 s* after stimulation. Note the cessation of OMN activity after stimulation.

In summary, these data show that OMN spontaneous activity does neither affect MCN1 nor the pyloric rhythm. These primary observations from extracellular recordings of the *ion* were followed by experiments in which the *ion* was stimulated to activate OMN. Spike size in extracellular recordings is known to be directly and positively correlated with axon diameter. A large axon diameter results in larger membrane area, thus the membrane capacitor can be charged more easily in larger axons. A gradually increased stimulus amplitude will thus cause the neurons with larger spike amplitudes to be activated first. Since the spike amplitudes of the OMN were consistently larger than those of MCN1, OMN is always activated at lower voltages as MCN1 and the voltage necessary to activate MCN1 always activates OMN as well. To test whether the OMN stimulation had any effect on the stomatogastric neurons stimulus voltage was raised manually, until OMN was activated. The stimulus (*20 Hz*) was applied for *10-20s*. The success of the stimulation, i.e. a sufficient stimulation am-

plitude was reached, when OMN showed a cessation of activity after the end of the stimulation This cessation is typical for this neuron after strong activation (see figure 18 bottom right and compare Hedrich et al. 2011). MCN1 activity as well as pyloric period before and after the simulation were analyzed. Before stimulation of OMN the MCN1 firing frequency had a value of ***6.5 ±1.3 Hz*** (***N = 4***); after stimulation the MCN1 firing frequency was ***5.9 ±0.9 Hz*** (***N = 4***). The activity of the pyloric neurons on the *dvn* remained equally unchanged (see figure 18 top right). Their mean firing frequency prior to stimulation ranged ***17.9 ±4 Hz*** (***N=7***) and after stimulation ranged ***16.5 ±3 Hz*** (***N=7***), demonstrating that OMN had no effect on the pyloric CPG (***p=0.42***, Student's t-Test).

This data shows that the targeted activation of MCN1, a projection neuron important for the CPGs in the stomatogastric ganglion, is possible *in vivo* despite the fact that the *ion* is a multiunit nerve. The following shows results of the MCN1 activation experiments and the effects *in vivo.*

4.1.3 Lesioning of MCN1 axon affects pyloric CPG *in vivo*

Termination of MCN1 activity *in vitro* terminates certain gastric mill rhythms, specifically the rhythms elicited by the sensory ventral cardiac neurons (VCN) and the inferior ventricular (IV) neurons, which descend to the commissural ganglia from the cerebral ganglion.

Although the pacemaker kernel of the pyloric central pattern generator network is capable of sustaining rhythmic activity without input from projection neurons, it is continuously excited by input from the commissural ganglia, for example by MCN1 (Bartos & Nusbaum 1997; Bartos et al. 1999). However, it is unknown if this is also the case in the intact animal. The simultaneous activity of other projection neurons may very well compensate for a cessation of MCN1 activity, or that projection neurons' activities have different effects on the pyloric pacemaker neurons altogether *in vivo*. Compensatory or modulatory effects may also emerge from the neuropeptides and neurohormones distributed via the bloodstream.Thus I conducted lesioning experiments *in vivo* to test whether MCN1 termination of activity had similar effects on the gastric mill CPG as in the *in vitro* preparation. Since the above experiments already demonstrated that OMN had no influence on the pyloric rhythm and MCN5 was not sufficient to affect the pyloric rhythm (Norris et al. 1996), the lesioning specifically affected MCN1. Lesioning the *ion* had significant effects on the rhythmic activities of motor neurons in the stomatogastric ganglion. The effects on the pyloric CPG are

shown in figure 16 C and D. The pyloric period increased from ***0.85 s*** (***±0.12***) to ***1.35 s*** (***±0.4***). This showed that effects on the rhythmic activity of pyloric neurons by the projection neuron MCN1 established in *in vitro* experiments were reproduced *in vivo* as well.

4.1.4 MCN1 activation *in vivo* has similar effects on the gastric mill CPG compared to *in vitro*

To test whether the effects of MCN1 activation on the STG pattern generators in vivo corresponded to those *in vitro*, the stimulus amplitude was raised manually until a response in the pyloric motor neurons could be seen. This voltage level was taken as the MCN1 activation threshold. MCN5 should not have been activated at this threshold due to its spike amplitudes being considerably smaller compared to MCN1 spikes on the *ion* recording (see fig. 17). The inferior ventricular (IV) neurons also project through the *ion* to the CoGs (Hedrich & Stein 2008). Their spike amplitudes are, however, even smaller than those of MCN5. While OMN was also activated by the *ion* stimulation, the results above showed that this had no effect on the activity of the motor neurons in the stomatogastric ganglion an on an important projection neuron in the CoGs (see chapter 4.1.2 on page 42). During *in vitro* experiments, the MCN1 neuron is necessary and sufficient to elicit and sustain a gastric mill rhythm and it also affects the pyloric rhythm. However, the situation *in vivo* might be such that not MCN1 alone can elicit these effects but rather a synchronous firing of several projection neurons is necessary to elicit changes in stomatogastric CPG activity.

The stimulus frequency was set according to previously published data (Smarandache & Stein 2007). The results are shown in a recording segment of an *in vivo* preparation in figure 19. Before (not shown) and after *ion* stimulation the gastric motor neuron LG was silent. During MCN1 activation LG was active in a burst-like fashion (***N=6***). Bursting ceased ***3-10 s*** after *ion* stimulation stopped. The intraburst firing frequency of LG during MCN1 activation was ***6.36 ±1.4 Hz.*** The duty cycle of LG during the gastric mill rhythms was short (***0.29 ±0.04***) compared to *in vitro* data from Wood et al. (2004).

The pyloric CPG was also affected by MCN1 stimulation (see fig. 19). The pyloric period was ***1.08 ±0.24*** before and during *ion* stimulation and increased to ***1.95 ±0.59*** after *ion* stimulation (***p=0.05,*** Mann-Whitney Rank-Sum test; ***N=5***).

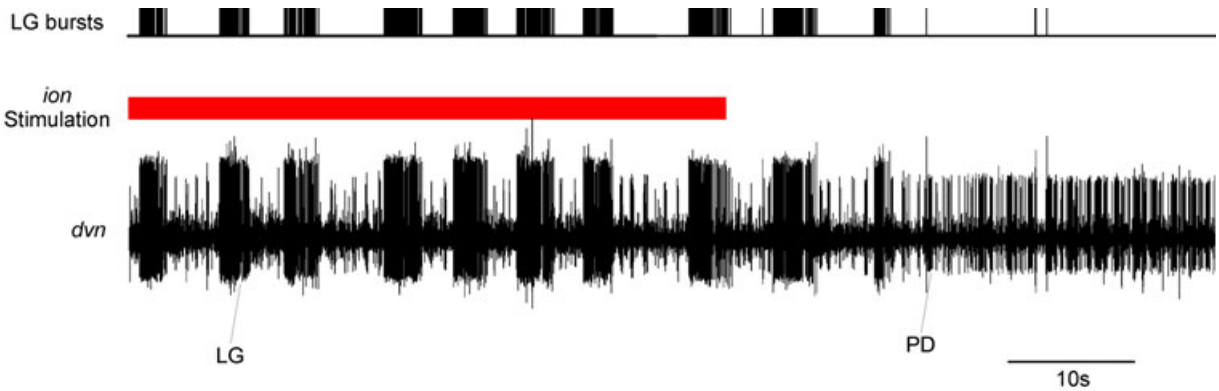

Figure 19: LG is activated during MCN1 stimulation *in vivo*. Data from *in vivo* experiment. LG (gastric) and PD (pyloric) bursts are visible. Due to recording quality no other pyloric neurons were discernible in the recording. Duration of *ion* stimulation shown in red.

4.1.5 Summary

The previous chapter showed that it is possible to stimulate a known modulatory neuron *in vivo*. Analogous to data established *in vitro* the projection neuron MCN1 has effects on the pyloric as well as the gastric mill CPG *in vivo*. Thus, MCN1 plays a similarly important role in pattern selection and modification as in the isolated preparation. It could also be show that it is possible to selectively stimulate single units on the *ion*, which might be helpful for future experiments.

The experiments shown in this chapter established MCN1 as a projection neuron important for pattern selection *in vivo*. Nonetheless, neuronal control of behavior is often controlled by more than one part of the system. A complex interplay of several parts of the nervous system generates characteristic activation pathways, which enable customized behavioral output. These pathways of initiation and modulation of rhythmic activity in the STG motor neurons have been described in-depth the isolated nervous system. It is not yet known, however, if these pathways have comparable effects on the output of the CPGs *in vivo*. In the following chapter, I will investigate two different activation pathways in the *in vivo* preparation.

4.2 Activation of distinct pathways initiating gastric mill rhythms *in vivo*

The previous chapter revealed that the selective activation of a single neuron is possible *in vivo*. This chapter shows how neuronal pathways, involving several projection- and/or sensory neurons, activate the gastric mill central pattern generators in the STG. It is known from *in vitro* studies that the gastric mill CPG only elicits rhythmic

bursting in the motor neurons when projection neuron(s) are activated (Blitz & Nusbaum 2012; Hedrich et al. 2009; Wood et al. 2000). If this holds also true for the *in vivo* preparation it would be ideal system for the investigation of neuronal control of behavior *in vivo.*

The concerted activities of several projection neurons have been known to elicit gastric mill rhythms *in vitro* (Bartos et al. 1999; Stein 2009). Several activation pathways have been described from the sensory- to the motor neuronal level (see chapter 2.2.4 and following). Not all of these pathways are feasible for the work in the intact preparation, however.

The ventral cardiac neurons (VCN) are mechanoreceptors, which transmit information about the state of pressure in the cardiac gutter. Activation of these sensory neurons causes the initiation of a distinct gastric mill rhythm *in vitro* and *in situ* (Beenhakker & Nusbaum 2004). It is still unclear whether this distinct rhythm is similar to that elicited by the VCNs *in vivo*, or if the VCNs can at all elicit gastric mill rhythms *in vivo.* Many factors such as coactivation or neurohormones might change or override the effects of the VCNs on the gastric mill CPG. Therefore, I conducted experiments in which I activated the VCN in the intact animal using mechanic stimuli applied via a plastic probe to the cardiac gutter.

The second pathway, which was investigated in *in vivo* experiments involves the previously described post-esophageal commissure (POC) neurons (Blitz et al. 2008). As oppose to the VCNs these are not sensory neurons but neuromodulatory interneurons, which elicit a characteristic gastric mill rhythm. *In vitro* the LG neuron shows pyloric-timed gaps during the bursts, which result from inhibitory actions of the AB neuron onto MCN1 (Blitz & Nusbaum 2008). This factor makes it easy to discriminate this type of gastric mill rhythm from others; however, it is still unknown whether this is also the case *in vivo*. Experiments were conducted in which the POC neurons were activated via extracellular stimulation.

4.2.1 Mechanical activation of the VCN-pathway *in vivo*

The ventral cardiac neurons are located in the cardiac gutter between the lateral cardiac ossicles and they are activated by mechanical stimuli to that area at the inside of the stomach. Beenhakker et al. (2004) showed that the VCN can be stimulated *in situ* by applying mechanical stimuli to the cardiac gutter via a pointed probe.

In my *in vivo* experiments, a plastic probe with a rounded blunt end was inserted through the esophagus and past the endoscope to stimulate the cardiac gutter. The gutter was stimulated with light constant pressure under visual control via the live feed of the endoscopic camera. The stimulation was applied until a GMR was initiated. If a GMR was initiated, the stimulation was immediately stopped. If no GMR could be induced after *100 s*, the stimulus was stopped. If a gastric mill rhythm was elicited, it took *3.4 ±1.7 s* (*N = 31*) to induce it. The rhythm persisted for several seconds, ranging from a minimum of *30 s* to a maximum of *13 min (8.7 ±11 min*, *N = 31)*.

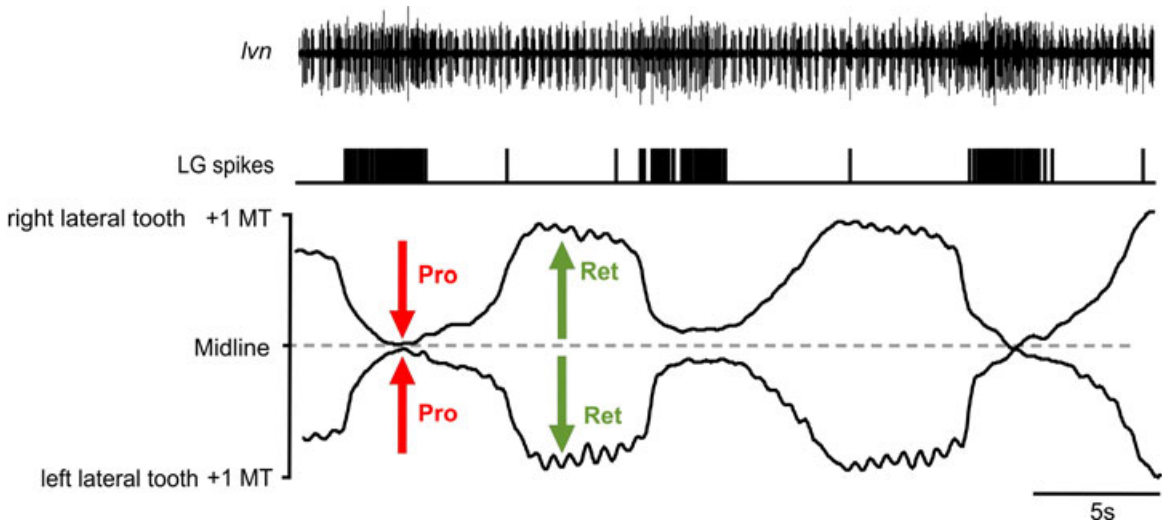

Figure 20: VCN stimulation elicits distinct neuronal activity and tooth movement. **Top:** Extracellular recording of left *lvn.* **Middle:** LG spikes. **Bottom:** Trajectories of the two lateral teeth are shown. Midline marks the middle of the medial tooth for reference. Protraction (red) and Retraction (green) are shown.

An example of the gastric mill is shown in figure 20. During LG bursting, both lateral teeth move towards the midline of the cardiac sac. To calibrate each video frame correctly, the middle of the medial tooth was assigned to represent the midline (see dotted line in fig. 20). During relaxation, the lateral teeth performed pyloric "twitching", visible in the smaller dents in the movement trajectory. Such pyloric-timed dents were present in about half (*N = 31*) of all the preparations (*N = 67*). They were most likely due to pyloric-timed activity of the inferior cardiac (IC) motor neuron, which projects via the mvn and innervates the gm5a muscle (Weimann et al. 1991). However, since IC was not recorded in these experiments this aspect of the gastric teeth movement repertoire was not investigated further.

In *12* experiments, a recording electrode was successfully placed on the *lvn* to record LG activity during an ongoing gastric mill rhythm. A total of *5* experiments showed the necessary signal quality to extract the LG spikes from the raw data and were used for further analysis. The bursts from each specimen were averaged and then statistically analyzed. Across all *5* preparations LG was firing at a mean rate of *18.25 ±4.8 Hz*. The average burst was *2.61 ±1.4 s* long, and a cycle was *11.33 ±10.3 s* long. The cycle period corresponds with previously acquired data (see Beenhakker et al. (2004)), although the standard deviation was higher in the *in vivo* data sets. In the *in vivo* experiments the intraburst firing rate was significantly higher than the *in vitro* values of *14.76 ±4.5 Hz* (*p<0.001,* Mann-Whitney Rank Sum test, *N=4*). The same was true for the mean burst duration of *4.21 ±0.8 s (N=3)* in the *in vitro* preparation (*p<0.001,* Mann-Whitney Rank Sum test, *N=4*). These experiments thus showed that the VCNs elicited a motor pattern that was at least partly similar to the one described *in vitro*.

4.2.1.1 Characterization of lateral tooth movement during VCN stimulation

In the previous chapter, it was established that the motor neurons are activated by VCN stimulation in the intact preparation. It is one goal of this work to investigate how neuronal activity is translated into movement. In experiments in which the stimulation of the VCNs was successful and a gastric mill rhythm was initiated, the movement of the teeth was recorded via the endoscopic camera. This protraction was translated into two-dimensional data by a motion tracking software. Pro- and Retraction amplitudes of the teeth were measured by a relative scale calibrated to the width of the medial tooth (Medial Tooth unit = *MT*) (see chapter 3.5 on page 36). During a gastric mill rhythm, the lateral teeth move towards and away from the midline in the horizontal plane. The medial tooth moves vertically but is obscured by the lateral teeth during each protraction phase. Therefore, the data of tooth movements presented in the following displays movement trajectories of the lateral teeth only. One of the two lateral teeth was analyzed in any given preparation. The mean maximum protraction amplitude of the lateral tooth was *0.94 ±0.2 MT (N=11)*. The duration until the midline was reached was *1.62 ±0.5 s (N=11)*. In figure 21 a sequence of rhythmic tooth movements, which were elicited by stimulation of the VCN neurons in the cardiac gutter, is shown. The stimulation of the VCN neurons initiated the gastric mill rhythm, since the teeth of the gastric mill did not move before the stimulation.

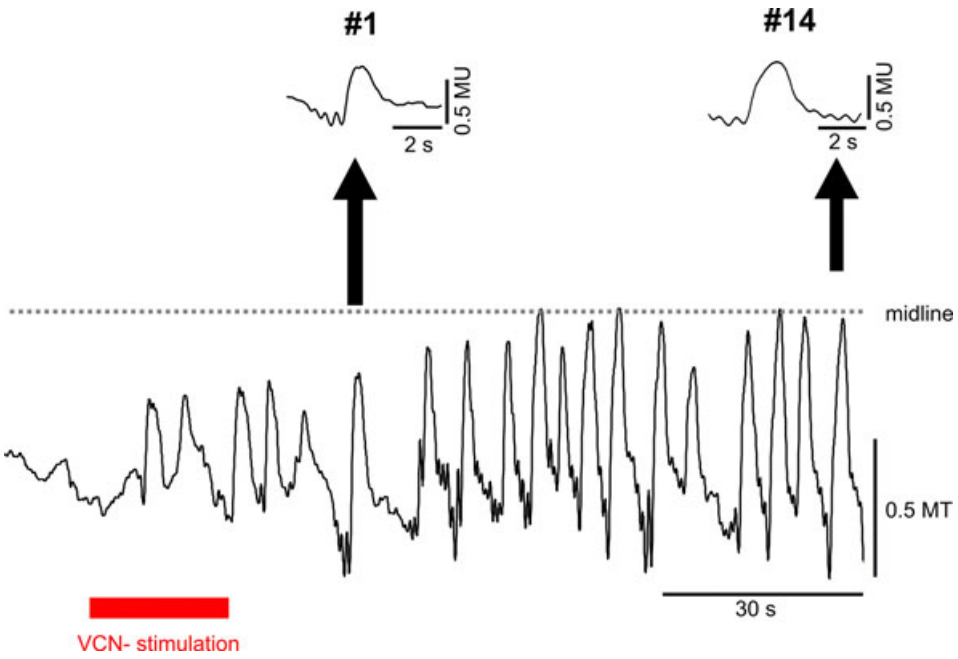

Figure 21: Variability of tooth movement in VCN-elicited GMR. Variability of movement output in one animal after VCN stimulation is shown. First burst is shown in expanded view above (#1). For comparison, 14th burst in the sequence is also shown in expanded view above (#14). Note that protraction is represented by upward deflection in movement trajectory.

4.2.1.2 Hepatopancreatic duct activity affects the initiation of the VCN-elicited gastric mill rhythm

It was not possible to elicit a GMR by stimulating the VCNs all preparations that were used (***N = 31*** of ***67*** were successful), although care was taken to keep conditions constant across experiments. When reviewing the video data, it became evident that activity of the gastric mill correlated positively with activity of the hepatopancreatic duct. In ***12*** animals in which the hepatopancreatic duct was active and digestive fluid (yellow, brown color) was flowing into the cardiac sac (see fig. 22 A) a gastric mill rhythm could faithfully be elicited. The other preparations, which did not show an active hepatopancreatic duct and thus no influx of digestive enzymes into the cardiac sac (see fig. 22 B), did not exhibit a long-lasting gastric mill rhythm. These specimen showed either no reaction ***(N=48)*** or just single contractions of the teeth ***(N=7)***. Repeated stimulations at changing intervals ***(1 min, 5 min, 10 min)*** did not change these results. A gastric mill rhythm could thus not be elicited when the hepatopancreas was inactive.

Spontaneous gastric mill activity, i.e. before the experiments was conducted, was recorded in ***48%*** of all preparations, which is comparable to previous studies conducted in intact preparations of the lobster *Panulirus interruptus* (Heinzel 1988).

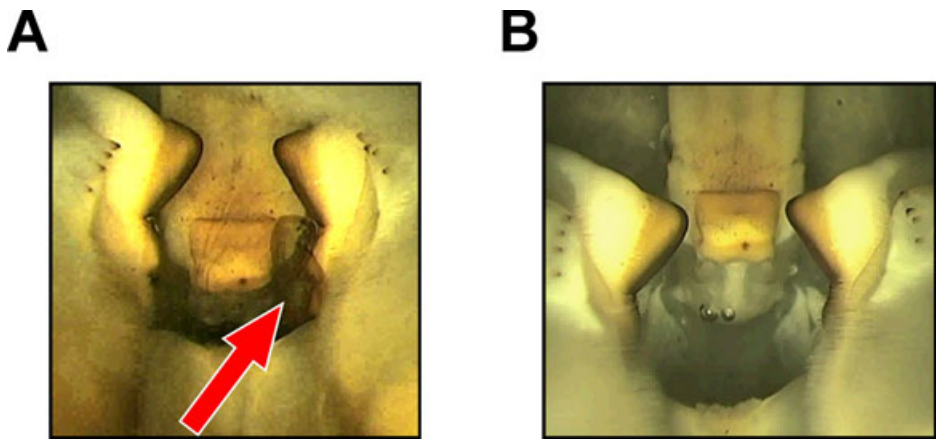

Figure 22: Induction of digestive enzymes via hepatopancreatic duct visible via endoscopy *in vivo*. **A** shows the gastric mill teeth and digestive enzymes (arrow) flowing from direction of the pyloric valve into the cardiac sac. **B** shows same without hepatopancreatic duct active and enzymes flowing.

In figure 23 a sample recording of the reaction of a lateral tooth during a stimulation which did not elicit a VCN-type rhythm is shown. The single protraction of the tooth during stimulation shows that the stimulation itself worked as demonstrated and that the absence of a gastric mill rhythm was not due to technical error or insufficient stimulation.

Figure 23: Example of VCN-stimulation not eliciting a GMR *in vivo*. The figure shows the response of the lateral tooth to tactile stimulation of the cardiac gutter (shown in red); stimulation duration was ***12 s*** (marked in red). Downward deflection of trajectory represents contraction towards midline.

Apparently, thus, the influence of the hepatopancreas was specific to the VCN-elicited gastric mill rhythm. These experiments demonstrated that despite similar conditions in the experimental setup, the initiation and maintenance of a gastric mill rhythm could not be guaranteed in every preparation. The simultaneous induction of digestive enzymes into the cardiac sac may be an indicator for another parameter (or parameters) of control of gastric mill activity *in vivo.*

4.2.2 Electrophysiological activation of the POC-pathway *in vivo*

The POC neurons are neuromodulatory neurons. Extracellular stimulation of these neurons faithfully elicits a gastric mill rhythm in *in vitro* experiments (Blitz & Nusbaum 2012; Blitz et al. 2008). To test whether the gastric mill rhythms elicited *in vitro* correspond to the rhythms in the intact animal the axons of the POC neurons were stimulated extracellularly (see chapter 2.3.I.2) and the tooth movement in the gastric mill was recorded.

Additionally, in ***4*** experiments an extracellular electrode was successfully placed onto the *lvn* and a sufficiently good signal-to-noise ratio was achieved to extract the action potentials of the lateral tooth protractor neuron LG (see figure 24 top and middle).

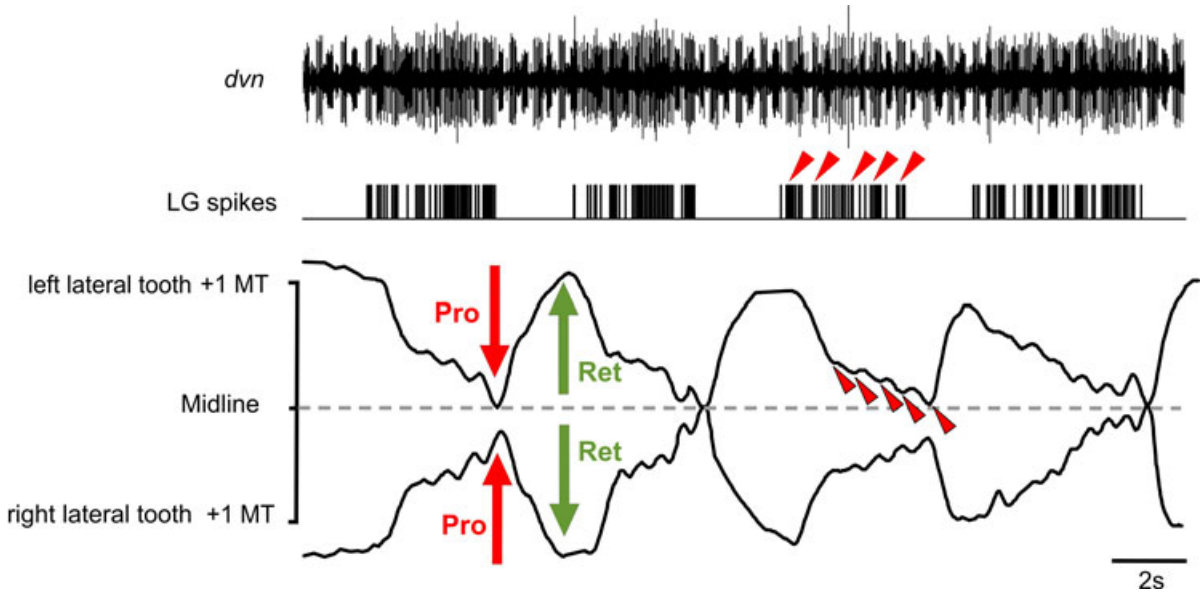

Figure 24: POC stimulation elicits distinct neuronal activity and tooth movements. **Top:** Data from extracellular recording of left *lvn.* **Middle:** LG spikes. Note the pyloric-timed gaps in LG bursts (red arrows). **Bottom:** Trajectories of the two lateral teeth are shown. Midline marks the middle of the medial tooth for reference. Protraction (red) and retraction (green) movement are marked. Interburstlet gaps are marked (red arrows).

Data from a total of *60* bursts was averaged for each animal and the burst characteristics of LG were calculated. After POC stimulation LG was firing at a mean rate of *13.32 ±3.2 Hz* (*N=4*) in all experiments. The burst duration was *4.24 ±3.6 s* and the interburst interval was *3.74 ±1.6 s*. *In vitro* data from the laboratoy of M.P. Nusbaum and the laboratory of W. Stein (Illinois State University, USA) was used for comparison. When the POC neurons were activated in *in vitro* experiments, LG elicited a firing rate of *6.56 ±2.6 Hz* (*N=4*). Average LG bursts *in vitro* were *6.57 ±2.6 s* long. The interburst interval of LG was an average of *5.74 ±1.7 s* long in the *in vitro* preparation. Statistical comparison of the data showed that firing frequencies were significantly different between the *in vitro* and the *in vivo* preparations (*p<0.001*, Mann-Whitney Rank Sum test). Also the burst duration of LG was significantly longer in the *in vitro* and the *in vivo* preparations (*p<0.033*, Mann-Whitney Rank Sum test). Interburst interval duration was significantly longer *in vitro* compared to *in vivo* (*p<0.001*, Mann-Whitney Rank Sum test).

An additional property of the LG firing patterns during a POC rhythm is that *in vitro* the LG burst is subdivided into short burstlet which are caused by a loss of excitation due to the MCN1 being inhibited by the pyloric pacemaker neuron AB (Beenhakker et al. 2004). This causes LG to stop firing while the pyloric pacemakers AB & PD are active. My data shows for the first time that LG shows the same pyloric-timed interruptions *in vivo* during a POC rhythm (fig. 24 bottom trace & red arrows). The timing of LG bursting relative to the pyloric phase is shown in figure 25. The X-Axis in each panel gives the phase in the pyloric cycle which was calculated from PD burst onset to the next burst onset. The number of spikes per pyloric phase was counted and plotted relative to all the spikes counted all preparations (*N=5*). The distribution of the events (*BIN* size *= 20 ms*) is plotted in figure 25 A and shows an inhomogenous distribution of the spikes. Due to the inhibitory effects of the pyloric pacemaker neurons, fewer LG spikes occured during the PD duty cycles at the beginning of each pyloric phase. For comparison, LG shows no pyloric-timed firing during a VCN-elicited gastric milll rhythm (figure 25 B).

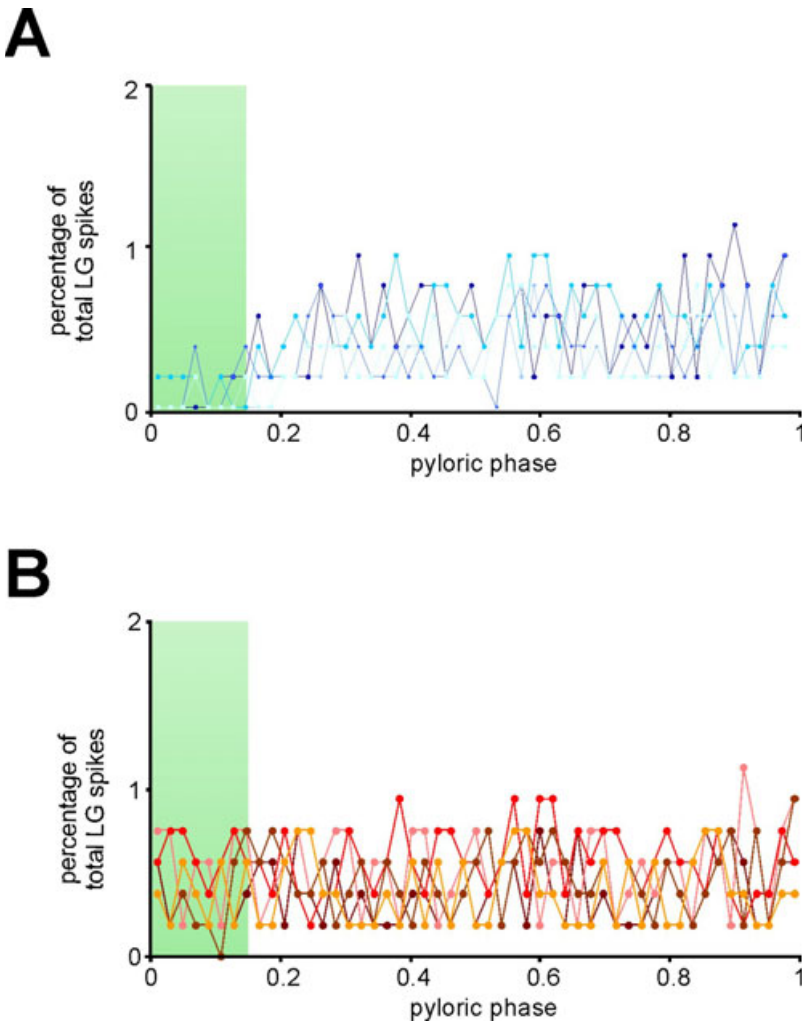

Figure 25: Distribution of LG spikes in reference to the pyloric cycle *in vivo*. Y-Axis show percentage of LG spikes per burst relative to total spike coun **A** Bluish traces represent POC-type rhythms. **B** Reddish traces represent VCN-type rhythms. Green boxes show the time frame for the statistical comparison (see text).

Spikes occured evenly across the whole pyloric period suggesting that the spike activity of LG was not affected by the pyloric neurons during this type of gastric mill rhythm. A comparison of the percentage of LG spikes during the average activity phase of PD (***0.15 ±0.08 s***, corresponding to ***9 BINs***) showed a significant difference between VCN and POC rhythms (***p<0.001***, Student's t-Test, ***N=5***).

In summary, there were significant differences in some respects of burst activity (burst duration, firing frequency, interburst duration) in LG between the VCN and POC GMRs. The characteristic LG firing pattern with pyloric-timed interruptions was also found *in vivo*. Although not controlled in this work, it can be assumed that the same pathway constituted by AB, the projection neuron MCN1 and LG is being activated *in vivo.*

4.2.2.1 Characterization of lateral tooth movement during POC stimulation

The previous chapter showed that certain characteristics in the activity patterns of motor neurons in the STG are preserved *in vivo* as well as *in vitro*. Investigation of neuronal activities, however, tells only part of the story since the motor neurons themselves innervate the musculature, which causes the actual movement responsible for behavior. The previous chapters demonstrated that VCN and POC stimulation elicited gastric mill rhythms *in vivo.* Whether these burst characteristics have effects on the movement level, however, is unknown, in particular because the gastric mill muscles are known to be slow non-twitching muscles (Govind et al. 1975; Hooper & Weaver 2000). It was therefore worthwile to investigate whether the neuronal characteristics previously described have an effect on the movement output of the gastric mill teeth as well. For this analysis, data from *in vivo* experiments with successful initiation of a GMR and simultaneous extracellular motor nerve-recordings were used. The PD burst onsets were extracted from the extracellular recordings on the *lvn* and correlated with the movement trajectories of the lateral teeth. In the following, the trajectories of just one lateral tooth are shown, since both teeth are innervated by the same motor neuron and therefore move as mirror images of one another.

To quantify the pyloric timing of tooth movement during the POC-elicited gastric mill rhythm statistically, the movement trajectory of the lateral tooth was examined for inflection points. Theoretically, each pyloric-timed burstlet during an LG burst should be represented by a positive and a negative inflection in the movement trajectory of the tooth. Due to the response delay of the musculature, the positive inflection overlapped with the burstlet gap after the burstlet, and the negative inflection overlapped with the ensuing burstlet. There were significantly more positive and negative inflection points during the POC-elicited LG bursts (***9.19 ±2.4, N=5***) than during the VCN-elicited LG bursts (***5.86 ±1, N=5***; ***p<0.05***, paired t-Test). This analysis showed that these two gastric mill activation pathways elicit different ouputs on the behavioral level. To examine these different ouputs in more detail, another method of analysis was applied, as shown in figure 26.

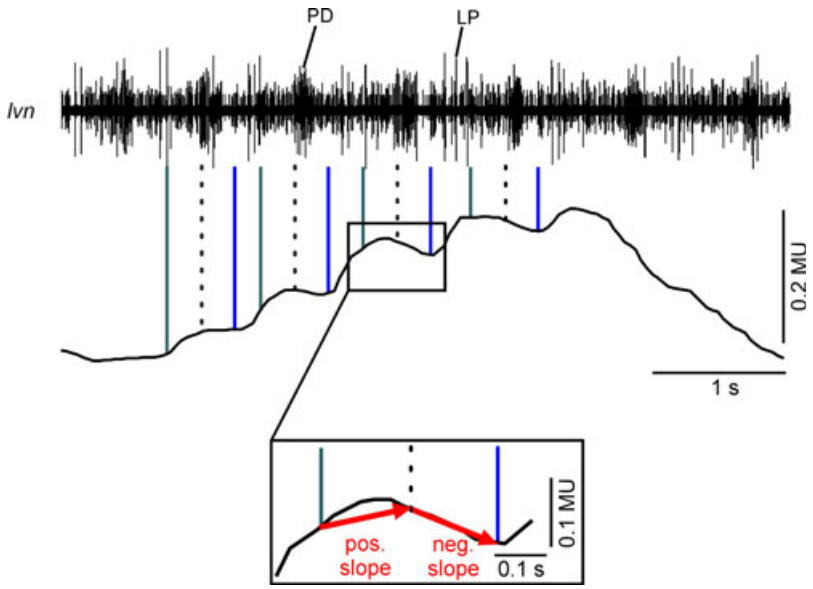

Figure 26: Schematized analysis of compliance of tooth movements to pyloric CPG. Burst onset of pyloric neuron PD on *lvn* recording (top trace) is used as reference (dashed line) on the movement trajectory (bottom trace). For sake of clarity LG spikes were omitted in the extracellular recording. Values of the movement trajectory ***200 ms*** before the onset of PD bursting (green line) and values of the movement trajectory ***200 ms*** after PD burst onset (blue line) were determined. Between these two data points the slopes were calculated. The inset shows exemplary the calculation of the slope values (positive & negative).

The PD bursts occuring during the lateral tooth protraction phase were identified (see *lvn* trace in fig. 26). In the following analysis, the onset of a PD burst was defined as point of reference (dashed line in fig. 26). After an LG burst onset the teeth started their movement with a certain delay due to the transduction speed of the action potentials and the time needed by the muscle to build up sufficient force to initiate the movement. This delay was approximately ***200 ms*** long. Hence the movement trajectory ***200 ms*** before the reference point was determined (green line in fig. 26). Same was done for the value of the movement trajectory ***200 ms*** after PD burst onset (blue line in fig. 26). Now the slope between these two data points was determined and the velocity of movement was calculated. A protraction movement of the teeth therefore resulted in a positive velocity value. Retraction movement resulted in a negative velocity. This produced one-dimensional sets of data, which are shown in figure 27. Black dots show the slope values occuring during the "before PD burst onset" time-frame; the grey dots show slope values during the "after PD burst onset" time-frame, respectively. All LG bursts from all animals are shown (data from each preparation was pooled).

For the VCN-elicited gastric mill rhythms (***N=4***) there was an even distribution of velocities (fig. 27 B), and therefore no influence of PD bursting on the tooth movement. The protraction velocities before a pyloric-timed LG burstlet were distributed around the *0*-line (***mean: 0 mN/0.12 s; 95%-ile: 0.6 mN/0.12 s; 5%-ile: -0.6 mN/0.12 s***), as were the protraction velocities after a pyloric-timed LG burstlet (***mean: -0.04 mN/0.12 s; 95%-ile: 0.5 mN/0.12 s; 5%-ile: -0.4 mN/0.12 s***). There was no statistical difference between the slopes in movement before and after a PD burst onset during the VCN-elicited gastric mill rhythms (***p=0.712, N=4***).

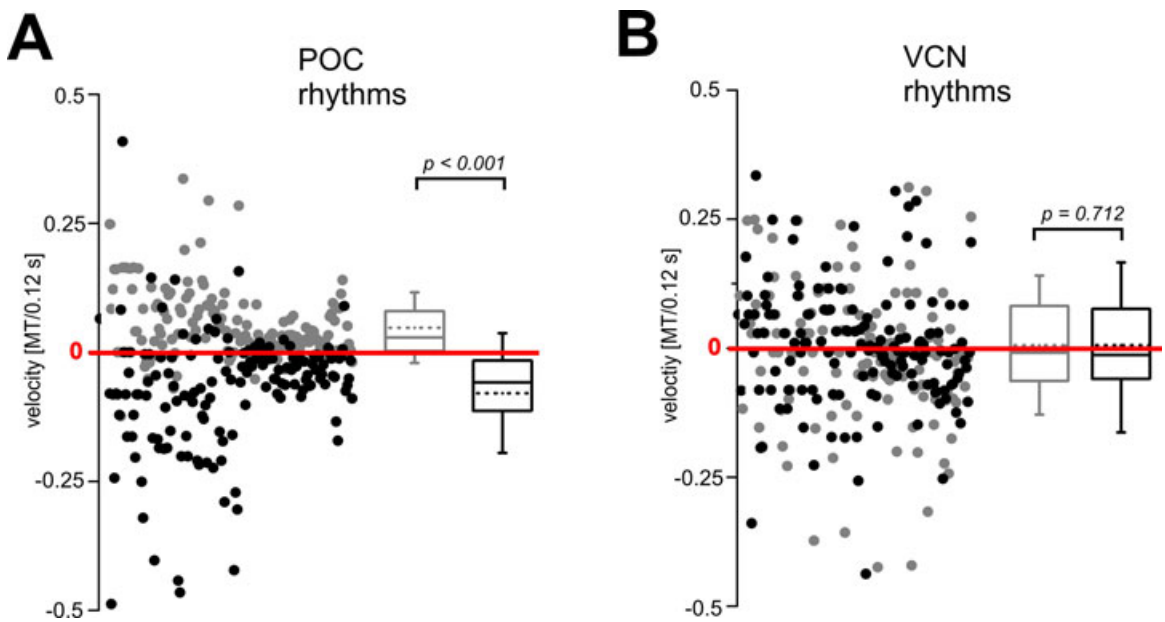

Figure 27: Compliance of tooth movement to pyloric CPG. **A** shows lateral tooth movement slopes before and after PD/AB burst onsets are shown for GMRs after stimulation of POC *in vivo*. The slopes occuring ***200 ms*** before LG-burstlet onset are shown in grey; slope values occuring ***200 ms*** after burstlet onset are shown in black. Distribution of slopes of the movement trajectory around pyloric-timed burstlet onsets is shown as box plots. Whiskers represent ***5 - 95 percentiles***; boxes represent ***25 - 75 percentiles***; median (straight line) and average (dashed line) are shown. **B** shows same for the tooth movement slopes before and after PD/AB burst onsets during mechanical stimulation of the VCNs.

For the POC-elicited gastric mill rhythms (***N=4***) however, the slope-distribution was unevenly distributed. There slopes occuring before PD burst onset (grey dots in fig. 27) were significantly different from those occuring in the time frame after PD burst onset (black dots in fig. 27). The protraction velocities before a pyloric-timed LG burstlet were shifted into the positive regime (***mean: 0.2 mN/0.12 s; 95%-ile: 0.5 mN/0.12***

s; 5%-ile: -0.03 mN/0.12 s). The protraction veloctities after a pyloric-timed LG burstlet were shifted into the negative regime (*mean: -0.3 mN/0.12 s; 95%-ile: 0.2 mN/0.12 s; 5%-ile: -0.7 mN/0.12 s*). This was also confirmed by the statistical analysis ($p<0.001$, Mann-Whitney Rank Sum test, $N=4$).

The analyses of the inflection points, as well as the velocity of movement, show for the first time that the differences in motoneuronal spike patterns caused by the activation of different pathways (VCN or POC) are preserved at the behavioral output *in vivo*.

Secondly, the duration of the maximum protraction was calculated (see fig. 28). For this, the time of maximal protraction in each burst was determined. The beginning of a plateau is characterized by a drop in the velocity (slope) of the protraction and the end of the plateau by a quick increase in negative slope (i.e. retraction movement). In other words, the movement decelerates at the beginning of the plateau and it accelerates after the end of the plateau. Thus, to determined the duration of the plateau, the slope of the movement around the time of the maximum protraction was measured. To do this, the data was divided into *0.04 s BINs* (which corresponds to the temporal resolution of the video recording). The velocity (slope) of the movement was then calculated between each *BIN*. The rate of change of the slope (i.e. the acceleration) movement was calculated for each *BIN* relative to the preceding *BIN* and given in percent change (see fig. 28). The *BIN*, during which the change of slope dropped below *63%* before the time of maximum protraction, was defined as the start of the plateau. The *63%* were used because the movement was assumed to roughly follow an exponential function.

Conversely, the end of a protraction plateau phase was defined as the time *BIN* during which the change of the slope first exceeded *63%* after the maximum protraction (see fig. 28). In the following, the edges (*63%*) of the plateau phase are defined as the peak protraction duration. These parameters were also statistically analyzed - the results are shown in figure 29.

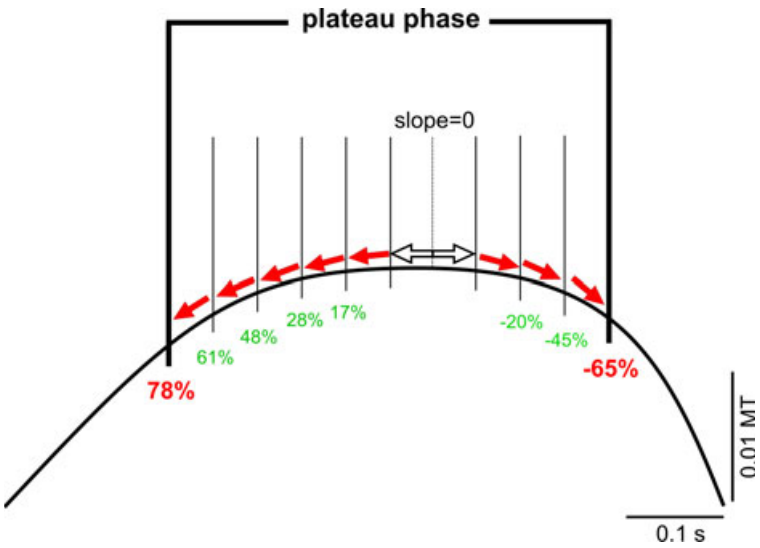

Figure 28: Schematic explaining how the peak protraction duration was determined. The maximum protraction was taken as the turning point of the trajectory with a slope of ***0***. The changes in the slope (red arrows) were then calculated between time ***BINs***. Slope changes ***>63%*** (red values) defined the edges of the plateau phase (thick lines).

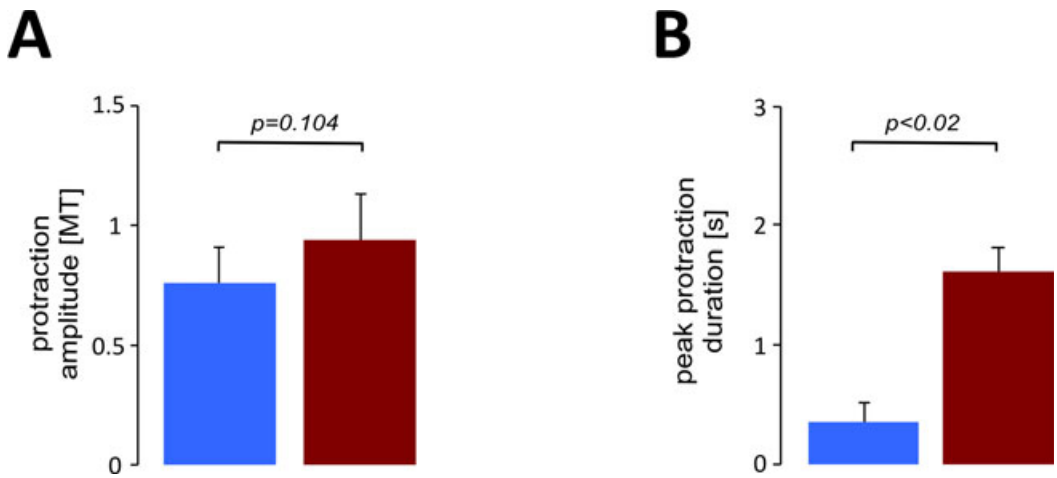

Figure 29: Protraction amplitudes and peak protraction durations show different characteristics during VCN and POC rhythms. **A** shows average amplitudes of protraction normalized to the width of the medial tooth (***MT***); POC-elicited GMRs and VCN-elicited GMRs are shown. **B** shows duration of maximum protraction in ***seconds***; POC-elicited GMRs and VCN-elicited GMRs are shown.

The protraction amplitudes were not significantly different during POC-elicited gastric mill rhythms and VCN-elicited gastric mill rhythms (***p=0.104;*** Student's t-Test, see fig. 29 A). In contrast, the duration of the maximum contraction showed a significant difference between the two types of gastric mill rhythms (***p<0.02;*** Student's t-Test, see fig. 29 B). This data corresponds to the previous finding, that tooth movements are pyloric-timed during POC-elicited gastric mill rhythms (see fig. 27). The maximum protraction of the lateral teeth is shorter during a POC-elicited GMR because the bursting of LG is interrupted by the pyloric pacemakers. Interestingly, the overall maximum protraction does not show a significant difference between the two types of rhythms (see fig. 29 A), despite the pyloric gaps during the POC-elicited gastric mill rhythms.

4.2.2.2 Hepatopancreatic duct activity affects the initiation of the POC-elicited gastric mill rhythm

Similar to the experiments in which gastric mill rhythms were elicited via stimulation of the VCNs, the extracellular stimulation of the POC did not result in a gastric mill rhythms in all of the specimen. A total of ***35*** animals were used during these types of experiments. Only ***12*** produced long-lasting gastric mill rhythms. In ***8*** animals, single protractions of the lateral teeth were noted, but could not be used for data analysis.

Figure 30 shows the reaction of a lateral tooth to a POC stimulation, which did not elicit a log-lasting gastric mill rhythm. The single retraction of the tooth during the stimulation suggests that the stimulation of the POC was successful.

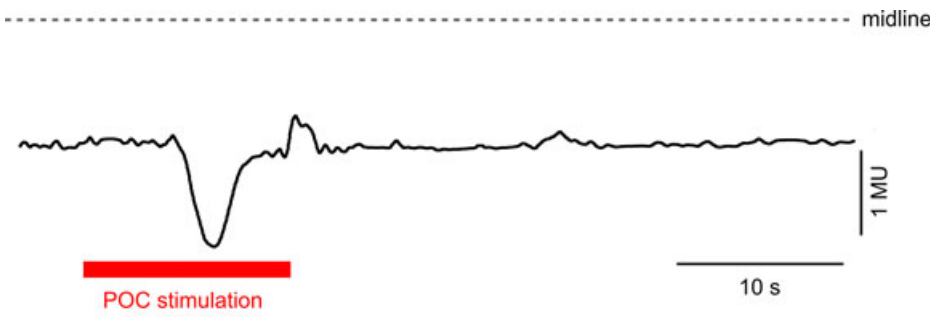

Figure 30: Example of a POC-stimulation, which did not elicit a GMR *in vivo*. The response of the lateral tooth to stimulation of the connective (shown in red) is shown. Downward deflection of trajectory represents retraction of the lateral tooth away from midline.

This indicates that other factors besides the release of neuromodulators of the projection neurons control the initiation of rhythmic motor neuron activity in the STG *in vivo*. In a total of *19* preprations continuous gastric mill rhythms could not be elicited by stimulation of the POC neurons. This showed that the initiation of a gastric mill rhythm was dependent on additional factors in the *in vivo* preparation. Despite the same experimental conditions present in all experiments, the stimulation of the POC pathway (or the VCN pathway) was not sufficient in all preparations to elicit and sustain a gastric mill rhythm. Whether the hepatopancreas or other factors might play a role in the successful initiation of a POC-type gastric mill rhythm could not be determined.

4.2.2.3 Variability of tooth movement changes during POC-elicited gastric mill rhythms

The previous chapters showed that in some preparations rhythmic movement of the gastric mill teeth was recorded after stimulation of the POC neurons. These movements showed the characteristic pyloric-timed interruptions (see fig. 25). In this chapter the variability of the protractions during a gastric mill rhythm will be investigated further. An ongoing POC-type rhythm *in vitro* is highly regular and shows pyloric-timed interruptions in LG activity in each burst (Saideman et al. 2007a). *In vivo* however, sensory feedback or variations in the neuromodulator cocktail in the hemolymph might change the rhythmic pattern. To characterize the rhythmic activity during POC- and VCN-type gastric mill rhythms, which persisted for at least *30 s* were analyzed.

The variability of movement output is shown in figure 31, which shows a recording from one *in vivo* preparation. The stimulation of the POC lasted for *20 s* and was successful, since during stimulation the gastric mill teeth (and the motor neurons) were activated (bouts of movement) and the gastric mill teeth did not move prior to stimulation. The first protraction of the rhythmic pattern is shown in expanded view above (see fig. 31, inset #1), which shows a short protraction duration.

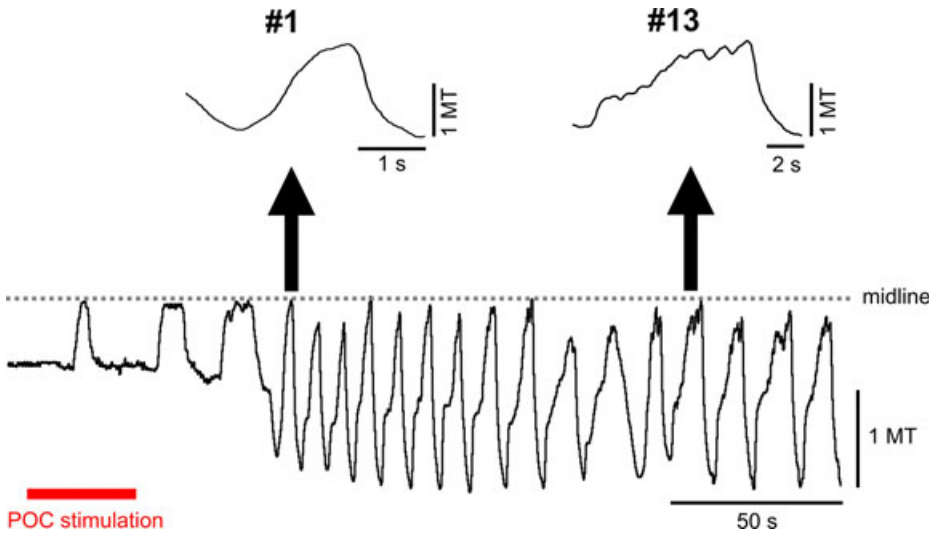

Figure 31: Example of a succession of variable tooth movements during a POC-elicited gastric mill rhythm. Variability of movement output of one lateral tooth in one preparation after POC stimulation is shown. First burst is shown in expanded view above (#1). Note different duration and pyloric timing in second burst shown in expanded view above (#13 in the sequence). Note the different time scales of the insets. The protraction is represented by upward deflection in movement trajectory in ***MT***.

There was no apparent pyloric timing of the protraction movement. A protraction that occured later in the pattern, however, looked very different (see fig. 31, inset #13). A pyloric-timed interruption during the protraction was visible in this protraction. Also, the protraction duration was increased. It is not yet clear what mechanism(s) cause this high variability in bursting *in vivo.*However, a significant difference was found between the first cycles of these types of gastric mill rhythms and the last cycles. The data in Figure 32 A shows the cycle duration for all cycles in the gastric mill rhythms (***N=5***). The X-Axis shows all cycles in their temporal sequence during a GMR. The number of cycles per gastric mill rhythms varied, ranging from ***15*** cycles to ***36*** cycles. In each preparation the duration of the first 5 cycles and the last ***5*** cycles were averaged and then statistically compared with the other preparations. The difference between these two sets of bursts was significant, as represented by the bar graphs (***p<0.001***, Student's t-Test, ***N=5***). This showed that there was a significant difference between the intial cycles and the last cycles of these types of gastric mill rhythms. The protraction duty cycle of each protraction of the teeth was also analyzed (see fig. 32 B). The average protractions during the first ***5*** cycles are plotted relative to the gastric mill phase (see fig. 32 B bottom). Same was done for the last ***5*** cycles (see fig. 32 B top).

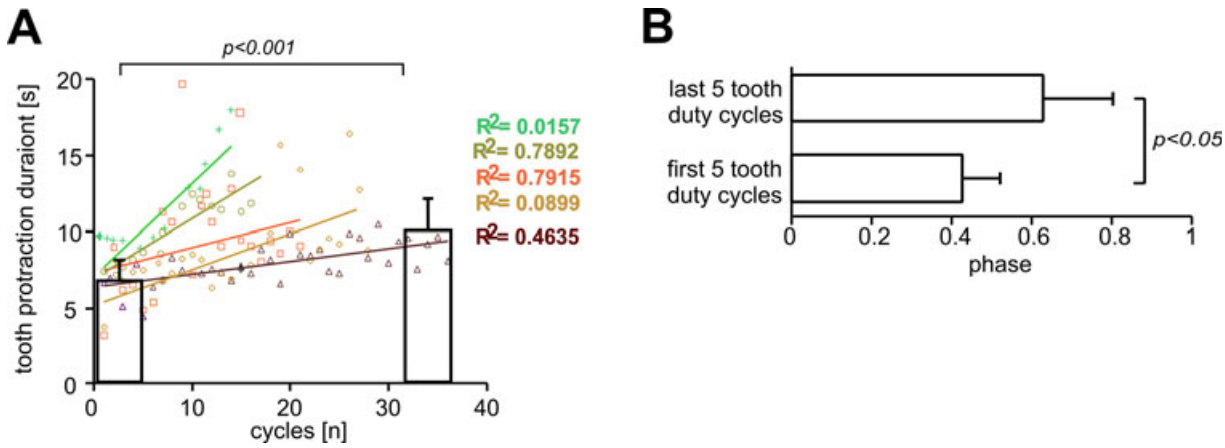

Figure 32: Statistical analysis of variability of tooth movement during POC-elicited gastric mill rhythms. **A** Durations of pro- and retraction cycles are plotted over the number of cycles after the stimulation end. Different colors depict different experiments. Linear regressions to the data points from each preparation are shown (straight lines). The bars show mean data from the first ***5*** cycles of each animal (left bar) and the last ***5*** cycles of each animal (right bar). **B** shows the average protraction duty cycles of the first ***5*** (bottom bar) and the last ***5*** cycles (top bar) relative to gastric phase.

A statistically significant difference was found between these cycles (***p<0.05***, Student's t-Test, ***N=5***). The protraction duty cycle was shorter during the earlier (and shorter) cycles compared to later (longer) cycles of the rhythms. This shows that not only the gastric mill period (cycle) was increasingly prolonged during these gastric mill rhythm but that even more so the relative contribution of the protraction movement during the cycle increased.

Interestingly, some of the elicited POC-elicited gastric mill rhythms did not change in the fashion shown above (***N = 4*** of ***12***). In these variants of the POC-elicit gastric mill rhythms recorded *in vivo, p*rotraction phases were of equal duration throughout the whole gastric mill rhythm sequence (see fig. 33, insets #1 and #8). In this example there was a noticeable deflection of the lateral tooth during the ***25 s*** of stimulation. Rhythmic pro- and retraction of the teeth started immediately after end of stimulation, as oppose to the previously shown stimulation (see figure 31, bottom trace), in which initiation of a gastric mill rhythm was delayed by ***27 s***. In all POC-elicited gastric mill rhythms, the protraction shows pyloric-timed dents. This was tested analogous to the analysis shown in figure 32. The following figure shows data from specimen (***N=5***),

which initiated gastric mill rhythms with homogenous cycle durations (see fig. 34). The shortest sequence was ***12*** cycles long, the longest sequence was ***35*** cycles long. The linear fits did indeed show a slope, i.e. increasing interburst interval duration, but the slopes of the fits was shallower than in figure 32.

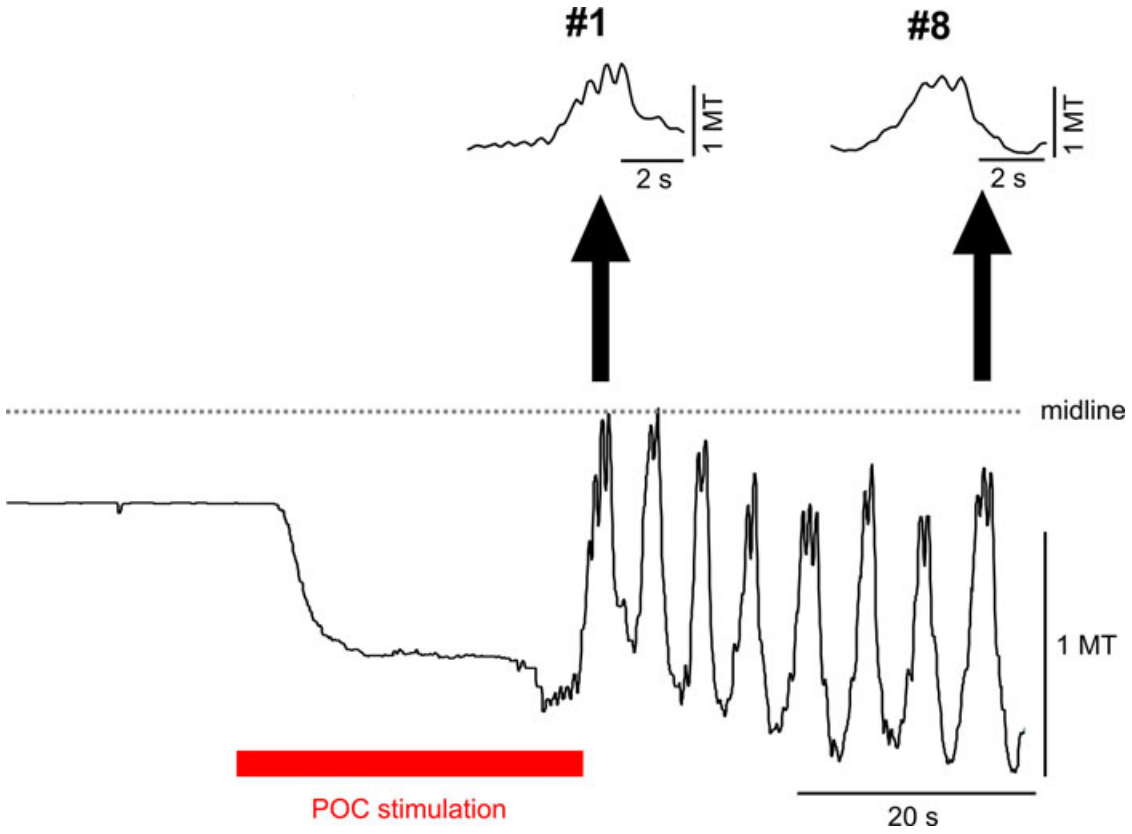

Figure 33: Example of a succession of constant tooth movements during a POC-elicited gastric mill rhythm. Tooth movement output in one animal after POC stimulation is shown. First burst is prolonged (#1, above), similar to 8th burst in the sequence (#8, above). Note the protraction is represented by upward deflection in movement trajectory. Midline of the stomach is marked by dashed line.

The average durations of protraction first ***5*** and the last ***5*** bursts of each gastric mill rhythm sequence are shown as bar graphs in figure 34 A. No significant difference could be found between these two data sets (***p=0.101***, Student's t-Test).

Additionally, the duty cycles of lateral tooth protraction during a gastric mill cycle were calculated (see fig. 34 B). No significant difference between the duty cycles at the beginning and at the end of the gastric mill sequences could be found (***p=0.2***, Student's t-Test). This showed that protraction duration as well as protraction duty cycle stayed constant in these variants of POC-elicited gastric mill rhythms.

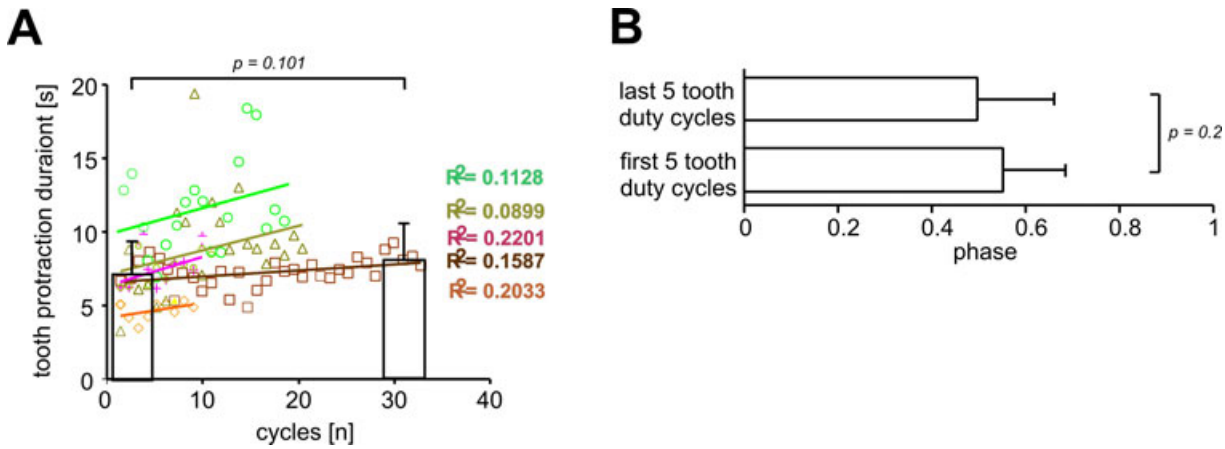

Figure 34: Tooth protraction did not change during some POC-elicited gastric mill rhythms. **A** Tooth protraction duration of ***5*** animals (colored data points) is plotted over the number of cycles after the end of POC stimulation. Linear fits to these data points are also shown (straight lines). The bars show mean data from the first ***5*** (left bar) and the last ***5*** interburst cycles (right bar). **B** shows average protraction duty cycles of the first ***5*** (bottom bar) and the last ***5*** cycles (top bar) relative to gastric phase.

These results show that POC-elicited gastric mill rhythms are more variable *in vivo* than *in vitro*. Interestingly, the variability of the duration of all protractions was similar in all POC-elicited rhythms. The standard deviation (as a marker of variability) was not significantly different between the "constant" (***8.9 ±4 s***) and the "variable" (***7.7 ±1.4 s***) versions of POC-elicited gastric mill rhythms (***p=0.29***, Student's t-Test, ***N = 5***).

4.2.2.4 Protraction movement of teeth during VCN-elicited gastric mill rhythms does not change over time

In the following the analysis of the gastric mill teeth movements during VCN-elicited patterns was performed analogous to the previous chapter. Figure 35 shows data from one experiment, in which stimulation of the VCN neurons successfully initated a long-lasting gastric mill rhythm. The cardiac gutter was stimulated for less than ***10 s*** and after several initial protractions, a VCN-type rhythm started. This concurred with previous stimulations of the VCNs in the *in situ* preparation (Beenhakker et al. 2004). The first full protraction cycle is marked as ***#1*** in the figure. Compared to the last protraction (#14) shown in the sequence, no difference in duration and amplitude could be detected visually in the movement trajectory. In all experiments the stimulus was applied for ***2 - 20 s*** and a gastric mill rhythm started ***5 - 10 s*** after stimulus initiation.

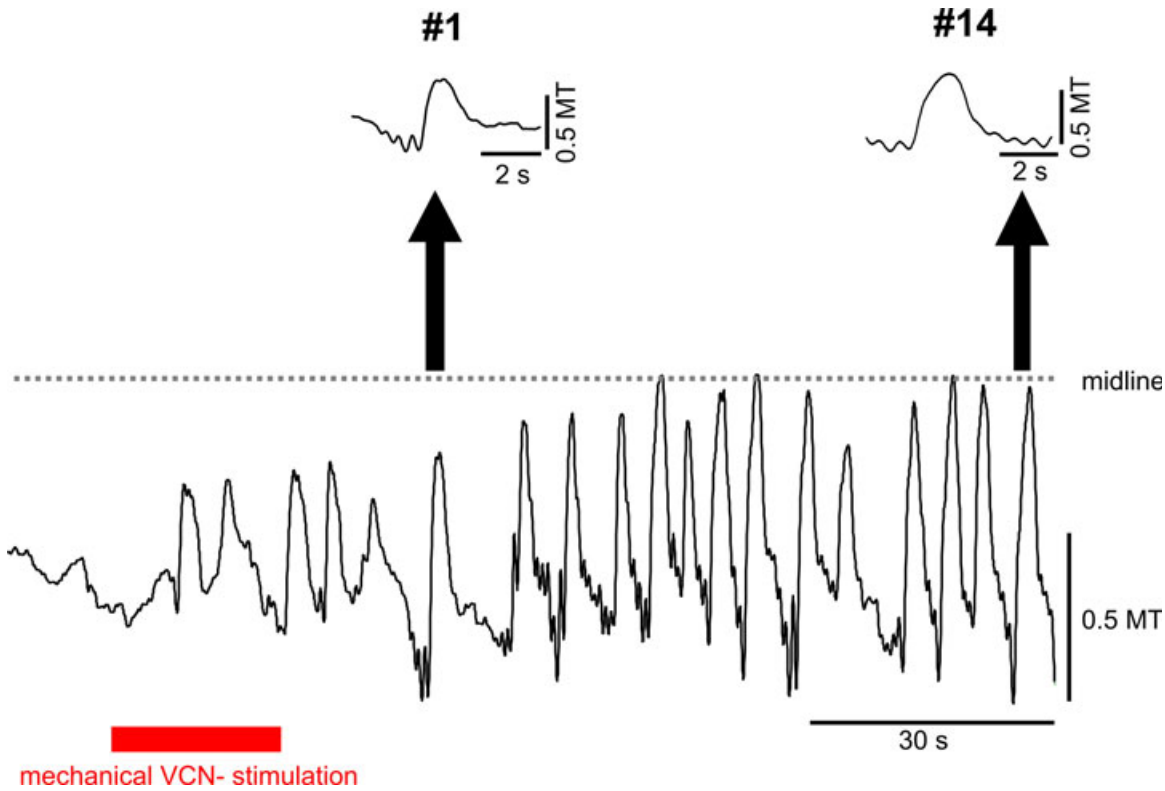

Figure 35: Example of a succession of tooth protractions during a VCN-elicited gastric mill rhythm. Tooth movement output in one animal after VCN stimulation (red bar) is shown. The protraction duration of the first burst (***#1***, inset above), similar to that of the 14th burst in the sequence (***#14***, inset above). Note that protraction is represented by upward deflection.

10 specimen showed successful initiation of a VCN-elicited gastric mill rhythm and also persistent rhythmic activity for at least ***9*** cycles. The cycle period was calculated by measuring from onset of tooth protraction to the next onset. The averaged values and standard deviations of the first and last ***5*** cycles of each gastric mill rhythm are shown as bar graphs in figure 36 A. The analysis shows that there was no statistical significant difference between the initial and final cycles produced during mechanically elicited VCN-type gastric mill rhythms (***p=0.23***, Rank Sum Test, ***N=5***). Thus, the VCN-elicited gastric mill rhythms show a similar amount of variability compared to the POC-elicited gastric mill rhythms (see fig. 31). The duration of each protraction of the teeth was also analyzed. The summarized data in the protraction durations figure 36 B shows that duty cycle of protraction phase relative to the gastric mill phase did not significantly vary between the initial ***5*** protraction and the final ***5*** protractions (***p=0.4,*** Rank Sum Test, ***N=5***).

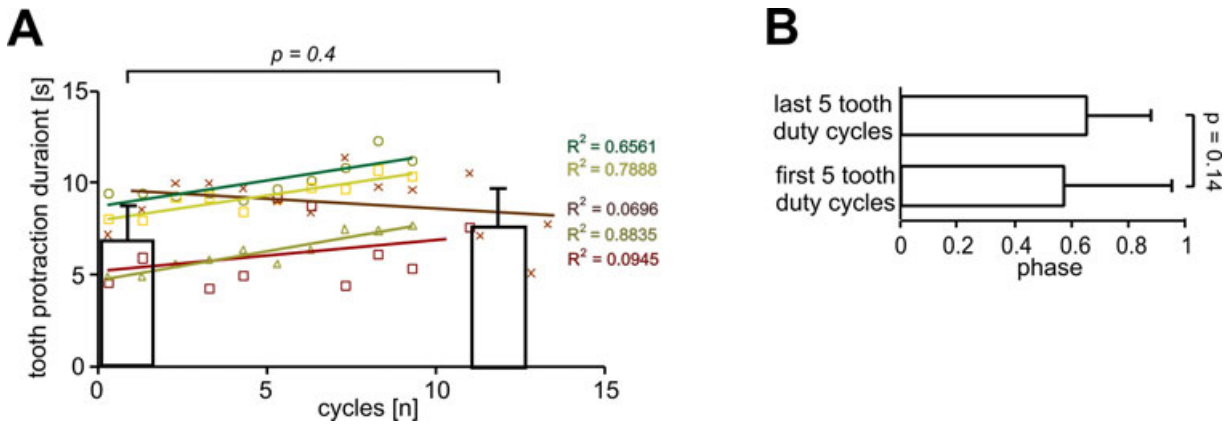

Figure 36: Statistical analysis of constancy of tooth movements during VCN-elicited gastric mill rhythms. **A** Tooth protraction duration of ***5*** animals (colored data points) is plotted over the number of cycles after the end of VCN stimulation. Linear fits to these data points are also shown (straight lines). The bars show mean data from the first ***5*** (left bar) and the last ***5*** interburst cycles (right bar). **B** shows average protraction duty cycles of the first ***5*** (bottom bar) and the last ***5*** cycles (top bar) relative to gastric phase.

These analyses show that duty cycle as well as protraction duration do not vary significantly during mechanically elicited VCN-type gastric mill rhythms. It is also worthy to note that the VCN-elicited gastric mill rhythms were shorter than the POC-elicited gastric mill rhythms. The POC-elicited rhythms were ***5*** to ***17*** cycles long, the VCN-elicited rhythms, however, were ***6*** to ***26*** cycles long (no significant difference: ***p=0.14***, Student's t-Test, ***N=5***).

4.2.3 Summary and characterization of VCN- and POC elicited rhyhms *in vivo*

The neuronal data, which has been obtained *in vivo* (see chapter 4.2.1 on page 48) showed high variability in parameters such as intraburst spike freqency and burst duration, which are likely to be important parameters for movement output. Despite this high variability it was possible to discriminiate the movement outputs elicited by the two activation pathways. The VCN-pathway elicited short protraction movements of the lateral teeth with fast pro- and retractions. The POC-pathway elicits longer movements of the lateral teeth with pyloric-timed gaps during the protraction phase.

The variability of duty cycles during gastric mill rhythms was also investigated and differences between the two types of gastric mill rhythms were found. The VCN-elicited gastric mill rhythms showed constant duty cycles the course of a rhythm. Not all POC-elicited GMRs did show this continuity. In several cases (***N=4***), the initial pro-

tractions resembled the VCN-elicited patterns in that they were shorter in duration and missing the pyloric timing. These types of protractions always occured at the beginning of a rhythm. Duty cycles were also shorter in this part of the gastric mill rhythm, underlining a faster rhythmic activity. The final cycles in these rhythms exhibited longer protraction durations as well as longer cycle durations. On the other hand I also observed POC-type gastric mill rhythms, which showed constant protraction and duty cycles. These types of rhythms were slower that the VCN-type gastric mill rhythms and each protraction of the lateral teeth showed pyloric-timed interruptions.

4.3 Application of *in vitro* spike patterns in the *in vivo* preparation

The rhythmic activities of the motor neuron LG were highly variable *in vivo*. Many factors could cause this variability, including sensory feedback and neuromodulator actions that affect the gastric mill CPG. In *in vitro* experiments the activity patterns are usually more constrained. To test whether these characteristics of the *in vitro* patterns are mapped onto the teeths' movements. To test whether the obtained *in vivo* rhythms, and the differences found between them can be attributed to the pathways stimulated (VCN vs. POC) - as opposed to influences from other sensory or modulatory structures - gastric mill tooth movements during motor neuron stimulation, with patterns that were recorded previously, were performed. Three samples types of POC-like patterns of LG bursting obtained from *in vitro* experiments and three samples of VCN-like burst patterns (obtained from a total of ***6*** *in vitro* preparations) were used. Each of these ***6*** patterns contained ***10*** consecutive LG bursts. They were selected to represent the range of obtained gastric mill rhythm *in vitro*.

The *in vitro* data sets were then used as stimuli in the *in vivo* preparation to selectively activate the lateral teeth protactor muscles and record the lateral tooth movement. This movement output was analyzed and compared to the *in vivo* data presented in the previous section. To exclude perturbations from the intrinsic activity of STG neurons, the motor nerves were between the STG and the stimulation electrode (see chapter 3.2.1.1 (page 26). This guaranteed selective stimulation of the motor neurons and eliminated backpropagation of action potentials to the LG soma or other STG neurons.

4.3.1 Quantitative analysis of differences between two types of *in vitro* patterns

To choose patterns that were easily identifyable as "POC-like" and "VCN-like" all available data was analyzed for burst duration, interburst duration and interspike interval duration. The mean values of these parameters have been presented in chapter 4.2.1 and chapter 4.2.2 and are presented again in this chapter in graphical form in figure 37. The term "-like" was chosen to emphasize that these spike patterns were elicited during *in vitro* experiments with most of the sensory feedback as well as interneuronal pathways severed or at least partly interrupted.

The chosen POC-like and VCN-like data sets should be as variable as possible to ensure that a broad spectrum of rhythmic patterns is used for stimulation. The top three rows of figure 37 A and B show sections of three bursts of the complete sets of *in vitro* recordings used for stimulations (total sets contained ***10*** bursts each). However, the variability of burst duration, interburst duration and interspike interval duration is rather low within each given data set. This is emphasized by the lines (representing the linear regression for each data set) added in figure 37 A and B. The lines representing the fits are all parallel and do not deviate significantly from each other in terms of slope, except for parameter "burst duration" in the dataset "POC 3". This example of a POC-elicited *in vitro* gastric mill rhythm shows a decrease in burst duration from burst ***#1*** (longest duration) to burst ***#10*** (shortest duration). The other parameters of POC 3 (and the other patterns) showed no such change over time. A quantitative analysis between the different rhythms was performed by calculating the averages over all ***10*** bursts from each data set.

The POC-like bursting shows the already described pyloric gaps. These gaps produce shorter segments of spike activity within a burst ("burstlets"). The same parameters assessed previously (burst duration, interburst frequency and ISI) were gathered for the burstlets in the POC-like data sets (see fig. 38).

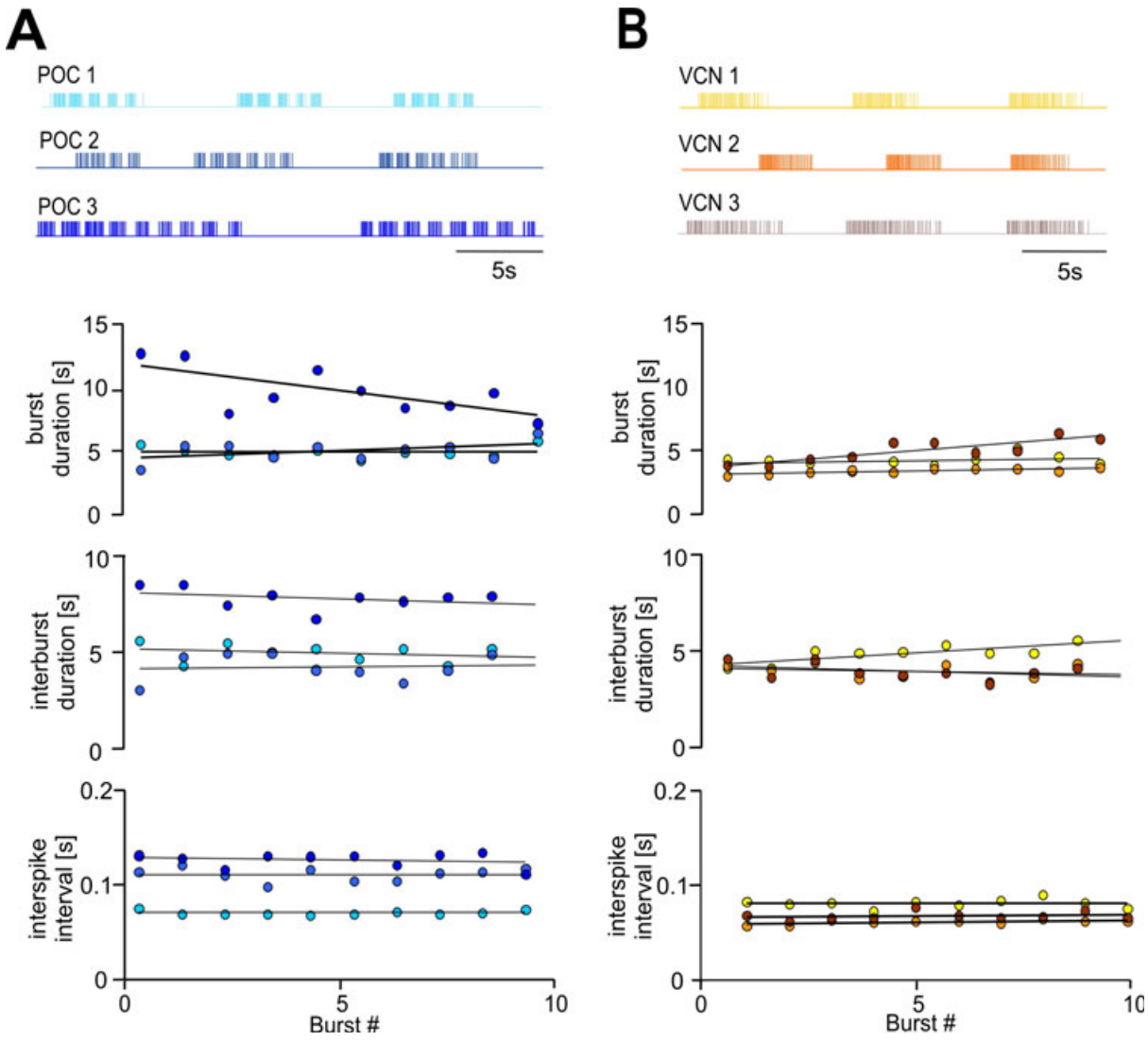

Figure 37: Diagrams showing several parameters of LG activity during POC- and VCN-elicited gastric mill rhythms. **A** shows three bursts of each POC-like patterns (light to dark shades of blue represent POC patterns 1-3). Below, mean burst duration, interburst duration and mean interspike interval (ISI) are shown. **B** shows same for VCN-like patterns (light to dark shades of orange represent VCN patterns 1-3). Black lines represent linear fits for each data set.

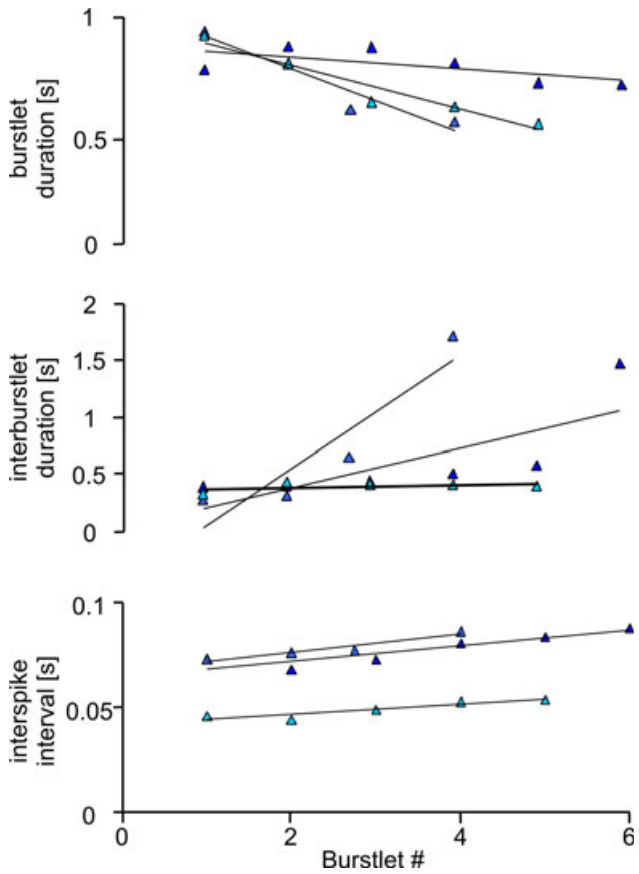

Figure 38: Diagrams show mean burstlet duration (top), interburstlet duration (middle) and mean interspike interval (ISI, bottom) during LG burstlets. Mean ISIs are shorter than those of the whole burst (see fig. 37) because the long ISIs between burstlets are not present here. Black lines represent linear fits for each data set.

The burstlet duration decreased in the course of each bursts, recognizable by the downward slope of the lines representing the linear fit for each data set. The *in vitro* data sets were also analyzed quantitatively. This is summarized in figure 39. The same parameters presented before (burst duration, interburst duration, number of spikes per burst and interspike intervals) were calculated for all ***10*** bursts within each data set and was then averaged. The graph in figure 39 A i) shows significant longer burst durations in the POC ***#3*** data set compared to the other two data sets ***#1 & #2*** (***p<0.001***, One Way ANOVA with Tukey post-hoc test, ***N=5***). The VCN data set ***#2*** showed significantly shorter average burst duration compared to the other two data sets #1 and ***#3*** (***p<0.05***, One Way ANOVA with Tukey post-hoc test, ***N=5***).

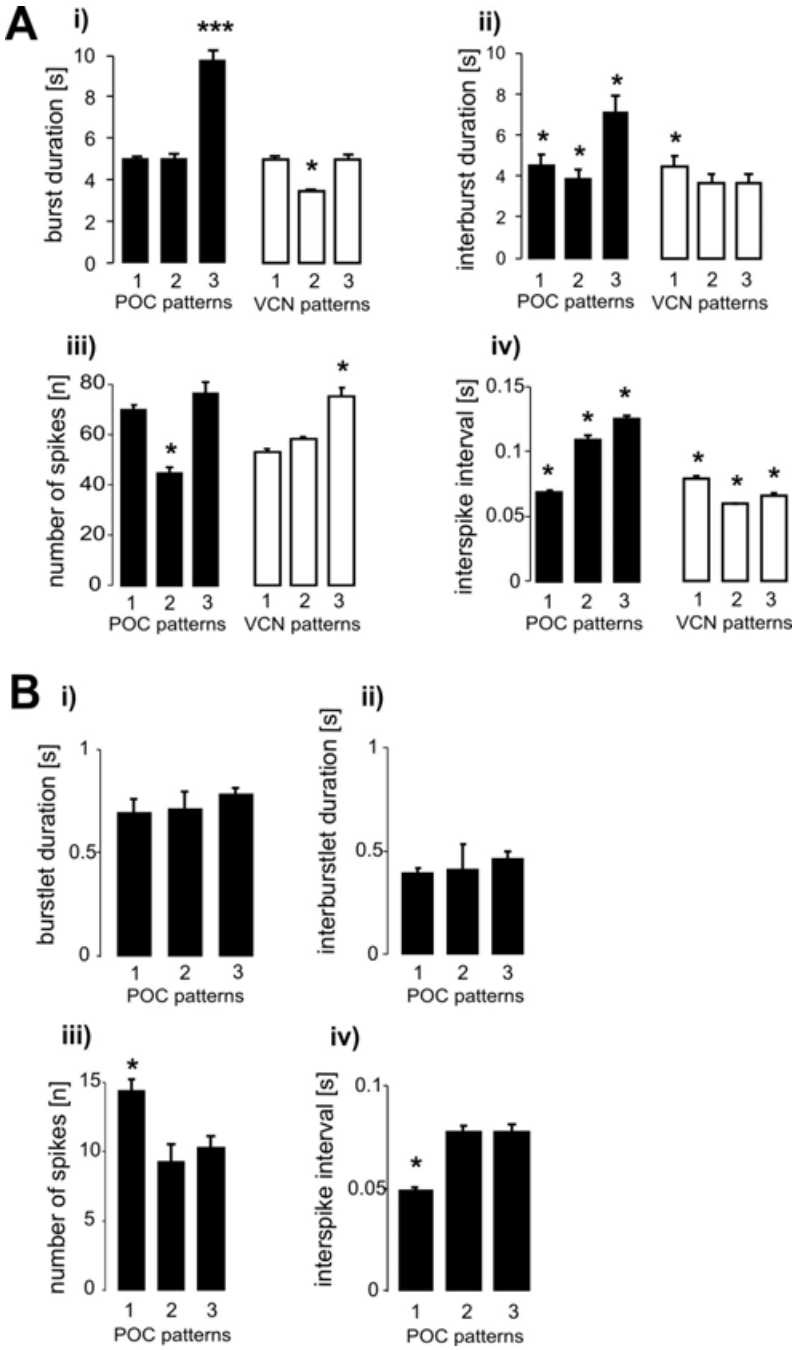

Figure 39: Quantitative analysis of LG activity during POC- and VCN-GMRs elicited *in vitro*. **A** shows LG activity parameters burst duration **(i)**, interburst duration **(ii)**, number of spikes per burst **(iii)** and interspike interval **(iv)** for POC-type rhythms 1-3 (black boxes) and VCN-type rhythms 1-3 (white boxes). **B** shows parameters of each burstlet during POC-type rhythms: burstlet duration **(i)**, interburstlet duration **(ii)**, number of spikes per burstlet **(iii)** and interspike interval **(iv)**. For legibility significance levels in all plots are indicated as follows: $p<0.05$ = ***** ; $p<0.001$ = *******. VCN data sets were compared among themsevles, as were the POC data sets.

The interburst durations of each POC-type rhythm differed significantly from each other (***p<0.05***, One Way ANOVA with Holm-Sidak post-hoc test, ***N=5***, see fig. 39 A ii)), which, in combination with the rather constant burst duration (see fig. 39 A i)), suggests that the gastric mill cycle periods were also variable in these *in vitro* preparations.

In the preparations, which displayed a VCN-type rhythm, only one data set (VCN ***#1***) differed significantly from the other two (***p<0.05***, One Way ANOVA with Tukey post-hoc test, N=5, see fig. 39 A ii)). The number of spikes was high during POC data sets ***#1 & #3***, and significantly lower during POC data set ***#2*** (***p<0.05,*** One Way ANOVA with Holm-Sidak post-hoc test, ***N=5***, see fig. 39 A iii)). As can be seen in figure 39 A iv), the average interspike intervals vary greatly between all three POC patterns (all ***p<0.05***, One Way ANOVA with Holm-Sidak post-hoc test, ***N=5***, see fig. 39 A iv)). The interspike intervals of the three VCN data sets was variable as well (all ***p<0.05***, One Way ANOVA with Holm-Sidak post-hoc test, ***N=5***, see fig. 39 A iv)).

Further analysis of the burstlets within the POC-LG bursts revealed that the burstlet characteristics varied little among all three patterns. The interspike intervals during the POC data set ***#2*** were significantly shorter compared to the other two data sets (***p<0.05,*** One Way ANOVA with Holm-Sidak post-hoc test, ***N=5,*** see fig. 39 B iv)). The low interspike intervals in the burstlets of this data set correlate with the high number of spikes in this same dataset (see figure 39 B iii), which was significantlz higher compared to the other two data sets (***p<0.05,*** One Way ANOVA with Holm-Sidak post-hoc test, ***N=5***).

This detailed analysis of the characteristic spike patterns of LG recorded *in vivo* allowed for a better appreciation of the tooth movements and the muscle contractions elicited by the stimulation of both with these recorded data sets.

4.3.2 Distinct characteristics in lateral tooth movements during stimulation with *in vitro* patterns

After the analysis of the motor neuronal data gathered *in vitro,* this data was used for stimulation in the *in vivo* preparation. The purpose of these experiments was to test whether POC and VCN elicited motor activity elicited functionally different behaviors. Here POC and VCN patterns were compared without the effects of other sensory inputs or neuromodulatory influences. A total of ***5*** animals was used for these experiments. All motor nerves were transected and the *lvn* was used to simulate LG activity The movement output of the teeth was monitored via the endoscope.

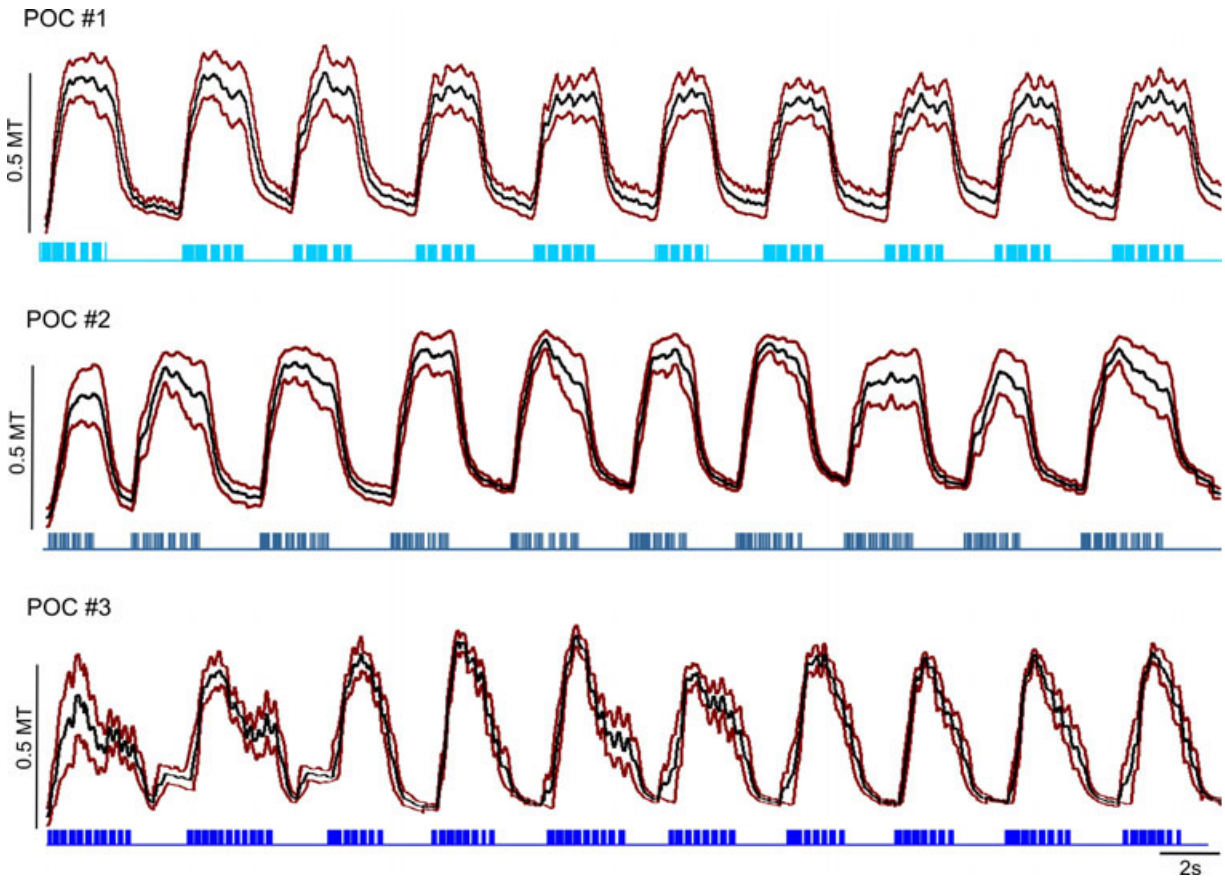

Figure 40: Lateral tooth movements elicited by stimulation with three POC-like *in vitro* patterns. All ***10*** bursts of each data set (POC1-3) and the average movement outputs of the lateral tooth (***N=5***) are shown. Black traces represent mean values, red traces represent standard deviation from the mean.

The averages from all preparations stimulated with the three *in vitro* POC-like patterns are shown in figure 40. The movement elicited by all three data sets reached similar peak amplitudes of protraction (all data sets: ***0.53 ± 0.08 MT***). Main characteristic of the patterns POC ***#1 & #2*** was that the pyloric-timed twitching of the teeth occured during a plateau-like phase (see fig. 40, top and middle traces). Concurrence of short inter-burstlet duration and high intra-burstlet spike frequency during the initial phase of the bursts resulted in a fast and large initial protraction, which ended in a plateau-like state (see fig. 40 bottom). This is shown in detail in figure 41, which shows a single protraction from one preparation during a burst of stimulus pattern ***#1***.

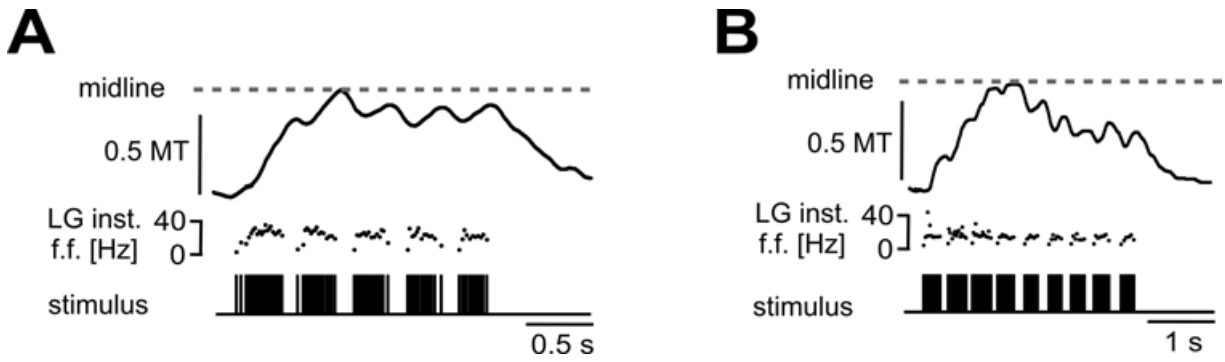

Figure 41: Two individual POC-like LG bursts and resulting tooth movements. **A** shows protraction of left lateral tooth (top) caused by single burst from POC-like stimulus pattern ***#3*** (bottom). Instantaneous firing frequency of stimulus is also shown (middle). **B** shows same for a single burst from POC-like stimulus pattern ***#1***. Note the differences in the time scale bars.

The POC-like stimulus-pattern ***#3*** showed the longest burstlet duration and lowest spike frequency compared to the other two data sets. This combination of parameters resulted in a larger retraction movement during the LG burst (while pyloric-timed twitching occured (see fig. 40, bottom trace)). To show this more clearly, figure 41 B shows a single protraction during POC-like pattern ***#3***.

The analysis of the movement output of the gastric mill teeth during stimulation with VCN-like data sets was performed as well. In contrast to movements elicited by POC-like patterns, the trajectory was smoother during VCN-like stimulations. The tooth movements elicited by all three VCN-like data sets reached similar peak protraction amplitudes (all data sets: ***0.53 ±0.05 MT***).

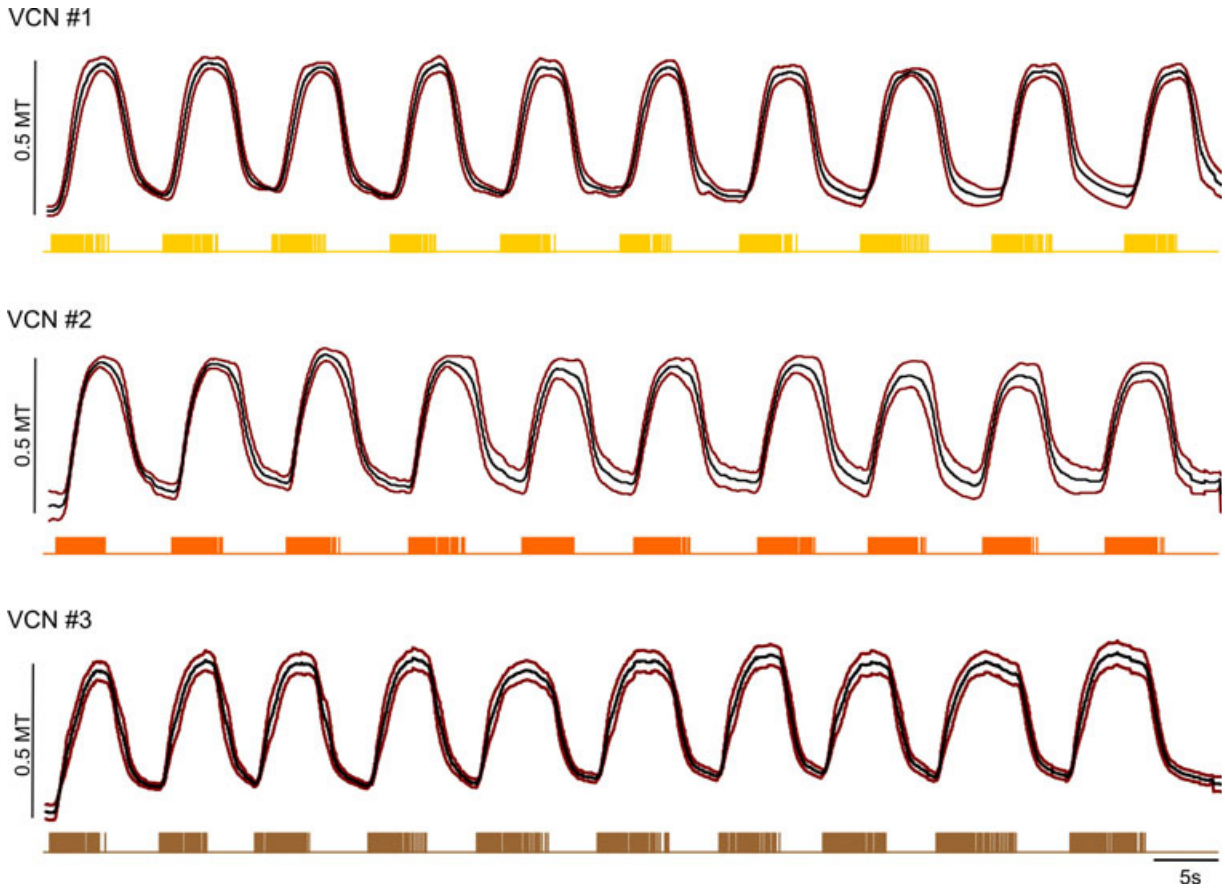

Figure 42: Tooth movements elicited by stimulation with three VCN-like *in vitro* patterns. All 10 bursts of each data set (VCN1-3) and the average movement outputs of the lateral tooth (N=5) are shown. Black traces represent mean values, red traces represent standard deviation from the mean.

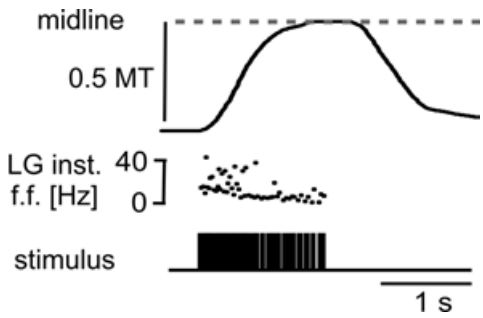

Figure 43: One individual VCN-like LG burst and resulting tooth movement. Protraction of left lateral tooth (top) caused by single burst from VCN-like stimulus pattern #2 (bottom) is shown. Instantaneous firing frequency of stimulus is also shown (middle).

This constancy in motor neuronal firing was mapped onto the movement output of the teeth, shown in figure 42. Similar to the tooth movements during stimulation with POC-like patterns, the protraction phase begins with a steep initial contraction of the tooth. This contraction was, however, smoother since pyloric-timed gaps were missing in the bursts (see fig. 43).

Additionally, a persistent protraction for the duration of the burst was achieved, which is shown in more detail in figure 43. In contrast, in some of the POC movement patterns (for example fig. 41 B), the maximum protraction of the tooth was only fully reached for a short period during the LG burst.

To quantify the apparent differences between POC-like and VCN-like patterns on the behavioral level, two parameters of movement output were selected. Firstly, the average maximal amplitudes of protraction were calculated for all patterns (POC *1-3* & VCN *1-3*). There was no significant difference in maximal protraction amplitude, neither between the different POC-like data sets (POC *#1: 0.54 ±0.08 MT*; POC *#2: 0.5 ±0.07 MT*; POC *#3: 0.56 ±0.08 MT*), nor VCN-like data sets (VCN *#1: 0.44 ±0.03 MT*; VCN *#2: 0.53 ±0.05 MT*; VCN *#3: 0.62 ±0.08 MT*, see fig. 44 A), nor between POC-like and VCN-like patterns (*p>0.18* for all comparisons*,* ANOVA with Repeated Measures, *N=5*). Thus, analogous to the tooth movement after stimulation of the POC itself (see chapter 4.2.2 on page 53 ff.), the pyloric-timed gaps in the LG burst during the POC-like stimulation of the motor neuron did not diminish maximum protraction amplitude.

Secondly the duration of the plateau phase of each protraction was calculated analogous to the method described in chapter 4.2.2.1 . The average maximum protraction durations (plateau phases) of movement were thus significantly longer during VCN-like stimulations (VCN *#1*: *1.9 ±0.1 s*; VCN *#2*: *1.9 ±0.2 s*; VCN *#3*: *2.4 ±0.2 s*), compared to the POC-like patterns (POC *#1*: *0.29 ±0.2 s*; POC *#2*: *0.36 ±0.3 s*; POC *#3*: *0.44 ±0.3 s*) with pyloric-timed interruptions (*p<0.001;* ANOVA with Repeated Measures, *N=5,* and see fig. 44 B).

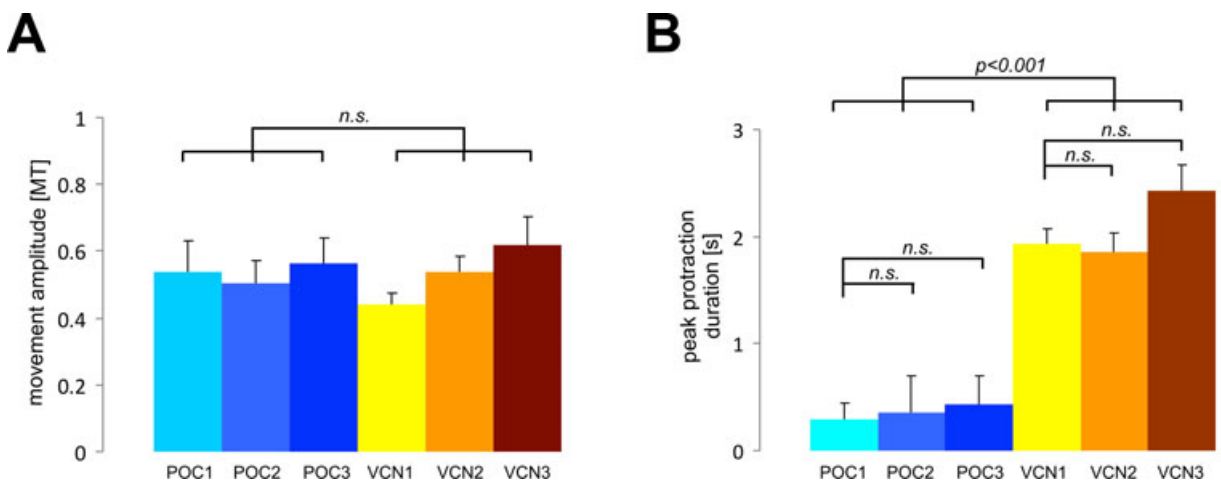

Figure 44: POC-and VCN-type stimulation elicit similar protraction peak amplitudes while protraction duration showed significant differences. **A** shows the amplitudes of protraction in medial tooth widths (MT) during POC-like stimulations (shades of blue) and VCN-like stimulations (shades of yellow). **B** shows durations of maximal protractions during POC-like stimulations (shades of blue) and VCN-like stimulations (shades of yellow).

The duration of the protraction plateau was therefore sufficient to separate POC-like from VCN-like patterns on the behavioral level. In addition, the protraction movement during the POC-like stimulation was not continuous, but rather showed many rippels that appeared to be caused by the pyloric-timed interruptions in the LG burst.

To test this, the movement trajectories were examined for inflection points, analogous to the anlysis shown in chapter 4.2.2.1 (page 56). For each POC-like stimulus pattern the number of (positive and negative) inflection points in the elicited protraction movement was determined (POC *#1*: *8.38 ±1.2*; POC *#2*: *6.34 ±1.1*; POC *#3*: *11.62 ±1*). Surprisingly, the number of inflection points in the movement trajectory was lower than the number of burstlet onsets & ends in the stimulation patterns (POC *#1*: *9.6*; POC *#2*: *9*; POC *#3*: *15.8*). The reason for this was that the first burstlets, which occured in the POC-like stimulation possessed short interburstlet intervals, which resulted in a steep increase in tooth protraction amplitude (figure 41 B). Intervals were too short for the muscle to exhibit relaxation, thus enabling stronger protraction, and resulting in a smoother protraction trajectory at the beginning of a burst with fewer inflection points.

The number of (positive and negative) inflection points in the tooth movement trajectory were examined for the VCN-like stimulations as well. The number of burstlets was *0* in these stimulations, therefore burst onset and end were counted for each stimulation pattern (VCN *# 1-3*: *2*). The number of inflection points in the movements

were: VCN *#1*: *2.28 ±0.4*; VCN *#2*: *2.16 ±0.3*; VCN *#3*: *2.48 ±0.2*, which matched very well the fact that now pyloric-timed interruptions in the LG burst during these stimulations. Therefore the number of inflection points during gm6 contractions was higher than the number of burst onsets and ends per VCN-like burst. The number of inflection points in the tooth movement elicited by VCN-like stimulation was thus also significantly lower compared to the tooth movement during POC-like stimulation (*p<0.001*, paired t-Test, *N=5*).

This analysis does not appreciate the qualitiy of tooth movement changes. All inflections in the tooth movement were counted, indifferent on the amplitude or trajectory slope. Therefore, in analogy to the analysis shown in figure 27, the pyloric timing of the tooth movement was analyzed. Since the nervous system was decentralized in this preparation the PD bursts were not measured via *in vivo* nerve recordings but were inferred from the *in vitro* burst patterns. In case of the POC stimulation the duration of each gap in the LG bursting patterns was determined and the velocity of movement was calculated before and during the gap. The results are shown in figure 45 A. After each LG burstlet onset the teeth started their protraction movement. Black dots show the velocities occuring during the "before LG burstlet" time-frame; the grey dots show velocities during the "after LG burstlet" time-frame, respectively. Positive velocities occurred during the interburstlet intervals ("before LG burstlet"), while negative velocities occurred after the intervals ("after LG burstlet"). The protraction velocities before a pyloric-timed LG burstlet were shifted into the positive regime (*mean: 0.32 MT/0.12 s; 95%-ile: 1.3 MT/0.12 s; 5%-ile: -0.5 MT/0.12 s*).

The protraction velocities after a pyloric-timed LG burstlet were shifted into the negative regime (*mean: -0.4 MT/0.12 s; 95%-ile: 0.2 MT/0.12 s; 5%-ile: -1.4 MT/0.12 s*). The boxplots and statistical analyses were performed on the averaged data from each preparation. There was a statistically significant difference between the slopes (*p<0.05*, U-Test, *N=5*). To analyze the tooth movements elicited by VCN-like stimuli, the movement trajectories were subdivided into segments of *0.79 s* duration. Due to the continuous spike distribution in LG bursts continuous protractions were elicited (see fig. 42 and fig. 43).

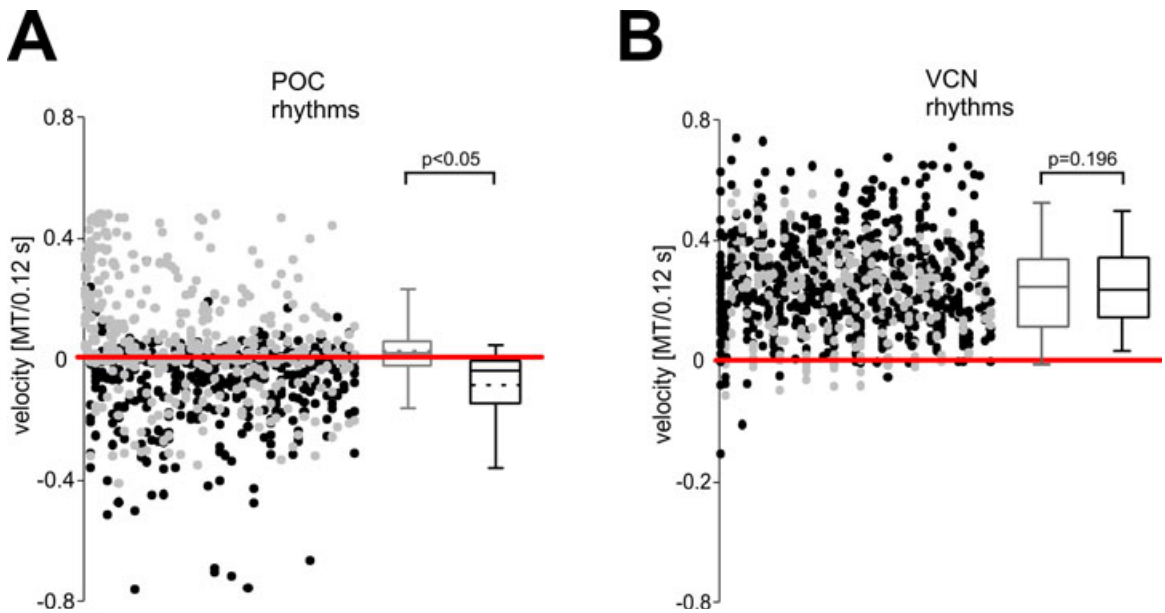

Figure 45: Changes in movement slope during pyloric-timed LG burst interruptions. **A** shows lateral tooth movement velocities during stimulation with LG activity during POC-elicited GMRs *in vitro*. The velocities occuring ***200 ms*** before LG-burstlet onset are shown in grey; velocities occuring ***200 ms*** after burstlet onset are shown in black. Distribution of velocities around pyloric-timed burstlet onsets is shown as box plots. Whiskers represent ***5-95 percentiles***; boxes represent ***25-75 percentiles***; median (straight line) and average (dashed line) are shown. **B** shows same for the stimulation with LG activity during VCN-elicited GMRs *in vitro*.

Analogous to the method described in chapter 4.2.2.1 (page 56), this duration was used to calculate the velocities of movement of the lateral tooth during the VCN-type stimulations figure 45 B. Similar to the POC-like stimulation, the protraction velocities before a pyloric-timed segment were shifted into the positive regime (***mean: -0.9 MT/ 0.12 s; 95%-ile: 2 MT/0.12 s; 5%-ile: -0.08 MT/0.12 s***). The protraction velocities after a pyloric-timed segment, however, were shifted into the positive regime as well (***mean: 1 MT/0.12 s; 95%-ile: 1.9 MT/0.12 s; 5%-ile: -0.2 MT/0.12 s***). There was no statistical difference between the velocities of movement before and the velocities after a pyloric segment during the VCN-elicited gastric mill rhythms (***p=0.196***, One Way ANOVA with Tukey post-hoc test, ***N=8***). The fact that more than ***80%*** of all velocities were positive indicates that the protraction movement was rather continuous and not interrupted by pyloric events.

4.4 The gm6 muscle faithfully reproduces stimulations with *in vitro* patterns

Clearly, VCN and POC-like patterns could be separated on the movement level. It is still unclear, however, how these differences are achieved. It is possible that steric properties of the stomach ossicle anatomy enable this behavior and that the combined activities of many muscles is necessary to faithfully reproduce VCN and POC rhythms. Another possibility is that even single muscles show dynamics, which enable them to produce contractions wich are tightly tuned to the spike pattern of the motor neuron.

To investigate this, I conducted *in situ* experiments (see chapter 3.2.2 on page 30) on the gm6 muscle. This muscle is one of the three muscles, which are innervated by LG and are part of the protractor-system of the lateral teeth (see chapter 4.7.1 on page 108). This muscle was investigated previously, and structure of sarcomeres (Jahromi & Govind 1976; Thuma et al. 2007) as well as contractile properties *in situ* (Stein 2006) are partially known. It was shown that amplitudes of excitatory junction potentials (EJPs) in the gm6 muscle were significantly higher when stimulated with standardized VCN-type bursts, compared to stimulations with standardized POC-type bursts (White 2011 page 150). Consequently, contraction force was different between the two rhythms. The question therefore remained why lower force amplitudes do not translate into lower tooth (protraction amplitudes of VCN-like and POC-like rhythms were not statistically different, see fig. 44).

Since the experiments by White (2011) tested the gm6 muscle properties by stimulations with standardized patterns (derived from averaged *in vitro* data), I conducted experiments on the gm6 muscle *in situ* as well, but applied the 6 types of stimulus patterns, which were already used in the *in vivo* stimulations described in chapter 4.3 (page 69). These patterns were not averaged, and therefore represent the natural spiking of LG. Comparing the *in situ* data with the standardized stimulations *in situ* and with the data from *in vivo* stimulations should shed some light on the effects of dynamics of a single muscle onto the movement in gastric mill.

4.4.1 Distinct characteristics of *in situ* muscle contractions during stimulation with *in vitro* data

A total of ***8*** preparations were stimulated with the VCN-like patterns as well as the POC-like patterns. Stimulations were applied via extracellularly, as described in chapter 3.2.2 (page 30). The elicited force trajectories are shown in figure 46 and figure 47.

Similar to the tooth movement elicited by stimulation with the *in vitro* data sets, the gm6 muscle showed a steep increase in the force trajectory, i.e. quick initial contraction during the stimulation with the POC-like data sets (see fig. 46). ***8*** of ***10*** bursts in the POC-like data set ***#1*** show a plateau during the contraction phase. Comparing this data to the *in vivo* experiments shown in chapter 4.3 (page 69) shows similarity in this aspect of the activity, since the tooth movements show this plateau during the protraction phase as well. Tight tuning of interburst spike frequency and inter-burstlet interval is responsible for this plateau phase. The POC-like stimulus-pattern #***3*** showed longest burstlet duration, longest inter-burstlet interval and lowest spike frequency compared to the other two data sets. This parameter combination resulted in a drop of contraction amplitude in some bursts while the pyloric-timed twitching occured (see fig. 46, bottom trace). Low intraburstlet firing frequency combined with high variability in burstlet duration and inter-burstlet interval caused more variability in the contractions of the gm6 muscle (POC-like pattern ***#2 & 3***). The strongest difference between *in vivo* and *in situ* POC-like stimulations was the maximum protraction duration (tooth movement) and the maximum contraction duration (gm6 muscle).

The difference between the tooth movement duration and contraction duration during POC-like stimulation was significant for all stimulation POC patterns (for all comparisons: $p<0.001$, One Way ANOVA).

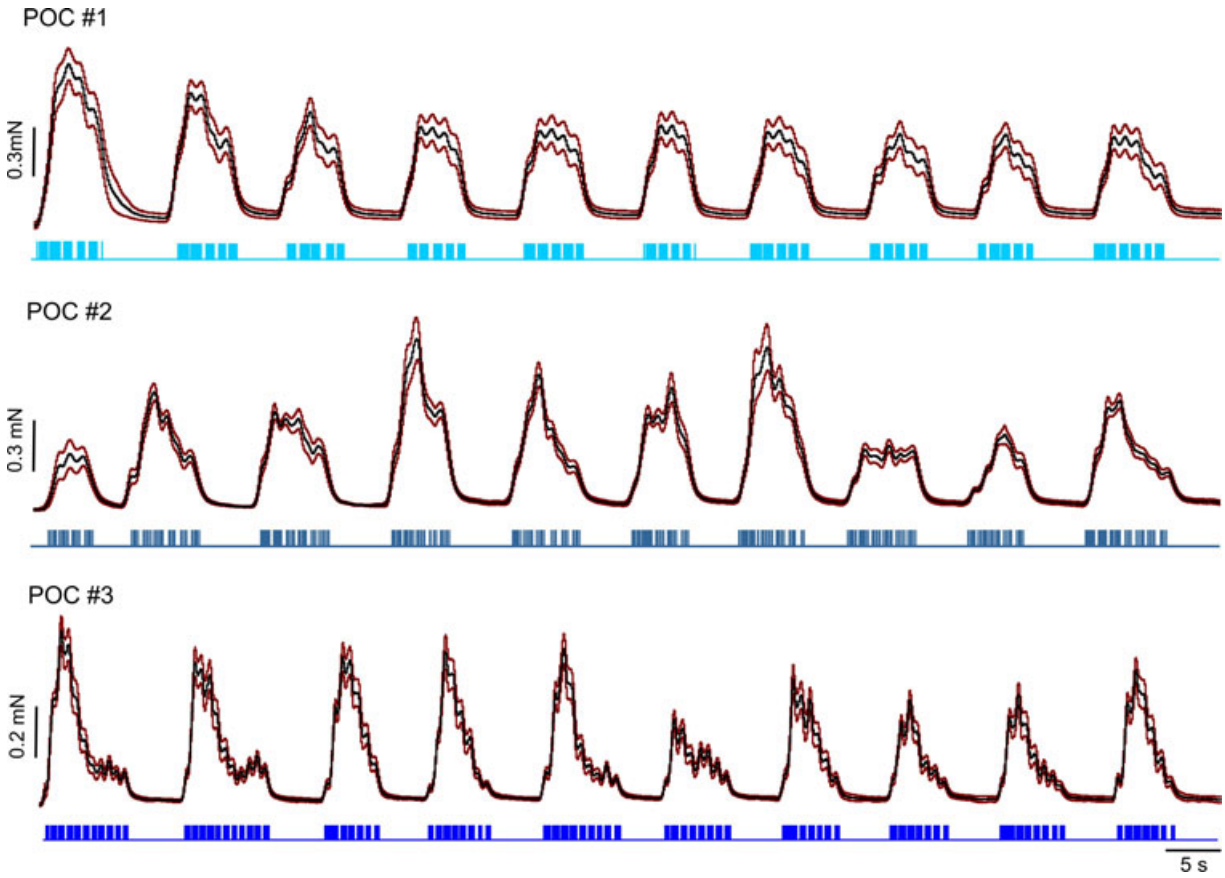

Figure 46: gm6 muscle force elicited by stimulation with three POC-like *in vitro* patterns. All 10 bursts of each data set (POC 1-3) and the average movement outputs of the lateral tooth (N=8) are shown. Black traces represent mean values, red traces represent standard deviation from the mean.

The VCN-like data sets also showed similar activity patterns compared to the *in vivo* tooth movement trajectories (see fig. 47). All three VCN-like data sets showed similar muscle force outputs (VCN ***#1: 0.8 ±0.1 mN;*** VCN ***#2: 1.5 ±0.2 mN;*** VCN ***#3: 0.7 ±0.1 mN***). Similar to the tooth movements *in vivo*, the muscle force depended on the stimulus parameters, such as interburst interval (for example: in VCN data set ***#1***, the interburst interval between gm6 contractions increases as well). All three POC-like data sets also showed similar muscle force outputs (POC ***#1: 0.26 ±0.07 mN;*** POC ***#2: 0.35 ±0.04 mN;*** POC ***#3: 0.33 ±0.02 mN***). Comparing the muscle force output of gm6 muscles during VCN-like stimulation to the outputs during POC-like stimulation shows

that the maximum contraction amplitudes were significantly different from one another (***p<0.05;*** Friedman Ranked Sum Test, see fig. 48 A). There was also a significant difference between VCN-like pattern ***#2*** and the other two patterns (***p<0.05;*** Friedman Ranked Sum Test, see fig. 48 and fig. 47 middle trace).

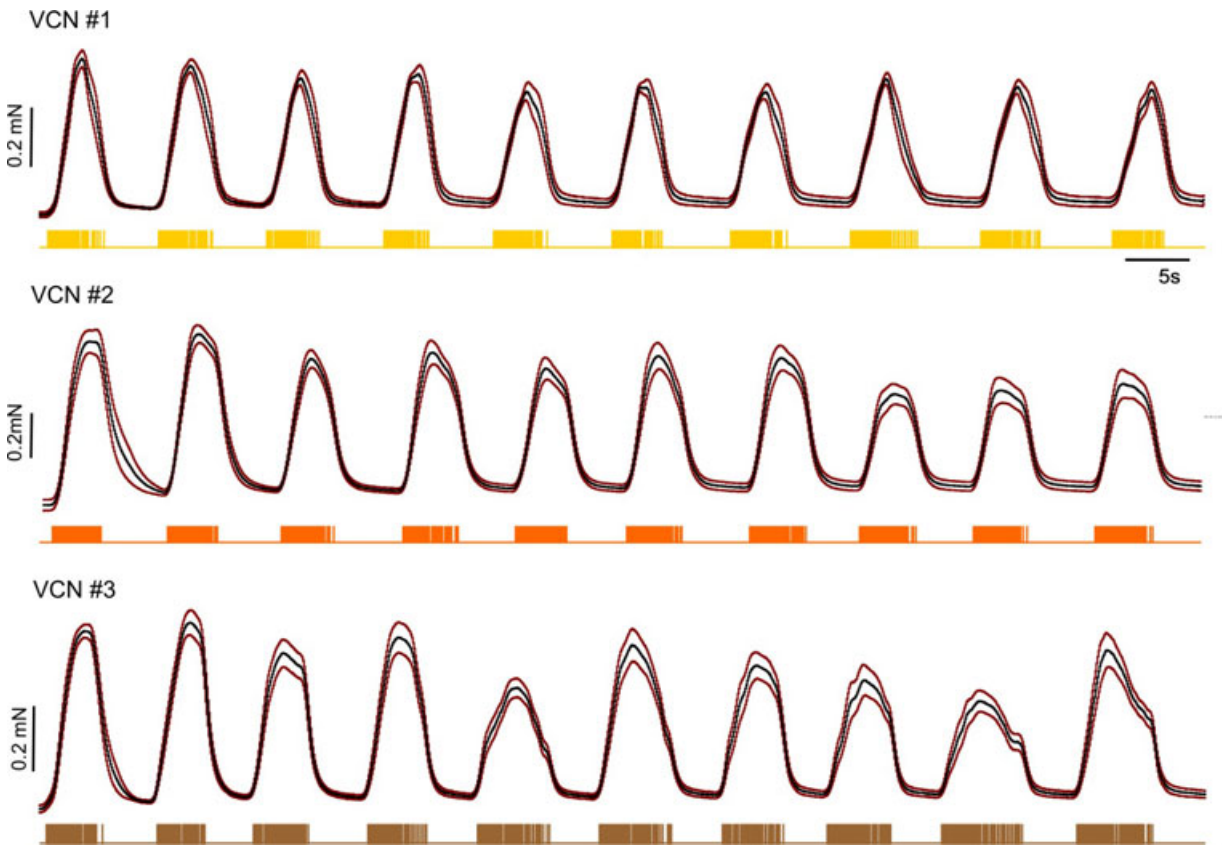

Figure 47: gm6 muscle force elicited by stimulation with three VCN-like *in vitro* patterns. All 10 bursts of each data set (VCN 1-3) and the average movement outputs of the lateral tooth (N=8) are shown. Black traces represent mean values, red traces represent standard deviation from the mean. Note the different scaling compared to figure 48 B.

Also the standard deviations, i.e. the variability was significantly different between the two types of gastric mill rhythms (***p<0.001***, Rank Sum Test).

This shows that, unlike in the *in vivo* experiments, the VCN-like stimulus patterns elicit significantly different maximum force amplitudes in the muscle. The mean interspike interval was lowest in the VCN-like stimulus pattern ***#2***, i.e. intraburst spike frequency was highest in this pattern, which, in the case of the force production, caused significantly higher values. The analysis of the tooth movement *in vivo*, however, did not show comparable differences.

The plateau phase during maximum protraction that was observed in the tooth movements during VCN-like stimulation was not as pronounced in the gm6 muscle force. Muscle relaxation was initiated immediately after the end of the LG burst. Comparing the tooth movement shown in figure 44 B with the force shown in figure 48 B demonstrates that the duration of the plateau was significantly longer for the tooth movement (for all comparisons: ***p<0.001***, One Way ANOVA on Ranks, ***N=8***).

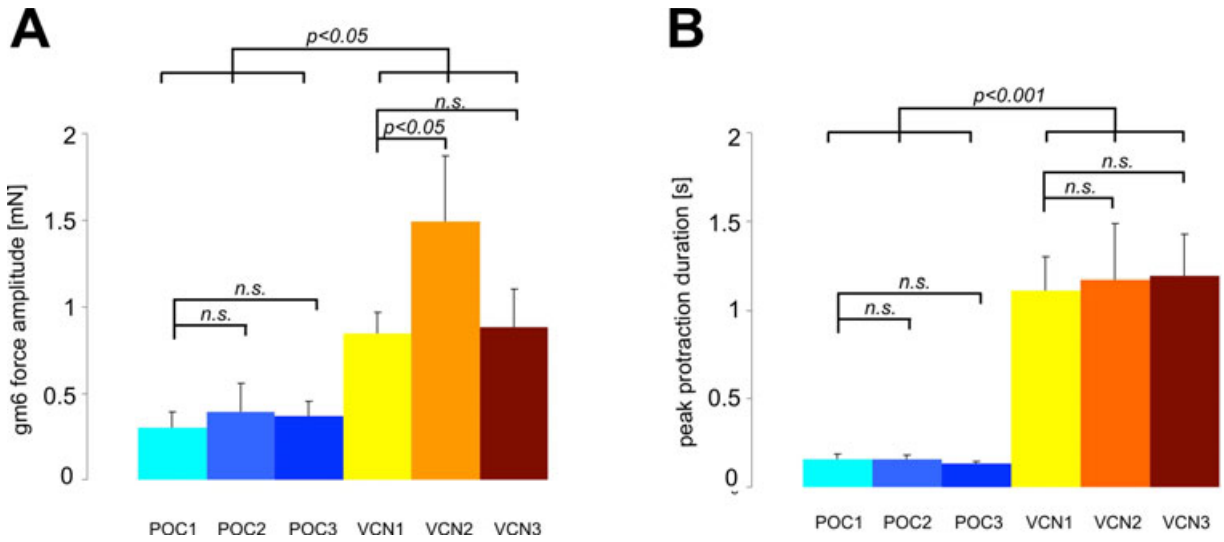

Figure 48: POC- and VCN-type stimulations elicit different force amplitudes and different peak contraction durations in the gm6 muscle. **A** shows the amplitudes of gm6 contraction force output (***mN***) during POC-like stimulations (shades of blue) and VCN-like stimulations (shades of yellow). **B** shows durations of maximal muscle force during POC-like stimulations (shades of blue) and VCN-like stimulations (shades of yellow). Note different scaling compared to figure 44 B.

To test whether muscle force faithfully represented the pyloric gaps in the POC-like pattern, the compliance of the gm6 muscle to the pyloric CPG period has been investigated. The number of (positive and negative) inflection points was measured for all three POC-like patterns (POC 1: ***7.93 ±1.1***; POC 2: ***8.83 ±1.7***; POC 3: ***12.77 ±0.8***). This matched rather well with the number of burstlet onsets and ends in the POC-like stimulation pattern (POC 1: ***9.6***; POC 2: ***9***; POC 3: ***15.8***; also). Similar results for the tooth movement shown in chapter 4.3.2 (page 75), muscle increased without interruption by the pyloric-timed burstlets at the beginning of the LG burst. This was most likely due to the short interburstlet interval and explains the slightly smaller number of inflection points.

The number of (positive and negative) inflection points in the gm6 contraction during the VCN-like stimulations was examined as well. The number of burstlets was *0* in these patterns, but burst onset and end were counted for each stimulus pattern (VCN 1-3: *2*). The number of inflection points in the force trajectory was counted for each pattern (VCN 1: *2.08 ±1.6*; VCN 2: *2 ±0*; VCN 3: *2.2 ±1.6*) and matched very well with the expected number. The number of inflection points during VCN-like stimulation was significantly lower than during the POC-like stimulation (*p<0.001*, U-Test, *N=8*).

A more detailed analysis of the progression gm6 muscle force velocity at the beginning of a pyloric-timed LG burstlet and at the end of a burstlet. Figure 49 A shows the distribution of negative (relaxing) and positive (contracting) trajectory slopes. Due to the response delay of the gm6 muscle to the stimuli the contraction measured before the onset of a burstlet was in fact elicited by the preceding burstlet. The contraction velocities before a pyloric-timed burstlet were thus shifted into the positive regime (*mean: 0.5 mN/0.12 s; 95%-ile: 0.18 mN/0.12 s; 5%-ile: -0.8 mN/0.12 s*). In contrast, the contraction velocities after a pyloric-timed burstlet were shifted into the negative regime (*mean: -0.7 mN/0.12 s; 95%-ile: 0.01 mN/0.12 s; 5%-ile: -0.19 mN/0.12 s*). The statistical analysis showed that the distribution of the contraction speeds was separated according to the pyloric timing (*p<0.001*, U-Test, *N=8*).

Analogous to the analysis described in chapter 4.3.2 (page 75 ff.) the force generated by the VCN-type stimulations was subdivided into pyloric-timed segments (*0.79 s*) corresponding to the interburstlet intervals during standardized POC-type stimulus patterns (see table 2). These segments were equidistant and thus not comparable to the pyloric-timed burstlet intervals during *in vitro* POC-type stimuli. Nonetheless, the subdivision allowed a better appreciation of the contraction process of the gm6 muscle during VCN-type stimulations. Force velocities before a POC-type interval were distributed around the zero line (*mean: 0.05 mN/0.12 s; 95%: 0.23 mN/0.12 s; 5%: -0.18 mN/0.12 s*). Force velocities after a POC-type showed the same result (*mean: 0.05 mN/0.12 s; 95%: 0.21 mN/0.12 s; 5%: -0.17 mN/0.12 s*). There is not significant difference between the two (*p=0.768*, U-Test, *N=8*). Interestingly, the distribution during tooth movement was skewed into the positive regime (see fig. 45 B) while muscle force velocity (see fig. 49 B) was distributed evenly across the negative and positive sectors. This suggests, that the gm6 muscle does not elicit constant force output until the end of the LG burst, but rather decreases force output before the end of the burst.

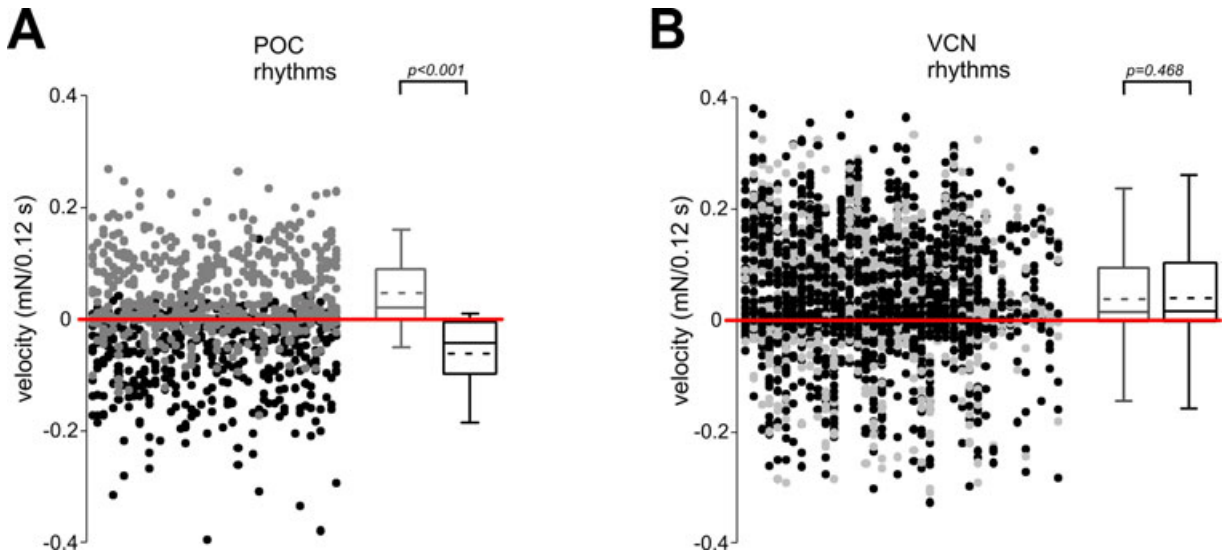

Figure 49: Muscle force velocities during stimulation with VCN- and POC-like patterns**. A** POC-type patterns. The velocities occuring ***200 ms*** before burstlet onset are shown in grey; slope values occuring ***200 ms*** after burstlet onset are shown in black. Distribution of slopes of gm6 contraction is shown as box plot on the right. Whiskers represent ***5-95 percentiles***; boxes represent ***25-75 percentiles***; median (straight line) and average (dashed line) are shown. **B** shows same for the VCN-type stimulation.

In summary, the *in situ* experiments showed that the pyloric-timed interruptions of LG-bursting during the POC-like stimulations could also be seen in the gm6 muscle force. VCN-like pattern ***#2*** showed significantly stronger response amplitude compared to the other two VCN-like patterns. Force amplitudes was significantly lower during POC-like stimulations than during VCN-like stimulations.

4.5 Characterization of tooth movements during three distinct gastric mill rhythms *in vivo*

The previous chapters showed that the investigation of muscle activity can account for some, but not all, properties of the movement output of the gastric mill teeth. It has been shown previously (Doya et al. 1993) that the anatomy of the stomach causes the muscles to move in a complex arrangement, which can cause passive stretch and

co-contractions in the system. Thus, it may be possible that the actual movement output of all the teeth, which form the gastric mill, the two lateral teeth and one medial tooth, causes emergent patterns, which cannot be anticipated by stimulation of the lateral tooth system alone.

To account for this, experiments were conducted in, which all motor neurons responsible for pro- and retraction of all teeth in the gastric mill were stimulated via extracellular electrodes. The protractor neurons for the medial tooth, the gastric motor (GM) neurons, project through all motor nerves (Städele 2010). Hence, to activate the gm1 protractor muscles, the *dvn, dgn* and *mvns* were severed and the nerve endings proximal to the stomatogastric ganglion were all placed onto one hook electrode and stimulated. The dorsal gastric (DG) neuron, which innervates the retractor muscle gm4, was activated by stimulation of the *dgn*. The *dvn* was stimulated to activate the lateral gastric (LG) neuron, which innervates the lateral tooth protractor muscles gm5, gm6 and gm8.

Data shown in the work of Beenhakker et al. (2004) was used to construct the standardized stimulus for the VCN-type rhythm. The standardized stimuli for the POC-type rhythm were built from data used with permission from R. S. White from the group of Dr. M. P. Nusbaum (University of Pennsylvania, USA). So far this work focused on two types of gastric mill rhythms. A third type of gastric mill rhythm elicited by the inferior ventricular (IV) neurons (Smarandache et al. 2008) was also included in this set of stimuli. The stimuli used in the experiments were calculated from previously published data (Hedrich et al. 2009; Hedrich 2008). While the POC and VCN patterns differ mainly in the bursting properties of LG and DG, the IV-type gastric mill pattern elicits a characteristic phasing of LG and DG that is distinct from that of the POC and VCN patterns. This unique stimulus pattern should help clarify the interaction of ossicles and muscles during coordinated movements of the gastric mill teeth. The characteristics of all three types of gastric mill rhythms are be described in the following in more detail.

4.5.1 Duty cycles of motor neurons in standardized gastric mill patterns

The duty cycles of the three gastric mill motor neurons during the IV-type gastric mill rhythm were distinct from those of the other rhythms in that they were rather short: none of the motor neurons occupied more than ***20%*** of the cycle (see table 2 and fig. 50 A). Consequently, there was a long pause where no motor neuron was active, which occupied ***51%*** of the gastric mill cycle.

	POC			VCN			IV		
				Intraburst firing frequencies (Hz): 50%, 100%, 150%					
LG	4.9	9.8	**15.7**	6.8	11.5	**17.3**	3.9	7.8	**11.7**
DG	5.5	10.9	**16.4**	6.8	13.6	**20.4**	5.8	11.5	**17.3**
GMs	5.8	11.6	**17.4**	6.5	13.0	**19.5**	7.2	14.4	**21.6**

		Burst duration (s)	
LG	5.6 [0.79]	6.5	2.6
DG	3.5	3.5	1.8
GMs	6.4	5.4	2.6

		phase onset / end	
LG	0 [0] 0.4 [0.29]	0 0.5	0 0.2
DG	0.5 0.8	0.7 1.02	0.3 0.5
GMs	-0.2 0.4	0.1 0.6	0.04 0.2

		period duration (s)	
	13.45	10.9	12.0

Table 2: Parameters of standardized gastric mill rhythms based on averaged *in vitro* data. Four parameters were used to build the standardized stimuli from described in the text. Values in brackets represent the duration and onset/end of the burstlets during POC-type LG spiking.

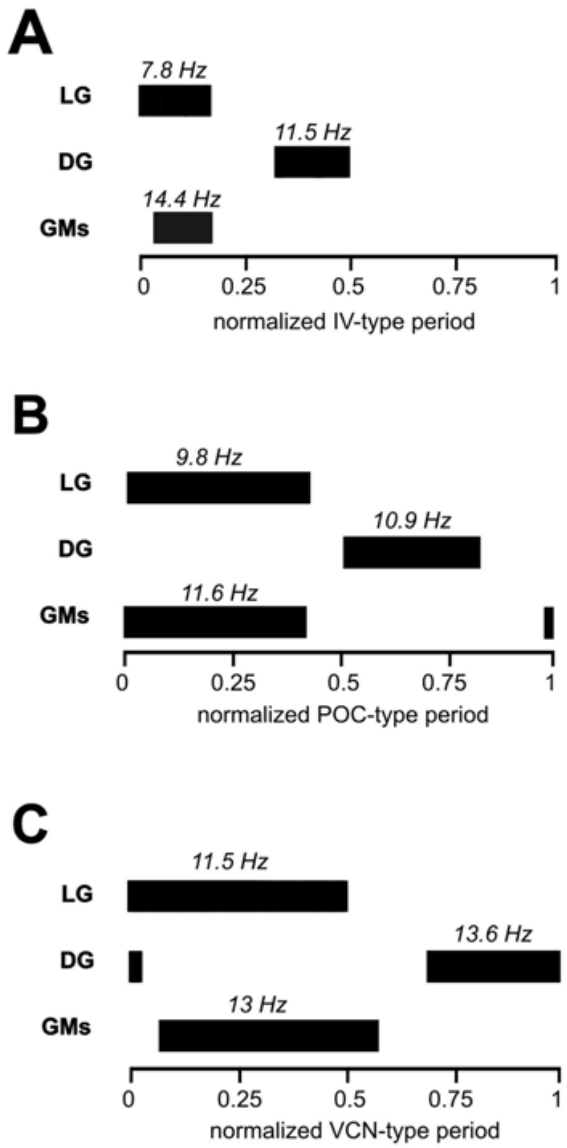

Figure 50: Phase diagrams of the three distinct stimulus patterns. **A** IV-type gastric mill rhythm. **B** POC-type gastric mill rhythm. **C** VCN-type gastric mill rhythm.

The POC-type rhythm showed an individual distribution of bursts of three motor neurons (see fig. 50 B). As oppose to the other two rhythm types, the GM burst was initiated before the LG burst. Each motor neuron occupied an average ***43.3%*** of the period. During the VCN-type rhythm the end of the DG burst overlapped with the beginning of the LG burst during the VCN-type rhythm (see fig. 50 C). Each motor neuron had a duty cycle of approximately ***44.0%*** of the gastric mill period.

4.5.2 Burst characteristics and gastric mill periods in standardized gastric mill patterns

The IV-type gastric mill rhythm exhibited a gastric mill period of ***12 s*** and was thus in between VCN- and POC-rhythms. The long gastric mill period contained the shortest motor neuron bursts of all gastric mill rhythm patterns. The GM burst started shortly after the LG burst onset.

The POC-type gastric mill rhythm possessed the shortest period (***10.9 s***). The burst duration of the GMs, however, was the longest (***5.6 s***) compared to the other rhythms. The LG burst was longer than in the VCN-type rhythm. All three, LG, DG and the GMs, exhibited longer bursts than during the IV-type rhythm. The LG and GM bursts started approximately simultaneously. As shown in previous chapters, the LG neuron shows a characteristic firing pattern during the POC-type rhythm. The stimulus patterns generated in the Spike2 software had to be adjusted to simulate this effect realistically. For this, the LG burst was split into ***5*** burstlets of equal duration and the corresponding ***4*** burstlet gaps (duration ***0.79 s,*** see table 2, section: burst duration, squared brackets).

The VCN-type gastric mill rhythm showed the longest period (***13.45 s***) and the longest LG burst (***6.5 s***). DG and GM exhibited longer burst durations compared to the IV-type rhythm. The DG burst overlapped with the LG burst, which implies a coactivation of antagonistic muscles *in vivo*. The GM burst overlapped with the LG burst as well, but started after LG in the gastric cycle.

4.5.3 Intraburst firing frequencies in standardized gastric mill patterns

The average intraburst firing frequencies measured for each motor neuron type *in vitro* was used to design the standardized stimulus patterns. The value labeled ***"100%***" in table 2 corresponds to the average firing frequency from the *in vitro* experiments. To test the how the movement output changed when stimulus frequencies varied, lower frequency stimulus (***50%***) and higher frequency stimulus (***150%***) paradigm were also applied. This retained relative firing frequencies between the motor neurons within a given gastric mill pattern as well as the phasing of the neurons. In all gastric mill rhythm types, with the exception of the VCN-type rhythm, LG was firing with the lowest intraburst firing frequency, while the GMs showed the highest frequency. In the VCN-type gastric mill rhythm DG showed highest intraburst firing frequency.

The GM firing frequency shown in table 2 represents the average firing frequencies of one of the four GM neurons. The gm1 muscle is innervated by several GM neurons simultaneously, but there is no reproducible pattern of innervation between individuals (Städele 2010). This makes it impossible to assess how many GM neurons innervate the gm1 protractor muscles in an individual preparation before an experiment is conducted. Since the exact pattern of innervation cannot be anticipated, a stimulation of individual GM neurons via extracellular electrodes applied to the motor nerves was impossible. Thus, a single stimulation electrode was used to stimulate the *dgn, dvn* and *mvn*, in order to activate all GM neurons simultaneously. The best approximation was found by increasing the stimulus amplitude (voltage) until maximal protraction of the medial tooth was affirmed via the endoscopic video recording. It was assumed that such voltage amplitude was sufficient to retrogradely activate most, if not all, of the GM neurons.

4.5.4 Analysis of gastric mill teeth movement elicited by standardized stimulation

The different stimulus patterns based on averaged activity of motor neurons during POC-, VCN- and IV-type rhythms were applied to the *in vivo* preparation in order to measure the movement output of the teeth in the gastric mill. The disconnected motor nerves were stimulated, which disabled all sensory or neuronal feedback from the STG or other parts of the nervous system during the experiments. The stimulation with standardized data allowed for comparable movement output of the teeth across preparations.

The movement of the teeth was recorded through an endoscope with a wide-angle lens. Since the exact position of the optics relative to the teeth varied among preparations, and the size of the preparations varied as well, the movement output was quantified similar to previous tooth movement measurements using a relative measure: the width of the medial tooth at the fusion point of the urocardiac and the mesocardiac ossicle ("Medial Tooth unit", ***MT***).

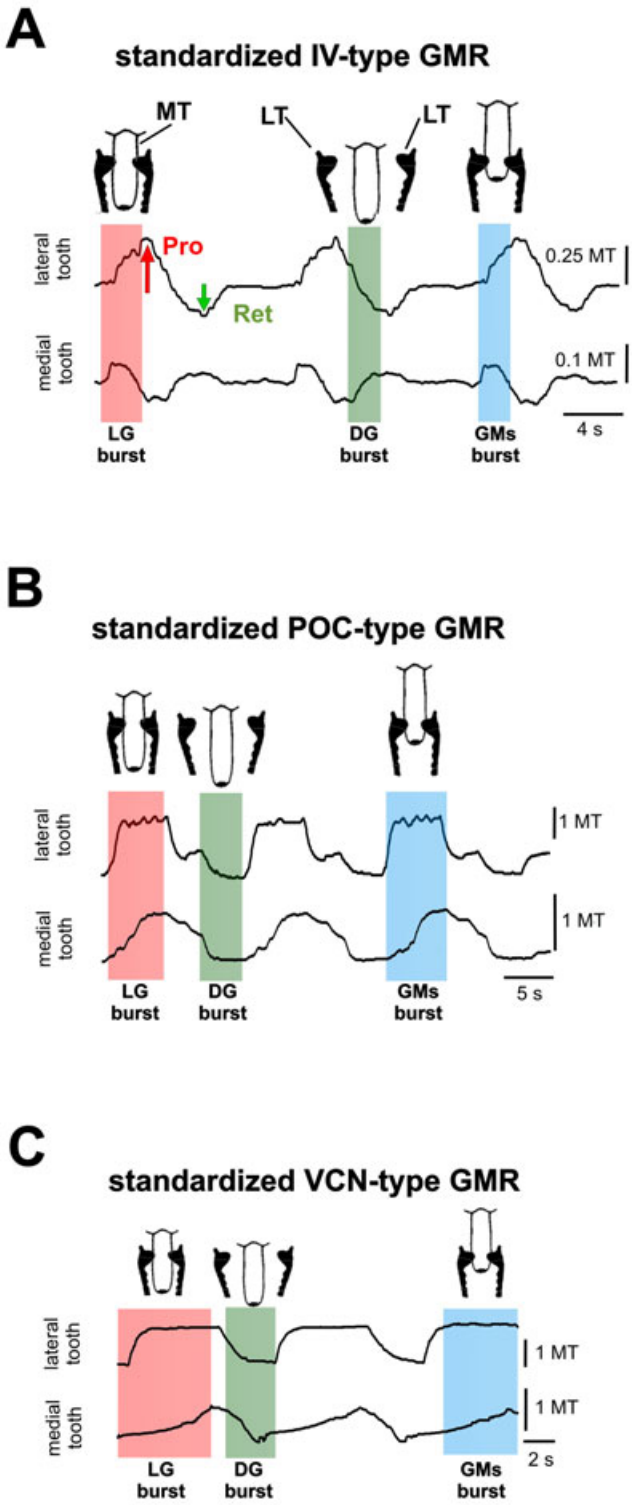

Figure 51: Standardized stimulus patterns and evoked tooth movements. **A** shows a schema of the teeth during movement (top). Movement of left lateral tooth and medial tooth during the IV-type rhythm are shown below. Stimuli applied to the motor nerves are also shown. Burst durations and corresponding movements are highlighted. **B** shows the tooth movements and stimuli applied during the POC-type rhythm. **C** shows the tooth movements and stimuli applied during the VCN-type rhythm.

The velocity of the tooth movement is given in ***MT*** per unit time (***MT*** × ***0.12 s***$^{-1}$). This time frame was chosen to prevent aliasing effects, since the video frame resolution was ***0.04 s***. Additionally, absolute amplitudes of movement were measured as well (also given as ***MT***).

An example of movement outputs of the gastric mill teeth during stimulation with the three types of gastric mill patterns is shown in figure 51. The movement of the teeth during activation of the respective motor neuron is schematized at the top of each panel. Below, the movement trajectories of the medial tooth and the left lateral tooth is shown. To accentuate the concurrence of stimulus and tooth movement the functional groups "protractor neuron LG & lateral tooth" (red bar, fig. 51), "protractor neurons GM & medial tooth" (blue bar, fig. 51) and "retractor neuron DG & teeth" (green bar, fig. 51) are highlighted. The corresponding stimulus trains, which were applied on the respective motor nerves are shown below.

Here, differences between the three rhythm types become evident on the behavioral level. The long burst duration of LG during the VCN-type rhythm (see fig. 51 C) seems to elicit long protractions of the lateral tooth. The short bursts durations during the IV-type rhythm (see fig. 51 A) elicited equally short pro- and retractions in the teeth. In IV-type and the POC-type rhythms retraction movement of the lateral tooth beyond the baseline during DG stimulation becomes evident. In the following the characteristic properties of each gastric mill rhythm pattern on the movement level is investigated more closely.

4.5.4.1 Standardized gastric mill rhythms elicit distinct movement output in the lateral teeth

Since both lateral teeth are innervated by the same motor neuron (LG), the movement trajectory of one lateral tooth was measured for each experiment and used for the statistical analyses to represent both lateral teeth. Each paragraph focuses on the movement velocity and amplitude of the lateral tooth during one of the three types of gastric mill rhythm patterns used for stimulation.

The IV-type stimulus (***0.82 (±0.04) MT***), the POC-type stimulus (***1.17 (±0.04) MT***) and the VCN-type stimulus (***1.09 (±0.1) MT***) did not elicit statistically stignificant differences in average protraction amplitudes of lateral tooth movement (***p=0.46***, One-way ANOVA with repeated measures, ***N=11,*** see fig. 52 A). This finding corresponds to the results from decentralized *in vivo* experiments (see fig. 44), in which similar protraction amplitudes, resulting from different gastric mill rhythm types (POC & VCN), could be demonstrated. Additionally, the IV-type pattern also shows equal protraction amplitudes compared to the POC- & VCN-type patterns. All amplitudes were large enough to enable the teeth to reach the midline, i.e. "clench".

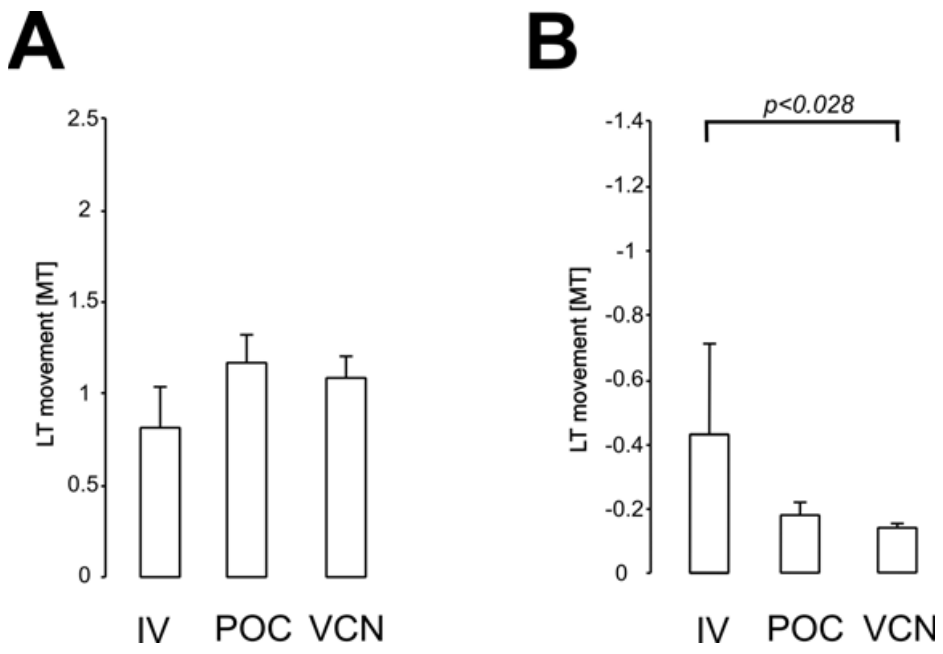

Figure 52: Amplitudes of lateral tooth movement differ during retraction but not during protraction. **A** Amplitudes of lateral tooth protraction during IV-, POC- and VCN-type rhythms. **B** Amplitudes of lateral tooth retraction. Please note the negative scale.

During the retraction phases (*dgn* stimulation) the lateral teeth retracteded beyond the resting position (see fig. 52 B). This was measured as negative movement (***MT***) of the teeth relative to baseline. The baseline was defined as the resting position of the teeth, in which neither pro- nor retractor muscles were active. In all three types of gastric mill rhythms this retractive movement of the lateral teeth was evoked (IV-type: ***-0.44 (±0.3) MT***; POC-type: ***-0.18 (±0.05) MT***; VCN-type: ***-0.14 (±0.01) MT***). The retraction amplitudes elicited during VCN-type rhythms were significantly smaller than those of the IV-type rhythm (***p<0.001***, One-Way ANOVA with Repeated Measures, ***N=8***) and those of the POC-type rhythm (***p<0.002***, One-Way ANOVA with Repeated Measures, ***N=8***). This effect was then investigated in more detail because retraction of the lateral teeth that occured during the DG neuron activity phase had never been described previously (see chapter 4.7 on page 108).

The movement velocities of the teeth during a gastric mill rhythm phase were calculated as well. Shown in figure 53, the movement process was subdivided into four segments: protraction during the LG burst, passive retraction after the LG burst, retraction during the DG burst and passive protraction after the DG burst. The lateral teeth protracted with an average velocity of $1.12 \pm 0.5\ MT \times 0.12\ s^{-1}$ (***N = 10***) during the POC gastric mill rhythm patterns (see fig. 53 A). The gap between LG burst end and DG burst onset was long enough for the lateral teeth to retract back to baseline, due to relaxation of the protractor muscles after the end of the LG burst. The retraction velocity of this passive movement was $-0.16 \pm 0.13\ MT \times 0.12\ s^{-1}$ (***N=10,*** see fig. 53 B). During the DG burst, however, the lateral teeth retracted beyond the baseline at an average velocity of $-0.55 \pm 0.9\ MT \times 0.12\ s^{-1}$ (***N=9***, see fig. 53 C). After the DG burst, when all stimuli ceased, and the gm4 muscle relaxed at the end of the cycle, the lateral teeth moved back to baseline position at an average velocity of $0.3 \pm 0.7\ MT \times 0.12\ s^{-1}$ (***N=10***, see fig. 53 D).

The movement of relaxation after the LG burst during VCN-type rhythm showed faster velocities (see fig. 53 B) than during the IV- and POC-type rhythms. The strong clenching during the LG burst (high intraburst firing frequency) induced a fast tooth movement during relaxation of the protractor muscles $-1.1\ (\pm 1.74)\ MT \times 0.12\ s^{-1}$ (***N=10***). Due to the short interval between the end of the LG burst and the beginning of the DG burst, this passive retraction never reached the baseline. Instead, with the onset of the DG burst, the teeth retracted beyond the baseline at a velocity of $-0.52\ (\pm 0.6)\ MT \times 0.12\ s^{-1}$ (***N=10***, see fig. 50 C).

Similar to the VCN-type rhythm, the gap between LG and DG burst during the IV-type rhythm was short enough for the DG burst onset to occur during the retraction phase of the teeth caused by relaxation of the protractor muscles. During the passive retraction phase the teeth moved at a velocity of $-0.48 \pm 0.51\ MT \times 0.12\ s^{-1}$ ($N=8$, see fig. 53 C). Despite the early onset of the DG burst, the movement velocities were lower compared to the ones during VCN-type stimulations (see previous section). This was pobably due to the short LG burst and the missing clenching-phase preceding relaxation. During the DG burst the teeth still retracted beyond baseline, however, at a velocity of $-0.54 \pm 0.5\ MT \times 0.12\ s^{-1}$ ($N=8$, see fig. 53 C) during the IV-type rhythm.

The velocity of the retractive movement towards baseline after the LG burst differed among the three types of rhythms. The movement velocity during the POC-type rhythm was significantly different from all other rhythm types ($p<0.001$, Kruskal-Wallis test, $N=8$); the IV-type and the VCN-type rhythms differed from each other as well ($p<0.05$, Kruskal-Wallis test, $N=8$). Thus, passive relaxation was the slowest during the POC-rhythm. Please note that during the IV- and VCN-type stimulation patterns the DG burst started during this retraction phase. During the POC-type stimulation the lateral teeth retracted to baseline before DG stimulation (and further retraction) started.

From previous studies it has been assumed that the protractor muscles always initiate protraction movements, and the retractor always retraction. Same is true for the medial tooth pro- and retraction system. The experiments with highly controlled application of stimuli shown in this work provided further proof for this hypothesis. However, negative velocity of movement velocities in both types of teeth (medial and lateral) were recorded during DG stimulation. This showed that emergent effects, which are not specifically controlled by the nervous system, have an impact on the movement output of the gastric mill teeth.

In summary, these data show that the degrees of freedom of movement of the teeth are limited during three types of gastric mill rhythms and different motor nerve stimulus frequencies. Additionally, these *in vivo* experiments showed that unexpected dynamics in the movement of gastric mill teeth, which could emerge rhythmic activation of the gastric mill musculature, occur *in vivo.* Whether these emergent dynamics in movement have an impact on the behavior, could not be clarified in these experiments. As mentioned before, the POC-type stimulus pattern reflected the characteristic burstlet-pattern during the LG burst caused by pyloric timed interruptions of LG activity.

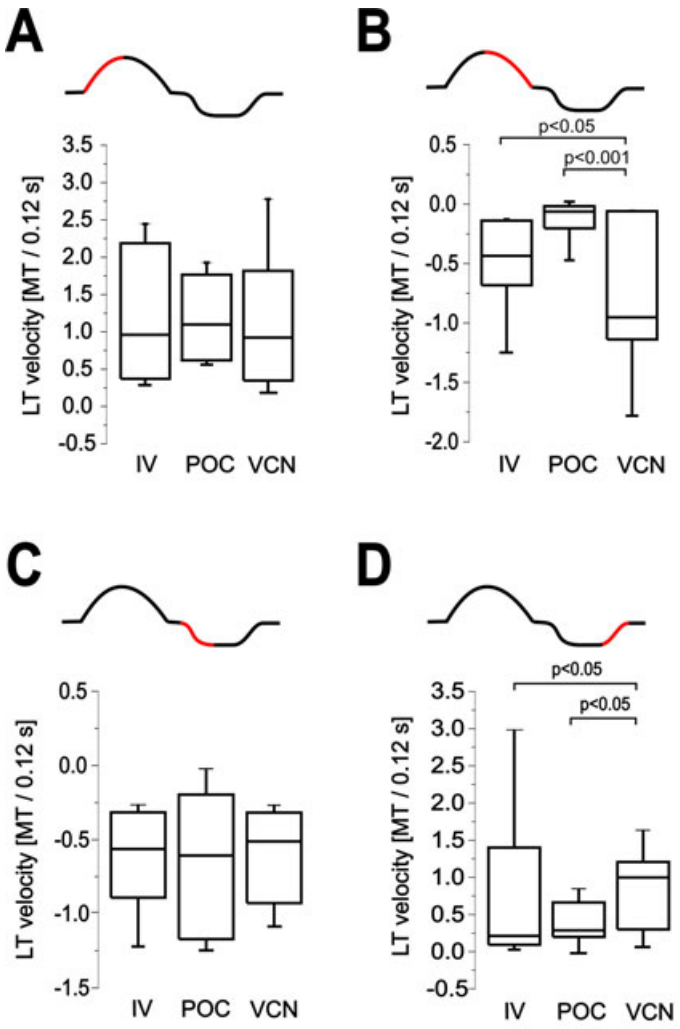

Figure 53: Characteristics of lateral tooth movement velocities during standardized stimulation. **A** shows the velocity of movement of the lateral tooth during LG stimulation. **B** shows the tooth velocity after LG stimulation. **C** shows tooth velocity during DG stimulation. **D** shows velocity after DG stimulation. Movement velocity is shown as medial tooth width $MT \times 0.12\ s^{-1}$. Above each plot a schema of tooth trajectory is shown. Edges of red sections mark the maxima and minima, which were used to calculate the velocity of movement for the respective plot. Boxplots show values for each standardized gastric mill pattern (IV, POC and VCN). Straight lines in boxplots show median of the data; whiskers show ***5-95% percentiles***; boxes show ***25-75% percentiles***.

To test whether the tooth movements followed the standardized burstlets *in vivo* the tooth movement trajectories were divided into sections based on the onsets and ends of the burstlet. A time-window of ***200 ms*** set before burstlet onset and after burstlet end, respectively, was used. For each one of these windows the velocity of tooth movement was calculated (see fig. 54). Velocities occuring during the "after LG burstlet end" time-window are represented by black dots. The velocities occuring during the "before LG burstlet onset" are represented by grey dots. The velocities occuring before an LG burstlet were shifted into the positive regime during the POC-type stimulation (***mean: 0.3 MT × 0.12 s^{-1}; 95%-ile: 0.6 MT × 0.12 s^{-1} 5%-ile: -0.05 MT × 0.12 s^{-1}***), while the protraction velocities after the LG burstlet were shifted into the negative regime (***mean: -0.1 MT × 0.12 s^{-1}; 95%-ile: 0.08 MT × 0.12 s^{-1}; 5%-ile: -0.4 MT × 0.12 s^{-1}***, see fig. 54 A). and were thus significantly different from velocities before the LG burstlet (***$p<0.001$***, Mann-Whitney Rank Sum test, ***$N=13$***). This separation of velocities of movement during POC-type tooth movements thus correlated with the short LG burstlets. The VCN-type stimulation (see fig. 54 B) did not show a correlation with the LG burstlets since this burst pattern consisted of a constant intraburst stimulus frequency without gaps. To be able to compare these data to the data from POC-type stimulations the VCN-type protraction velocities were divided into the same segments as shown previously for the POC-type tooth movement data sets. The protraction velocities before the burstlets (grey dots, fig. 54 B) were shifted into the positive regime (***mean: 0.1 MT × 0.12 s^{-1}; 95%-ile: 0.4 MT × 0.12 s^{-1}; 5%-ile: -0.06 MT × 0.12 s^{-1}***). The protraction velocities after the burstlets were shifted into the positive regime as well (***mean: 0.2 MT × 0.12 s^{-1}; 95%-ile: 0.7 MT × 0.12 s^{-1}; 5%-ile: -0.05 MT × 0.12 s^{-1}***, black dots, fig. 54 B). Similar to *in vivo* experiments presented previously, which were conducted with stimuli from individual (but not averaged) motor patterns (see fig. 45 B), the slope trajectories during the VCN-type rhythm were not significantly different from each other (***$p=0.468$***, Mann-Whitney Rank Sum test, ***$N=8$***), thus indicating that the teeth protracted in a smooth, uninterrupted, fashion during the VCN-type stimulations.

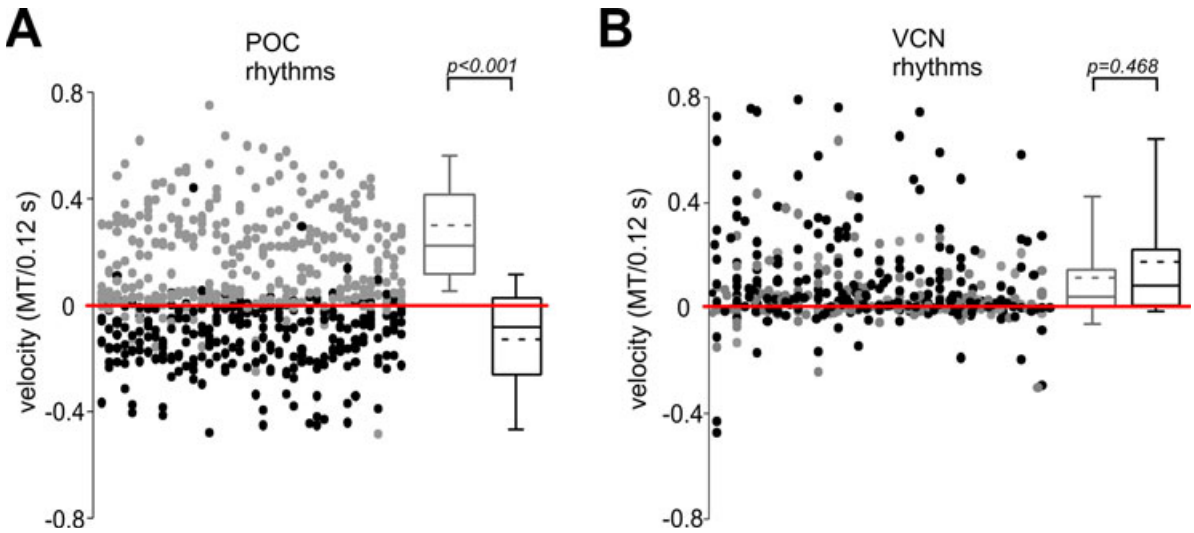

Figure 54: Timing of lateral tooth movement to standardized POC- and VCN-type stimuli. **A** shows lateral tooth movement velocities during POC-type stimulation (*N=13*). The velocities occuring *200 ms* before burstlet onset are shown in grey; velocities occuring *200 ms* after burstlet end are shown in black. Box plots: whiskers represent *5-95* percentiles; boxes represent *25-75* percentiles; median (straight line) and average (dashed line) are shown. **B** shows same for the VCN-type stimulation.

4.5.4.2 Standardized gastric mill rhythms elicit distinct movement output of the medial tooth

So far, the different movement patterns of the lateral teeth have been investigated. The following shows analyses of the protraction of the medial tooth during GM stimulation, as well as the retraction of the medial tooth during DG stimulation with standardized gastric mill patterns.

The maximal protraction amplitudes of the medial tooth during GM stimulation and retraction amplitudes during DG stimulation are shown in figure 55. The protraction (see fig. 55 A) was significantly smaller in amplitude during the VCN-type stimulation (*0.36 ±0.09 MT*) compared to the IV-type and POC-type stimulation (IV: *0.74 ±0.2 MT*, POC: *0.79 ±0.2 MT; p<0.001*, Friedman Test, *N=12*).

The amplitudes of the retraction movement of the medial tooth during the IV- and POC-type gastric mill rhythms were not significantly different from each other (*p=0.495*, ANOVA on Ranks, *N=10*, see fig. 55 B). The low average protraction amplitude may be due to the clenching of the lateral teeth when the serrated edges move towards the midline and hinder the protraction of the medial tooth.

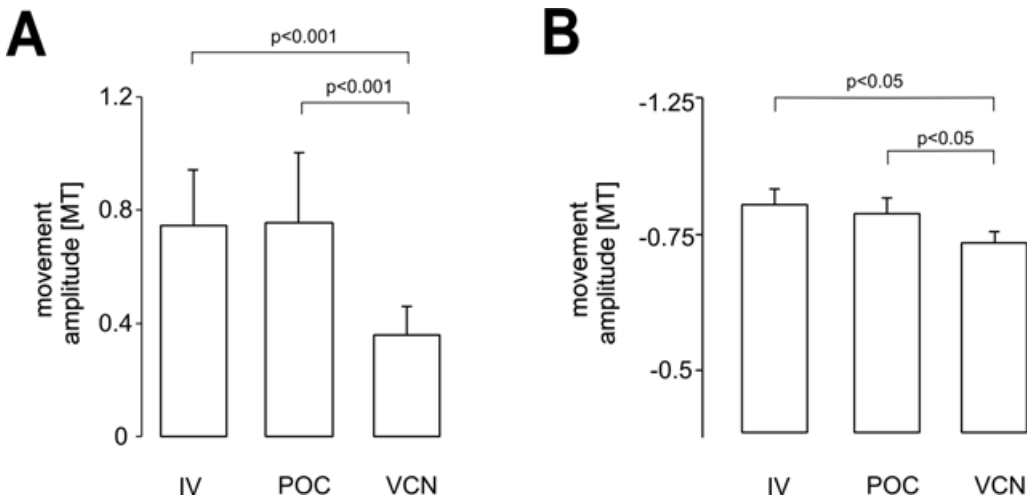

Figure 55: Significant differences in pro- and retraction amplitudes of the medial tooth during standardized gastric mill rhythm stimulation. **A** shows amplitudes of medial tooth protraction during standardized stimulation of the GM neurons with standardized gastric mill rhythm stimulations. **B** shows amplitudes of medial tooth retraction during stimulation of GM neurons with standardized IV-, POC- and VCN-type rhythms. Note the inverted scale in **B**.

Since the protraction of the medial tooth is not as pronounced during VCN-type rhythms, the retraction amplitude is also smaller. The amplitudes of retraction movement elicited during the VCN-type rhythm were also significantly smaller than in the other two types of rhythms (***p<0.05***, ANOVA on Ranks, ***N=10,*** see fig. 55 B).

Analogous to the analyses of the lateral tooth movements shown in figure 53 the velocities of medial tooth movement occuring during the stages of rhythmic tooth movement are shown in figure 56. The extracellular stimulation of the motor neuron axons during the IV-type gastric mill rhythm elicited a protraction rate of ***0.50 ±0.06 MT × 0.12 s^{-1}*** in the medial tooth. The POC-type stimulation elicited a movement velocity of ***0.72 ±0.08 MT × 0.12 s^{-1}***, the VCN-type stimulation elicited a velocity of ***0.62 ±0.05 MT × 0.12 s^{-1}*** (see fig. 56 A). All of these velocities of movement during protraction were significantly different from each other (***p<0.001***, ANOVA on Ranks, ***N=10***). Similar results were found for the velocities of movement during retraction after the GM stimulation (see fig. 56 B). At the end of GM stimulation the gm1 muscle relaxed and caused retraction of the medial tooth back to baseline. The retraction velocities were all significantly differen from one another (IV***: -0.84 ±0.04 MT × 0.12 s^{-1}***, POC: ***-0.79 ±0.05 MT × 0.12 s^{-1}***, VCN: ***-0.71 ±0.03 MT × 0.12 s^{-1}***; ***p<0.001***, ANOVA on Ranks, ***N=10***). In all rhythm types the medial tooth retracted beyond the baseline towards the pyloric valve during DG stimulation.

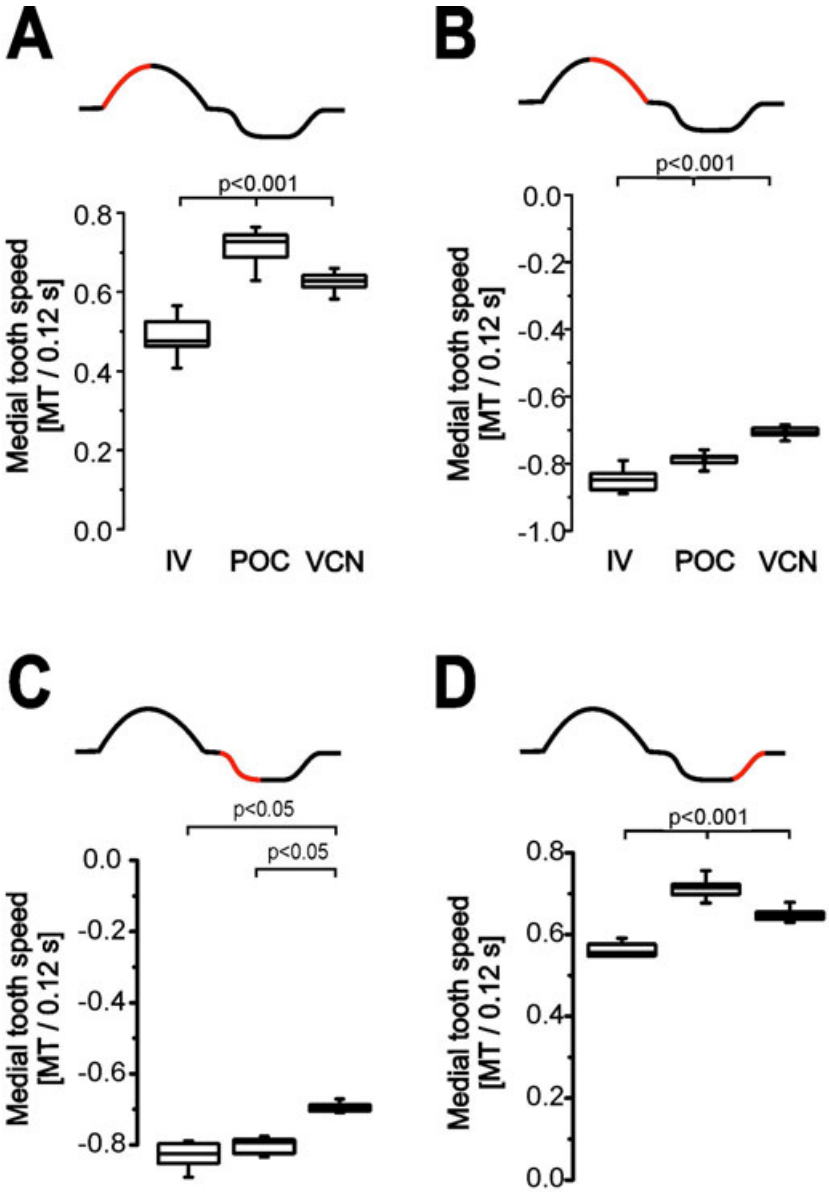

Figure 56: Characteristics of medial tooth movement velocity during standardized stimulation. **A** shows the velocity of movement of the medial tooth during *GM* stimulation. **B** shows the movement velocity after *GM* stimulation and before DG stimulation. **C** shows medial tooth movement velocity during *DG* stimulation. **D** shows movement velocity of medial tooth after *DG* stimulation. Movement velocities are shown as medial tooth width MT × 0.12 s-1. Above each plot a schematic of the corresponding movement trajectory is shown. Edges of red sections mark the maxima and minima, which were used to calculate movement velocity. Box plots: whiskers show 5-95% percentiles; boxes show 25-75% percentiles.

Tooth velocities beyond the baseline were not significantly different between IV-type (*-0.84 ±0.06 MT × 0.12 s^{-1}*) and POC-type stimulations (*-0.80 ±0.06 MT × 0.12 s^{-1}*; *p=0.12*, ANOVA on Ranks, *N=10*, see fig. 56 C). The medial tooth velocity of movement during the VCN-type stimulation (*0.70 ±0.04 MT × 0.12 s^{-1}*), however, was significantly smaller compared to the other two stimulus paradigms (*p<0.05*, ANOVA on Ranks, *N=12*). When the DG stimulation ended the retractor muscle relaxed and the medial tooth returned back to baseline (positive movement velocity). The movement velocities in this stage showed significant differences between all three types of gastric mill rhythms (IV*: 0.57 ±0.03 MT × 0.12 s^{-1}*, POC: *0.71 ±0.06 MT × 0.12 s^{-1}*, VCN: *0.65 ±0.03 MT × 0.12 s^{-1}*; *p<0.001*, ANOVA on Ranks, *N=10*).

4.5.5 Summary of chapter 4.5

These data show the movement characteristics of the lateral teeth and the medial during the standardized stimulation based on averaged *in vitro* data sets. The experiments demonstrate that the movement output of the chewing mechanism in the gastric mill differs during the different types of rhythmic stimulus patterns. This provides evidence for the hypothesis that variations in the motor neurons' spiking during these gastric mill rhythms has an impact on the effectors, i.e. on the musculature in the gastric mill. As shown in figure 53 (A & C) the mean velocities of lateral tooth movements that occured during the different rhythms were not significantly different from each other. This was true for both, pro- and retraction (LG stimulation: *p=0.68*, ANOVA on Ranks, *N=8*; DG stimulation: *p=0.48*, ANOVA on Ranks, *N=8*) and despite the fact that stimulation frequencies varied quite substantially between rhythms. This means that LG bursts with evenly distributed spike events elicits similar movement trajectories rather independently of motor neuron spike frequency.

For the medial tooth a slightly different picture developed. Here, the medial tooth movement velocities were significantly different in all gastric mill rhythm stimuli during protraction (see fig. 56 A), and significantly different in two gastric mill rhythm stimuli during retraction (see fig. 56 C). This shows that the movement output of the medial tooth was more sensitive to variations in intraburst firing frequencies than the lateral teeth.

4.6 Lateral- and medial tooth movement depends on motor neuron spike-frequency

The previous experiments based on averaged *in vitro* data showed that the intraburst firing frequency is a key parameter in the control of muscle contraction and therefore movement. This has been shown in the previous chapter for the medial tooth movement. Whether the lateral teeth are generally insensitive to changes in firing frequency was tested in the following experiments. High firing frequencies in the motor neurons elicit summation in the musculature and thus stronger contraction (Hooper & Weaver 2000). Albeit variations in properties of individual muscles, the gm6 (White 2011), the gm1 (Städele 2010) and the gm4 muscles (Ahn et al. 2006) all show this dependency on firing frequency.

The *in vivo* stimulation with standardized gastric mill patterns allowed for a systematic investigation of the effects of increased stimulus frequencies onto the behavior. The intraburst frequencies of the three gastric mill stimuli were altered to simulate at ***50%, 100%*** and ***150%*** intraburst firing frequencies. The values for each paradigm are shown in table 2 (top row). The intraburst firing frequency was the only parameter that was changed in these stimulus paradigms. All other parameters (burst duration, cycle duration, duty cycle) were left the same to keep the data comparable. First, the data analysis for the pro- and retraction movement of the lateral teeth is shown. Then the same data analysis is shown for the medial tooth movement.

The lateral teeth movement during the ***50%***, ***100%*** and ***150%*** intraburst frequency stimulations is shown and summarized in figure 57. The bar graphs show the results grouped according to the type of gastric mill pattern. Each group shows the lower than average stimulus frequencies (light grey bars), average stimulus frequencies (grey bars) and higher than average stimulus frequencies (black bars) used during each stimulus paradigm.

The protraction of the lateral teeth during LG stimulation is shown in Figure 57 A. Statistical analysis of the movements caused by the different intraburst stimulus frequencies (***50%, 100%, 150%***) across all three types of gastric mill patterns is presented in the following. All burst at ***50%*** stimulation frequency never elicited significantly different movement amplitudes (***p=0.095,*** One-Way ANOVA Repeated Measurements, ***N=7***). Similarly, there was no difference with ***100%*** stimulus frequency (***p=0.46,*** One-Way ANOVA Repeated Measures, ***N=7***). Only the bursts elicited during POC-type patterns at ***150%*** stimulus frequency were significantly different from the other two patterns (***p<0.05,*** One-Way ANOVA Repeated Measures, ***N=7***).

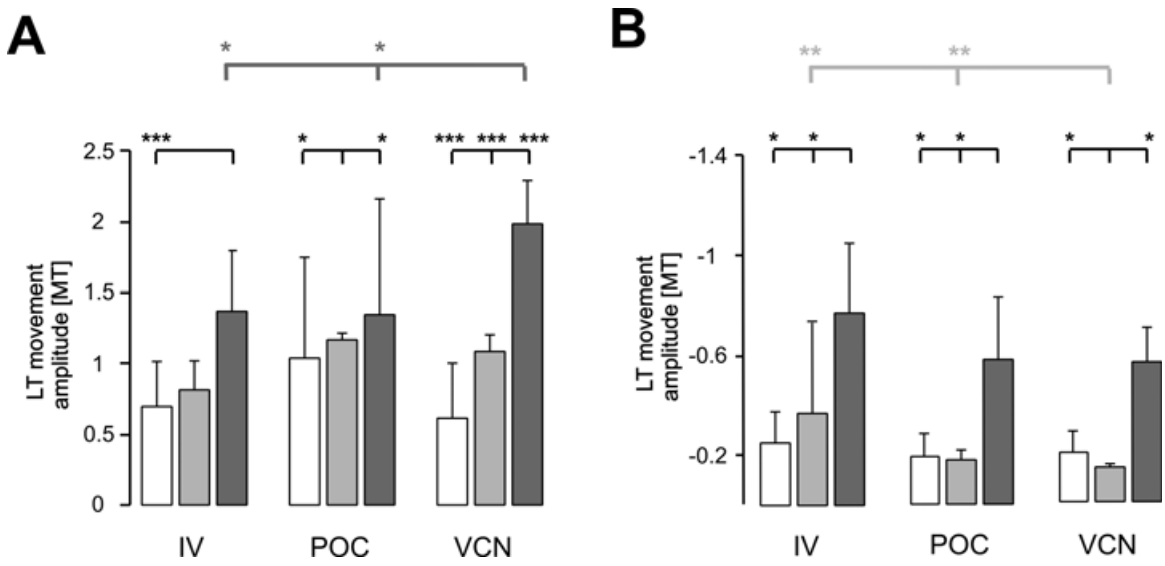

Figure 57: Movement amplitudes of lateral tooth during various intraburst spike frequencies and gastric mill rhythms. **A** The intraburst stimulus frequency of each rhythm type was modulated by ***50%*** (white bars) and ***150%*** (dark grey bars) of the original stimulus frequency (***100%***, grey bars). **B** shows retraction amplitudes of lateral tooth elicited by three types of gastric mill patterns. All else as described in **A**. Please note the inverted Y-Axis and different scaling in **B**. Significance levels are shown above each bar (***p<0.001 = ***, p<0.002 = **, p<0.05 = ****).

The differences in amplitudes of protraction movement output among the different "versions" (***50%, 100% & 150%***) of a given gastric mill rhythm was performed as well. Firstly, for the IV-type rhythm, only the ***50%*** and the ***150%*** intraburst stimulus frequencies elicited protraction amplitudes, which were significantly different from another (***p<0.001,*** One-Way ANOVA Repeated Measures, ***N=7***, see fig. 57 A, left grouped set of data), but each showed no difference not from the ***100%*** stimulus paradigm. For the POC-type stimulation the ***50%*** and ***150%*** stimulus frequency paradigms were both significantly different from the standard (***100%***) stimulus frequency paradigm (***p<0.05***, One-Way ANOVA Repeated Measures, ***N=7***, see fig. 57 A, middle grouped set of data). For the VCN-type stimulus pattern, all three types of stimulus frequency paradigms were significantly different from each other (***p<0.001,*** One-Way ANOVA Repeated Measures, ***N=7,*** see fig. 57 A, right grouped set of data). The same type of analysis shown in the preceding section was applied to the retraction of the teeth during DG stimulation. The data is shown in figure 57 B.

The statistical analysis of the three stimulus frequency paradigms (***50%, 100%, 150%***) across all three types of gastric mill patterns revealed that only the VCN-type stimulation with the ***100%*** stimulus paradigm elicited significantly different retraction movement amplitudes compared to the other gastric mill rhythm types (both: ***p<0.002,*** One-Way ANOVA Repeated Measures, ***N=7***, see fig. 57 B, top). The other two stimulus frequency paradigms (***50%*** and ***100%***) did not show a significant difference in lateral tooth retraction amplitude in any type of gastric milll rhythm.

The amplitudes of retraction movement beyond baseline upon DG stimulation elicited by the different stimulus frequency paradigms (***50%, 100% & 150%***) is shown in the following. For the IV-type rhythm the ***150%*** stimulus frequency paradigm was significantly different from the other two paradigms (***p<0.05,*** One-Way ANOVA Repeated Measures on Ranks, ***N=6***, see fig. 57 B, left grouped set of data). The ***150%*** stimulus frequency paradigm during the POC-type rhythm showed significant difference of the retraction amplitude of the teeth (***p<0.05,*** One-Way ANOVA Repeated Measures on Ranks, ***N=6,*** see fig. 57 B, middle grouped set of data). Lastly, during the VCN-type rhythm the ***100%*** stimulus paradigm, however, was significantly different from the other two (***p<0.05,*** One-Way ANOVA Repeated Measures on Ranks, ***N=6***, see fig. 57 B, right grouped set of data).

4.6.1 Summary of chapter 4.6

These experiments provided some additional insights into the dynamics of movement in the gastric mill of the crab. Firstly, the effects of DG onthe lateral teeth was proven to be effective during the low (***50%)*** stimulus frequency paradigm, because retraction of the lateral teeth could still be elicited in all gastric mill rhythms. The ***150%*** stimulus frequency paradigm elicited higher pro- and retraction amplitudes in all gastric mill rythm types. The LG stimulation during VCN-type rhythms elicited the strongest variability in tooth movement output. The standardized LG bursts during the VCN-type rhythm showed the highest intraburst spike frequencies (***11.5 Hz***) therefore making the frequency drop (for ***50%***) and rise (for ***150%***) larger compared to the other two rhythm types (IV and POC). This large range of interburst firing frequencies was very likely responsible for the large range of protraction amplitudes of the lateral teeth

movements. Hence, lateral tooth protraction was indeed sensitve to changes in motor neuron firing frequency. Apparently, however, the naturally occurring LG firing frequencies are, however, not sufficiently different to cause a difference in lateral tooth protraction (see chapter 4.5 on page 88 ff.).

In the following chapter the effect of DG on the lateral tooth retraction was investigated more closely and the anatomical interplay of musculature and skeleton during lateral tooth retraction was elucidated.

4.7 Emergent effects during rhythmic muscle contractions influence tooth movement

For the presented work I analyzed the interactions of all ossicles participating in the movements during gastric mill rhythms. I differentiate three functional systems in the gastric mill system:

1. Medial tooth protraction system
2. Lateral tooth protraction system
3. Medial- and lateral tooth retraction system

In the following I will focus on the functional aspects of the foregut anatomy. The data is based on photographs of dried stomach preparations of *C. borealis* and *C. pagurus,* as well as on the findings in the previous chapters showing effects in the teeth movement that could not be anticipated from the analysis of the activity of the motor neurons. Due to findings that shed new light on the functionality of the retractor muscle gm4 I will also discuss the retraction of the medial tooth in more detail. In the following paired, symmetric structures are referred to in singular nomenclature.

4.7.1 Lateral and medial tooth protractions are decoupled

The protractors of the lateral tooth are the gm5ab,6 and 8ab muscles (Weimann et al. 1991; Heinzel 1988). During the movement of the lateral tooth, a hinge-structure serves also a key function as in the medial tooth protractor system. This hinge is formed where the subdentate ossicle fuses with the zygocardiac ossicle. Whilst contracting, the gm8 and gm6 muscles pull these two ossicles towards each other. This leads to a closing movement of the zygocardiac ossicle, which forms the lateral tooth inside the stomach.

The functioning of the medial tooth protraction has been discussed previously (Heinzel 1988) for the Nephropidae (*H. gammarus*). Since the protractors (gm1 & gm2 & 3) and retractors (gm4) are arranged in the same fashion in the Cancridae (*C. pagurus* & *C. borealis*) around the stomach and also insert extrinsically into the similar locations in the carapace it was assumed that the functioning and movement output of the medial tooth is the same in both groups.

Experiments conducted for this work, however, show that the lateral and medial tooth protraction systems are independent from each other. Exclusive stimulation of the LG axon *in vivo* elicited a protraction of the lateral teeth, while the medial tooth remained still. Vice versa, stimulation of the axons of the GM neurons exclusively elicited a protraction of the medial tooth.

4.7.2 Retractions of the medial- and lateral tooth are coupled

The protractions of the lateral tooth and the medial tooth proceed independently of each other - the two types of teeth are "decoupled". The retractor system on the other hand consists of a single muscle, which performs the retractions of the medial as well as the lateral tooth. Thus, the retraction of the the two types of teeth is "coupled". This coupling is enabled by the gm4 muscle, which inserts rostrally into the mesocardiac ossicle and caudally into the pro- and exopyloric ossicles.

A closer investigation of the caudal insertion areas reveales that the gm4b muscle inserts at the exopyloric ossicle and the (medial) gm4c muscle inserts at the propyloric ossicle. As will be shown later, each muscle fiber bundle of the gm4 has distinct effects on the retractive movement of the teeth.

4.7.2.1 The medial tooth retractor subsystem

The actions of the gm4 muscle onto the medial tooth retraction were investigated in the fully intact preparation using successive transsections of the gm4 fiber bundles (b and c). In each situation (intact and lesioned) the *dvn* was stimulated for ***5 s*** with stimulus frequencies ranging from ***10 Hz*** to ***50 Hz*** (in ***10 Hz*** steps). The movement of the teeth to the various stimulation frequencies were recorded on video file and the retraction amplitudes were analyzed. The results are summarized in figure 58.

The retraction amplitude with fully intact gm4 muscles reached ***-1.29 (±0.4) MT*** (***N=4***) during the highest stimulus frequency (***50 Hz***). The gm4c fibers insert rostrally into the propyloric ossicle. In my observations of the fully intact gm4c *in vivo*, I could show that the mesocardiac ossicle is moved in caudal direction, and the propyloric

ossicle is moved in rostral direction. The propyloric and the pyloric ossicle are fused and because the pyloric ossicle is moved dorsocaudally and the mesocardiac ossicle is moved caudally, the medial tooth performs a retraction. The medial tooth protractors (gm1 and gm2/3) are passively stretched because the innervating motor neurons are silent during the retraction phase. Transection of the gm4c bundle was performed and the stimulation was then repeated, resulting in a retraction movement amplitude of *-0.78 (±) MT* (*N=4*) in amplitude. A similar reduction in amplitude compared to the fully intact condition, was seen for all of the tested stimulus frequencies (see fig. 58, blue bars, ***p<0.001***, One Way ANOVA on Ranks, *N=4*). This demonstrated that the gm4c bundles contribute to the retraction movement of the medial tooth.

Then, the lateral gm4b fiber bundles were successively severed and changes in medial tooth retraction amplitudes were recorded. In each experiment the left gm4b bundle was sectioned first (see fig. 58, light blue bars) leaving only the right gm4b bundle intact. Due to the symmetrical anatomy of the gm4 muscle, experiments with mirrored transection of gm4b bundles (right gm4b fiber bundle lesioned before the left gm4b bundle) were omitted.

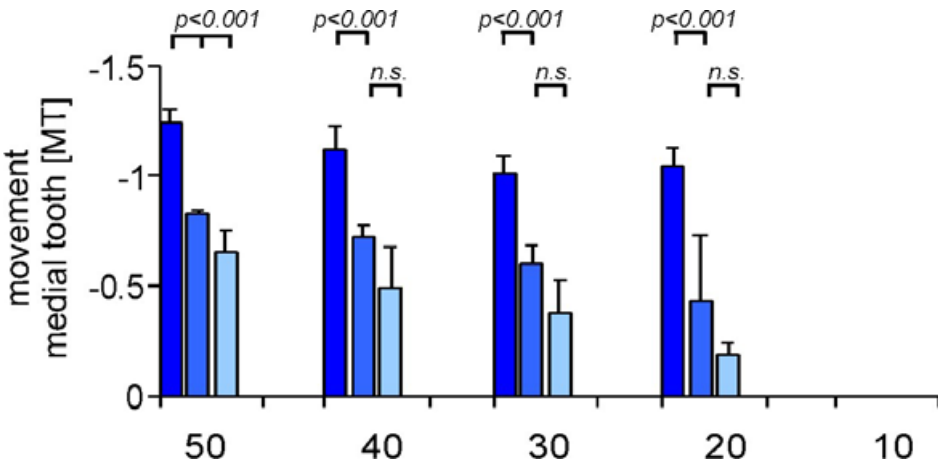

Figure 58: Retraction amplitude of the medial tooth diminishes after successive transection of gm4 muscle bundles. Bar graphs show amplitudes of medial tooth retraction. X-Axis shows the stimulus frequencies (Hz) used to activate the motor neurons' axons. Colors of bars indicate the state of the preparation. **Dark blue**: fully intact gm4 muscle. **Blue**: gm4c bundles sectioned. **Light blue**: gm4b left bundle sectioned.

After the first of the gm4b bundles (gm4b left) was lesioned, the DG stimulation was performed and the medial tooth performed a retraction of *0.65 (±0.2) MT* (*N=4*) upon *50 Hz* stimulation. Finally, the right gm4b bundle was transected as well, which abolished all retraction movements (not shown fig. 58). The retractions of the medial tooth were significantly different from the other two conditions (fully intact & gm4c bundles sectioned), showing that the lateral gm4b bundles also affect movement of the medial tooth (*p<0.001*, One Way ANOVA with Repeated Measurements, *N=4*). However, this was only the case for the strongest stimulus paradigm (*50 Hz*); the other stimuli did not evoke a significantly different movement compared to the previous experiments with only the gm4c sectioned. The *10 Hz* stimulation did not elicit any movement in the medial tooth. This seems to be the threshold for eliciting movement in the medial tooth.

4.7.2.2 The lateral tooth retractor subsystem

The gm4b bundles insert at the exopyloric ossicle. This ossicle is functionally combined via connective tissue with the zygocardiac ossicle, i.e. the lateral tooth (Brösing et al. 2002; Pearson 1908). When the gm4b muscles contract, the exopyloric- and the zygocardiac ossicles are moved rostrally. Simultaneously, the mesocardiac- and the pterocardiac ossicles are pulled in caudal direction.

The actions of the gm4 muscle during lateral tooth retraction were investigated in the intact preparation and after the gm4c and gm4b fiber bundles were successively transsected. In each situation (intact and lesioned) DG was stimulated for *5 s* with stimulus frequencies ranging from *50 Hz* to *10 Hz*, producing the same conditions compared to experiments shown in chapter 4.7.2.1 (page 109). The response of the lateral tooth to the various stimulation frequencies was recorded.

The retraction amplitudes of the lateral tooth elicited by fully intact gm4 muscles were -*0.52 (±0.2) MT* (*N=3*) for the right lateral tooth and *-0.51 (±0.2) MT* (*N=3*) for the right lateral tooth during the strongest stimulus frequency (*50 Hz*). The fully intact gm4 muscles retract the lateral tooth ossicles synchronously and symmetrically; as shown in figure 59 A. No significant difference in retraction amplitude was found between the two lateral teeth (*p=0.92*, One Way ANOVA, *N=3*). Since the gm4b fiber bundles inserts rostro-laterally into the exopyloric ossicle, they were assumed to be the main contributors to the retractive movement of the lateral teeth.

Next, the lateral gm4b fiber bundles were transected and DG stimulations were repeated after each lesion and the changes in lateral tooth retraction amplitudes were recorded (see fig. 59 B). In each experiment the left gm4b bundle was transected first, followed by the right gm4b bundle.

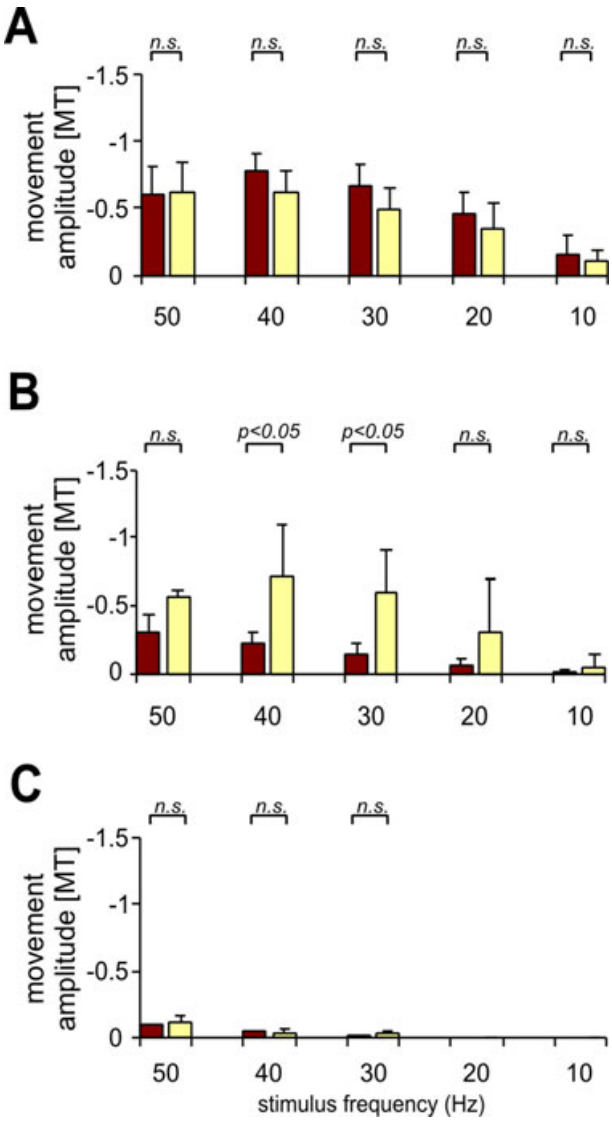

Figure 59: Retraction amplitude of the lateral tooth diminishes after successive transection of gm4 bundles **A** shows the maximal retractions of the right (yellow bars) and left (red bars) lateral teeth with intact gm4 muscle. X-Axis shows stimulus frequencies decreasing from left to right. Y-Axis shows movement amplitude in *MT*. **B** shows same as **A** after transection of left gm4b muscle. **C** shows same as **B** with the right gm4b severed.

After the left gm4b bundle was transected, the right lateral tooth showed a retraction amplitude that was very close to control (*-0.57 ±0.03 MT*; *N=3*) during *50 Hz* stimulation. The retraction amplitude of the left lateral tooth, however, was smaller (*-0.31 ±0.1 MT; N=3*) during the same stimulation, but no statistically significant retraction amplitude, compared to the right lateral tooth, was elicited (*p=0.29*, paired t-Test, *N=3*). *40 Hz* and *30 Hz* stimulations produced significantly smaller retraction amplitudes in the left lateral tooth movement compared to the ipsilateral tooth (both *p<0.05*, paired t-Test, *N=3*). The lower frequencies tested (*20 Hz* and *10 Hz*) produced very small amplitude movements in all teeth, and also not significantly different movements between the ossicles with intact gm4b and severed gm4b bundles (*20 Hz: p=0.48*, paired t-Test, *N=3*; *10 Hz: p=0.61*, paired t-Test, *N=3*). After both gm4b fiber bundles were transsected, only the medial gm4c bundles were intact. DG stimulation in these preparations produced low amplitude retractions in both lateral teeth (*0.06 (±0.04) MT*), all of which were not significantly different from each other (*50 Hz: p=0.65*; *40 Hz: p=0.79; 30 Hz: p=0.81*, paired t-Test, *N=3*). No movement could be recorded for stimulations at *20 Hz* and *10 Hz* in these preparations (see fig. 59 C). Interestingly, the *10 Hz* stimulation of the fully intact gm4 muscle did not evoke movement in the medial tooth (see chapter 4.7.2.1 on page 109) but did so in the lateral teeth.

4.7.2.3 Muscles gm2 & gm3 do not participate in retraction

From experiments in *H. gammarus* first conducted by Heinzel (1988) it was shown that the gm2 and gm3 muscles are an integral part of the medial tooth protraction system, as well as the retraction system of the medial and lateral tooth. In the lobster the gm2 & gm3 muscles are innervated by the lateral posterior gastric (LPG) neuron. The role of LPG in the crab, however, appears to be different: it acts as part of the pyloric pacemaker ensemble (Stein, 2009) and only rarely contributes to the gastric mil rhythm (W. Stein, personal communication). I conducted preliminary experiments to examine whether activation of the gm2 & gm3 muscles also has retractive effects on the lateral tooth. In these experiments, all muscles were left intact, except the gm2 & gm3 muscles, which were transected caudally of the pyloric and propyloric ossicle.

The retraction movement of the lateral teeth after the transsection was monitored during DG stimulation. DG was stimulated with a stimulus frequency of ***50 Hz***. As shown in figure 60 the complete transection of the gm2 & gm3 muscles had no effect on the retraction of the lateral teeth. Also there was no significant difference between the retraction amplitude between the left and right lateral tooth after transsection of these muscles (***p=0.54***, Student's t-Test, ***N=3***).

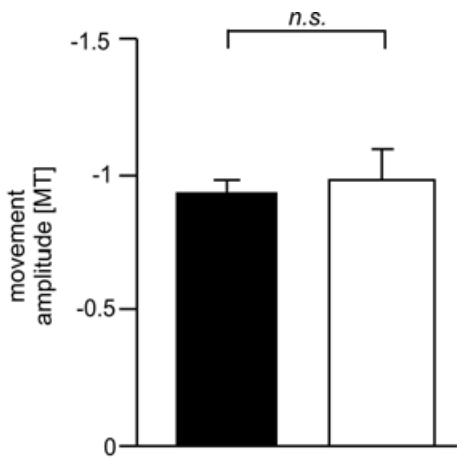

Figure 60: No change in lateral tooth retraction amplitude after transection of muscles gm2 & 3. Graph shows the maximal retractions of the right lateral tooth before (black bar) and after (white bar) the gm2 & gm3 muscles were transected.

4.7.3 3D-modeling visualizes functional coupling of gastric mill teeth

These findings show that a complex interaction of ossicles and muscles occurs during rhythmic movement. The above experiments indicate that the medial tooth retractor neuron DG also affected the retraction of the lateral teeth during gastric mill rhythms. Previous studies of the neuronal network in the STG and the musculature did not reveal such effects of DG on the lateral teeth. To study a possible mechanical influence of the medial tooth retractor system on the the lateral teeth a 3D model was created to visualize and help understand the emergent movement patterns, with particular emphasis on the lateral teeth.

The 3D model is a purely anatomical reconstruction and no data about neuronal innervation, muscle properties or ossicle stiffness was implemented. It is based on photographs of dried foregut preparations (own work; see chapter 3.7 on page 37 ff.) as well as anatomical data on the ossicles' structure from previous publications (Brösing et al. 2002; Hobbs & Hooper 2009; Kennedy & Cronin 2006; Maynard & Dando 1974; Pearson 1908; Patwardhan 1935a). The relative sizes and insertion points of

the gastric mill muscles were deducted from schematic drawings (Heinzel et al. 1993; Maynard & Dando 1974; Weimann et al. 1991) and included into the model. Since figures from the aforementioned publications are inconsistent in scaling and composition, only manual sculpting and arrangement of the 3D models (meshes) of ossicles and muscles was possible.

In addition to a 3D representation of the stomach ossicles and muscles in the 3D rendering software Blender the model allows to simulate movement of each ossicle and the inserting muscles. Solely the moments of maximal pro- and retractions of the teeth were simulated. This was done by manually shortening the muscle-meshes (to simulate contraction) and rearranging the ossicle-meshes to reconcatenate them with the respective muscle-mesh at the correct insertion point. For example, the movement of one of the lateral teeth was simulated by shortening the meshes of the protractor muscles (gm5, 6 & 8). Afterwards the zygocardiac ossicle-mesh was moved in order to realign with the ends of the muscle-meshes (see fig. 61). For demonstration purposes the protraction was simulated for the right side only.

Contraction of the aforementioned group of lateral tooth protractor muscles causes a total of four ossicles to move. The gm8 muscle inserts dorsally into the zygocardiac ossicle (***# 5*** in fig. 61 A) and ventrally into the inferior lateral cardiopyloric ossicle (***# 13*** in fig. 61 A). The gm6 muscle inserts dorsally into the subdentate ossicle (***# 14*** in fig. 61 A). The gm5 muscle inserts dorsally into the prepectineal ossicle (***# 9*** in fig. 61 A). The preperinecteal ossicle, however, is fused with the zygocardiac ossicle, thus allowing the assumption that gm5 and the muscles gm6 and gm8 belong to the same functional group. Contractions of this group of muscles and the aforementioned movement of ossicles causes the calcified protrusion of the zygocardiac ossicle inside the cardiac sac (the lateral tooth) to move towards the midline, thus performing a protraction of the lateral tooth. This is depicted in figure 61 B by changing the image plane in Blender to a frontal view, which corresponds to the view through the endoscopic camera *in vivo*. The frontal view of the gastric mill in the intact animal showed only parts of the ossicles and no muscles due to the non-transparency of the tissue constituting the stomach wall. The 3D model of the gastric mill, however, showed an unobstruced view of the ossicles and muscles. This model supports the assumption that the protraction of the lateral teeth is performed by a movement of the zygocardiac and the subdentate ossicle towards each other, performed by the gm8 muscle.

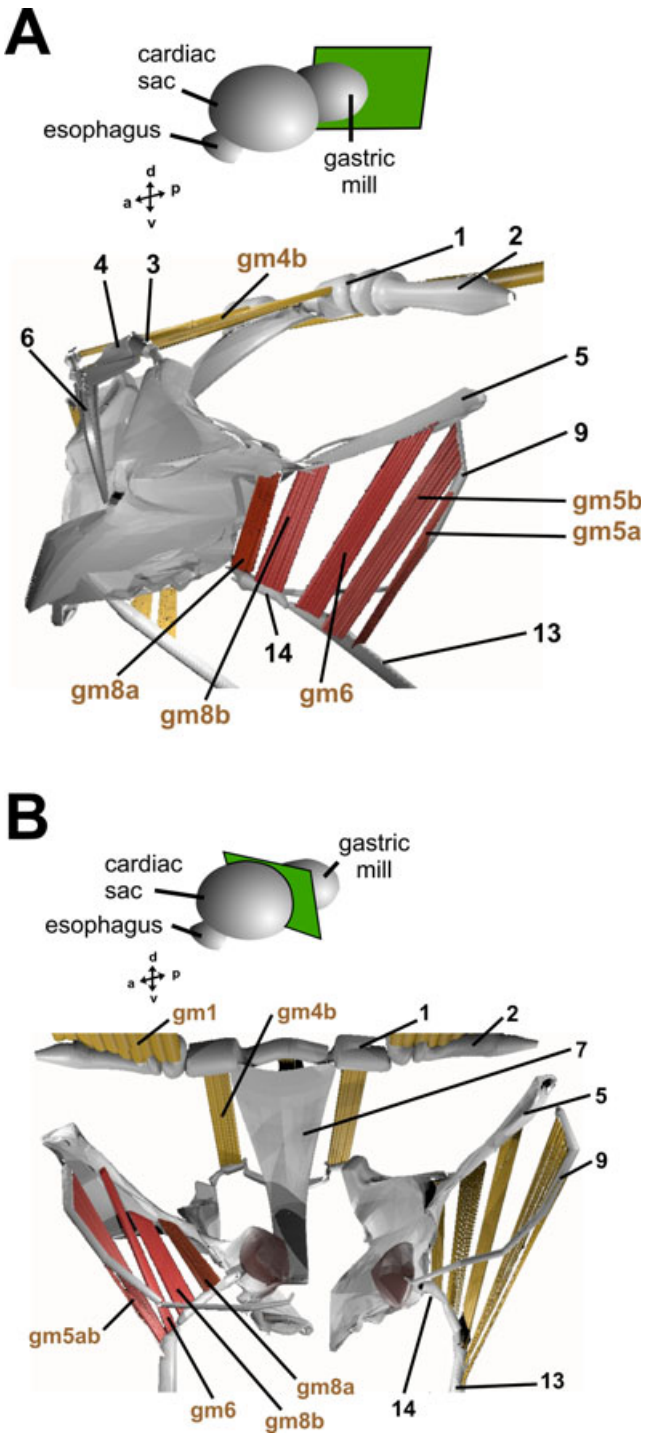

Figure 61: 3D model of the gastric mill ossicles, muscles and nerves showing the right lateral tooth protraction. **A** Top shows the image plane onto the foregut depicted in the graphic below (d=dorsal; v=ventral; a=anterior; p=posterior). Graphic shows ossicles (grey, numbering according to nomenclature in table 1), muscles (brown) and nerves (green) in posterolateral view. Protractor muscles gm5, gm6 and gm8ab are shown in red. **B** Top shows the image plane onto the foregut depicted in the graphic below. Graphic shows ossicles and muscles in frontal view. Note that only right-side protractors contracted. Left-side and dorsal muscles are all in relaxed position.

The protraction of the lateral teeth was thus managed by simultaneous contraction of several muscles inserting in multiple ossicles. After the end of a protraction the gm5,6,8 muscles relax and the ossicles return to the baseline position. This has also been described in detail during the analysis of standardized stimulations of the motor nerves *in vivo* (see chapter 4.5.1 and fig. 53). These experiments also showed that this retraction due to muscle relaxation was followed by an additional retraction beyond the baseline upon commencement of the DG burst.

As shown in figure 62 A, contraction of all fiber bundles of the gm4 muscle simultaneously affected the medial tooth ossicles and the lateral tooth ossicles. To illustrate the effects of the gm4 contraction on the gastric mill teeth, figure 62 A shows the 3D simulation of the gastric mill in the vetral view (same as in fig. 61 B), in which the transparency of the medial tooth mesh was increased to fully reveal the gm4 muscles. The keys to the medial tooth retraction were the exopyloric and propyloric ossicles, at which the gm4c and gm4b muscles insert. Contraction of the gm4 muscle moved the propyloric ossicle and the meso- and pterocardiac ossicles (***# 1*** & ***2*** in fig. 62 A), thus pulling the medial tooth (urocardiac ossicle, ***# 7*** in fig. 62 A) posteriorventrally towards the pyloric valve and the cardiac gutter (not shown in fig. 62 A).

The retraction movement of the lateral teeth was affected by the contration of the gm4 muscles as well. The exopyloric ossicle is fused to the zygocardiac ossicle ***(# 5*** in fig. 62 A). Contraction of the gm4b muscle, which moved the exopyloric ossicles in rostral direction, also affected the zygocardiac ossicle. This caused a movement of the lateral tooth inside the cardiac sac away from the midline. Finally, the relaxation of the gm4 muscle, after the end of a DG burst, reversed the retraction of medial and lateral teeth (see fig. 62 B). The gm4 muscles were passively stretched by the gm1 muscles and the gm2/3 muscles (not shown).

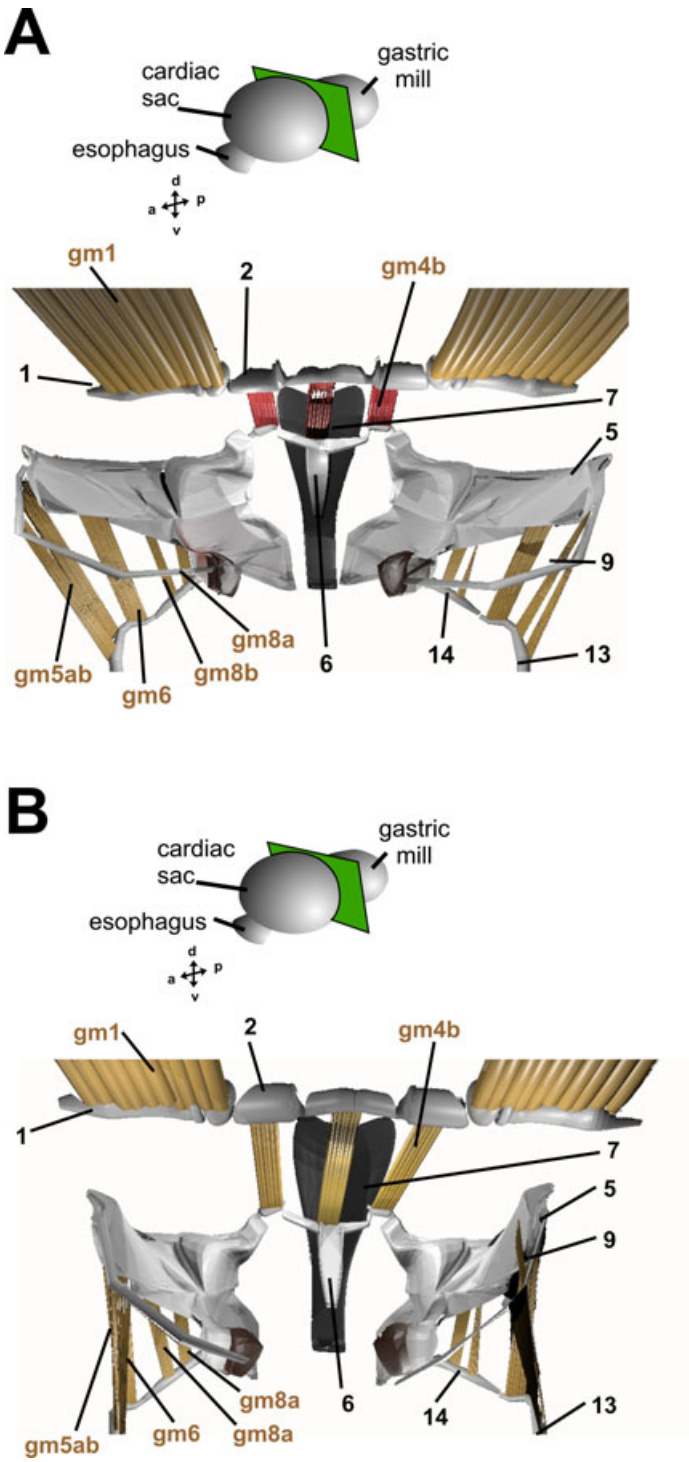

Figure 62: 3D model of the gastric mill ossicles, muscles and nerves showing the lateral and medial tooth retraction. **A** Top shows the image plane onto the foregut depicted in the graphic below. (d=dorsal; v=ventral; a=anterior; p=posterior). Graphic shows ossicles (grey, numbering according to nomenclature in table 1), muscles (brown) and nerves (green) in posterolateral view. Protractor muscles gm5, gm6 and gm8ab are shown in red. **B** Top shows the image plane onto the foregut depicted in the graphic below. Graphic shows ossicles and muscles in frontal view.

4.7.4 Summary of chapter 4.7

The calcified bones and muscles forming and moving the decapod crustaceans' foregut have been described in the last century from a purely anatomical perspective.

This chapter illuminated the movement of the three teeth in the gastric mill and revealed interesting properties of the movement output. The standardized stimulus paradigm allowed for a thourough and comparable investigation. In general, the functional interaction of the musculature was confirmed for the protraction movements of the lateral teeth and the medial tooth. One new finding was the retraction movement of the lateral teeth that was caused by a mechanical coupling to the retraction system of the medial tooth. Consequently, the retraction of all teeth is performed by the gm4 muscle, which was formerly assumed to elicit only the retraction of the medial tooth. The gm4 muscle was investigated by transsection experiments conducted in the *in vivo* preparation. Lesioning of the gm4 muscle prevented this retraction of the lateral teeth as well as the medial tooth. Partial lesions of the individual gm4 fiber bundles revealed that the medial gm4c has stronger effects on the medial tooth retraction, while the lateral gm4b bundles have stronger retractive effects on the lateral teeth. Preliminary experiments on the gm2 & gm3 muscles were performed as well, revealing that these muscles do not participate in medial and lateral teeth retraction in the crab.

5. Discussion

In this work the effects of changes in the activity of the neuronal network in the crabs *Cancer pagurus* and *Cancer borealis* on the behavioral output were investigated. The nervous system of decapod crustaceans is, like all invertebrate nervous systems, organized in spatially separated ganglia. One of those ganglia, the stomatogastric ganglion (STG), accomodates ***26*** synaptically interconnected neurons (Bartos et al. 1999; Kilman & Marder 1996). These neurons form two central pattern generators (CPGs) with distinct characteristics (Marder et al. 2005). The motor neurons in the STG innervate intrinsic and extrinsic muscles, which elicit digestive movements by the gastric mill teeth in the foregut of the animal (Heinzel et al. 1993; Patwardhan 1935a; Russell 1985). Extensive studies on the neuronal network in the STG and its connections to other parts of the nervous system revealed intricate simultaneous interactions of cellular (Golowasch et al. 2009; Marder et al. 1996), synaptic (Bartos & Nusbaum 1997; Beenhakker et al. 2007) and hormonal factors (Marder & Bucher 2007; Nusbaum & Beenhakker 2002; Stein 2009). This allows the two central pattern generators in the STG to elicit a highly flexible, yet stable, output (Golowasch et al. 1999; Nusbaum et al. 2001; Parker 2006; Prinz 2006). It is not yet fully understood, however, whether and if so, how these various neuronal outputs affect the behavior of the animal. It is possible that the purpose of the modulation of neuronal activity is to assure maximum stability of the nervous system at all times (Marder & Prinz 2002; Saideman et al. 2007a), rather than to alter the behavior. If this were the case, it would be highly inefficient for the behavioral output to mimic the variability in neuronal activity. Another option is that this variability in neuronal activity is indeed of behavioral relevance. Studies on the proprioceptors, which modulate the output of the CPGs, support this hypothesis (Daur et al. 2009; Smarandache & Stein 2007).

To find experimental proof for either of these hypotheses the behavioral output and the neuronal network activity were investigated simultaneously in the intact animal. I developed an *in vivo* assay, which provides the experimental tools for this task. The behavioral output was monitored via endoscopic video equipment, which filmed the movement of the gastric mill teeth. Neuronal activity was recorded and induced by extracellular electrodes applied directly to the designated nerves.

It is known that the motor neurons in the STG are modulated by projection neurons in the commissural ganglia (Hedrich et al. 2009; Smarandache & Stein 2007; Hedrich 2008). Depending on the activity patterns in these projection neurons the rhythmic activity of the motor neurons in the stomatogastric ganglion is initiated or modulated. The motor neurons, which are part of the gastric mill CPG are only active when the projection neurons in the commissural ganglia provide sufficient activation (Blitz &

Nusbaum 2012; Stein 2009). The projection neurons themselves are activated by different sensory neurons as well as by neurons from other parts of the nervous system (Beenhakker & Nusbaum 2004; Beenhakker et al. 2005; Blitz et al. 2008). Previous studies showed that projection neurons retain their influencence on pattern selection, which has been shown in *in vitro* studies, as well as in *in vivo* preparations (Hedrich & Stein 2008; Smarandache et al. 2008). These studies show that neuromodulation has important effects on the flexibility on the nervous system *in vitro* and *in vivo.* Whether this flexibility is also conveyed to the behavioral level is not known.

To clarify whether the flexibility of neuronal output is important for the behavior of the animal, or whether it rather has a stabilizing function of the neuronal network output, was the main goal of my work.

5.1 Contribution of a single projection neuron on motor output *in vivo*

The experiments presented in chapter 4.1 (page 39) show that activation of a single projection neuron (MCN1) in the stomatogastric nervous system is sufficient to activate the gastric mill CPG and to modulate the pyloric CPG. This is coherent with data gathered *in vitro* where the projection neuron MCN1 was exposed as an important element, which is necessary and sufficient to initiate gastric mill rhythms (Coleman et al. 1995; Stein 2009). My data shows that at least one of the projection neurons (MCN1) serves as command-like neuron, which integrates sensory input and activates the central pattern generators in the STG *in vivo*. This data is coherent with previously published *in vitro* studies, which showed that variations in activity of MCN1 alone is sufficient to modulate the rhythmic activity of the gastric mill motor neurons as well as the pyloric motor neurons (Bartos & Nusbaum 1997; Coleman & Nusbaum 1994).

MCN1 is not the only source of neuromodulation in the STNS. There are at least three more modulatory neurons in the CoGs, which also affect the STG central pattern generators (Stein 2009). Simultaneous activation of these neurons can affect the output of the motor neurons (Beenhakker & Nusbaum 2004). Additionally, the release of neurohormones into the bloodstream can modulate the effects of any of the projection neurons onto the pattern generators (Wood et al. 2010). The neurohormone pyrokinine (PK) even elicits a gastric mill rhythm *in vitro* without the synaptic inputs of any of the projection neurons (Saideman et al. 2007b). In a system, which is influenced by many neuromodulators and -hormones, it is not clear whether a single projection neuron MCN1 (or any projection neuron) is of similar importance.

The recording of MCN1 *in vivo* revealed that the projection neuron MCN1 is sufficient and neccessary for the initiation of rhythmic activity in the gastric mill CPG in the *in vivo* preparation. Lesioning of the MCN1 axon supressed the initiation of gastric mill rhythms entirely and slowed down the pyloric rhythm. This suggests that MCN1 plays an equally important role in pattern selection *in vivo* as *in vitro.* The data showed that, despite the dynamic and uncontrollable influence of neuromodulators, a projection neuron in the commissural ganglia exhibits effects on the central pattern generators in the STG comparable to previously published data from *in vitro* experiments.

Previous studies showed that MCN1 and the other projection neurons are synaptically connected to sensory neurons (Barriere et al. 2008; Beenhakker et al. 2007) as well as to neurons in the cerebral ganglion (Hedrich & Stein 2008). The activation pathway utilized by the IV neurons in the cerebral ganglion has been confirmed *in vivo* and the elicited gastric mill rhythms were comparable to those obtained in *in vitro* preparations (Hedrich 2008). The activation pathways utilized by the sensory neurons have been studies *in vitro* as well as *in situ* (Beenhakker et al. 2004, 2005). In these preparations, however, the cerebral and the thoracic ganglion were removed prior to the experiments. For example, Mullins & Friesen (2012) show that interneuron E21 in the leech *Hirudo verbana* shows drastic differences in activity in preparations with an intact brain compared to decerebrated preparations. This could also be the case in the *in vivo* preparation of the crab, where MCN1 might be active in a different manner compared to the *in vitro* preparations. I thus performed extracellular recordings of the *ion* in the *in vivo* preparation, which showed that MCN1 possessed spontaneous activity that was similar to that *in vitro* (Hedrich et al. 2011). When activated, however, MCN1 effects on the burst patterns of the gastric mill protractor neuron LG were different from those *in vitro*. It is therefore possible that concurrent activity of other projection neurons, sensory neurons in the foregut modulate MCN1 activity in the *in vivo* preparation. The data gathered so far suggest that the activation pathways of MCN1 are not substantially different *in vivo* compared to the isolated preparation. Modulation of MCN1 activity, elicited by other neurons or neurohormones in the blood stream, alters the output of the gastric mill motor neurons *in vivo.* Whether these modulations of the motor neurons' activities have effects on the behavior was also investigated in this work.

In summary, these experiments showed that the stimulation and lesion of a single neuron in the intact animal is experimentally feasible. The experiments also showed that a single projection neuron is important for the initiation and maintaining of chewing behavior in the *in vivo* preparation. The observation that the activity of MCN1 is modulated, possibly via neurohormones from the blood stream and/or comodulation

via the other *20* projection neurons, suggests that such modulation adjusts the motor neuronal output to the behavioral context. Current research in vertebrates also reveals that neurohormonal modulation serves as important element in control of neuronal activity (Miles & Sillar 2011; Dickinson 2006; Harris-Warrick 2011). Further research on the peptidome in the *in vivo* preparation of decapod crustaceans (Chen et al. 2010) could reveal insights about the interaction of neurohormones and peptides, which are also helpful for vertebrate research.

5.2 Different gastric mill activation pathways elicit distinct behaviors *in vivo*

In the *in vitro* preparation, different sensory pathways can elicit various versions of the gastric mill rhythm. Hedrich & Stein (2008), for example, showed that activation of the IV neurons and elicits a unique type of gastric mill rhythm in the STG.

The gastric mill CPG is not only initialized by the pathway mediated by the IV neurons. Internal sensors in the foregut can also activate the gastric mill. The mechanosensory VCNs (Beenhakker & Nusbaum 2004; Dando & Maynard 1973; Ringel 1924) are mechanoreceptors in the cardiac sac, which elicit a different version of gastric mill rhythm. Yet another version is elicited by modulatory interneurons projecting through the post esophageal commissure (POC) (Blitz et al. 2008; Goldberg et al. 1988). Those neurons are no sensory cells, but they are assumed to be interneurons relaying activation from the thoracic ganglion to the commissural ganglia (M. P. Nusbaum, University of Pennsylvania, personal communication). The lateral gastric motor neuron shows very characteristic and easily discernible activity patterns during POC- and VCN-elicited gastric mill rhythms (Beenhakker et al. 2004; Blitz et al. 2008). Whether these activity patterns are behaviorally relevant, however, has not been clarified. The *in vivo* preparation presented in this work was ideal to test if differences in motor neuronal output mapped onto the movement output of the teeth in the gastric mill. The motor neuron LG elicits protractive movement of the lateral teeth, which can be recorded and analyzed easily in the *in vivo* preparation. Thus, LG was ideal to clarify whether changes in neuronal output are transferred to the behavioral level.

5.2.1 Investigation of a mechanosensory gastric mill activation pathway

It was shown previously that a gastric mill rhythm can be initiated *in vitro* when the VCN neurons are stimulated extracellularly. Similarly, a gastric mill rhythm was initiated in semi-intact preparations when the VCNs were activated by mechanical stimulation of the cardiac gutter (Beenhakker et al. 2004). The work presented here showed

that it is possible to elicit a gastric mill rhythm *in vivo* by activation of the VCNs alone. As will be dicussed in more detail in chapter 5.2.8 (page 142), the stimulation of the cardiac gutter *in vivo* did not always initiate rhythmic movements of the gastric mill teeth. This suggests that, since this pathway involves several projection neurons, inhibitory effects via other neurons or neurohormones in the CoGs could supress the initiation of gastric mill rhythms in these preparations.

In the preparations, in which a gastric mill rhythm was successfully initiated, the activity of the lateral tooth protractor neuron was measured and compared to *in vitro* data (obtained from W. Stein & M. P. Nusbaum). The data presented in chapter 4.2.1 (page 48) shows firing characteristics of LG after activation of the VCN pathway *in vivo*. The period of LG bursting showed high variability *in vivo*, which suggests that other factors in the intact animal influenced the output of the motor neuron. The electrode, which recorded the LG activity was insufficient to determine whether these factors were proprioceptors or projection neurons. Despite the variability across preparations, a striking constancy of burst durations was observed during a given gastric mill rhythm. The burst duration during the initial phase of a gastric mill rhythm was not statistically different from the burst duration at the end of the rhythm. This showed that while the protraction phases during gastric mill rhythms varied largely during several preparations, the phases and protraction durations within a preparation, remained constant. It is not known, however, whether this was actively controlled by the nervous system or due to missing sensory feedback, since the animals were chewing with empty stomachs. Experiments could be performed on the *in vivo* preparation in the future in, which the pro- and retraction of the teeth during an ongoing VCN-elicited gastric mill rhythm is perturbed. Measuring the protraction phase durations and gastric mill periods before and after perturbation would provide insights about how stable the patterns of certain types of gastric mill rhythms are after a disruption. During walking in insects (Ekeberg et al. 2004) and in humans (McAndrew et al. 2011), for example, quick recovery of the locomotor CPGs after disruptions is vital for survival. Since locomotion through a changing environment poses different demands onto the nervous system and the musculature than the digestion of food, it is sensible to assume that biological organisms have evolved specialized neuronal networks, optimized for walking and chewing, respectively. Locomotor systems have several sensors (visual, tactile, proprioceptive and equilibioceptive), which allow precise control of the limbs (Levine & Loeb 1992; Pearson et al. 2006). During chewing of food, however, information about consistency and size of the food particles can only be assessed indirectly via proprioceptors and mechanosensors. It would thus be interesting to examine whether different types of gastric mill patterns elicit different responses during perturbation. Since the underlying neuronal network is very well understood in

decapod crustacteans, this would provide insights into the control of variability in biological systems. Research on the dynamic control of behavior in the stomatogastric system may be a promising approach to increase flexibility in robotic systems. Shortcomings in battery life and weight of current robots, have presented miniaturization as a promising approach to alleviate energy shortage. The problems of scaling and neuronal control have been tackled in various ways by nature already (Hooper 2012). Another problem correlated with energy consumption is the very limited sensory outfit of autonomous robots (Tikanmaki & Roning 2009; Playter 2006), which makes the precise reaction to environmental changes difficult. The stomatogastric system is one promising model to investigate sensory control of movement as well as emergent effects beyond neuronal control, and thus provide prospects for robot design.

The different LG activities that were obtained after *in vivo* and *in vitro* VCN stimulation were also different on the movement level. Tooth movement during mechanically elicited VCN patterns were compared with those obtained during LG stimulations with either standardized or spikes patterns that were obtained in *in vitro* experiments.

The movement of the lateral teeth after mechanical stimulation of the VCNs showed both negative and positive velocities, i.e. protractive as well as retractive movements during bursting of LG. The two main characteristics of the mechanically elicited VCN pattern were that tooth protraction increased with a rather constant velocity and that the plateau phase interspersed with irregular bouts of movement. In some cases, retraction of the lateral teeth initiated while LG was still actively bursting.

When the LG axon was stimulated with the *in vitro* data, a different behavioral output emerged. The movement velocities were faster (compared to the mechanical stimulation) and the plateau phase was more pronounced and regular. In other words, the irregular bouts and retractions during LG bursting did not appear during the stimulations with *in vitro* data, which is also reflected in the data presented in chapter 4.2.2.1 (page 56). In addition to the aforementioned stimuli with *in vitro* patterns and mechanical stimulation of the cardiac gutter, standardized stimuli were applied to the motor nerves in the *in vivo* preparation.

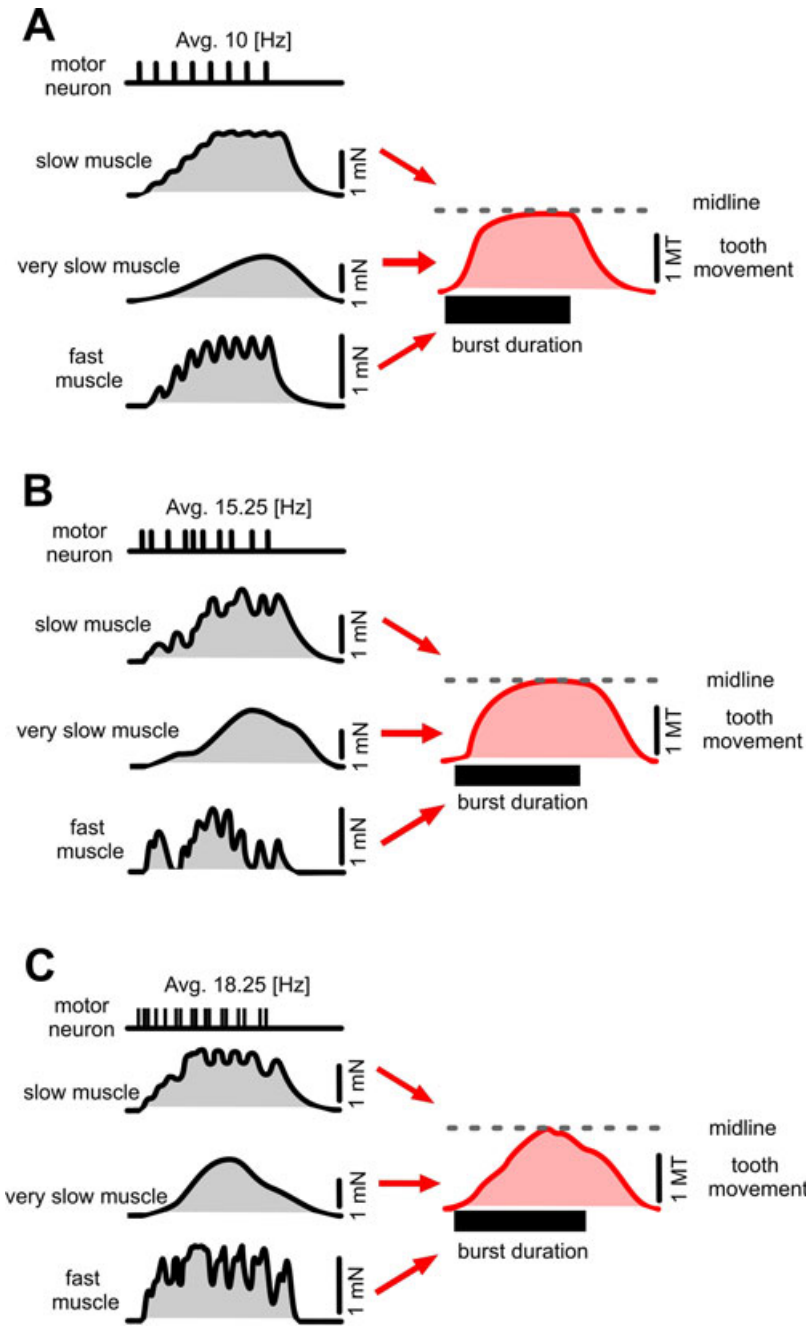

Figure 63: Model for behavioral output of the gastric mill protractor system to standardized, *in vitro* and natural activation. **A** shows contractions of three protractor muscles upon standardized stimuli (top). The protraction of the lateral tooth is shown on the right (red curve). **B** shows contractions of the muscles upon stimulation with *in vitro* data (***15.25 Hz***). The elicited protraction of the lateral tooth is shown on the right (red curve). **C** shows contractions of the muscles during even higher LG average intraburst spike frequency (***18.25 Hz***). The protraction of the lateral tooth is shown on the right (red curve). Tooth protractions are actual recordings. Depictions of muscle contractions are based on data from (Stein 2006; White 2011). The fast muscle represents gm5, the slow and very slow muscles represent gm5 and gm6, respectively.

Interestingly, LG stimulation with the standarized VCN pattern caused a more rapid protraction than the non-standarized version and than the mechanically evoked VCN pattern. Protraction was not uniform: it was initially quick, but slowed down eventually before it reached a sustained plateau. This was surprising since the average firing frequency of LG was lowest in the standardized version of the VCN pattern and the intervals between single LG spikes were constant. Intuitively, this should lead to a uniform and, in comparison to the other, more natural (noisy) stimulations, slower protraction. However, in the case of the lateral tooth protractor system three individual muscles are innervated by the same motor neuron (LG). Muscles can possess very different characteristics in elasticity and contractability (Hill et al. 1975). If such differences exist between the gastric mill muscles it could cause a different movement output of the teeth. The three muscles gm5, gm6 and gm8 indeed have distinct contraction and relaxation characteristics (Jahromi & Govind 1976), which is even obvious from the temporal dynamics of their response to LG spike input (White 2011). While gm5 responds faster to stimuli and elicits high EJP amplitude, the gm6 muscle shows slower responses to stimulations (Stein 2006). The gm8 muscle shows response delays, which are comparable to the gm6 muscle, but it elicits larger EJPs (White 2011). Consequently, an uneven distribution of spikes, as obtained during the mechanical and *in vitro*-data stimulations, can thus have smoothing effects on the movement output of the gastric mill teeth. Figure 63 summarizes this hypothesis: during standardized stimulation force output of all three protractor muscles increases continuously, resulting in fast protraction and a long plateau phase of the tooth movement at the midline. The plateau phase represents the isometric "clenching" phase during a VCN-rhythm (see fig. 63 A). The question arose why the non-standardized LG activity from in vitro experiments causes a movement output that is more similar to that of standardized stimuli than to that of the mechanical stimulation of the VCNs. Once of the reasons could be that the in vitro LG activity was recorded (per definition) without any sensory feedback, which may occur in intact animals and could modulate the output of the motor neuron. The pattern shown in figure 63 C illustrates this assumption. This pattern is based on one LG burst elicited by mechanical stimulation of the VCNs shown in figure 20. The contraction patterns of the three muscles cause a slower protraction, even retraction, of the teeth during LG bursting. This is counter intuitive at first, because the average LG interburst spike frequency was higher (see chapter 4.2.1) compared to standardized (see chapter 4.3.1) and *in vitro* stimulation patterns (see chapter 4.5). The key must therefore lie in the way the muscles respond to the distribution of the three different types of stimuli. As shown in previous studies, muscles in decapod crustaceans can exhibit nonlinear contraction properties (Hooper & Weaver 2000; Morris & Hooper 1997). Studies on the gastric mill protractor muscles

(Stein 2006; White 2011) showed that these muscles also exhibit such nonlinear characteristics. Another gastric mill muscle, which has been investigated in detail, the medial tooth protractor (gm1), has been shown to elicit complex responses to stimuli as well (Städele 2010). These preliminary results suggest that the complex intrinsic characteristics of the musculature are not adding variability to the movement of the gastric mill teeth. On the contrary, the data presented in this work suggests that, at least for the lateral tooth protractor system, the musculature can stabilize behavioral output. The functional specialization of intrinsic muscle properties has been shown to be a key element for stabilization of behavior in mammals as well (Graziotti et al. 2012). In a simulation study the integration of nonlinear muscle dynamics into the simulation of a bipede computer model, which elicited a hopping behavior greatly reduced the sensitivity of the system to perturbation (Haeufle et al. 2012). Interestingly, the study also showed that the stabilizing effects of the musculature were preserved across a wide range of stimulus paradigms. Similarly to the different outputs of lomotor systems (walking, running, hopping), the gastric mill elicits very different modalities of behavior as well. The hypothesis that the musculature in the gastric mill seems to elicit similar stabilizing effects needs, of course, further experimental affirmation. It would be nonetheless interesting to investigate how, despite differences in evolutionary starting situations as well as environmental conditions, the methods of behavioral control in vertebrates and invertebrates converge to similar mechanisms.

5.2.2 Implications of noise and functional relevance of variability of behavior in the gastric mill

The aforementioned results from the comparison of LG activity after mechanical VCN stimulation with standardized and *in vitro*-data stimuli, suggest that some factor(s) in the intact animal modulate the output of LG activity. This variability causes different movement outputs and it is possible that these are functionally relevant during behavior. The higher variability in LG bursting *in vivo* may be due to the actions of neurohormones in the blood stream. Another trigger for the observed variability in activity of the motor neuron LG could be the feedback from sensory neurons in the foregut or external sensors. Previous experiments have shown that the anterior gastric receptor (AGR) and the gastro-pyloric receptors (GPR) modulate motor neuronal output during VCN rhythms (Beenhakker et al. 2007; Daur et al. 2009; Delong et al. 2009). In my studies I could not conclusively show what role each of these factors (proprioceptors and neurohormones) play in the fully intact animal. The data did show, however, that the protraction of the teeth was slower and the plateau phase was interspersed with retractive movements. It has been shown in humans that strong isometric contractions can cause muscle damage (Jubeau et al. 2012). During

the plateau phase of lateral tooth protraction the protractor muscles esssentially elicit isometric contractions, because the teeth are pressing together at the midline. It is thus possible that strong isometric force production during behavior is avoided by the computation of feedback from the proprioceptors. Interestingly, there are no known proprioceptors, which measure the state of contraction of the lateral tooth protractor muscles. It is also possible that the characteristics of the muscles themselves help to avoid stress during contractions. To fully understand the complex interactions of different types of muscles during movement, however, one must also appreciate the functional properties of the ossicles, at which the intrinsic muscles insert. Hobbs (2009) showed with computer tomographic imaging that some ossicles exhibit spring-like functionality during chewing. Thus, the bone structure could also provide ways to reduce muscle strain during isometric contractions. Spring-like structures could help to elongate the isotonic contraction phase, thus reducing the phase of isometric force production, and thus lowering the likelihood of muscle damage during strong contractions. Passive stretch and steric effects are not only important for behavior in the foregut of decapod crustaceans. In bipedal walking the bones and muscles in the leg and spine elicit damping effects, thus stabilize the movement output (Blickhan et al. 2007). In humans and other mammals these effects play a larger role than in insects, for example, because their legs have more mass and have higher inertia (Hooper 2012). The study of mechanical feedback of ossicles and muscles in the foregut of crabs could therefore be insightful to research on locomotion in other animals as well.

The observation that the stimulation with *in vitro* data sets produced similar tooth movements as the standardized stimulation opens another interesting realm of research that could be investigated using the *in vivo* preparation of decapod crustaceans: the impact of noise on a biological system. The investigation of methods, via which neuromuscular networks can reduce noise, and even use noise to optimize behavioral output (Douglass et al. 1993; McDonnell & Ward 2011; Narendra 1996), has been started relatively recently but is nonetheless very intriguing. Generally speaking, noise is inherent to every system, and the reduction of noisiness in one part, usually enhances noisiness in another (Faisal et al. 2008; Hooper 2004). To perceive the world organisms use a manifold of sensors. No matter what type, each sensor amplifies a (usually low) signal and then turns it into a digital signal (action potential), which is transduced to the central nervous system. Animals pay high metabolic costs to keep noise during this detection and conversion process minimal (Laughlin et al. 2008). It is thus feasible to assume that animals also try to find ways to reduce the susceptibility to noise in the effectors as well. The arrangement of ossicles in the gastric mill may be optimal to minimize degrees of freedom in movement of the teeth. This might be a way for the organism to reduce the variability (noisiness) of the be-

havioral output, but also to make the gastric mill less sensitive to perturbations during chewing of food. In other biological systems such approaches to optimizing behavioral output have been observed as well. To perform turning during running behavior, the motor neuron, which innervates the ipsilateral extensor muscle elicits phase-advanced action potentials in the cockroach (Sponberg et al. 2011b). This initates the contraction in the femoral extensor muscle on one side sooner than in the contralateral extensor muscle. The actual turning is managed, without neuronal control, by the intrinsic muscle characteristics and the anatomical structure of the leg (Sponberg et al. 2011a). This allows the cockroach to perform fast turns, which are controlled by mechanical feedback, which reduces reaction time and metabolic cost.

In the crab foregut, targeted behavioral output could be elicited without the nervous system's participation, via the intrinsic properties and organization of the muscles in the foregut. The stomatogastric ganglion contains only *26* neurons, which control a system of *39* muscles to perform coordinated movements. It is unlikely that, despite multiple sensory cells measuring the state of the system at any given moment, the nervous system can predict movement output of the system of the gastric mill in sufficient detail. It is argued that the human brain is capable to optimize movement output by motor learning (Sanger 2010). This allows for precise behavioral output despite noisy (sensory) inputs. In the stomatogastric nervous system a specialized neuronal structure for motor learning (cerebellum) does not exist. Despite the fact that the number of neurons in the nervous system of decapod crustaceans is low, it would also not be useful to implement such a structure. Movements during digestion in the foregut cannot be anticipated the same way as movements of the leg or the hand. Thus, as some researchers suggested previously, the best approach to solving the problem of prediction of motor output, may be to ignore it completely (Beer & Gallagher 1992; Chiel & Beer 1997). It was discussed previously that slow muscles can have a smoothing effect on the irregularities in neuronal firing, thus rendering the need for a neuronal feedback controller unnecessary in most situations (Krylow & Rymer 1997). The results presented in this work support the hypothesis that the slow protractor muscles facilitate the smooth protraction characteristics of the lateral teeth in the *in vivo* preparations despite the variability in motor neuronal input. All gastric mill muscles are slow, non-twitching muscles (Morris & Hooper 1997; Thuma et al. 2007). Further research on the intrinsic properties of gastric mill muscles, in the fashion of the *in situ* experiments on the gm6 muscle presented in this work, may provide evidence for stabilizing effects of several coactivated muscles on an oscillatory system. In case of the protractor system of the lateral tooth the distribution of work load onto three individual muscles could indeed be capable of decreasing noisy input from motor neurons, thus rendering the behavioral output less prone to interference.

Observations of leg muscles in the frog during jumping (Sundar 2009) and in bipedal walking in humans (Blickhan et al. 2007) showed that the autonomous interaction of contractile and elastic elements in muscles stustains stability and conserves energy without sensory feedback.

Organisms have evolved methods to minimize metabolic cost and reduce noise in behavioral output at the same time. It is, however, also the case that noise can be helpful for successful behavioral output of an organism. Proekt et al. (2008) show that noisy behavior can be advantageous for the snail *Aplysia* during feeding. With a combination of electrophysiological and ecological experiments as well as computer simulations, the authors demonstrate that egestive and ingestive movement patterns of the esophagus are irregular (noisy). In several studies, the authors showed that the tolerance of noise in less important aspects of the behavior can increase the accurateness of more important aspects (Proekt et al. 2004, 2008). Irregular (noisy) ingestion, which causes the food to be ingested in a less than optimal fashion, can be managed easily by the animal by slightly prolonging the feeding periods. More important is the egestion of seaweed that cannot be cut by the radula of *Aplysia*. If the seaweed cannot be fully ingested, the nervous system has to elicit egestive behavior. The animal has to egest the whole leaf and start over on a different one. Irregularities during egestion could cause a reinitiation of ingestive behavior on the same, uncuttable, leaf. Therefore, the CPG which controls the egestive behavior needs to be stable and resistive to perturbations. Thus, acquiescence of increased noisiness of one part of the system (ingestion) can highly reduce noisiness in another part (egestion).

5.2.3 Different methods to investigate the neuronal network, musculature and anatomy of the stomatogastric system in the crab

The stomatogastric nervous system is one of the best understood neuronal networks in neurobiology (Grillner et al. 2005; Marder et al. 2005; Hooper 2000). Most experimental knowledge comes from classical *in vitro* preparations (see fig. 64 A). The vast knowledge of the neural circuits involved in generating the pyloric and gastric mill motor patterns, however, now allow to test the neuronal control of behavior in experiments, in which the structural integrity of the stomach and the nervous system remains intact. Computer-aided simulation of conductances (see fig. 64 B) allows simulating the complex neuron-neuron interactions (Nadim et al. 2008; Prinz et al. 2003; Prinz 2006), as well as sensor-neuron interactions (Arsiero et al. 2007; Daur et al. 2012). *In situ* preparations (see fig. 64 C), which allow the study of proprioceptors and neuromuscular interactions, have been presented in this work and previously published studies in crabs (Beenhakker et al. 2004; White 2011).

These experimental paradigms are conducted on preparations, from which the other organs, sensors and nervous system have been partly, or completely, removed. In this thesis I described a preparation, which allows the investigation of the nervous system and the behavior using minimally invasive methods. These experiments were conducted in the (restrained) *in vivo* preparation of the crab (see fig. 64 D) where the environment was kept constant to minimize behavioral output variation. Neuroethological studies have been performed in decapod crustaceans *in natura* (Hemmi & Pfeil 2010; Smolka et al. 2011), which allow the animal to respond to a complex environment (see fig. 64 E). The neurobiological and -ethological investigation of decapod crustations can thus widen of our knowledge about the interaction of the nervous system with the body and the environment.

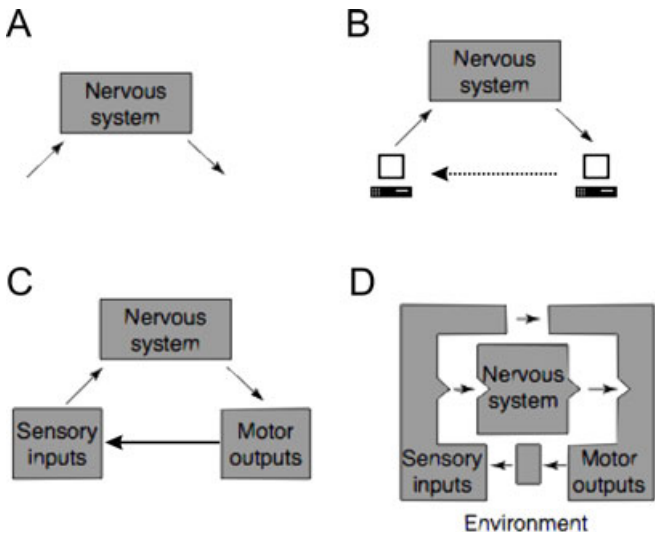

Figure 64: Schematic showing different paradigms of neurobiological experimentation Classical research *in vitro* (**A**) provides detailed, yet limited understanding of the nervous system architecture. Computer-aided closed-loop experiments (**B**) provide a method to partly close the gap without loosing benefits of *in vitro* preparations. *In situ* experiments (**C**) provide a natural way of sensory and motor activitation but are not always experimentally feasible. **D** Experiments conducted *in vivo* may provide further insights in the mechanisms controlling behavior than in more reduced preparations. Adapted from Chiel & Beer (1997).

A systematic unveilment of the intricacies of the foregut of the crab is neccessary before any of the aforementioned interactions of the nervous system and the musculature can be fully understood. The concept of the "neuromuscular transform" may provide the most promising approach to accomplish this (Brezina & Weiss 2000; Brezina et al. 2000a, b). The neuromuscular transform allows the reconstruction of muscle force output via analysis of the neuronal firing patterns. From analysis of the

spike-train and overall response to it, it is possible to extract the elemental kernel of the response. This mathematical technique is not based on initial assumptions as most other models, and it is designed to optimally fit the data at hand (Magleby & Zengel 1975). It rather uses a model-free approach by combination of several linear algebraic functions, which allows the transform to map all output modalities, while retaining structural simplicity (Sen et al. 1996; Marmarelis 2004). This technique has already been used to model the cardiac-ganglion & heart-muscle neuromuscular network (Stern et al. 2009). To simplify implementation of the neuromuscular transform in a complex system such as the gastric mill in the foregut of the crab, detailed anatomical analysis will be helpful to facilitate transform construction and limit possible simulation outcomes. As a first attempt providing the experimental tools necessary, we reconstructed the activity patterns of the proprioceptor AGR from the analysis of the motor neuronal data (Daur et al. 2012; Diehl 2008; Daur 2009). Expanding this onto the other receptors in this system and combining them with the neuromuscular transforms of all gastric mill muscles would provide an extensive data set sufficient to describe every behavioral aspect of all components of the foregut (neurons, muscles and ossicles). To simulate all components in concert, i.e. integrate all transforms into one coherent model, which generates controllable output, it is neccessary to apply optimal control methods (Levine & Loeb 1992; Loeb et al. 1990; Theodorou & Valero-Cuevas 2010). These methods are applied to control nonlinear stochastic models by implementing cost functions. Generally speaking, these functions allow the mathematical quantification of how efficient the output of any given neuromuscular system(s) is (are) in respect to stability, robustness and performance (Stengel 1994). The groundwork for implementing this theory into computer simulations has been provided as well (Todorov 2005, 2009). The simulation could then be run in Animatlab software, which provides the graphical user-interface and simulation environment (Chen & Zeltzer 1992; Cofer et al. 2005).

5.2.4 Varying contribution of a protractor muscle on movement during several modes of VCN-type stimulations

The protraction movement of the lateral teeth during rhythmic chewing depends on three separate muscles, which are innervated by the same motor neuron (LG). One muscle specifically, the gm6 muscle, was stimulated previously by White (2011) with a standardized stimulus paradigm in order to quantify the differences between VCN-type and POC-type patterns on the muscle level. The stimulus patterns were based on averaged data and consisted of constant interstimulus interval durations. In my work I used the realistic, non-averaged spike activity from *in vitro* data sets that were also used to stimulate the motor nerves *in vivo*, and in the *in situ* preparation where I

measured the force output of the gm6 muscle. Analysis of the spike patterns of all VCN-type and all POC-type patterns showed significant differences between those two types of gastric mill rhythms. Additionally the stimulus paradigm I used in my experiments (non-standardized *in vitro* LG activities) show different distribution of spikes within bursts, although average intraburst spike frequencies were similar to the standardized stimulus paradigm used by White (2011). I could show that the differences in rhythmic patterns (POC & VCN), but also the different spike distributions in the two stimulus paradigms (standardized and non-standardized), were faithfully mirrored by the force output of the gm6 muscle. The analysis of the muscle force output showed that the number of inflections in the trajectory was larger during POC-type stimuli compared to VCN-type stimuli. Thus, the differences between the two types of gastric mill patterns are conserved on the level of the musculature. The analysis of contraction velocities elicited by the gm6 muscle during stimulation with non-standardized VCN-type patterns showed that the contraction velocities were distributed aroung the zero line (see fig. 49 B), suggestsing that relaxation occured before the end of the LG burst. These results become especially interesting when compared to the analysis of the movement output *in vivo*, which was elicited by the same stimulus paradigm (see fig. 45 B and 64 B). In this case the distribution of movement velocities showed predominantly high, positive values. The question therefore arises why the contractions in the gm6 muscle experiments *in situ* did not replicate the findings from the stimulations with identical stimulus paradigms *in vivo*?

One explanation could be provided by in the movement pattern of the teeth during VCN-type activity of the gastric mill. During VCN-type stimulation *in vivo* the teeth reached the midline and touched, thus hindering further movement. This resulted in a clenching behavior in the gastric mill. During the VCN-type rhythms the muscles thus intially perform an isotonic contraction that protracts the tooth. During clenching, the muscles perform an isometric contraction. The fact that contraction ceases (plateau phase, contraction speed ***= 0***) or even reverses (negative contraction speed) during the isometric phase (figure 49 B) suggests that the gm6 muscle is not contributing to the (isometric) clenching phase during the VCN-type rhythm.

Another explanation for the observed effects of the relaxing gm6 muscle during clenching (isometric) phase may be due to the surgery prior to *in situ* experiments. The transsection and removal of ossicles in the foregut necessary for these experiments could allow the muscle to shorten more than it would in the intact animal, thus affecting the force output during stimulation. This seems unlikely, however, since

most ossicles that the gm6 connects to are preserved and since these effects were not described previously by (White 2011) during standardized stimulation of the gm6 muscle, although experimental setup as well as surgery were conducted in the same fashion.

5.2.5 Investigation of a non-sensory gastric mill activation pathway

In addition to the sensory pathway constituted by the VCN neurons a second pathway was investigated in this work. Neuromodulatory neurons projecting through the post esophageal commissure to the commissural ganglia have been shown to modulate gastric mill CPG output *in vitro* (Blitz et al. 2008). I could show for the first time that extracellular stimulation of the POC neurons elicits a gastric mill rhythm *in vivo*, which shows similar characteristics to that elicited *in vitro*. *In vitro* experiments had shown that POC-elicited gastric mill rhythms can continue for up to several hours. Even when other pathways were stimulated afterwards, the gastric mill CPG output resorted back to the POC-type firing patterns after a few cycles in the isolated preparation (Blitz et al. 2008).

In the *in vivo* preparation, however, POC-elicited rhythms were rather variable. Compared to the gastric mill CPG output recorded *in vitro*, the gastric mill rhythms elicited *in vivo* were significantly shorter in duration, lasting for only a few minutes. Other burst parameters were also analyzed and compared to previously published *in vitro* data. This showed that average burst duration was longer and the intraburst firing frequency was higher during the POC-elicited gastric mill rhythms *in vivo* when compared to POC-elicited gastric mill rhythms in the isolated preparation. Intracellular recordings on gastric mill muscles in intact crabs performed by Powers (1973) showed variable contraction durations and periods during ongoing gastric mill rhythms as well. The author did not discriminate between distinct types of rhythms in their study and it is therefore not known which types of gastric mill rhythms were recorded in each preparation. It has been suggested, however, that high variability during behavior might not be a bug but a feature, especially during the chewing of food (Hooper 2004): although consistency and taste of food are evaluated by the animal before ingestion (Hughes & Seed 1981; Nunes & Parsons 1998). Modulation of gastric mill motor output by the system-wide release of endocrine substances have been shown to regulate production and mixture of the cocktail of digestive enzymes (Icely & Nott 1992; Muhlia-Almazan & Garcia-Carreno 2003) and control ingestion and digestion during molting (Ceccaldi 1989). Sensory feedback from proprioceptors and other sensors in the foregut (VCNs) during the actual act of chewing in the foregut provides the most valuable information for the modulation of CPG output,

however. The indirect detection of food structure during chewing by sensory cells and the computation of these signals by the nervous system provides a fast method to respond to changes in food consistency and to avoid potential damage to the teeth. In the work presented here these hypotheses about neuronal control of ongoing rhythmic behavior during digestion could not be tested. The experiments conducted in the *in vivo* preparations were conducted with empty stomachs in order to maintain video endoscopic recordings of the teeth. Consequently the teeth did not actually chew any food, which might have altered the feedback from proprioceptors in the muscles of the gastric mill.

Due to the missing feedback a homogenous rhythmic output could be expected in the *in vivo* preparation. Nevertheless, several *in vivo* experiments showed a change in the tooth protractions over the course of a gastric mill rhythm. In these preparations (see fig. 31) the initial (first ***5***) protractions were lacking the pyloric-timed bouts and were of shorter duration compared to protractions occuring later in the cycle. Since the stomach contained no food during all experiments an accidental activation of the VCNs during POC stimulation was rather unlikely. The lack of clenching in these early protractions further indicated that this interspersed pattern was not due to an unintended activation of the VCNs. Other variants of POC-elicited gastric mill rhythms were also observed *in vivo*. Here, the protractions showed a process, uninterrupted by bouts, from the beginning to the end of the rhythm (see fig. 33). This suggest that the execution of a whole POC-elicited gastric mill rhythm in the intact preparation can be modulated as well. Whether this modulation is elicited by sensory feedback at the beginning or at some point during a rhythm, or whether it is elicited by the endocrine (neurohormones) or the paracrine system, which set the state of the organism and therefore the types of gastric mill rhythms that are elicited, could not be shown conclusively in this work.

Why some gastric mill rhythms elicited patterns with gradually shifting protraction characteristics (initially short, then longer protractions) and others did not, could not be explained conclusively by the experiments conducted for this work. Since exteroceptors, such as olfactory or visual receptors, were not activated specifically in these experiments, triggers for a shift in protraction patterns may be enteroceptors in the foregut. Proprioceptors, in contrast, may have been activated in these experiments. The muscle tendon organ AGR (anterior gastric receptor), for example, has been shown to slow down the gastric mill rhythm by prolonging the protraction phase

(Smarandache et al. 2008). This could explain the increase of the protraction phase duration during the POC-rhythms shown in figure 31. To test this hypothesis, however, an additional electrode would have to be applied to the *dgn* in the *in vivo* preparation in order to record AGR activity.

The recordings of POC-elicited behavioral output in the gastric mill showed for the first time that the recently discovered neuromodulatory POC pathway can be stimulated *in vivo* and that this elicits a distinct behavioral output. Some elicited rhythms contained tooth movement patterns (in the initial phase of the rhythm), which are not readily assignable as "typical" POC-elicited behavior. This suggests, that the POC neurons response can be modulated downstream by sensory feedback or neurohormones. The triggers for such downstream modulation of rhythmic motor patterns could neither be isolated nor determined conclusively in the experiments presented in this work. Further investigation on the interaction of neuronal (sensors) as well as paracrine and endocrine systems *in vivo* could help evaluate the functional relevance of each system during specific types of behavioral output. Nonetheless, these experiments provided further proof for the hypothesis that different outputs of the motor network also elicit functionally different output on the behavioral level. These experiments also showed that the shift in movement patterns (from intially short to longer protraction durations) during some POC-elicited gastric mill rhythms was directional, i.e. the shift always proceeded in the same manner, from short to long protraction durations. In hominids the mouth is not only used for chewing but also for speaking. This is a unique system where the musculature has to perform precise, mainly placid, movements during speaking and more forceful movements during chewing. Shepherd et al. (2012) showed that the rhythmic contractions of several facial muscles were rather variable during chewing. While the test subjects (*Macaca fascicularis*) were producing sounds, however, the same muscles produced highly rhythmic and synchronous contractions. This example from the vertebrate realm shows that such behaviors are not elicited randomly. Muscle force and movements are tightly controlled by the nervous system and used when necessary (and only then) in the appropriate environmental context. To revert to the stomatogastric system, this suggests that the variability seen in the motor patterns may not be elicited randomly, but rather serve a purpose behavior.

Despite the implications of sensory feedback on behavior, the question of the advantage of eliciting a POC-type rhythm during chewing is still extant. Previous observations of standardized patterns *in situ* (White 2011) showed that the amplitude of muscle contraction is progressively gaining in amplitude during protraction, which suggested that the induced protraction of the teeth is used to shatter or smash the food. In contrast, the GMRs elicited *in vivo* via extracellular stimulation of the POC

neurons, revealed that all, or at least several, pyloric-timed bouts of movement reached the midline (see fig. 34 insets ***#1*** and ***#8***). This resulted in a plateau-like phase, in which the teeth touched lightly during each bout at the midline. The teeth did not clench, however, as they do during the VCN-elicited GMRs. Based on these observations it can be assumed that during this touching of the teeth during POC-elicited rhythms at the midline no extra (isometric) force is elicited. Consequentially, the switch from isotonic to isometric contractions of the protractor muscles is not likely to occur during POC-type rhythms. Thus, the argument could be made that the POC-type chewing pattern is rather used for squeezing or softening elastic and facile types of food.

5.2.6 Consistent contribution of a protractor muscle on movement during several modes of POC-type stimulations

When stimulated with POC-type patterns in the *in situ* preparation, the gm6 muscle showed good compliance with the pyloric-timed gaps of the stimuli (burstlets, see also White & Nusbaum 2011). The standardized stimuli applied in these experiments were designed with constant (inter)burstlet durations.

While in standardized stimulations, fixed burstlet and interburstlet durations were used, the analysis of the *in vitro* patterns revealed that at the beginning of the LG burst longer burstlets and shorter interburstlet intervals were present than at the end of the burst. The contraction force of the gm 6muscle mirrored these changes: the combination of long burstlets and short gaps facilitated continuous force output of the muscle. Instead of a step-like increase in force output during standardized stimulation, the muscle force reached a plateau-like state quickly after burst initiation (see fig. 46). The length of interburstlet gap durations within the POC-elicited LG bursts was thus progressing from gap durations, which were too short for the gm6 muscle to respond to, to gap durations, which were long enough to enable the muscle to elict the typical POC-elicited bouts in the movement trajectory. The prolongation of interburstlet gaps are produced by reduced transmitter release from MCN1 onto the pyloric CPG (Bartos & Nusbaum 1997). During LG bursting the synapse of MCN1 receives presynaptic inhibition from LG, which reduces transmitter release and causes an increase in pyloric cycle period. The pauses in LG spiking during the POC rhythm are induced by the pyloric timing of MCN1 (Blitz et al. 2008). Since the pyloric rhythm slows down during the LG burst, the pauses in MCN1 are prolonged as well, which consequently leads to longer LG interburstlet intervals. This also shapes the gm6, and ultimately, movement output of the teeth during behavior.

5.2.7 Behavioral relevance of three different types of gastric mill rhythms

In addition to the stimulation with non-standardized *in vitro* data and "natural" stimulation of the respective pathways, standardized stimulus patterns of three types of previously described gastric mill rhythms were applied *in vivo.* The IV-, POC- and VCN-type patterns elicited different amplitudes of protraction and retraction in the medial and lateral teeth (see chapter 4.5.4 on page 93 ff.). These data suggest that different types of gastric mill rhythms also elicit different types of behaviors.

The issue arose, however, whether these differences are behaviorally relevant during chewing. Are the short pro- and retractions during the IV-elicited gastric mill rhythm used for very hard and large bits of food? Is the POC-elicited gastric mill rhythm used for softer foods and the VCN-elicited rhythm for harder types of food? The question whether POC-type or VCN-type movement patterns have functionally relevant effects during chewing can be answered in multiple ways. The most straightforward one is to investigate the actual chewing of food *in vivo*. When the cardiac sac is filled with food endoscopy is not feasible because the view towards the gastric mill is obstructed. McGaw & Reiber (2000) showed a method to monitor the internal movement of food through the gut in crabs via X-ray photography and food blended with barium sulfate. In their studies the food had a gel-like consistency, because of the question posed in the publication. To test the capabilities of the gastric mill harder food pellets could be used. If the pellets are of oblonged shape, their directionality in the cardiac sac could be determined as well. New advancements in the temporal resolution of computer tomography could also provide a promising method to monitor movement of teeth during chewing (Reimer et al. 2009; Ziegler et al. 2008). A relatively new non-invasive method to optically monitor voltage changes across membranes of neurons is Optical Coherence Imaging (OCI, see Graf et al. 2009). This method utilizes the observation that optical properties in the membrane of a neuron changes during a change in membrane potential (Hill & Keynes 1949) and has been applied in rats (Aguirre et al. 2006) as well as crustaceans (Akkin et al. 2004; Fang-Yen et al. 2004). It has been shown that this technique is also applicable in feline cerebral cortices *in vivo* (Maheswari et al. 2003). Current development of functional optical coherence imaging techniques (fOCT) focuses on penetration depth rather than focal diameter. Since the ganglia of invertebrates are much smaller than cortices of larger mammals, it is unclear whether it is possible to produce reliable data with this method in the *in vivo* preparation of the crab. If such non-invasive monitoring of neuronal activity *in vivo* will be possible, however, this would allow a less restrictive experimental setup, in which

rhythmic activity in the STG neurons could be elicited via multiple sensory modalities, which could also be applied simultaneously. The simultaneous regordings of all motor neurons in the STG could then be used to extract the neuromuscular transform for each specific behavioral output. The additional monitoring of the gastric mill teeth via endoscopy would provide a sufficient method to validate the accuracy of the neuromuscular transforms.

Another, experimentally simpler, approach could be to investigate other species of the decapod crustacea with diets consisting of either hard, fibrous or soft components. Previous studies showed that adaptations in the shape of the gastric mill teeth occur in aquatic andsemi-terrestrial crayfish (Linton et al. 2009). They showed that the gastric mill of *Cherax destructor* is best suited for the grinding of food material while the gastric mill of *Engaeus sericatus* appears to be better suited to cutting of food. Given this, the gastric mill of *E. sericatus* may be better able to cut the resilient cellulose and hemicellulose fibres occuring in fibrous plant material. In contrast, the gastric mill of *C. destructor* appears to be more efficient in grinding soft materials such as animal muscle tissue and algae. In another study on terrestrial crabs the gastric mill teeth of a specialized herbivorous species (*G. natalis*) and a generalized omnivorous species (*C. perlatus*) were photographed in a scanning electron microscope and compared (Allardyce & Linton 2009). The authors argued that the gastric mill teeth in these species showed drastic morphological differences, which optimized the grinding of different foods. Does the stomatogastric nervous system of these species also show specializations? Do spezialized herbivores elicit different types of gastric mill rhythms than omnivores? The aforementioned techniques to monitor gastric mill activity noninvasively during chewing could be applied for these species of crabs as well. This would help to clarify if the output of the nervous system shows adaptations to the dietary situation of the animal. Such experiments would be interesting from an evolutionary standpoint as well. In mammals the central nervous system contains millions of cells and billions of synapses, and therefore believed to be the most dynamic part of the neuromuscular system. ***5*** types of gaits are performed by icelandic horses, for example. Despite similar anatomical structure, other horse breeds are incapable of performing that many forms of locomotion. Recent studies showed that a single gene, which controls spinal motor neurons in horses and rats is neccessary (not sufficient) to enable the animal to perform *pass* and *tölt* (Andersson et al. 2012). Whether such mutations in the nervous system of decapod crustaceans have similar effects, or occur at all, remains to be debated.

The number of cells contained in the crustacean ganglia is tiny compared to the cell number in mammalian nervous systems. The number of cells in decapod crustaceans does not change after the larval stage (Fénelon et al. 2004). Also, decapod crustaceans grow out of their old exoskeleton via molting (Lovett & Felder 1989; Mangum 1992). It was also shown that gastric mill ossicles also grow at each adult molting (Leland et al. 2009). Genetic mutations or fluctuations during ecdysis could result in changes of the ossicle shapes (at each molting), while the nervous system remains largely unmodified.

Thus, crustacean ossicle structures in the foregut may be the dynamic part of the neuromuscular system in invertebrates. The investigation of environmental effects on invertebrate organs and behavior could provide interesting additional data on the process of evolutionary change in general (Bitsch & Bitsch 2002; Katz & Harris-Warrick 1999).

5.2.8 An active hepatopancreatic duct enables the induction of gastric mill rhythms *in vivo*

This work showed that it is possible to elicit gastric mill rhythms by stimulating one type of pathway at a time in the intact animal. Interestingly, however, in only a few *in vivo* preparations activity in the gastric mill could be elicited. In less than ***18%*** of all the preparations this was the case. The other preparations showed no rhythmic behavior, i.e. no chewing was elicited after appropriate stimulation.

Most responsive preparations showed activation of the hepatopancreatic duct (Schultz 1976). The hepatopancreas produces digestive enzymes, which are released into the cardiac sac via the hepatopancreatic duct (Icely & Nott 1992; McGaw & Reiber 2000). These enzymes play an important role in the foregut where the food particles are broken down into bits small enough to pass on into the pylorus. It is known that starvation can drastically lower the concentration of protein in the hemolymph (Djangmah 1970). This also includes neuromodulatory active hormones, which can affect the central pattern generators in the STG. To exclude such effects as additional blockers for the initiation of gastric mill rhythms during experiments conducted for this work, animals were fed twice a week to ensure a regular activation of the whole digestive system. Prior to each experiment, possible candidates were checked via an endoscope for stomach content. If the animal had recently fed, it was assumed that gastric mill initiation should be easier. All experiments were thus con-

ducted on animals, which had food contents and digestive enzymes in the cardiac sac. Also environmental factors such as water temperature and pH, as well as the day/night cycle were kept constant. Nonetheless not all animals showed gastric mill activity during experiments.

Since the animals were kept in groups in the tanks it is possible that interactions between the animals occur. Very little is known about social factors, which could alter the animals' inclination for feeding. Since only animals of the same sex were kept in the tanks, mating behavior or competition among males prior to mating can be excluded. It is known however that brayurian species perform territorial defence behavior (Mariappan et al. 2000). If this behavior causes the defending animals to supress feeding or digestion has not been investigated yet, but it is conceivable that social stress can change the inclination to feeding (Weissburg et al. 2012).

Furthermore, the experimental conditions could have affected the success of the stimulation: all animals had to be taken out of the water and kept on ice for the duration of the experiment. The combination of inhibited functionality of the gills and the cooling might have had effects on some animals and hindered the activation of rhythmic movement of gastric mill teeth. The crab is an aquatic organism and therefore requires water for breathing through its gills. Constrained or blocked function of the gills increases hypoxic effects resulting in increasing blood pH, for example. Unlike other species, such as *Cancer magister* (Bernatis et al. 2007), *C. pagurus* did not have to evolve methods to cope with hypoxic waters (L. Burnett, College of Charleston, USA, personal communication). Arterial partial O_2 pressure has been shown to have effects on the pyloric and gastric mill CPGs in *H. gammarus* in *in vivo* and *in vitro* preparations (Clemens et al. 1998). The conditions during experiments imposed such conditions onto the animals. Still, some animals exhibited chewing behaviors. Since the experiments were conducted similarly for all preparations, variability in body size or other individual differences might have caused this higher resilience in some animals. Another effect, which temporarily inhibits chewing behavior in crabs is a sudden onset of illumination (Fleischer 1981). To date, it was not empirically measured if sudden changes of other environmental factors (exposition to air, salinity, social stress) have comparable effects on the gastric mill and digestion in general.

In combination with the previous chapter, in which the environmental reasons for neuronal control of behavior were discussed the effect of the hepatopancreas, or the part of the nervous system innervating the hepatopancreas, on the foregut may be another pathway, by which the chewing behavior is controlled. A possible reason for control of digestive behavior in invertebrates shall be mentioned here. Poikilothermia allows invertebrates to save significant amounts of energy by not sustaining a certain level of body heat. Freshwater lobsters (*Cherax tenuimanus*) have been recorded to

exhibit a metabolic rate of ***5.4 J/g,*** which is about ***5%*** of the metabolic rate of an average human (Villarreal 1991). This low metabolic rate enables crustaceans to survive long phases of starvation (Storch & Anger 1983). A second reason for the control of digestion lies in the fact crustaceans do not grow continuously as, for example, mammals do. This means that the amount of nutrient intake has to be regulated and adapted to the molting cycle (Weis 1976). One possible mechanism to regulate the ingestion and digestion behavior is the use of the hepatopancreas as a controlling agent. Release of peptides from this organ into the blood stream could be a possible method to control whether stomatogastric CPGs can or cannot be activated by sensors or other modalities.

5.3 Coupling and decoupling of tooth movement systems in the gastric mill is mediated by an intrinsic muscle

The coordinated contractions of the gastric muscles elicit pro- and retraction of the teeth in the gastric mill. For the purpose of this work I categorized the muscles into four "tooth movement systems". The lateral tooth protractors (gm5,6 and 8) constitute the lateral tooth protraction system and have been described extensively in this work (see chapter 2.2.7 on page 16). The medial tooth protractor system consists of the gm1 muscle, which elicits dorso-rostral movement of the medial tooth. The medial tooth retraction system contains the gm4 muscle, which has been described previously (Heinzel et al. 1993) in the lobster *H. gammarus*. Additionally, the lateral tooth retraction system is described in this work for the first time. This retraction is also performed by the gm4 muscle, thus functionally combining lateral and medial tooth retraction.

Experiments were conducted, in which three distinct types of gastric mill rhythms (IV, VCN & POC) were applied via concerted stimulation of the truncated motor nerves *in vivo*. These standardized stimulus patterns made it possible to discriminate and analyze the different tooth movement systems. These experiments also revealed a fourth movement system, which elicits retraction movement of the lateral tooth during gm4 muscle activation. A lateral tooth retraction system had not been described previously in the crab. In particular, the gm4 muscle has only been implicated in the retraction of the medial tooth. My results show that this muscle is also involved in retraction of the lateral teeth. As such, a single muscle moves three ossicles and elicits the retraction phase of all teeth. Figure 65 summarizes the working hypothesis of the

functionality of the gm4 muscle *in vivo.* In the protraction phase the gm4 muscle is passively stretched (see fig. 65 A). During the retraction phase the gm4 muscle contracts and pulls the pterocardiac and mesocardiac ossicles in rostral direction. Simultaneously the propyloric and exopyloric ossicles are moved rostrally.

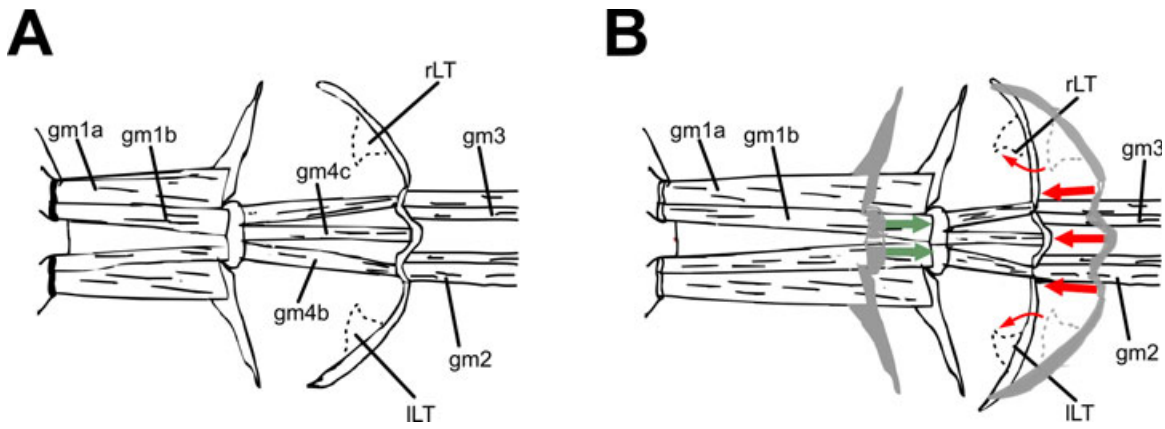

Figure 65: Schematics showing the movement of ossicles during gm4 contraction. **A** shows the protraction phase with contracted gm1 and gm2/3 muscles. The left (lLT) and right lateral tooth (rLT) do not move in this configuration and are shown in relaxed position. **B** shows the zygocardiac and pyloric ossicles moving rostrally (red arrows) after protraction phase (grey) thus deflecting the lateral teeth in lateral direction (small red arrows). The caudal movement of the meso- and pterocardiac ossicles (green arrows) after protraction phase (grey) is shown as well.

Since the gm4 muscle is not connected to the carapace (in contrast to the gm1 and gm2/3 muscles) it is an intrinsic muscle, which means that contraction moves the ossicles on both ends of the muscle (red, bold arrows in fig. 65 B). During protraction phase of a gastric mill rhythm, two separate protraction systems are activated. The protractors of the medial tooth and protractors of the lateral tooth are anatomically separated. Thus, protraction of the medial tooth is independent of the protraction of the lateral teeth. In the retraction phase, however, the medial and lateral teeth are coupled into one retraction system. The influence of the gm4 muscle on the retraction of the lateral teeth was observed during stimulation with standardized activity patterns. It is therefore unclear whether retraction is also coupled during natural chewing *in vivo*. Given that the ossicle arrangement and connectivity does not change, it appears likely that retraction is always coupled. In fact, coupling might be important behaviorally by preventing the teeth from getting stuck during the protraction phase. Full retraction of the teeth (beyond baseline) before the next protraction phase may also be useful when maximal force needs to be elicited, for example when chewing hard

foods. It has been shown in previous studies that muscles can elicit higher force output after passive stretching (Bosco & Komi 1979). The observation that the passive response to stretch in stomatogastric musculature is not mediated by actomyosin (Thuma & Hooper 2010) further supports the hypothesis that pre-stretching of the lateral tooth protractor muscles could at least elicit longer protraction and faster movement velocities of the teeth. Gastric mill rhythms elicited in the fully intact animal exhibited a fast transition between protraction and retraction, which made the subdivision into separate phases impossible. It could thus not be shown conclusively that the gm4 muscle elicits the coupled retraction of the teeth in the fully intact animal.

Another indication for the retractive actions of the gm4 muscles on both types of lateral and medial teeth lies in the structure of the gm4 muscle. The gm4 muscle consists of three fiber bundles (Govind et al. 1975; Maynard & Dando 1974). The paired gm4b muscle inserts caudally at the exopyloric ossicle, which are fused to the zygocardiac ossicles. The hypothesis that the gm4 muscles are primarily responsible for the retraction of the lateral teeth is also supported by experiments, in which one gm4b bundle was transsected. After ipsilateral transection, a reduced retraction of the lateral tooth was recorded on the ipsilateral side. Interestingly, lesion of the gm4c bundle had less dramatic effects: the remaining gm4b bundles still elicited enough force to retract medial as well as lateral teeth simultaneously.

In the lobster, the retraction mechanism for the lateral teeth was described previously (Heinzel 1988). Here, retraction of the lateral teeth is performed by the gm2/3 muscles. These muscles are innervated by the lateral posterior gastric (LPG) neuron (Selverston et al. 2009). Activation of the motor neurons causes contraction in the gm2/3 muscles, which insert at the caudal side of the propyloric and exopyloric ossicles. Upon contraction these ossicles are pulled latero-caudally (Maynard & Dando 1974), thus exercising lateral torque on the zygocardiac ossicle. The carapace of the crab, however, does not from a tubular hull as in the lobster. Thus, the gm2/3 muscles insert parallel to the gm4 muscle into the dorsal carapace. The gm2/3 muscles do therefore not excert torque on the zygocardiac ossicles, which I confirmed in the crab *in vivo*. In these experiments all muscles (including the gm4 muscles) were left intact except for the gm2 and gm3 muscles and the DG neuron was stimulated. The results showed that retraction of the teeth peristed despite transsection of these muscles, which suggests that the gm2/3 muscles do not participate in retraction of the teeth in the crab. In the crab stomatogastric nervous system the function of the LPG neuron is thus not as clearly assigned as in the lobster (Weimann et al. 1991). In fact, in the crab, LPG is typically active in pyloric rhythm (Stein 2009) and only rarely participates in the gastric mill rhythm (M. P. N. Nusbaum, personal communication). LPG in the crab is electrically coupled to the pyloric pacemaker AB, which does not fit well

as a retractor of the lateral teeth as well. Apparently, thus, the difference in carapace shape and the ensuing change in the function of the musculature and ossicles went along with a change in the neuronal function of LPG. Current studies show that Brachyura and Astacidea developed separately into their current form, which makes it difficult to find evolutionary explanations concerning the differences in LPG function and tooth retraction in Cancridae and Nephropidae (Toon et al. 2009; Tsang et al. 2008).

Previous studies have appreciated the anatomically complex human hand (Valero-Cuevas 2005) as a structure that enables a maximum of precision and variability. The advantages for animals with hand extremities are undeniable, but such a complex organ poses immense demands to the nervous system (Schieber & Santello 2004; Lemon 1999). In the foregut of decapod crustaceans different demands are imposed on the system. Chewing of various different types of foods requires repeatability of movement. Similarly, the anatomical structure of head and mouth in humans enables the repetitive opening and closing and thus grinding of the food particles. Thus the anatomical structure of the chewing apparatus itself limits the degrees of freedom, in which the teeth can move (Scholz & Schöner 1999). This coupling of the retraction of lateral and medial teeth can be seen as a reduction of movement complexity. The gm4 muscle retracts the medial tooth as well as the lateral teeth simultaneously. These structures are decoupled during protraction, meaning that the medial tooth protraction system and the lateral tooth protraction system elicit movement output independently of each other. Functional coupling by an intrinsic muscle can have several advantages during behavior. Retraction of the medial tooth is belivied to push ground food past the cardiopyloric valve into the pylorus for further digestion (Heinzel et al. 1993). The retraction of the lateral teeth, however, is likely to serve as a safety measure during chewing because it prevents the blocking of the teeth. The VCN-elicited gastric mill rhythms used for the standardized stimulations presented in chapter 4.5 (page 88) elicit protraction phases, which are likely to crush more resisitive types of foods. In this type of rhythm the burst of the retractor neuron DG overlapped with the LG burst (see fig. 50). This overlap ensures a fast retraction of the lateral teeth after the clenching phase during protraction. Whether this coupling by the retractor muscle gm4 is actually employed during chewing behavior *in vivo* is not yet experimentally proven. Digital modeling of the structures in the foregut could provide helpful insights about their functional relevance.

Previous studies showed that the digital modeling of the functional anatomy in the foregut of the crab is feasible (Doya et al. 1993). This work presents a preliminary computer model in a state-of-the-art simulation environment and allows for further enrichment, for example by the implementation of muscle characteristics and ossicle stiffness. Such a detailed model would provide the platform to design and test hypotheses about the importance of the anatomical arrangement of ossicles and muscles.

5.4 Outlook

In the year 1994 I witnessed a spectacular event that should spark my ongoing fascination for astronomy. Debris of the comet SL-9 hit the planet Jupiter, an event so rare that it was never observed before (Shoemaker et al. 1994). This asteroid was very likely originated during the Late Heavy Bombardment in the solar system ***3.8*** billion years ago (Gomes et al. 2005). This convulsive event was caused by gravitational resonance. The rhythmic concurrence of the two planets Saturn and Jupiter at a single position caused a buildup of energy that ended in a catastrophy, spewing millions of asteroids into space and into the paths of planets. It is now believed that the explosive distribution of these asteroids, which contained mostly ice, is responsible for the spawning of life on earth (Rothschild 2009).

Analogous events occur during the life time of organisms when tissues develop diseases or are distorted by abnormal posture or movement. The changing environment and insufficient exercise have caused massive health issues (Cho et al. 2012) in an ever growing portion of the population (Røe et al. 2012). Recent developments in scientific research have initiated a new approach: it has been shown that singular treatment of individual components of the body, the classic impetus in scholar medicine, might not be as efficient as the integrated consideration of all components (El-Rich et al. 2004; Gardner-Morse & Stokes 1998).

The stomatogastric system of invertebrates serves as another promising tool in understanding the complex interaction of different tissues *in vivo.* Understanding of this system on multiple levels may also provide the scientific foundation for understanding the complex architecture of man - and how to heal it.

6. Bibliography

ABRAMSON C. & FEINMAN R. 1990. Lever-press conditioning in the crab. *J Physiol Behav* 48: 267-272.

AGUIRRE A.D., CHEN Y., FUJIMOTO J.G., RUVINSKAYA L., DEVOR A. & BOAS D.A. 2006. Depth-resolved imaging of functional activation in the rat cerebral cortex using optical coherence tomography. *Opt Lett* 31: 3459-3461.

AHN A.N., MEIJER K. & FULL R.J. 2006. In situ muscle power differs without varying in vitro mechanical properties in two insect leg muscles innervated by the same motor neuron. *J Exp Biol* 209: 3370-3382.

AKKIN T., DAVÉ D., MILNER T. & RYLANDER III H. 2004. Detection of neural activity using phase-sensitive optical low-coherence reflectometry. *Opt Expr* 12: 2377-2386.

ALLARDYCE B.J. & LINTON S.M. 2009. Functional morphology of the gastric mills of carnivorous, omnivorous, and herbivorous land crabs. *J Morphol* 271: 61-72.

ANDERSSON L.S., LARHAMMAR M., MEMIC F., WOOTZ H., SCHWOCHOW D., RUBIN C.-J., PATRA K., ARNASON T., WELLBRING L., HJÄLM G., IMSLAND F., PETERSEN J.L., MCCUE M.E., MICKELSON J.R., COTHRAN G., AHITUV N., ROEPSTORFF L., MIKKO S., VALLSTEDT A., LINDGREN G., ANDERSSON L. & KULLANDER K. 2012. Mutations in DMRT3 affect locomotion in horses and spinal circuit function in mice. *Nature* 488: 642-646.

ARSIERO M., LÜSCHER H.-R. & GIUGLIANO M. 2007. Real-time closed-loop electrophysiology: towards new frontiers in in vitro investigations in the neurosciences. *Arch ital de bio* 145: 193-209.

AYALI A. 2009. The role of the arthropod stomatogastric nervous system in moulting behaviour and ecdysis. *J Exp Biol* 212: 453-459.

BAL T., NAGY F. & MOULINS M. 1988. The pyloric central pattern generator in Crustacea: a set of conditional neuronal oscillators. *J Comp Physiol A* 163: 715-727.

BARKER P.L. & GIBSON R. 1977. Observations on the feeding mechanism, structure of the gut, and digestive physiology of the european lobster Homarus gammarus (L.) (Decapoda: Nephropidae). *J Exp Mar Biology & Ecol* 26: 297-324.

BARRIERE G., SIMMERS J. & COMBES D. 2008. Multiple mechanisms for integrating proprioceptive inputs that converge on the same motor pattern-generating network. *J Neurosci* 28: 8810-8820.

BARTOS M., MANOR Y., NADIM F., MARDER E. & NUSBAUM M.P. 1999. Coordination of fast and slow rhythmic neuronal circuits. *J Neurosci* 19: 6650-6660.

BARTOS M. & NUSBAUM M.P. 1997. Intercircuit control of motor pattern modulation by presynaptic inhibition. *J Neurosci* 17: 2247-2256.

BEENHAKKER M.P., BLITZ D.M. & NUSBAUM M.P. 2004. Long-Lasting Activation of Rhythmic Neuronal Activity by a Novel Mechanosensory System in the Crustacean Stomatogastric Nervous System. *J Neurophys* 91: 78-91.

BEENHAKKER M.P., DELONG N.D., SAIDEMAN S.R., NADIM F. & NUSBAUM M.P. 2005. Proprioceptor regulation of motor circuit activity by presynaptic inhibition of a modulatory projection neuron. *J Neurosci* 25: 8794-8806.

BEENHAKKER M.P., KIRBY M.S. & NUSBAUM M.P. 2007. Mechanosensory gating of proprioceptor input to modulatory projection neurons. *J Neurosci* 27: 14308-14316.

BEENHAKKER M.P. & NUSBAUM M.P. 2004. Mechanosensory activation of a motor circuit by coactivation of two projection neurons. *J Neurosci* 24: 6741-6750.
BEER R.D. & GALLAGHER J. 1992. Evolving Dynamical Neural Networks for Adaptive Behavior. *J Adapt Behav* 1: 91-122.
BERNATIS J.L., GERSTENBERGER S.L. & MCGAW I.J. 2007. Behavioural responses of the Dungeness crab, Cancer magister, during feeding and digestion in hypoxic conditions. *Mar Biol* 150: 941-951.
BIERMAN H.S. & TOBIN A.E. 2009. Gross dissection of the stomach of the lobster, Homarus Americanus. *J Vis Exp*
BITSCH C. & BITSCH J. 2002. The endoskeletal structures in arthropods: cytology, morphology and evolution. *Arthrop Struct & Develop* 30: 159-177.
BLICKHAN R., SEYFARTH A., GEYER H., GRIMMER S., WAGNER H. & G√ºNTHER M. 2007. Intelligence by Mechanics. *J Phil Trans Math Phys Eng* 365: 199-220.
BLITZ D.M., BEENHAKKER M.P. & NUSBAUM M.P. 2004. Different sensory systems share projection neurons but elicit distinct motor patterns. *J Neurophys* 24: 11381-11390.
BLITZ D.M. & NUSBAUM M.P. 2008. State-Dependent Presynaptic Inhibition Regulates Central Pattern Generator Feedback to Descending Inputs. *J Neurosci* 28: 9564.
BLITZ D.M. & NUSBAUM M.P. 2011. Neural circuit flexibility in a small sensorimotor system. *Curr Op Neurobiol* 21: 1-9.
BLITZ D.M. & NUSBAUM M.P. 2012. Modulation of circuit feedback specifies motor circuit output. *J Neurosci* 32: 9182-9193.
BLITZ D.M., WHITE R.S., SAIDEMAN S.R., COOK A., CHRISTIE A.E., NADIM F. & NUSBAUM M.P. 2008. A newly identified extrinsic input triggers a distinct gastric mill rhythm via activation of modulatory projection neurons. *J Exp Biol* 211: 1000-1011.
BLITZ D.M. & NUSBAUM M.P. 1999. Distinct functions for cotransmitters mediating motor pattern selection. *J Neurosci* 19: 6774-6783.
BOSCO C. & KOMI P.V. 1979. Potentiation of the mechanical behavior of the human skeletal muscle through prestretching. *Acta Physiol Scand* 106: 467-472.
BREZINA V., OREKHOVA I.V. & WEISS K.R. 2000a. Optimization of rhythmic behaviors by modulation of the neuromuscular transform. *J Neurophys* 83: 260-279.
BREZINA V., OREKHOVA I.V. & WEISS K.R. 2000b. The neuromuscular transform: the dynamic, nonlinear link between motor neuron firing patterns and muscle contraction in rhythmic behaviors. *J Neurophys* 83: 207-231.
BREZINA V. & WEISS K.R. 2000. The neuromuscular transform constrains the production of functional rhythmic behaviors. *J Neurophys* 83: 232-259.
BRÖSING A., RICHTER S. & SCHOLTZ G. 2002. The foregut-ossicle system of Dromia wilsoni, Dromia personata and Lauridromia intermedia (Decapoda, Brachyura, Dromiidae), studied with a new staining method. *Arthrop Struct & Develop* 30: 329-338.
CALABRESE R.L. 1995. Oscillation in motor pattern-generating networks. *Curr Op Neurobiol* 5: 816-823.
CALABRESE R.L. 2003. Behavioral choices: how neuronal networks make decisions. *Curr Biol* 13: R140-2.
CARR W. & DERBY C.D. 1986. Chemically stimulated feeding behavior in marine animals. *J Chem Ecol* 12: 989-1011.
CECCALDI H. 1989. Anatomy and physiology of digestive tract of crustaceans decapods reared in aquaculture.
CHEN D. & ZELTZER D. 1992. Computer animation of a biomechanically based model of muscle using the finite element method. *J Comp graph* 26: 89-97.

CHEN R., HUI L., CAPE S.S., WANG J. & LI L. 2010. Comparative Neuropeptidomic Analysis of Food Intake via a Multi-faceted Mass Spectrometric Approach. *ACS Chem Neurosci* 1: 204-214.

CHIEL H.J. & BEER R.D. 1997. The brain has a body: Adaptive behavior emerges from interactions of nervous system, body and environment. *Trends Neurosci* 20: 553-557.

CHO C.-Y., HWANG Y.-S. & CHERNG R.-J. 2012. Musculoskeletal Symptoms and Associated Risk Factors Among Office Workers With High Workload Computer Use. *J Manip & Physiol Therap* 35: 534-540.

CLEMENS S., MASSABUAU J.-C., LEGEAY A., MEYRAND P. & SIMMERS J. 1998. In Vivo Modulation of Interacting Central Pattern Generators in Lobster Stomatogastric Ganglion: Influence of Feeding and Partial Pressure of Oxygen. *J Neurosci* 18: 2788-2799.

COCHRAN D.M. 1935. *The skeletal musculature of the blue crab, Callinectes sapidus*. Washington, D.C.: Smithsonian Institution.

COFER D., REID J., ZHU Y. & EDWARDS D.H. 2005. A 3D graphics toolkit for studying neural basis of adaptive behaviors. *SIGGRAPH*

COLEMAN M.J., MEYRAND P. & NUSBAUM M.P. 1995. A switch between two modes of synaptic transmission mediated by presynaptic inhibition. *Nature* 378: 502-505.

COLEMAN M.J. & NUSBAUM M.P. 1994. Functional consequences of compartmentalization of synaptic input. *J Neurosci* 14: 6544-6552.

COLEMAN M.J., NUSBAUM M.P., COURNIL I. & CLAIBORNE B.J. 1992. Distribution of modulatory inputs to the stomatogastric ganglion of the crab, Cancer borealis. *J Comp Physiol A* 325: 581-594.

COMBES D., MEYRAND P. & SIMMERS J. 1999. Dynamic restructuring of a rhythmic motor program by a single mechanoreceptor neuron in lobster. *J Neurosci* 19: 3620-3628.

DANDO M.R. & LAVERACK M.S. 1969. The anatomy and physiology of the posterior stomach nerve (psn) in some decapod Crustacea. *Proc R Soc B* 171: 465-482.

DANDO M.R. & MAYNARD D.M. 1973. The sensory innervation of the foregut of Panulirus argus (Decapoda Crustacea). *J Mar & Freshw* 2: 283-305.

DAUR N. 2009. Charakterisierung intrinsischer Eigenschaften eines Propriozeptors und deren Beitrag zur sensorischen Informationsverarbeitung. *Institute for Neurobiology, Ulm University*

DAUR N., DIEHL F., MADER W. & STEIN W. 2012. The stomatogastric nervous system as a model for studying sensorimotor interactions in real-time closed-loop conditions. *Front Comput Neurosci* 6: 1-19.

DAUR N., NADIM F. & STEIN W. 2009. Regulation of motor patterns by the central spike-initiation zone of a sensory neuron. *Eur J Neurosci* 30: 808-822.

DEKEYSER S.S., KUTZ-NABER K.K., SCHMIDT J.J., BARRETT-WILT G.A. & LI L. 2007. Imaging Mass Spectrometry of Neuropeptides in Decapod Crustacean Neuronal Tissues. *J Prot Res* 6: 1782-1791.

DELONG N.D., BEENHAKKER M.P. & NUSBAUM M.P. 2009. Presynaptic inhibition selectively weakens peptidergic cotransmission in a small motor system. *J Neurophys* 102: 3492-3504.

DICKINSON P.S. 2006. Neuromodulation of central pattern generators in invertebrates and vertebrates. *Curr Op Neurobiol* 16: 604-614.

DIEHL F. 2008. Modellierung eines Rezeptorneurons im stomatogastrischen Nervensystem des Taschenkrebses (Cancer pagurus). *Institute for Neurobiology, Ulm University*

DIMANT B. & MALDONADO H. 1992. Habituation and associative learning during exploratory behavior of the crab Chasmagnathus. *J Comp Physiol A* 170: 749-759.
DJANGMAH J.S. 1970. The effects of feeding and starvation on copper in the blood and hepatopancreas, and on blood proteins of Crangon vulgaris. *J Comp Biochem & Physiol A* 32: 709-718.
DOUGLASS J.K., WILKENS L., PANTAZELOU E. & MOSS F. 1993. Noise enhancement of information transfer in crayfish mechanoreceptors by stochastic resonance. *Nature* 365: 337-340.
DOYA K., MARY E.T., BOYLE A. & SELVERSTON A.I. 1993. Mapping Between Neural and Physical Activities of the Lobster Gastric Mill. *Adv Neur Info Proc Sys* 913-920.
EKEBERG O., BLÜMEL M. & BÜSCHGES A. 2004. Dynamic simulation of insect walking. *Arth Struct & Develop* 33: 287-300.
EL-RICH M., SHIRAZI-ADL A. & ARJMAND N. 2004. Muscle activity, internal loads, and stability of the human spine in standing postures: combined model and in vivo studies. *Spine* 29: 2633-2642.
FAHRMEIR L. 1992. Posterior Mode Estimation by Extended Kalman Filtering for Multivariate Dynamic Generalized Linear Models. *J Americ Stat Soc* 87: 501-509.
FAISAL A.A., SELEN L.P.J. & WOLPERT D.M. 2008. Noise in the nervous system. *Nat Rev Neurosci* 9: 292-303.
FANG-YEN C., CHU M.C., SEUNG H.S., DASARI R.R. & FELD M.S. 2004. Noncontact measurement of nerve displacement during action potential with a dual-beam low-coherence interferometer. *Opt Lett* 29: 2028-2030.
FÉNELON V.S., LE FEUVRE Y. & MEYRAND P. 2004. Phylogenetic, ontogenetic and adult adaptive plasticity of rhythmic neural networks: a common neuromodulatory mechanism? *J Comp Physiol* 190: 691-705.
FLASH T. & HOCHNER B. 2005. Motor primitives in vertebrates and invertebrates. *Curr Op Neurobiol* 15: 660-666.
FLEISCHER A.G. 1981. The effect of eyestalk hormones on the gastric mill in the intact lobster, Panulirus interruptus. *J Comp Physiol A* 141: 363-368.
GABBAY M. 2000. A Principal Components-Based Method for the Detection of Neuronal Activity Maps: Application to Optical Imaging. *NeuroImage* 11: 313-325.
GARDNER-MORSE M.G. & STOKES I.A.F. 1998. The Effects of Abdominal Muscle Coactivation on Lumbar Spine Stability. *Spine* 23: 86-91.
GOLDBERG D., NUSBAUM M.P. & MARDER E. 1988. Substance P-like immunoreactivity in the stomatogastric nervous systems of the crab Cancer borealis and the lobsters Panulirus interruptus and Homarus americanus. *J Cell & Tiss Res* 252: 515-522.
GOLOWASCH J., CASEY M., ABBOTT L.F. & MARDER E. 1999. Network Stability from Activity-Dependent Regulation of Neuronal Conductances. *J Neur Comp* 11: 1079-1096.
GOLOWASCH J., THOMAS G., TAYLOR A.L., PATEL A., PINEDA A., KHALIL C. & NADIM F. 2009. Membrane Capacitance Measurements Revisited: Dependence of Capacitance Value on Measurement Method in Nonisopotential Neurons. *J Neurophys* 102: 2161-2175.
GOMES R., LEVISON H.F., TSIGANIS K. & MORBIDELLI A. 2005. Origin of the cataclysmic Late Heavy Bombardment period of the terrestrial planets. *Nature* 435: 466-469.
GOVIND C.K., ATWOOD H.L. & MAYNARD D.M. 1975. Innervation and neuromuscular physiology of intrinsic foregut muscles in the blue crab and spiny lobster. *J*

Comp Physiol A 96: 185-204.
GRAF B.W., RALSTON T.S., KO H.-J. & BOPPART S.A. 2009. Detecting intrinsic scattering changes correlated to neuron action potentials using optical coherence imaging. *Opt Expr* 17: 13447-13457.
GRAZIOTTI G.H., CHAMIZO V.E., RÍOS C., ACEVEDO L.M., RODRÍGUEZ-MENÉNDEZ J.M., VICTORICA C. & RIVERO J.-L.L. 2012. Adaptive functional specialisation of architectural design and fibre type characteristics in agonist shoulder flexor muscles of the llama, Lama glama. *J Anat* 221: 151-163.
GRILLNER S., MARKRAM H., DE S., ERIK, SILBERBERG G. & LEBEAU F.E.N. 2005. Microcircuits in action--from CPGs to neocortex. *Trends Neurosci* 28: 525-533.
GRILLNER S. & WALLEN P. 2002. Cellular bases of a vertebrate locomotor system. *Brain Res. Rev.* 40: 92-106.
HAEUFLE D.F.B., GRIMMER S., KALVERAM K.-T. & SEYFARTH A. 2012. Integration of intrinsic muscle properties, feed-forward and feedback signals for generating and stabilizing hopping. *J R Soc Interface* 9: 1458-1469.
HAMILTON K.A. & ACHE B.W. 1983. Olfactory excitation of interneurons in the brain of the spiny lobster. *J Comp Physiol A* 150: 129-140.
HARRIS-WARRICK R.M. 2011. Neuromodulation and flexibility in Central Pattern Generator networks. *Curr Op Neurobiol* 21: 685-692.
HEDRICH U.B.S. 2008. Charakterisierung einer vom Gehirn absteigenden Bahn. *Institute for Neurobiology, Ulm University*
HEDRICH U.B.S., DIEHL F. & STEIN W. 2011. Gastric and pyloric motor pattern control by a modulatory projection neuron in the intact crab Cancer pagurus. *J Neurophys* 105: 1671-1680.
HEDRICH U.B.S., SMARANDACHE C.R. & STEIN W. 2009. Differential activation of projection neurons by two sensory pathways contributes to motor pattern selection. *J Neurophys* 102: 2866-2879.
HEDRICH U.B.S. & STEIN W. 2008. Characterization of a descending pathway: activation and effects on motor patterns in the brachyuran crustacean stomatogastric nervous system. *J Exp Biol* 211: 2624-2637.
HEDRICK T.L. 2008. Software techniques for two- and three-dimensional kinematic measurements of biological and biomimetic systems. *J Bioinsp Biomim* 3: 034001.
HEINZEL H.G. 1988. Gastric mill activity in the lobster. I. Spontaneous modes of chewing. *J Neurophys* 59: 528-550.
HEINZEL H.G., WEIMANN J.M. & MARDER E. 1993. The behavioral repertoire of the gastric mill in the crab, Cancer pagurus: an in situ endoscopic and electrophysiological examination. *J Neurosci* 13: 1793-1803.
HEMMI J.M. & PFEIL A. 2010. A multi-stage anti-predator response increases information on predation risk. *J Exp Biol* 213: 1484-1489.
HERMANN A. 1977. Mechanism of command fibre operation onto bursting pacemaker neurones in the stomatogastric ganglion of the crab, Cancer pagurus. *J Comp Physiol A* 114: 15-33.
HILL D.K. & KEYNES R.D. 1949. Opacity changes in stimulated nerve. *J Physiol* 108: 278-281.
HILL T., EISENBERG E., CHEN Y. & PODOLSKY R. 1975. Some self-consistent two-state sliding filament models of muscle contraction. *J Biophys* 15: 335-372.
HILLE B. 1986. Ionic channels: molecular pores of excitable membranes. *Harvey lectures* 82: 47.
HOBBS K. & HOOPER S.L. 2009. High-resolution computed tomography of lobster

(Panulirus interruptus) stomach. *J Morphol* 270: 1029-1041.
HOLMES P., FULL R.J., KODITSCHEK D. & GUCKENHEIMER J. 2006. The Dynamics of Legged Locomotion: Models, Analyses, and Challenges. *SIAM Review* 48: 207-304.
HOOPER S.L. 2000. Central pattern generators. *Curr Biol* 10: 176-179.
HOOPER S.L. 2004. Variation Is the Spice of Life. Focus on “Cycle-to-Cycle Variability of Neuromuscular Activity in Aplysia Feeding Behavior”. *J Neurophys* 92: 40-41.
HOOPER S.L. 2012. Body size and the neural control of movement. *Curr Biol* 22: R318-R322.
HOOPER S.L. & WEAVER A.L. 2000. Motor neuron activity is often insufficient to predict motor response. *Curr Op Neurobiol* 10: 676-682.
HUGHES R.N. & SEED R. 1981. Size Selection of Mussels by the Blue Crab Callinectes sapidus: Energy Maximizer or Time Minimizer. *Mar Ecol Prog Ser* 6: 83-89.
HUMBOLDT A.V. 1797. *Versuche über die gestreifte Muskel- und Nervenfaser*. Berlin: Heinrich August Rottmann.
HUXLEY T.H. 1880. *The crayfish: an introduction to the study of zoology*. New York: Appleton.
ICELY J.D. & J.A. NOTT. 1992. Digestion and absorption: digestive system and associated organs, in F.W. Harrison & Humes A.G. (ed.) *Decapod Crustacea*: 147-201. New York: Wiley-Liss.
JAHROMI S. & GOVIND C.K. 1976. Ultrastructural diversity in motor units of crustacean stomach muscles. *Cell Tiss Res* 166: 159-166.
JOHNSON B.R. & S.L. HOOPER. 1992. Overview of the stomatogastric nervous system, in R.M. Harris-Warrick, Marder E., Selverston A.I. & Moulins M. (ed.) *Dynamic biological networks: the stomatogastric nervous system*.
JOHNSON P.T. 1980. *Histology of the blue crab, Callinectes sapidus: A model for the Decapoda*. New York: Praeger.
JUBEAU M., MUTHALIB M., MILLET G.Y., MAFFIULETTI N.A. & NOSAKA K. 2012. Comparison in muscle damage between maximal voluntary and electrically evoked isometric contractions of the elbow flexors. *Europ J Appl Physiol* 112: 429-438.
JURJUT O.F., NIKOLIC D., PIPA G., SINGER W., METZLER D. & MURESAN R.C. 2009. A Color-Based Visualization Technique for Multielectrode Spike Trains. *J Neurophys* 102: 3766-3778.
KATZ P.S. 1996. Neurons, networks, and motor behavior. *Neuron* 16: 245-254.
KATZ P.S. 2001. Comparison of extrinsic and intrinsic neuromodulation in two central pattern generator circuits in invertebrates. *J Exp Physiol* 83: 281-292.
KATZ P.S., EIGG M.H. & HARRIS-WARRICK R.M. 1989. Serotonergic/cholinergic muscle receptor cells in the crab stomatogastric nervous system. I. Identification and characterization of the gastropyloric receptor cells. *J Neurophys* 62: 558-570.
KATZ P.S. & HARRIS-WARRICK R.M. 1999. The evolution of neuronal circuits underlying species-specific behavior. *Curr Op Neurobiol* 9: 628-633.
KENNEDY V. & E. CRONIN 2006. *Anatomy of the post-larval blue crab*. Sea Grant Maryland.
KILMAN V.L. & MARDER E. 1996. Ultrastructure of the Stomatogastric Ganglion Neuropil of the Crab. *J Comp Physiol A* 374: 362-375.
KIRBY M.S. & NUSBAUM M.P. 2007. Central nervous system projections to and from the commissural ganglion of the crab Cancer borealis. *Cell Tiss Res* 328: 625-637.
KRYLOW A.M. & RYMER W.Z. 1997. Role of intrinsic muscle properties in producing

smooth movements. *Trans Biomed Eng* 44: 165-176.
LARIMER J.L. & KENNEDY D. 1966. Visceral afferent signals in the crayfish stomatogastric ganglion. *J Exp Biol* 44: 345-354.
LAUGHLIN S.B., C. JOHN, D.C. O'CARROLL & R.R. DE RUYTER VAN STEVENINCK 2008. *Information Theory and the Brain*. Cambridge: Cambridge Univ Press.
LELAND J.C., COUGHRAN J. & BUCHER D.J. 2009. A preliminary investigation into the potential value of gastric mills for ageing crustaceans. *Proc TCS Summer Meeting* 15: 57-68.
LEMON R.N. 1999. Neural control of dexterity: what has been achieved? *Exp Brain Res* 128: 6-12.
LEVINE W.S. & LOEB G.E. 1992. The neural control of limb movement. *Contr Sys, IEEE* 12: 38-47.
LINTON S.M., ALLARDYCE B.J., HAGEN W., WENCKE P. & SABOROWSKI R. 2009. Food utilisation and digestive ability of aquatic and semi-terrestrial crayfishes, Cherax destructor and Engaeus sericatus (Astacidae, Parastacidae). *J Comp Physiol B* 179: 493-507.
LOEB G.E., LEVINE W.S. & HE J. 1990. Understanding sensorimotor feedback through optimal control. *Cold Spring Harb. Symp. Quant. Biol.* 791-803.
LOHMANN K.J., LOHMANN C.M.F. & ENDRES C.S. 2008. The sensory ecology of ocean navigation. *J Exp Biol* 211: 1719-1728.
LOVETT D.L. & FELDER D.L. 1989. Ontogeny of gut morphology in the white shrimp Penaeus setiferus (Decapoda, Penaeidae). *J Morph* 201: 253-272.
MAGLEBY K.L. & ZENGEL Z.E. 1975. A quantitative description of tetanic and post-tetanic potentiation of transmitter release at the frog neuromuscular junction. *J Phys* 245: 183-208.
MAHESWARI R.U., TAKAOKA H., KADONO H., HOMMA R. & TANIFUJI M. 2003. Novel functional imaging technique from brain surface with optical coherence tomography enabling visualization of depth resolved functional structure in vivo. *J Neurosci Meth* 124: 83-92.
MANGUM C. 1992. Physiological aspects of molting in the blue crab Callinectes sapidus. *Amer Zool* 32: 459-469.
MARDER E., ABBOTT L.F., TURRIGIANO G.G., LIU Z. & GOLOWASCH J. 1996. Memory from the dynamics of intrinsic membrane currents. *Proc Nat Acad Sci USA* 93: 13481-13486.
MARDER E. & BUCHER D. 2001. Central pattern generators and the control of rhythmic movements. *Curr Biol* 11: R986-96.
MARDER E. & BUCHER D. 2007. Understanding circuit dynamics using the stomatogastric nervous system of lobsters and crabs. *Annu Rev Physiol* 69: 291-316.
MARDER E., BUCHER D., SCHULZ D.J. & TAYLOR A.L. 2005. Invertebrate central pattern generation moves along. *Curr Biol* 15: R685-99.
MARDER E. & PRINZ A.A. 2002. Modeling stability in neuron and network function: the role of activity in homeostasis. *Bio Ess* 24: 1145-1154.
MARIAPPAN P., BALASUNDARAM C. & SCHMITZ B. 2000. Decapod crustacean chelipeds: an overview. *J Biosci* 25: 301-313.
MARMARELIS V.Z. 2004. *Nonlinear dynamic modeling of physiological systems*. New York: Wiley Interscience.
MAYNARD D.M. & DANDO M.R. 1974. The structure of the stomatogastric neuromuscular system in Callinectes sapidus. *R Soc Phil Trans B* 268: 161-220.
MAYNARD D.M. & SELVERSTON A.I. 1975. Organization of the stomatogastric ganglion

of the spiny lobster. *J Comp Physiol A* 100: 161-182.
McAndrew P.M., Wilken J.M. & Dingwell J.B. 2011. Dynamic stability of human walking in visually and mechanically destabilizing environments. *J Biomech* 44: 644-649.
McDonnell M.D. & Ward L.M. 2011. The benefits of noise in neural systems: bridging theory and experiment. *Nat Rev Neurosci* 12: 415-426.
McGaw I.J. & Reiber C.L. 2000. Integrated physiological responses to feeding in the blue crab Callinectes sapidus. *J Exp Biol* 203: 359-368.
McGaw I.J. 2006. Feeding and digestion in low salinity in an osmoconforming crab, Cancer gracilis II. Gastric evacuation and motility. *J Exp Biol* 209: 3777-3785.
Miles G.B. & Sillar K.T. 2011. Neuromodulation of Vertebrate Locomotor Control Networks. *J Physiol* 26: 393-411.
Mocquard F. 1883. Recherches anatomiques sur l'estomac des crustacés podophtalmaires. *Faculté des sciences de Paris*
Möhl B. 1972. The Control of Foregut Movements by the Stomatogastric Nervous System in the European House Cricket. *J Comp Physiol* 80: 1-28.
Morris L.G. & Hooper S.L. 1997. Muscle response to changing neuronal input in the lobster (Panulirus interruptus) stomatogastric system: slow muscle properties can transform rhythmic input into tonic output. *J Neurosci* 18: 3433-3442.
Muhlia-Almazan A. & Garcia-Carreno F. 2003. Digestion physiology and proteolytic enzymes of crustacean species of the Mexican Pacific Ocean. *Contr Stud Pacif Crust* 2: 77-91.
Mullins O.J. & Friesen W.O. 2012. The brain matters: Effects of descending signals on motor control. *J Neurophys* 107: 2730-2741.
Nadim F., Brezina V., Destexhe A. & Linster C. 2008. State dependence of network output: modeling and experiments. *J Neurosci* 28: 11806-11813.
Nagy F. & Moulins M. 1981. Proprioceptive control of the bilaterally organized rhythmic activity of the oesophageal neuronal network in the lobster. *J Exp Biol* 90: 231-251.
Narendra K.S. 1996. Neural networks for control theory and practice. *IEEE Proc* 84: 1385-1406.
Ng P.K.L., Guinot D. & Davie P.J.F. 2008. Systema Brachyurorum: Part I. An annotated checklist of extant brachyuran crabs of the world. *Bull Zool* 17: 1-286.
NIH 1985. *Public Health Service Policy on Humane Care and Use of Laboratory Animals*. Office of Laboratory Animal Welfare: NIH.
Norris B.J., Coleman M.J. & Nusbaum M.P. 1996. Pyloric motor pattern modification by a newly identified projection neuron in the crab stomatogastric nervous system. *J Neurophysiol* 75: 97-108.
Nunes A.J.P. & Parsons G.J. 1998. Food handling efficiency and particle size selectivity by the southern brown shrimp penaeus subtilisfed a dry pelleted feed. *J Mar Freshw Behav & Physiol* 31: 193-213.
Nusbaum M.P. 2012. Neuropeptide modulation of microcircuits. *Curr Op Neurobiol* 22: 1-10.
Nusbaum M.P. & Beenhakker M.P. 2002. A small-systems approach to motor pattern generation. *Nature* 417: 343-350.
Nusbaum M.P., Blitz D.M., Swensen A.M., Wood D.E. & Marder E. 2001. The roles of co-transmission in neural network modulation. *Trends Neurosci* 24: 146-154.
Parker D. 2006. Complexities and uncertainties of neuronal network function. *Phil Trans R Soc B* 361: 81-99.
Patwardhan S.S. 1935a. On the structure and mechanism of the gastric mill in

Decapoda. II. A Comparative Account of the Gastric Mill in Brachyura. *Proc: Plant Sciences* 2: 155-174.
PATWARDHAN S.S. 1935b. On the structure and mechanism of the gastric mill in Decapoda. IV. The structure of the gastric mill in reptantous Macrura. *Proc Ind Acad Sci* 1: 414-422.
PEARSON J. 1908. *Cancer, the edible crab*. London: Price Six Shilling and Sixpence.
PEARSON K.G. 2006. Common Principles of Motor Control in Vertebrates and Invertebrates. *Ann Rev Neurosci* 16: 265-297.
PEARSON K.G., EKEBERG O. & BÜSCHGES A. 2006. Assessing sensory function in locomotor systems using neuro-mechanical simulations. *Brain Res Rev* 57: 222-227.
PILLOW J.W., AHMADIAN Y. & PANINSKI L. 2010. Model-Based Decoding, Information Estimation, and Change-Point Detection Techniques for Multineuron Spike Trains. *Neur Comput* 1-45.
PLAYTER R. 2006. BigDog. *Unm Sys Tech* VIII: 6230.
POWERS L.W. 1973. Gastric mill rhythms in intact crabs. *J Comp Biochem & Physiol* 46: 767-783.
PRINZ A.A. 2006. Insights from models of rhythmic motor systems. *Curr Op Neurobiol* 16: 615-620.
PRINZ A.A., BILLIMORIA C.P. & MARDER E. 2003. Alternative to Hand-Tuning Conductance-Based Models: Construction and Analysis of Databases of Model Neurons. *J Neurophys* 90: 3998-4015.
PROEKT A., BREZINA V. & WEISS K.R. 2004. Dynamical basis of intentions and expectations in a simple neuronal network. *Proc Nat Ac Sci* 101: 9447-9452.
PROEKT A., WONG J., ZHUROV Y., KOZLOVA N., WEISS K.R. & BREZINA V. 2008. Predicting adaptive behavior in the environment from central nervous system dynamics. *PLoS ONE* 3: e3678.
REDDY A.R. 1935. The structure, mechanism and development of the gastric armature in Stomatopoda with a discussion as to its evolution in Decapoda. *Proc: Plant Sci* 1: 650-675.
REIMER J.D., SINNIGER F., NONAKA M. & UCHIDA S. 2009. Non-invasive internal morphological examination of epizoic zoanthids utilizing CT scanners. *Cor Reefs* 28: 621-621.
RICE M.J. 1970. Cibarial stretch receptors in the tsetse fly (Glossina austeni) and the blowfly (Calliphora erythrocephala). *J Insect Physiol* 16: 277-289.
RINGEL M. 1924. Zur Morphologie des Vorderdarmes von Astacus fluviatilis. *Zeitschr für Wiss Zool* 123: 498-554.
ROBERTSON R.M. & LAVERACK M.S. 1979. Oesophageal sensors and their modulatory influence on oesophageal peristalsis in the lobster, Homarus gammarus. *Proc R Soc, B* 206: 235-263.
RØE C., BAUTZ-HOLTER E. & CIEZA A. 2012. Low back pain in 17 countries, a Rasch analysis of the ICF core set for low back pain. *Intl J Rehabil Res* 1: 1-12.
ROTHSCHILD L.J. 2009. Earth science: Life battered but unbowed. *Nature* 459: 335-336.
RUSSELL D.F. 1985. Neural basis of teeth coordination during gastric mill rhythms in spiny lobsters, Panulirus interruptus. *J Exp Biol* 114: 99-119.
SAIDEMAN S.R., BLITZ D.M. & NUSBAUM M.P. 2007a. Convergent motor patterns from divergent circuits. *J Neurosci* 27: 6664.
SAIDEMAN S.R., MA M., KUTZ-NABER K., COOK A., TORFS P., SCHOOFS L., LI L. & NUSBAUM M.P. 2007b. Modulation of Rhythmic Motor Activity by Pyrokinin

Peptides. *J Neurophys* 97: 579-595.
SANGER T.D. 2010. Controlling variability. *J Mot Behav* 42: 401-407.
SATTELLE D.B. & BUCKINGHAM S.D. 2006. Invertebrate studies and their ongoing contributions to neuroscience. *J Inv Neurosci* 6: 1-3.
SCHIEBER M.H. & SANTELLO M. 2004. Hand function: peripheral and central constraints on performance. *J App Physiol* 96: 2293-2300.
SCHMIDT M., VAN EKERIS L. & ACHE B.W. 1992. Antennular projections to the midbrain of the spiny lobster. I. Sensory innervation of the lateral and medial antennular neuropils. *J Comp Physiol A* 318: 277-290.
SCHOLZ J.P. & SCHÖNER G. 1999. The uncontrolled manifold concept: identifying control variables for a functional task. *Exp Brain Res* 126: 289-306.
SCHULTZ T.W. 1976. The ultrastructure of the hepatopancreatic caeca of Gammarus minus (crustacea, amphipoda). *J Morphol* 149: 383-399.
SELVERSTON A.I., SZÜCS A., HUERTA R., PINTO R. & REYES M. 2009. Neural mechanisms underlying the generation of the lobster gastric mill motor pattern. *Front Neur Circ* 3: 1-12.
SEN K., JORGE-RIVERA J.C., MARDER E. & ABBOTT L.F. 1996. Decoding synapses. *J Neurosci* 16: 6307-6318.
SHEPHERD S.V., LANZILOTTO M. & GHAZANFAR A.A. 2012. Facial Muscle Coordination in Monkeys during Rhythmic Facial Expressions and Ingestive Movements. *J Neurosci* 32: 6105-6116.
SHOEMAKER E.M., P.R. WEISSMAN & C.S. SHOEMAKER 1994. *Hazards Due to Comets and Asteroids*. University of Arizona Press.
SMARANDACHE C.R., DAUR N., HEDRICH U.B.S. & STEIN W. 2008. Regulation of motor pattern frequency by reversals in proprioceptive feedback. *Eur J Neurosci* 28: 460-474.
SMARANDACHE C.R. & STEIN W. 2007. Sensory-induced modification of two motor patterns in the crab, Cancer pagurus. *J Exp Biol* 210: 2912-2922.
SMITH R.I. 1978. The midgut caeca and the limits of the hindgut of Brachyura: a clarification. *Crustaceana* 35: 195-205.
SMOLKA J., ZEIL J. & HEMMI J.M. 2011. Natural visual cues eliciting predator avoidance in fiddler crabs. *R Soc Phil Trans B* 278: 3584-3592.
SPIRITO C.P. 1975. The organization of the crayfish oesophageal nervous system. *J Comp Physiol A* 102: 237-249.
SPONBERG S., LIBBY T., MULLENS C.H. & FULL R.J. 2011a. Shifts in a single muscle's control potential of body dynamics are determined by mechanical feedback. *R Soc Phil Trans B* 366: 1606-1620.
SPONBERG S., SPENCE A.J., MULLENS C.H. & FULL R.J. 2011b. A single muscle's multifunctional control potential of body dynamics for postural control and running. *R Soc Phil Trans B* 366: 1592-1605.
STÄDELE C. 2010. Gleiche Neurone - gleiche Effekte? Anatomie und multineuronale Innervation eines Muskels durch Neurone des gleichen Typs im stomatogastrischen Nervensystem des Taschenkrebses. *Institute for Neurobiology, Ulm University*
STEIN W. 2006. Functional consequences of activity-dependent synaptic enhancement at a crustacean neuromuscular junction. *J Exp Biol* 209: 1285-1300.
STEIN W. 2009. Modulation of stomatogastric rhythms. *J Comp Physiol A* 195: 989-1009.
STEIN W., DELONG N.D., WOOD D.E. & NUSBAUM M.P. 2007. Divergent co-transmitter

actions underlie motor pattern activation by a modulatory projection neuron. *Eur J Neurosci* 26: 1148-1165.
STEIN W., EBERLE C. & HEDRICH U.B.S. 2005. Motor pattern selection by nitric oxide in the stomatogastric nervous system of the crab. *Eur J Neurosci* 21: 2767-2781.
STENGEL R.F. 1994. *Optimal Control and Estimation*. New York: Wiley Interscience.
STEPHENS G.J., JOHNSON-KERNER B., BIALEK W. & RYU W.S. 2008. Dimensionality and dynamics in the behavior of C. elegans. *PLoS Comput Biol* 4: e1000028.
STERN E., GARCIA-CRESCIONI K., MILLER M.W., PESKIN C.S. & BREZINA V. 2009. Modeling the complete cardiac ganglion and heart muscle network of the crab Callinectes sapidus. *BMC Neurosci* 10: P295.
STEULLET P., KRUTZFELDT D., HAMIDANI G. & FLAVUS T. 2002. Dual antennular chemosensory pathways mediate odor-associative learning and odor discrimination in the carribean spiny lobster. *J Exp Biol* 205: 851-867.
STORCH V. & ANGER K. 1983. Influence of starvation and feeding on the hepatopancreas of larvalHyas araneus (Decapoda, Majidae). *Helgol Meeresunt* 36: 67-75.
SUNDAR K. 2009. The importance of muscle mechanics during movement. *Georgia Institute of Technology, Atlanta*
THEODOROU E. & VALERO-CUEVAS F.J. 2010. Optimality in neuromuscular systems. *Ann Intl Conf IEEE* 2010: 4510-4516.
THUMA J.B., HARNESS P.I., KOEHNLE T.J., MORRIS L.G. & HOOPER S.L. 2007. Muscle anatomy is a primary determinant of muscle relaxation dynamics in the lobster (Panulirus interruptus) stomatogastric system. *J Comp Physiol A* 193: 1101-1113.
THUMA J.B. & HOOPER S.L. 2010. Direct evidence that stomatogastric (Panulirus interruptus) muscle passive responses are not due to background actomyosin cross-bridges. *J Comp Physiol A* 196: 649-657.
TIKANMAKI A. & RONING J. 2009. Development of Mörri, a high performance and modular outdoor robot. *IEEE Intl Conf Robot & Autom* 1441-1446.
TODOROV E. 2005. Stochastic optimal control and estimation methods adapted to the noise characteristics of the sensorimotor system. *Neural Comput Phys Rev* 17: 1084-1108.
TODOROV E. 2009. Efficient computation of optimal actions. *Proc Nat Acad Sci* 106: 11478-11483.
TOMASCHKO K.H., GUCKLER R. & BÜCKMANN D. 1995. A new bioassay for the investigation of a membrane-associated ecdysteroid receptor in decapod crustaceans. *Neth J Zool* 45: 93-97.
TOON A., FINLEY M. & STAPLES J. 2009. Decapod phylogenetics and molecular evolution. *Dec Crust Phyl* 21: 613-622.
TSANG L.M., MA K.Y., AHYONG S.T., CHAN T.-Y. & CHU K.H. 2008. Phylogeny of Decapoda using two nuclear protein-coding genes: origin and evolution of the Reptantia. *J Mol Phylogen Evo* 48: 359-368.
VALERO-CUEVAS F.J.F.J. 2005. An integrative approach to the biomechanical function and neuromuscular control of the fingers. *J Biomech* 38: 673-684.
VILLARREAL H. 1991. A Partial Energy Budget for the Australian Crayfish Cherax tenuimanus. *J Aquacult Soc* 22: 252-259.
WEIMANN J.M., MEYRAND P. & MARDER E. 1991. Neurons that form multiple pattern generators: identification and multiple activity patterns of gastric/pyloric neurons in the crab stomatogastric system. *J Neurophys* 65: 111-122.
WEIS J.S. 1976. Effects of environmental factors on regeneration and molting in

fiddler crabs. *Biol Bull* 150: 152-162.
WEISSBURG M., ATKINS L., BERKENKAMP K. & MANKIN D. 2012. Dine or dash? Turbulence inhibits blue crab navigation in attractive–aversive odor plumes by altering signal structure encoded by the olfactory pathway. *J Exp Biol* 215: 4175-4185.
WHITE R.S. 2011. Distinct Neuromuscular Patterns from a Single Motor Network. *Department of Neuroscience, University of Pennsylvania*
WHITE R.S. & NUSBAUM M.P. 2011. Distinct Input Pathways elicit different motor patterns driven by the same core rhythm generator. *J Neurosci* 31: 11484-11494.
WOOD D.E., MANOR Y., NADIM F. & NUSBAUM M.P. 2004. Intercircuit control via rhythmic regulation of projection neuron activity. *J Neurosci* 24: 7455-7463.
WOOD D.E., STEIN W. & NUSBAUM M.P. 2000. Projection neurons with shared cotransmitters elicit different motor patterns from the same neural network. *J Neurosci* 20: 8943-8953.
WOOD D.E., VARRECCHIA M., PAPERNOV M., COOK D. & CRAWFORD D.C. 2010. Hormonal modulation of two coordinated rhythmic motor patterns. *J Neurophys* 104: 654-664.
YONGE C.M. 1924. Studies on the Comparative Physiology of Digestion. *J Exp Biol* 1: 343-389.
ZIEGLER A., FABER C., MUELLER S. & BARTOLOMAEUS T. 2008. Systematic comparison and reconstruction of sea urchin (Echinoidea) internal anatomy: a novel approach using magnetic resonance imaging. *BMC Biol A* 6: 1-33.

Acknowledgments

In the following, I would like to thank all people who were directly or indirectly involved in the completion of this work:

First of all, I want to thank Prof. Harald Wolf for allowing me to write my thesis in his institute and providing the work space. Is thoughts and remarks were of great help for this work.

I would like to earnestly thank my supervisor, Dr. Wolfgang Stein. Without his creativity and wisdom this work would not have been possible. I will miss the White Board Sessions and his door being always open for questions and discussions. His support and friendship during and beyond work made the years in the Crab Lab run by too quickly. I whish him all the best for all his future endeavors. So say we all.

I want to thank Prof. Michael P. Nusbaum for letting me finish the experimental part of my thesis in his laboratory. The fruitful discussions were a great help for the completion of this thesis. I also want to thank Jason Rodriguez and Aaron Cook for the outright support during my stay, the discussions on NPR in the lab and the great time.

I want to thank Dr. Wolfgang Mader for his helpful advice with any type of problems with computers and statistics.

I want to thank Ursula Seifert for her support in all administrative questions and for being the good soul of our institute.

I want to thank all students, colleagues and friends whom I had the pleasure to work and spend time with during the past years at the institute (in alphabetical order): Alex, Andrea, Astrid, Carmen, Carola, Frank, Jessica, Matthias, Nelly, Peter, Philipp, Raimund, Stefan, Steffi, Stephi, Siegfried, TingTing, Tino, Thorsten, Uli, Wafa.

I want to thank all members of the Institute for Neurobiology for the support and great work athmosphere.

I want to thank Denise Hummel for her support and understanding and for being the great person she is. You make me whole.

Last, but certainly no least, I want to thank my family and my parents who trusted and supported me throughout these years, and for giving me the opportunity to study and follow my dreams.

Declaration

I hereby declare that this thesis has been written independently and that I have used no other material than that I have specified. Those passages taken from other works, either verbatim or in spirit, I have identified in each individual case by indicating the source. I further declare that all my academic work has been written in line with the principles of proper academic research according to the valid “university statute for the safeguarding of proper academic practice.

Ulm, the 13th of November 2012

Publications

Scientific publications

Hedrich, U.B.S., Diehl, F., Stein, W. (2011). Gastric and pyloric motor pattern control by a modulatory projection neuron in the intact crab, Cancer pagurus. Journal of Neurophysiology 105(4): 1671-80. doi:10.1152/jn.01105.2010.

Daur N., Diehl F., Mader W., Stein, W. (2012) The stomatogastric nervous system as a model for studying sensorimotor interactions in real-time closed-loop conditions. Front Comput Neurosci 6(13) doi: 10.3389/fncom.2012.00013.

Presentations

Diehl, F. (2008). Simulation of a muscle tendon organ in the stomatogastric nervous system of the crab using the simulation software MadSim. BUGS meeting.

Diehl, F. (2010). Function of modulatory projection neurons in vivo and behavioral relevance. ANN-Meeting 2010 (DZG satellite symposium), Hamburg.

Diehl, F. (2010). In vivo recording and stimulation of MCN1: prospects and constraints. STG-Meeting 2010, San Diego, CA, USA.

Diehl, F. (2011). Neurons alone can't chew - Functional relevance of activity in the stomatogastric nervous system of the crab. Neuro DoWo 2011, Bonn.

Abstracts/Symposia

Diehl, F., Stein, W. (2008). A real-time model of a muscle tendon organ in the somatogastric nervous system of the crab. In: Society for Neuroscience, 376.10, Washington D.C., USA.

Diehl, F., Daur N., Stein, W. (2009). Investigating the effects of proprioceptive feedback on a central pattern generator with a real-time computer model. In: Meeting of the German Neuroscience Society, T21-1A, Göttingen, Germany.

Diehl, F., Stein, W. (2009). Characterization of proprioceptive feedback to the stomatogastric nervous system of the crab using a closed-loop experimental setup. In: Interdisciplinary College 2009, Guenne, Germany.

Diehl, F., Stein, W. (2009). Measuring the contraction properties of a gastric mill muscle in the crab Cancer pagurus for creating a real-time computer model. In: Society for Neuroscience, Chicago, IL, USA.

Other publications

Diehl, F. (2010). Literaturverwaltungsprogramme. Laborjournal (Vol. 16).

Curriculum Vitae

of Florian Diehl

born in Kempten (Allgäu) on 27th of November 1981.

Institute address
Institute for Neurobiology
Ulm University
89069 Ulm, Germany
Tel.: 0731-50-22644
e-mail: florian@neurobiologie.de

Private address
Spechtweg 29
87439 Kempten

Education

1987 - 1991	Konrad Adenauer Grundschule, Kempten
1991 - 2002	Allgäu-Gymnasium, Kempten
1999 - 2000	Frederic High-School, Wisconsin, USA
2003 - 2008	Studies of Biology at Ulm University
	Diploma (major: neurobiology; minors: computer science, ecology of the mediterranean, virology). Grade: 1.9
	diploma thesis: Modeling of a receptor neuron in the stomatogastric ganglion of the crab. Grade: 1.0
since 2009	PhD student at the Institute for Neurobiology, Ulm University and at the University of Pennsylvania, Philadelphia, PA, USA.

Scientific courses

Aug. 2011	"22. NeuroDoWo" Doktorandenworkshop, Universität Bonn participant & speaker
Jun. - Aug. 2009	Woods Hole, USA "Neural Systems & Behavior" course attendee
Mar 2009	Interdisciplinary Summer School, Günne Attendee & Poster presenter

Other activities

2008	Certificate for Extracurricular Dedication, awarded by Ulm University